

Novel Approaches to Probe the Activity of Deubiquitinating Enzymes



*A thesis submitted to the school of Chemistry, Trinity College Dublin,
The University of Dublin for the degree of Doctor of Philosophy*

Neil C. Taylor B.A. (Mod)

Under the supervision of Prof. Joanna McGouran

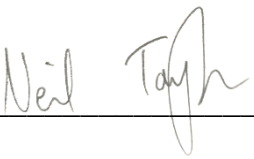
Trinity College Dublin, The University of Dublin

May 2021

Declaration

I declare that this thesis has not been submitted as an exercise for a degree at this or any other university and it is entirely my own work other than where acknowledged.

I agree to deposit this thesis in the University's open access institutional repository or allow the Library to do so on my behalf, subject to Irish Copyright Legislation and Trinity College Library conditions of use and acknowledgement.



Neil Taylor

Abstract

Ubiquitination is a highly conserved post-translational modification that regulates a multitude of critical cellular events. This process is orchestrated by a complex enzymatic network. Deubiquitinating enzymes (DUBs) are responsible for removal of ubiquitin from its conjugates. There are over 100 DUBs expressed in eukaryotes and several diseases are associated with their dysregulation, including cancer and neurodegeneration. Activity-based probes (ABPs) have been developed as an effective strategy to study DUBs.

ABPs targeting these enzymes are typically based on a ubiquitin scaffold and incorporate an electrophilic group that reacts with an active site cysteine. These probes have greatly enhanced the mechanistic and structural understanding of DUBs but offer no external control over the timing of the reaction. In this work, ABPs consisting of a monoubiquitin recognition element and warheads with reactivity previously unexplored in the context of ABPs were designed and synthesised. The reactivity of these novel ABPs with DUBs was examined and new labelling strategies were developed to improve the study of these enzymes.

New electrophilic probes with fluoride reactive groups were designed and synthesised. These probes were tested alongside previously reported electrophilic probes and demonstrated negligible reactivity with DUBs.

Latent ubiquitin-based probes that target DUBs *via* a site selective, photoinitiated thiol-ene coupling mechanism were developed. A novel labelling methodology was developed for these alkene-functionalised probes and reactivity was demonstrated against recombinant DUBs and endogenous DUBs within cell lysate. Specificity of this probe labelling was confirmed using inhibitor and proteomic studies. Novel assays to probe reversible and irreversible inhibitors for this enzyme were also demonstrated.

In order to enhance the biocompatibility of this methodology, a milder source of UV light was used to initiate the reaction between DUBs and the alkene-functionalised probes. Alternative radical initiators were examined for a visible light-mediated thiol-ene reaction. Successful labelling of recombinant DUBs was achieved in both strategies, but visible light activation was limited by off-target reactivity in more complex systems. The visible light-mediated thiol-ene reaction and the thiol-yne

reaction were also explored for non-templated protein conjugation, affording modest coupling in both cases.

Overall, the novel electrophilic probes presented do not improve upon existing probes of similar reactivity. However, the work on alkene functionalised probes enables more finely resolved investigations of DUB activity in complex systems. In contrast to existing cysteine reactive probes, control over the timing of the enzyme-probe reaction is possible for the alkene functionalised probes as they are completely inert under ambient conditions, even upon probe binding. This is expected to help provide a better understanding of these enzymes and aid in the study and development of novel inhibitors. The visible light-mediated thiol-ene and thiol-yne reactions were found to have limited applications for bioconjugations.

Acknowledgements

Firstly, like to thank my supervisor Prof. Joanna McGouran for not only providing me with the opportunity to work in her research group but the support and assistance she provided me at all stages throughout my PhD. I would also like to thank the School of Chemistry, Trinity College Dublin for funding my time as a PhD student.

I am grateful to Dr. John O'Brien and Dr. Manuel Rüther for their assistance with NMR. I would also like to thank Dr. Gary Hessman, Dr. Martin Feeney and Dr. Holger Kramer for all their assistance with the running and analysis of MS samples.

I would like to thank all past and present McGouran group members for being great colleagues and friends. It is a testament to the collaborative and helpful environment of the group that as a biochemist I (somewhat) successfully synthesised multiple compounds. Thank you to Werner for being a great tour guide and host on our visits to Switzerland. Mark, I appreciate all the times you have shared some of your endless science knowledge with me and good luck as the new lab alpha. Susie and Ellen, thank you for always bringing happiness and laughter to the lab. Sean, thank you for being the first person I could speak to about both chemical biology and football. Connor and Valerio, I appreciate your excellent proofreading and good luck with your PhDs.

Eva, thank you for being a great colleague and always being willing to help me with stupid chemistry questions. Most importantly, thank you for your support and the time we have had outside the lab during this period.

Finally, I would like to express my gratefulness to my family. I would not have gotten to this point without the education and support they provided me with.

Contents

Declaration	i
Abstract	ii
Acknowledgements	v
Contents	vi
Abbreviations	xii
1 Introduction	1
1.1 Ubiquitination as a post-translational modification.....	1
1.2 Deubiquitinating enzymes	3
1.3 Activity-based probes targeting DUBs	6
1.3.1 Monoubiquitin based probes	7
1.4 Advances in the application of DUB ABPs.....	11
1.4.1 Mass spectrometry-based techniques using DUB ABPs	11
1.4.2 Cell permeable DUB ABPs.....	12
1.4.3 Small molecule DUB ABPs	14
1.5 Ubiquitin conjugate probes targeting DUBs.....	16
1.5.1 Ubiquitin peptide probes	17
1.5.2 Diubiquitin ABPs.....	18
1.5.3 Ubiquitin-protein conjugate probes	20
1.6 Probes for Ubiquitin Conjugation Machinery.....	21
1.6.1 Ubiquitin-adenine probes.....	21
1.6.2 Ubiquitin-protein Probes for E3 ligases.....	23
1.7 Radical chemistry in biological systems	24
1.7.1 Cysteine selective radical-mediated bioconjugations	25
1.7.1.1 Photocatalysts for visible light-mediated thiyl radical generation... 26	
1.7.2 Tyrosine selective radical-mediated bioconjugations.....	27
1.7.3 Tryptophan selective radical-mediated bioconjugations.....	28

1.7.4	C-terminal and Dha selective radical bioconjugations	30
1.8	Radicals and other activatable chemistry in ABPP	31
1.8.1	Photoactivatable groups for ABPP	32
1.9	Objectives.....	34
2	Electrophilic probes for DUBs	38
2.1	Synthesis and testing of reported electrophilic probes.....	40
2.1.1	Expression and purification of HA-Ub ₇₅ -thioester.....	40
2.1.2	Synthesis and reactivity of the HA-Ub ₇₅ -CH ₂ CH ₂ Br probe.....	42
2.1.3	Optimisation of the immunoprecipitation protocol using the HA-Ub ₇₅ -CH ₂ CH ₂ Br probe.....	46
2.1.4	Synthesis and reactivity of HA-Ub ₇₅ -propargylamine probe.....	50
2.2	Synthesis and reactivity of fluoride probes.....	51
2.3	Conclusions	54
3	The thiol-ene reaction for ABPP of DUBs.....	57
3.1	Introduction and probe design.....	57
3.2	Synthesis, characterisation and testing of HA-Ub ₇₅ -propene.....	59
3.2.1	Recombinant enzyme experiments using HA-Ub ₇₅ -propene 38.	60
3.2.2	Cell lysate experiments and optimisation of thiol-ene reaction conditions.....	63
3.3	Investigating the specificity of the thiol-ene labelling using PR-619	69
3.4	Design, synthesis and testing of substituted alkene probes.	72
3.5	Immunoprecipitation analysis of thiol-ene labelling.....	76
3.6	Conclusion	84
4	Towards the application of the thiol-ene reaction for ABPP in cells	87
4.1	Examining a milder UV source for the thiol-ene methodology.....	89
4.2	Ambient light-mediated thiol-ene labelling experiments.....	91
4.2.1	Recombinant enzyme ambient light labelling	91
4.2.2	HEK 293T lysate experiments using ambient light	94

4.3	Controlled visible light source thiol-ene labelling experiments	96
4.3.1	Recombinant enzyme 10 W lamp thiol-ene labelling	96
4.3.2	HEK 293T lysate experiments using a 10 W lamp	99
4.4	Investigating the influence of degassing on the Eosin Y catalysed labelling	101
4.5	Investigating the off-target reactivity of Eosin Y	103
4.5.1	Fluorescent gel studies	103
4.5.2	Analysing the effects of certain amino acids on the Eosin Y labelling..	106
4.6	Using Eosin Y for non-templated thiol-ene conjugation of proteins	110
4.7	Conclusions	113
5	Conclusions and outlook	116
6	Experimental	120
6.1	General biological methods	120
6.1.1	Buffers	120
6.1.2	SDS-PAGE	120
6.1.3	Silver staining	121
6.1.4	Coomassie blue staining	121
6.1.5	Western Blotting	121
6.1.6	Expression and purification of WT ubiquitin	122
6.1.7	Expression and purification of OTUB1	122
6.2	Mass spectrometry	123
6.2.1	CHCl ₃ /MeOH extraction	123
6.2.2	In-solution digest following CHCl ₃ /MeOH extraction	124
6.2.3	In-gel digest	124
6.2.4	Filter Aided Sample Preparation (FASP)	125
6.2.5	Zip-tip purification	125
6.2.6	MALDI-TOF mass spectrometry	125
6.2.7	Orbitrap mass spectrometry	126

6.2.8	Captive spray ionisation mass spectrometry	127
6.3	Synthesis of HA-tagged activity-based monoubiquitin probes	128
6.3.1	Expression and purification of HA-Ub ₇₅ -thioester	128
6.3.2	Synthesis of HA-Ub ₇₅ -CH ₂ CH ₂ Br 5	129
6.3.3	Synthesis of HA-Ub ₇₅ -alkene probes 38–40	129
6.3.4	Synthesis of HA-Ub ₇₅ -alkyl fluoride probes 36–37	130
6.3.5	Synthesis of HA-Ub ₇₅ -PA 6	130
6.4	<i>In vitro</i> DUB labelling	131
6.4.1	HEK 293T cell lysate preparation	131
6.4.2	<i>In vitro</i> HA-Ub ₇₅ CH ₂ CH ₂ Br 5 labelling	131
6.4.3	Optimised <i>in vitro</i> thiol-ene labelling with alkene probes	131
6.4.4	Lysate labelling with <i>N</i> -ethylmaleimide (NEM)	132
6.4.5	Screening of alternative initiators	132
6.4.6	Investigating increasing DPAP and MAP concentrations	132
6.4.7	Optimisation of labelling conditions for LC-MS/MS	133
6.4.8	<i>In vitro</i> thiol-ene labelling with alkene probes and denatured OTUB1	133
6.4.9	PR-619 (55) pre-incubation assay	133
6.4.10	Probe displacement assay	134
6.4.11	Determining the K _d of the probe-OTUB1 complex	134
6.5	Immunoprecipitation (IP)	135
6.6	Optimised Eosin Y lysate labelling	135
6.6.1	Optimised Eosin Y recombinant enzyme labelling	136
6.6.2	Amino acid spike OTUB1 labelling using Eosin Y	136
6.6.3	Eosin Y for the conjugation of ubiquitin monomers and BSA	137
6.6.4	Bi ₂ O ₃ labelling	137
6.7	General chemical methods	137
6.7.1	Synthesis of (<i>E</i>)-1-phenyl-3-phthalimido-2-propene 59	138

6.7.2	Synthesis of (<i>E</i>)-3-phenyl-prop-2-en-1-amine 56.....	139
6.7.3	Synthesis of (<i>E</i>)-1-phthalimido-2-butene 61	140
6.7.4	(<i>E</i>)-but-2-ene-amine hydrochloride 62	141
6.7.5	(<i>E</i>)-tert-butyl but-2-en-1-ylcarbamate 63	141
6.7.6	(<i>E</i>)-but-2-ene-amine trifluoroacetate 64	142
7	References.....	144

Abbreviations

°C	Degrees Celsius
AAPH	2,2'-Azobis(2-amidinopropane) dihydrochloride
ABP	Activity-based probe
ABPP	Activity-based protein profiling
Acm	Acetamidomethyl
ACPA	4,4'-Azobis(4-cyanopentanoic acid)
Aha	L-Azidohomoalanine
Ala	Alanine
AMP	Adenosine monophosphate
APCI	Atmospheric pressure chemical ionisation
APS	Ammonium persulfate
Arg	Arginine
Asn	Asparagine
Asp	Aspartic acid
ATP	Adenosine triphosphate
BAP	BRCA1-associated protein
BOC	<i>tert</i> -Butyloxycarbonyl
BODIPY	Boron dipyrromethene fluorophore
bpy	Bipyridine
BRCA	Breast cancer type
BSA	Bovine serum albumin
CAP-GLY	Cytoplasmic protein with three cytoskeletal-associated protein-glycine-conserved
CASTp	Computed Atlas of Surface Topography of proteins
CBD	Chitin binding domain
Cit	Citrulline
CPP	Cell-penetrating peptide
CPY	Cytochrome P45 enzyme
CSF	Colony-stimulating factor
Cys	Cysteine
Da	Dalton
Dab	2,4-Diaminobutyric Acid
DCM	Dichloromethane
Dha	Dehydroalanine
DiUb	Diubiquitin
DMF	<i>N,N</i> -Dimethylformamide
DMSO	Dimethyl sulfoxide
DNA	Deoxyribonucleic acid
DPAP	2,2-Dimethoxy-2-phenylacetophenone
DTT	Dithiothreitol
DUB	Deubiquitinating enzyme
E1	Ubiquitin-activating enzyme

E2	Ubiquitin-conjugating enzyme
E3	Ubiquitin ligase
ECL	Enhanced chemiluminescence
EDTA	Ethylenediaminetetraacetic acid
ESI	Electrospray ionization
Et	Ethyl
<i>et al.</i>	<i>et alii</i> , and others
EWG	Electron withdrawing group
FA	Formic acid
FAD	Flavin adenine dinucleotide
FANCD2	Fanconi anaemia group D2
FASP	Filter aided sample preparation
Gly	Glycine
GPX4	Glutathione peroxidase 4
GSH	Glutathione
GST	Glutathione S-transferases
h	Hour
H2A	Histone 2A
HA	Hemagglutinin
HAT	Hydrogen atom transfer
HCCA	α -Cyano-4-hydroxycinnamic acid
HECT	Homologous to the E6-AP Carboxyl Terminus
HEK	Human embryonic kidney
HeLa	Henrietta Lacks immortal cancer cell line
His	Histidine
HMBC	Heteronuclear Multiple Bond Correlation
HRMS	High resolution mass spectrometry
HSQC	Heteronuclear single quantum correlation
IAA	Iodoacetamide
ID	Identity
IP	Immunoprecipitation
IPA	Isopropyl alcohol
IPTG	Isopropyl β -D-1-thiogalactopyranoside
IR	Infrared
IsoT	IsopeptidaseT
JAMM	JAB1/MPN/MOV34 family
K _d	Equilibrium dissociation constant
LAP	Lithium phenyl-2,4,6-trimethylbenzoylphosphinate
LB	Lysogeny broth
LC	Liquid chromatography
LFQ	Label free quantification
Lys	Lysine
MALDI	Matrix-assisted laser desorption/ionisation
MAP	Methoxyacetophenone
MCPIP	Monocyte chemotactic protein-induced protein

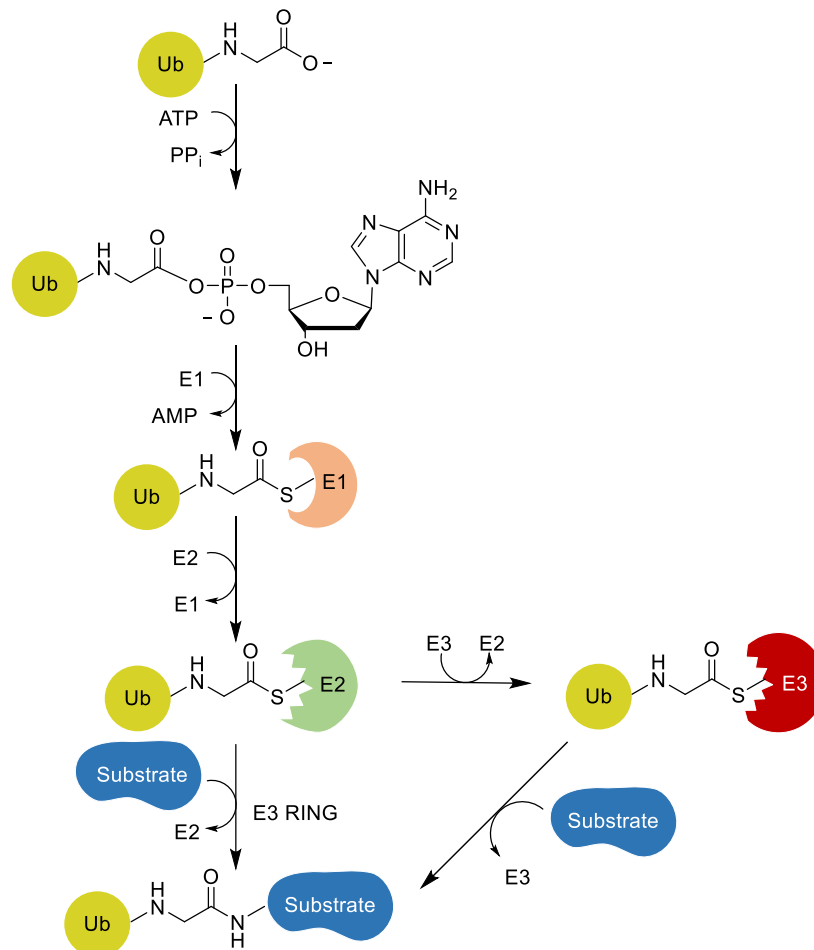
Me	Methyl
MESNa	Sodium 2-mercaptoethanesulfonate
Met	Methionine
min	Minute
MINDY	Motif interacting with Ub-containing novel DUB family
MJD	Machado-Josephin domain proteases
mp	Melting point
MS	Mass spectrometry
MW	Molecular weight
NCL	Native chemical ligation
NEDD	Neural precursor cell expressed developmentally down-regulated protein
NEM	<i>N</i> -Ethylmaleimide
NFκB	Nuclear factor kappa-light-chain-enhancer of activated B cells
NHS	<i>N</i> -Hydroxysuccinimide
NMR	Nuclear magnetic resonance
NP-40	Nonylphenoxypolyethoxyethanol
OD	Optical density
OTU	Ovarian tumour proteases
p53	Tumour protein p53
PA	Propargyl amine
PAGE	Poly acrylamide gel electrophoresis
PARK	Parkinson disease protein
PBS(T)	Phosphate buffered saline (tween)
PCNA	Proliferating cell nuclear antigen
PEG	Polyethylene glycol
PET	Photoinduced electron transfer
PFO	Perfringolysin O
Ph	Phenyl
Phth	Phthalimide
Plpro	Coronavirus papain-like proteases
PMSF	Phenylmethylsulfonyl fluoride
PMT	Photomultiplier tubes
Ppi	Pyrophosphate
Pro	Proline
Rf	Retention factor
RING	Really Interesting New Gene
RNA	Ribonucleic acid
ROS	Reactive oxygen species
rpm	Revolutions per minute
RT	Room temperature
SARS	Severe Acute Respiratory Syndrome
SDS	Sodium dodecyl sulfate
SeCys	Selenocysteine
Ser	Serine

SET	Single electron transfer
SUMO	Small ubiquitin-related modifier
TCEP	Tris (2-carboxyethyl) phosphine
TDAE	Tosyl-substituted doubly activated ene
TEMED	Tetramethylethylenediamine
TEMPO	2,2,6,6-Tetramethyl-1-piperidine-1-oxyl
TFA	Trifluoroacetic acid
TGF- β 7	Transforming growth factor beta
TLC	Thin layer chromatography
TMR	Tetramethylrhodamine
TOF	Time of flight
TRIM	Tripartite motif-containing protein
Trp	Tryptophan
Tyr	Tyrosine
U2OS	Human Bone Osteosarcoma Epithelial Cells
Ub	Ubiquitin
UBA	Ubiquitin activating enzyme
UBD	Ubiquitin binding domains
UBEN	Ubiquitin conjugating enzyme
UCH	Ubiquitin C-terminal hydrolases
Ulp	Ubiquitin like protein
USP	Ubiquitin-specific proteases
UV	Ultraviolet
VME	Vinyl methyl ester
WT	Wild-type
XML	Extensible mark-up language
ZUFSP	Zinc finger with UFM1-specific peptidase domain protein/C6orf113/ZUP1

1 Introduction

1.1 Ubiquitination as a post-translational modification

Ubiquitination is a post-translational modification wherein ubiquitin is conjugated to substrate proteins.¹ The conjugation of this 76 amino acid protein changes the activity of the substrate proteins and their interactions with other proteins.¹ The ubiquitination process is carried out by a series of enzymes that comprise what is known as the ubiquitin cascade. This cascade consists of the highly conserved E1, E2 and E3 enzymes that carry out a series of activation and ligation reactions to ultimately conjugate the C-terminus of ubiquitin to a lysine (Lys) residue or the N-terminus of substrates (**Scheme 1.1**).^{2,3}



Scheme 1.1: The ubiquitin cascade. Ubiquitin monomers travel through the ubiquitin cascade via a series of transthioesterification reactions before conjugation to a lysine (Lys) residue of a substrate protein.

The array of these enzymes in eukaryotes and the differences in their relative promiscuity results in highly complex enzymatic networks that regulate numerous

cellular events. Initially, the cascade was understood to provide the early signals for the ATP-dependent degradation of short-lived proteins by the proteasome.⁴ Since then, the cascade has also been identified to play a major role in DNA repair,⁵ transcriptional regulation,⁶ the cell cycle^{7,8} and stress responses^{7,8} among many other processes.⁹

The cellular pool of ubiquitin-substrate conjugates is highly dynamic, with rapid removal and addition of monomers.^{10,11} The E1 ubiquitin-activating enzymes catalyse the formation of a high-energy adenylate intermediate that is transferred to the E2 and E3 enzymes *via* transthioesterification reactions with the active site cysteine (Cys) of each enzyme (**Scheme 1.1**).¹² Ultimately, an isopeptide bond is formed between a lysine (Lys) residue of a substrate protein and the C-terminus of the ubiquitin monomer by an E3 enzyme.¹² Alternatively, RING E3 enzymes can act as scaffolds, templating the interaction between E2 enzymes and the substrate proteins to facilitate isopeptide bond formation.

Substrates can be monoubiquitinated, as seen in proliferating cell nuclear antigen (PCNA)¹³ and the transcription factor p53.¹⁴ Alternatively, multiple ubiquitin monomers can be conjugated to multiple Lys residues of a protein in a process known as multimonoubiquitination. A well-established example of this is the epidermal growth factor receptor.¹⁵ Isopeptide bonds can also be formed with the N-terminus of another ubiquitin monomer, or one of its seven surface-exposed Lys residues to construct polyubiquitin chains.¹⁶ These chains vary in length and linkage type, affording distinct topologies which determine the substrate protein's interactions.¹⁷

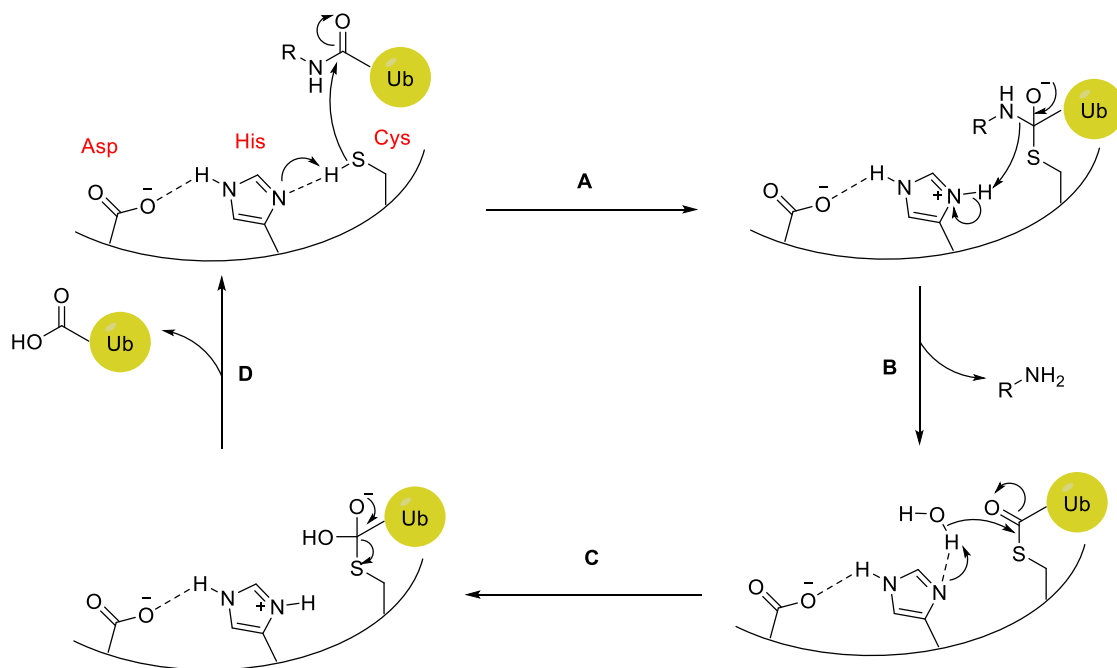
All possible polyubiquitin linkage types have been found in eukaryotic cells, with chains adopting either an 'open' or 'compact' conformation depending on this linkage type.^{18,19} These differing topologies are recognised by subsets of other enzymes, allowing for numerous different processes to be regulated by ubiquitination. The best studied of these chains is the Lys 48 linkage type.⁹ Proteins with Lys 48 linked polyubiquitin chains of at least four units long are marked for degradation by proteasome.²⁰ Ubiquitin receptor proteins have been demonstrated to escort these ubiquitinated proteins to the proteasome and certain deubiquitinating enzymes (DUBs) such as Rpn11 associate with the proteasome to regulate this process.^{20,21} In contrast, chains linked *via* the Lys 63 residue are known to be

involved in DNA damage signalling.²² The exact function of chains linked *via* other Lys residues or chains of mixed linkage type remains unclear, and the complexity of the process is added to by the occurrence of chains containing other ubiquitin-like proteins such as NEDD and SUMO.¹⁸ The importance of the ubiquitin cascade is underlined by the range of pathologies that have been linked to mutations of enzymes within the cascade. These include cancer,²³ genetic syndromes²⁴ and neurodegenerative diseases.²⁵ The ubiquitination process therefore requires tight regulation and the enzymes that oppose the action of this cascade and remove ubiquitin monomers from substrates play an critical role.

1.2 Deubiquitinating enzymes

DUBs possess ubiquitin C-terminal hydrolytic activity and are responsible for removal of ubiquitin from its conjugates.²⁶ The human genome encodes for approximately 100 of these enzymes, and they are split into eight classes based on sequence similarity and mechanism of action: ubiquitin-specific proteases (USPs), ubiquitin C-terminal hydrolases (UCHs), ovarian tumour proteases (OTUs), Machado-Josephin domain proteases (MJDs), the JAB1/MPN/MOV34 family (JAMMs), the motif interacting with Ub-containing novel DUB family (MINDY), monocyte chemotactic protein-induced proteins (MCPIPs) and the recently discovered Zn-finger and UFSP domain proteins (ZUFSPs).^{27,28} This wide range of enzymes adds to the intricacy of the ubiquitin system already afforded by the conjugation machinery and array of linkage types for polyubiquitin chains.

All families, except the JAMM metalloproteases, are Cys proteases.²⁷ Their active site contains a Cys and histidine (His) residue, which together form a catalytic diad. Often a third residue, typically an asparagine (Asn) or aspartate (Asp), also contributes to form a catalytic triad (**Scheme 1.2**).²⁹ The catalytic Cys residue is deprotonated by the adjacent His, promoting nucleophilic attack by this Cys. If present, the third residue polarises and aligns the His to promote hydrogen bonding with the Cys (**Scheme 1.2**).³⁰ DUBs cleave the amide bond between C-terminal glycine (Gly 76) of ubiquitin and the Lys side chain of the protein that is conjugated to the monomer.



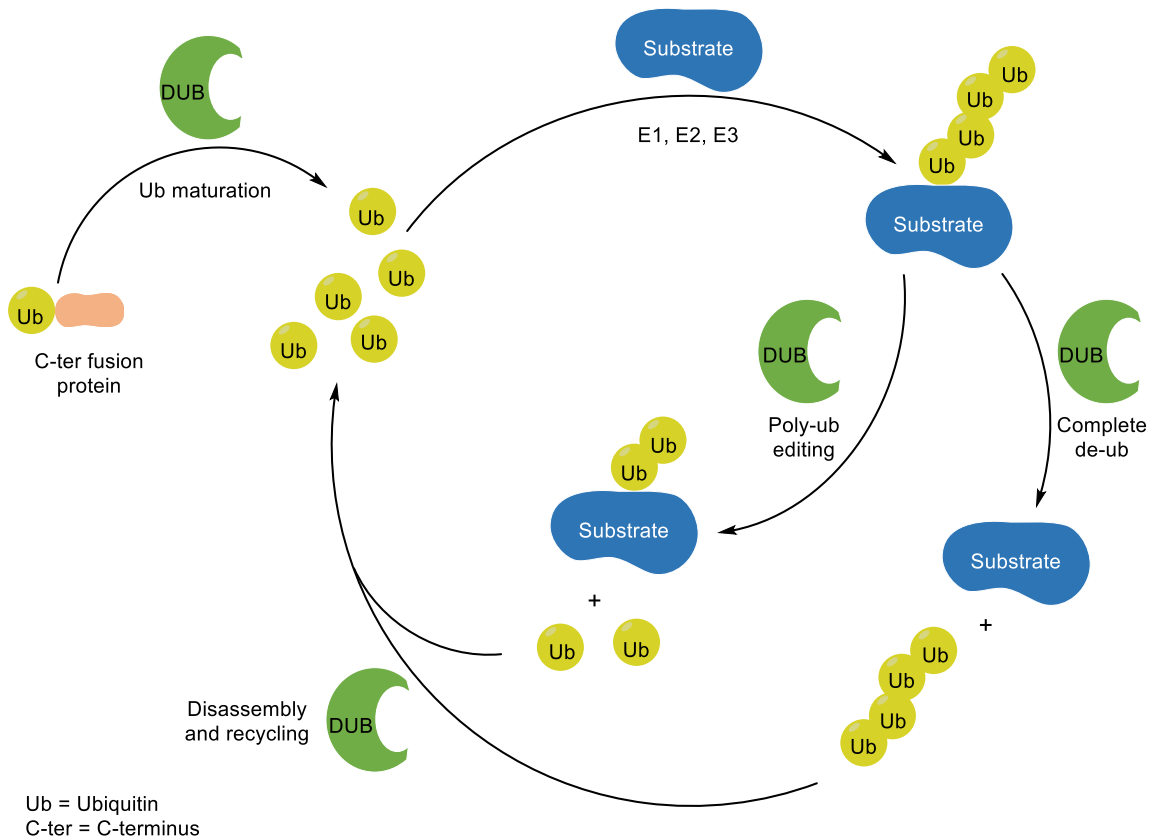
R = Substrate protein

Scheme 1.2: Mechanism of action for Cys protease classes of DUBs. (A) Nucleophilic attack at the carbonyl carbon of Gly 76 by Cys, (B) Elimination of amine to form thioester, (C) Hydrolysis of thioester, (D) Elimination of Cys and release of ubiquitin.

The JAMM family of DUBs are zinc metalloproteases.³¹ Two zinc ions are coordinated within the active site by conserved His and Asn residues. The zinc ions activate a water molecule to attack the isopeptide bond, creating a charged catalytic intermediate which then collapses to release the amino group.^{32,33} As with the Cys protease DUBs, the isopeptide bond between the Gly 76 residue of ubiquitin and the conjugated Lys residue is cleaved.

DUB-ubiquitin binding interactions are mediated by various ubiquitin binding domains (UBDs). Examples include the ubiquitin associated domain, the ubiquitin interacting motif and the zinc-finger ubiquitin-specific protease domain.³⁴ The C-terminal sequence of ubiquitin, in particular the arginine (Arg) 74 and Gly 75 residues, is fundamental for recognition by DUBs, with the final Gly residue orientated immediately adjacent to the active site Cys.³⁵ DUBs display varying specificities for different polyubiquitin linkage types. For example, OTUB1, a member of the OTU family, has high specificity for Lys 48 linked chains.³⁶ OTUB1 therefore plays a crucial role in the protein degradation pathway. Conversely, some members of the USP family demonstrate little linkage preference, suggesting they

play a more general role in the ubiquitin network.³⁷ The primary roles of DUBs in cells are summarised below (**Scheme 1.3**).



Scheme 1.3: Summary of the roles of DUBs in cells. The general roles of DUBs are the processing of immature ubiquitin monomers, the complete removal of polyubiquitin chains, editing poly ubiquitin chains and the disassembly and recycling of these chains. Figure adapted with permission from Todi et al.³⁸

Ubiquitin precursors are first synthesised in the cell as C-terminally extended proteins, fused to ribosomal proteins or as ubiquitin polymers. DUBs are responsible for processing these precursors, adding to the pool of free ubiquitin monomers available for the conjugation machinery to add to substrate proteins.³⁹ The complete disassembly and recycling of ubiquitin chains is also carried out by DUBs and is critical in sustaining ubiquitin homeostasis. The partial disassembly or editing of these chains is also performed.⁴⁰ PA700-isopeptidase has been reported to associate with parts of the proteasome and perform a ‘proofreading’ role, ensuring no protein is mistakenly degraded.⁴¹ Several DUBs have been implicated in the developmental processes of *Drosophila*, including Fat facets (faf)⁴² and members of the OTU family.⁴³ Similarly, DUBs are established to have important roles in the development of mice.⁴⁴ Furthermore, the role of DUBs in stem cell maintenance and

differentiation is also well established.⁴⁵⁻⁴⁷ The DUB USP1 has been demonstrated to have a close relationship with the DNA repair enzyme Fanconi anaemia group D2 protein (FANCD2).⁴⁸ Several other DUBs, including USP3, are believed to be involved in DNA repair and maintenance.^{49,50} Finally, USP16,⁵¹ USP22⁵² and USP3⁵³ have all been strongly implicated in cell cycle regulation. DUBs are known to regulate several other cell signalling pathways in combination with the ubiquitin conjugation machinery *via* the controlled addition and removal of ubiquitin monomers. Regulating effects have been demonstrated on the p53,⁵⁴ NFκB,⁵⁵ TGF-β⁵⁶ and Csf3⁵⁷ signalling pathways, all of which are critical to the homeostasis of a cell.

Dysregulation of DUBs can promote the development of certain disease states. Genes encoding the DUBs CAP-GLY and BAP1 are established tumour suppressor genes and are often mutated in cancer phenotypes.⁵⁸ Additionally, upregulation in the expression of members of the OTU family is linked to the development of many cancer types.⁵⁹ An increasing number of studies also link mutations and changes in the expression levels of DUBs and members of the ubiquitin cascade to neurological diseases.^{25,60-63} The apparent importance of DUBs in a number of cellular processes and disease states has created a significant demand for new tools and methods to increase the understanding of these enzymes.⁶⁴

1.3 Activity-based probes targeting DUBs

Traditional methods to understand and profile an enzyme's influence on a cell rely on monitoring the abundance of the associated messenger ribonucleic acid (mRNA) sequence using transcriptomic techniques.⁶⁵ These methods are limited as they assume that all mRNA present will be translated into active enzyme. They do not account for regulation of a protein's expression at the mRNA level or the regulation of an enzyme's activity *via* post-translational modifications or interactions with other molecules. Therefore, transcriptomic analysis does not provide a complete picture of enzyme activity. Activity-based probes (ABPs) were developed to overcome these limitations.⁶⁶ These probes target only the active form of an enzyme and allow for the identification and characterisation of active enzymes within complex cellular milieu, giving a more accurate picture of an enzyme's influence in a cell. ABPs contain three common elements; a reactive group, or 'warhead', that covalently reacts with the enzyme's active site, a recognition element that mimics the enzyme's

substrate, and a reporter tag to allow for the visualisation and purification of the probe-enzyme adduct (**Scheme 1.4**). This tag also facilitates the identification of bound proteins through quantitative proteomics. The probes are designed such that when the target enzyme binds to the recognition element of the probe, the warhead is positioned proximal to the active site residue and a covalent bond is formed, typically by nucleophilic attack of the active site residue.



Scheme 1.4: Design and application of ABPs. Probes contain a recognition element that directs binding to the enzyme of interest. The warhead covalently traps the enzyme upon binding and the tag facilitates downstream analysis.

1.3.1 Monoubiquitin based probes

Probes targeting DUBs that use a monoubiquitin recognition element have been successful in the identification and characterisation of new DUB family members,⁶⁷ helping in crystallisation studies of DUBs⁶⁸ and evaluating inhibitors for these enzymes.⁶⁹ The first example of an ABP targeting DUBs consisted of a vinyl sulfone warhead in place of the C-terminal Gly 76 residue of ubiquitin (**Figure 1.1A**).⁷⁰ The Michael acceptor of the vinyl sulfone is positioned such that the site of attack is equivalent to that on the natural substrate of DUBs, a ubiquitin-protein conjugate. Many subsequent probes follow this same pattern, positioning an electrophilic warhead to mimic the site of attack on the natural substrate. The vinyl sulfone probe was synthesised using a transpeptidation approach and since then a variety of thiol-reactive electrophiles have been reported. Lactone⁷¹ and alkyl halide⁶⁷ based warheads are two further examples of probes that work *via* nucleophilic attack (**Figure 1.1B and C**). The vinyl methyl ester (VME) warhead (**Figure 1.1D**) has the same reactivity as the vinyl sulfone, labelling DUBs *via* conjugate 1,4-addition.⁶⁷

Unexpectedly, propargyl amide groups (**Figure 1.1F**) were found react with the active site Cys by direct 1,2-addition to form a vinyl thioether.⁷² Crystal structure

experiments confirmed the formation of a vinyl thioether with the active-site Cys of DUBs. This was explained by stabilisation of the unfavourable vinylic anion intermediate formed during the labelling by acidic residues within the nearby oxyanion hole. More recently, a disulfide probe (**Figure 1.1G**) capable of reversibly labelling DUBs by a thiol-specific exchange reaction was described.⁷³

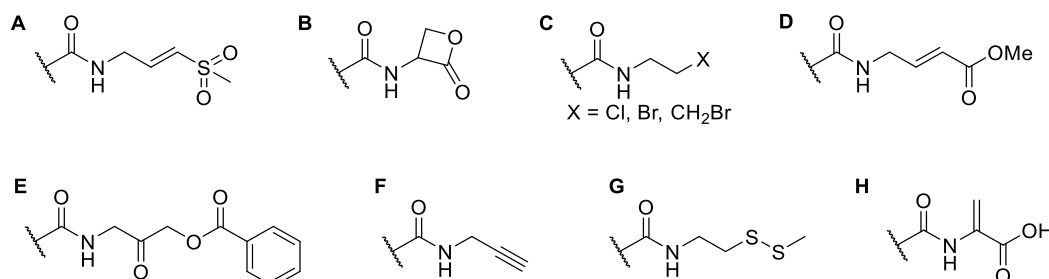


Figure 1.1: A selection of warhead structures targeting the Cys protease DUBs.

An alternative strategy towards monoubiquitin ABPs uses the random mutation of wild-type (WT) ubiquitin followed by a phage display assay to examine the effects of these mutations on the binding affinity between ubiquitin and DUBs and select for those that improve binding.⁷⁴ The method was originally developed to inhibit or enhance DUB activity through endogenous expression of such ubiquitin mutants. Certain mutations resulted in class specific ubiquitin variants and several of these DUB classes and some of the conjugation machinery have been targeted in this manner.⁷⁵⁻⁷⁸ The methodology was extended to ABPs by *Gjonaj et al.* who functionalised these mutants with tags and warheads to generate USP7 selective probes using some of the previously developed ubiquitin variants along with novel variants made using computational models as starting points.^{74,75,77,79} The probes consisted of a C-terminal alkyne warhead along with an N-terminal rhodamine dye. This strategy is limited as although some mutations enhance binding affinity, they appear to alter the position of the C-terminus when the probe is bound to a DUB, and this influences the covalent capture of the enzyme.⁷⁹

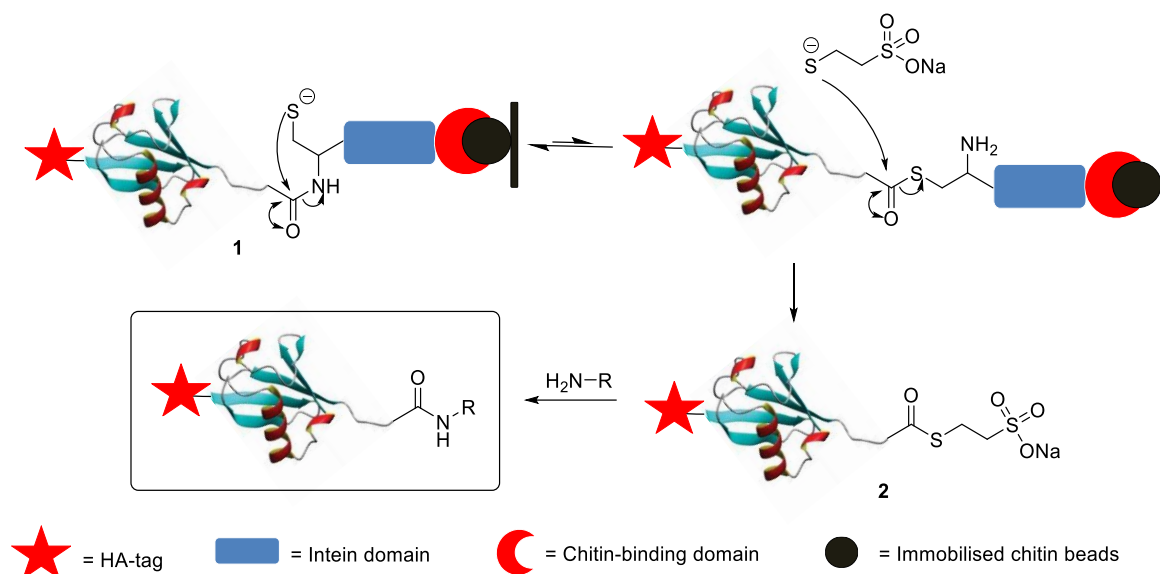
Interestingly, certain warheads also show reactivity towards the ubiquitin conjugation machinery as well as DUBs.⁷¹ The majority of enzymes also employ an active site Cys and are ATP dependent.¹² One example of a ubiquitin-based ABP designed to target these enzymes is the Ub₇₅-dehydroalanine (Dha) probe reported by Mulder *et al.* (**Figure 1.1H**).⁸⁰ This probe contains the unnatural amino acid Dha at its C-terminus. Like WT-ubiquitin, the Ub₇₅-Dha probe can travel down the ubiquitin cascade through a series of transthioesterification reactions following

conjugation to ADP in the active site of an E1 enzyme. At each step the probe can trap the enzyme *via* nucleophilic attack of the Michael acceptor in the Dha residue or be processed as normal *via* cleavage of the peptide bond.

Using a NCL approach, ubiquitin probes have been generated by fragment based approaches and total synthesis using Fmoc solid-phase peptide synthesis (SPPS).⁸¹⁻⁸³ One such approach developed by Erlich *et al.* demonstrated that the synthesis of ubiquitin analogues could be achieved starting from two peptide fragments.⁸¹ An Ala46Cys mutation in the N-terminal fragment facilitated NCL of the two fragments and a C-terminal *N*-methylcysteine was then converted to a thioester under acidic conditions. Amines functionalised with reactive groups were coupled to this thioester to afford the final probe. The total synthesis of C-terminal ubiquitin analogues using NCL has been achieved using a chlorotrityl resin.⁸³ The mild conditions required to cleave peptides from this resin meant that a ubiquitin peptide with all protecting groups intact was cleaved and the free C-terminus was coupled selectively to the desired nucleophile. Global deprotection using trifluoroacetic acid (TFA) provided the desired probe.

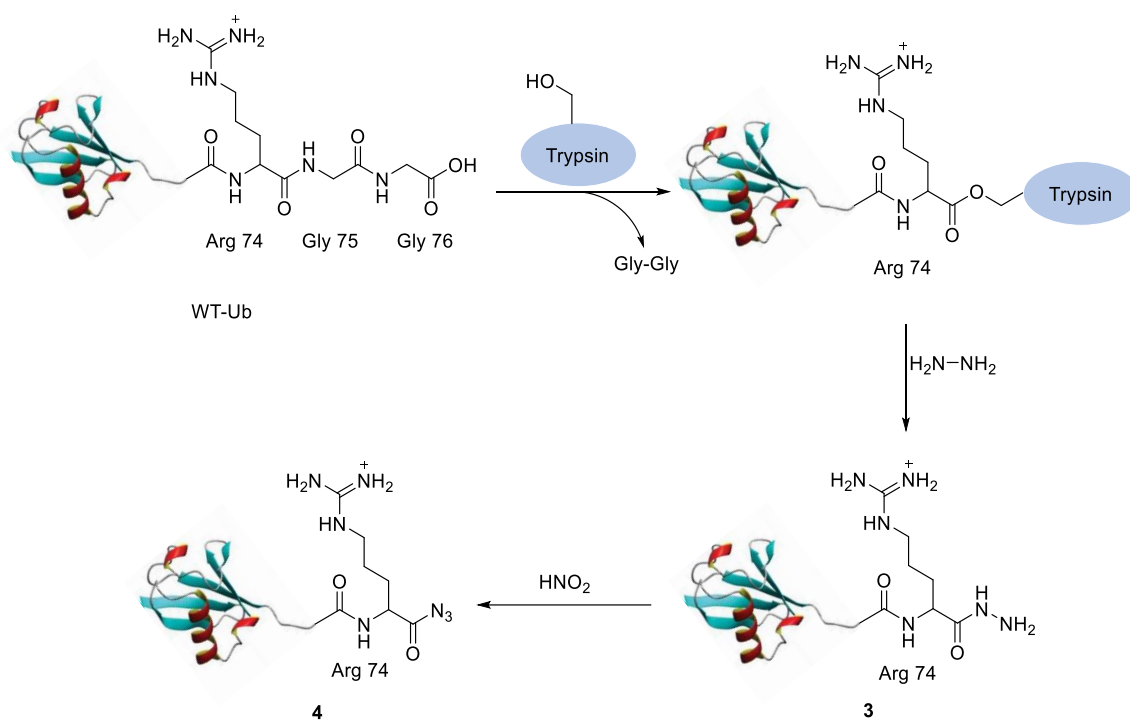
In addition to NCL, other enzymatic and semi-synthetic methods have been used to synthesise these monoubiquitin probes. A common semi-synthetic method for monoubiquitin probe preparation starts by expressing a fusion protein containing an intein and chitin-binding domain (CBD) **1** and proceeds *via* a reactive thioester **2** (**Scheme 1.5**).⁶⁷ Inteins are protein motifs which are observed across several organisms and act as auto-processing domains that post-translationally modify proteins *via* splicing events.⁸⁴ The splicing typically involves the cleavage of two peptide bonds, the excision of the intein domain and the ligation of the two flanking extein sequences. The process is spontaneous and requires no external driving force other than the correct folding of the domain. These domains have been repurposed to facilitate tagless protein purification.⁸⁵ An Asp to alanine (Ala) mutation results in a trapped equilibrium forming between an amide and thioester bond at the N-terminus of the intein (**Scheme 1.5**). An affinity binding domain is usually included C-terminally to the intein domain that immobilises the construct on a column. At this point other proteins are removed by affinity purification. Following purification, base is added to induce hydrolysis of the thioester or alternatively, cleavage can be induced through the attack of a nucleophile. In the context of monoubiquitin probes, addition of sodium 2-mercaptoethanesulfonate (MESNa) to

induce thiolysis is most commonly employed (**Scheme 1.5**).⁶⁷ The resulting thioester **2** can be reacted with an amine warhead which replaces the C-terminal glycine, providing an efficient and convenient method to obtain a monoubiquitin probe.



Scheme 1.5: Formation of a reactive HA-ubiquitin-thioester 2 on an immobilised chitin column by MESNa-mediated thiolysis. The protein construct is expressed in bacteria consists of HA-ubiquitin without the C-terminal glycine residue (Ub_{75}), an intein domain and a CBD. The construct can be purified on an immobilised chitin column and then eluted as the reactive thioester following MESNa induced thiolysis.

Transpeptidation is an enzymatic strategy used for the synthesis of monoubiquitin ABPs (**Scheme 1.6**). When the tertiary structure of ubiquitin is retained, the only site efficiently cleaved by trypsin is Arg 74, resulting in the release of the final two Gly residues.⁸⁶ This knowledge was used to design an approach to synthesise ubiquitin reagents such as the fluorogenic Ub-7-amido-4-methyl coumarin (UbAMC) probe before being adapted to make ABPs.^{70,87-89} The method adapted for ABP synthesis starts with the treatment of ubiquitin with trypsin followed by the addition of excess hydrazine to promote proteolysis to $Ub_{75}-NHNH_2$ **3** (**Scheme 1.6**).⁷⁰ Oxidation with nitrous acid leads to the formation of $Ub_{75}-N_3$ **4** and the final probe is formed by coupling $Ub_{75}-N_3$ **4** to a Gly residue conjugated to the desired warhead. The reactivity of E2 enzymes has been used in a similar way to generate ubiquitin modified C-terminally with small molecules or whole proteins, although it has not yet been used to synthesise ABPs.⁹⁰



Scheme 1.6: Transpeptidation approach towards the synthesis of monoubiquitin ABPs.

1.4 Advances in the application of DUB ABPs

1.4.1 Mass spectrometry-based techniques using DUB ABPs

Several studies have effectively demonstrated the power of monoubiquitin DUB ABPs by coupling their use with advanced proteomic techniques. Hewings *et al.* developed an enhanced chemoproteomic technique using an on-bead digest protocol that not only allowed for comprehensive identification of captured DUBs, but also permitted precise identification of the labelled residues.⁹¹ Probe labelling of the active-site Cys for multiple DUBs was confirmed as well as unexpected off-target labelling of non-catalytic Cys residues within active sites. The results of this study provided a valuable insight into the promiscuity of monoubiquitin ABPs and provides further opportunities for the identification of the reaction sites of covalent molecules. A total of 61 DUBs were identified in this study, which was the most comprehensive study at that time. Furthermore, a novel DUB class, ZUFSP, was identified in this study and its chain selectivity was assessed.

More recently, Pinto-Fernandez *et al.* performed an even larger study of DUB activity using the haemagglutinin (HA)-tagged probes HA-Ub₇₅CH₂CH₂Br **5** and HA-Ub₇₅-PA **6** (Figure 1.2).⁹² An extended chemoproteomic workflow identified 74

DUBs and was able to distinguish between enzyme isoforms. This was achieved by incorporating an additional high-pH fractionation step prior to analysis by LC-MS/MS. This extra step reduced sample complexity, resulting in a 92% increase in the number of DUBs observed relative to existing ABPP workflows using the same equipment.

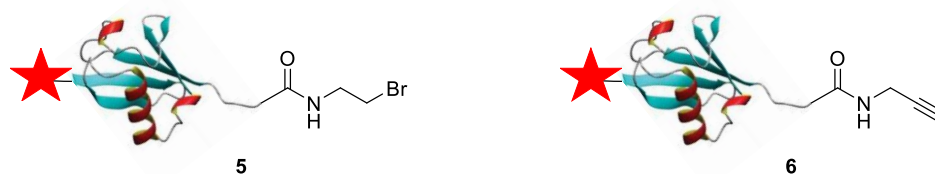


Figure 1.2: Structure of ABPs used for in studies by Pinto-Fernandez *et al.*⁹²

Comparative transcriptomic experiments looking at the presence of DUB-associated mRNA demonstrated the value of this methodology, with certain DUBs only detected at the mRNA level while others were only found as proteins. These results suggest distinct regulatory pathways are at play at both these levels, confirming that using ABPs provides distinct and valuable information relative to transcriptomic analysis. This study provides a framework for future analysis of DUBs and small molecules targeting these enzymes as the number of DUBs detectable was equivalent to the DUBs known to be expressed in the examined cell lines. Analysis is therefore more accurate and provides a more complete picture of the activity of the DUBome.

1.4.2 Cell permeable DUB ABPs

The large size of ABPs incorporating a ubiquitin recognition element means that they are generally cell impermeable. This is limiting as cell lysis is known to impact protein function. Upon cell lysis, protein-protein interactions, which are known to be important to DUB function, are affected and ubiquitination patterns have been observed to change.^{91,93,94} Efforts have therefore been made to enable the use of these probes in more physiologically relevant systems. One way this has been addressed is by using pore-forming toxins. The first example of this by Claessen *et al.* employed perfringolysin O (PFO) which is known to bind to cholesterol and form large pore complexes (**Figure 1.3B**).⁹³ Used in combination with a ubiquitin ABP, this facilitated its transport across the cell membrane and a comparative study of DUBs in chlamydia-infected HeLa cells was carried out.

Electroporation is generally used for transfecting impermeable small molecules or DNA into cells.^{95,96} It creates transient micropores on the surface of a cell, meaning it can be used in the same way as the pore forming toxins but with less impact on cell viability (**Figure 1.3B**). Its use for ubiquitin ABPs was first reported by Mulder *et al.* when examining the activity of their Ub₇₅-Dha probe (**Figure 1.1H**).⁸⁰

More recently, the Zhuang group incorporated a variety of cell-penetrating peptides (CPPs) into existing DUB probes (**Figure 1.3A and B**).⁹⁴ The CPPs were conjugated by a disulfide bond, meaning once inside the reducing environment of the cell the CPP is cleaved from the probe. Uptake of these ABPs was visualised using fluorescent tags in combination with live-cell fluorescent confocal microscopy. Alternative HA-tagged probes permitted immunoblotting and affinity purifications for quantitative mass spectrometry. Interestingly, the results obtained by these measures were different to those observed in equivalent cell lysate labelling experiments, demonstrating the importance of accessing tools to study these enzymes in more physiologically relevant systems. Furthermore, some of the DUBs identified in whole cells are known to localize to specific organelles, suggesting that the probe can permeate different sub-cellular compartments.

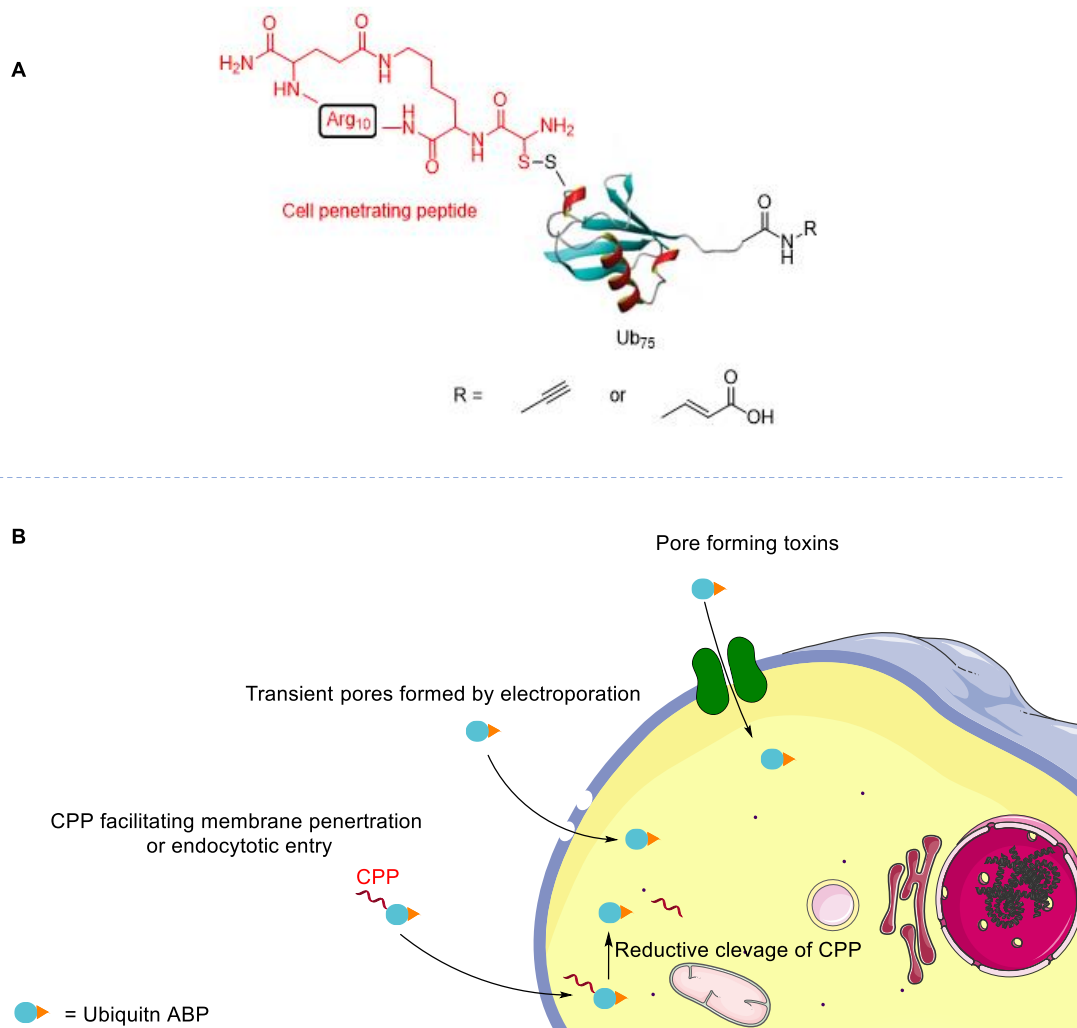


Figure 1.3: Methods to facilitate ubiquitin ABP transport into whole cells. (A) Structure of ubiquitin ABP conjugated to a cell peptide. (B) Methods to profile DUB activity in whole cells using ABPs with ubiquitin recognition elements.

1.4.3 Small molecule DUB ABPs

Probes using ubiquitin recognition elements offer a convenient scaffold to selectively target DUBs and they have provided significant advances in the understanding of DUB biology. However, as discussed, their size means they are generally cell impermeable. Their use is therefore limited to cell lysate or with recombinant enzymes unless they are used in combination with the methodologies previously discussed. To provide an alternative to these techniques, significant efforts have been made to develop small molecule DUB ABPs. These molecules are cell permeable and therefore offer a powerful alternative to the existing ubiquitin-based probes.

The first example of this type of probe was adapted from a compound that was initially identified as a potent USP4 and USP11 inhibitor by high-throughput screening.⁹⁷ The original chloroacetylpyrrole scaffold was furnished with an alkyne handle to afford the ABP **7** (**Figure 1.4**) which was demonstrated to label twelve DUBs in live U2OS cells. Unsurprisingly, this probe demonstrated increased off-target labelling relative to probes with a ubiquitin scaffold but it represented a significant advance as a tool to study DUB inhibitors in whole cells.^{91,97} This was validated by experiments showing that the parent molecule could compete for binding with the ABP **7** in a concentration dependent manner with several DUBs.

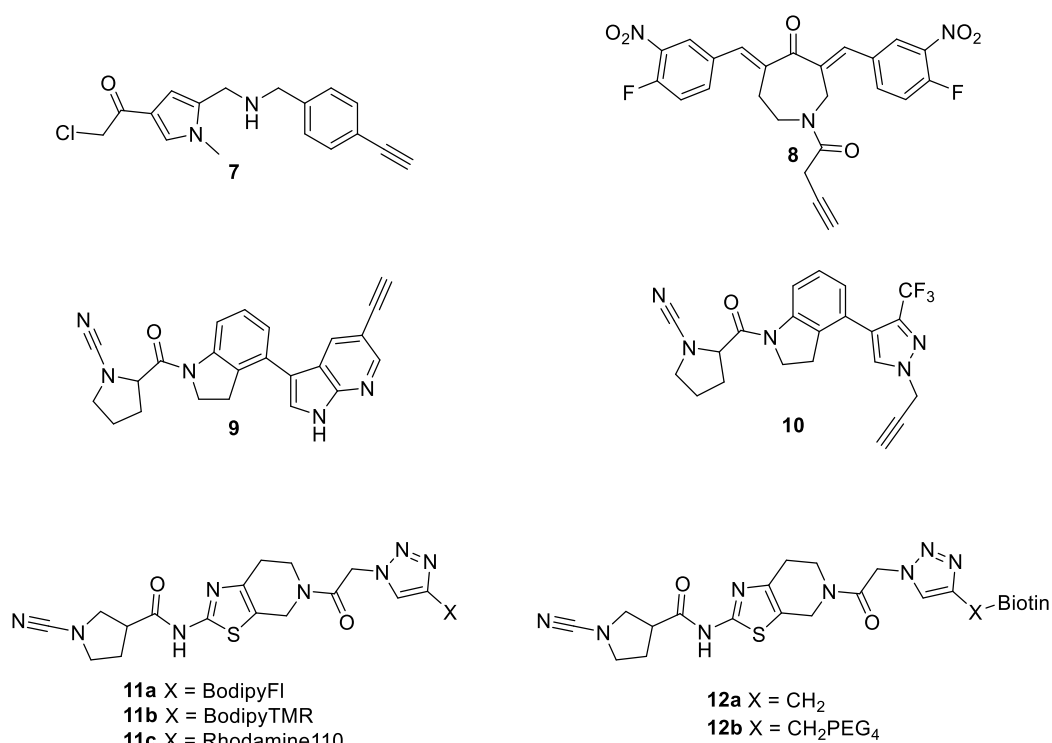


Figure 1.4: Structures of small molecule DUB ABPs.

A similar approach was taken to equip a small molecule USP14 inhibitor with an alkyne handle affording the probe **8** (**Figure 1.4**).⁹⁸ However, this probe was found to be even more promiscuous than the previous small molecule probe **7**, causing protein aggregation and affecting cell viability. UCHL specific probes designed using the same concept have been more successful. One example, IMP-1710 **9** (**Figure 1.4**), was based on a cyanopyrrolidine scaffold known to covalently inhibit UCHL1.⁹⁹ This scaffold was functionalised with an alkyne handle to make a highly selective ABP for UCHL1. Only the S-enantiomer of the probe was bound by the

enzyme. The value of these cell permeable probes was demonstrated by using this IMP-1710 probe **9** to show that the previously reported UCHL1 inhibitor LDV-57444 is not bound by UCHL1 in whole cells. A closely related probe **10** based on a similar cyanopyrrolidine skeleton was reported more recently but was significantly less potent than IMP-1710 **9** and less specific (**Figure 1.4**).¹⁰⁰

Geurink *et al.* also employed a cyanopyrrolidine scaffold in the design of fluorescently labelled and biotinylated derivatives of UCHL1 specific probes **11a–c** and **12a–b** respectively (**Figure 1.4**).¹⁰¹ These derivatives were strongly selective for UCHL1 over other DUBs but some off-target labelling was observed with PARK7, a human deglycase, limiting its utility relative to the original IMP-1710 probe **9**.

1.5 Ubiquitin conjugate probes targeting DUBs

Probes incorporating a monoubiquitin recognition element are extremely useful research tools that provide valuable information about global DUB activity.^{91,92} In addition to the small molecule probes which demonstrate specificity, a generation of ubiquitin-conjugate probes was developed to allow for more focused investigations of DUB activity.¹⁰² These probes target subsets of the ubiquitin conjugation/deconjugation machinery to help elucidate enzyme specificity. They provide a more precise picture of enzyme activity compared to the existing monoubiquitin probes. Ubiquitin conjugate probes were designed using the knowledge that DUB specificity is largely mediated by the C-terminal adduct or substrate protein proximal to the ubiquitin, as well as the linkage type in cases where the substrate is a polyubiquitin chain (**Figure 1.5A**). In ABPs, the isopeptide bond is replaced by a linker containing a reactive group (**Figure 1.5B**).

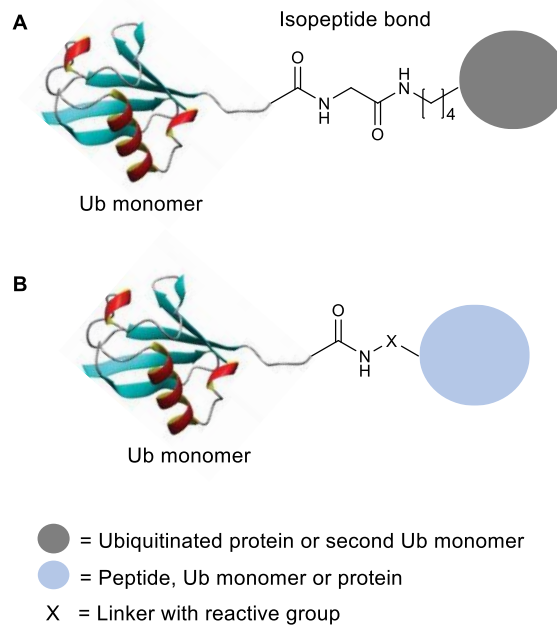


Figure 1.5: Structure of (A) WT ubiquitinated protein or ubiquitin dimer (B) Ubiquitin probes resembling these WT conjugates.

1.5.1 Ubiquitin peptide probes

The first probes using this concept were designed by Iphöfer *et al.* and consisted of ubiquitin monomers conjugated to peptides mimicking certain ubiquitin linkages **13** (**Figure 1.6**).¹⁰³ Sequences mimicking the regions around Lys 48 and Lys 63 were tested, and a lower number of enzymes were captured relative to the existing Ub₇₅-VME probe (**Figure 1.1D**). Further examples of Ub-peptide probes **14** were synthesised using selenocysteine (SeCys) ligation (**Figure 1.6**).¹⁰⁴ The peptide used was centred around the Lys 117 residue of the TRIM25 protein, a known ubiquitination target that is specifically bound by USP15. Deselenisation furnished the probe **14** with a Dha residue by in place of the Gly 76 which acted as the electrophilic trap.

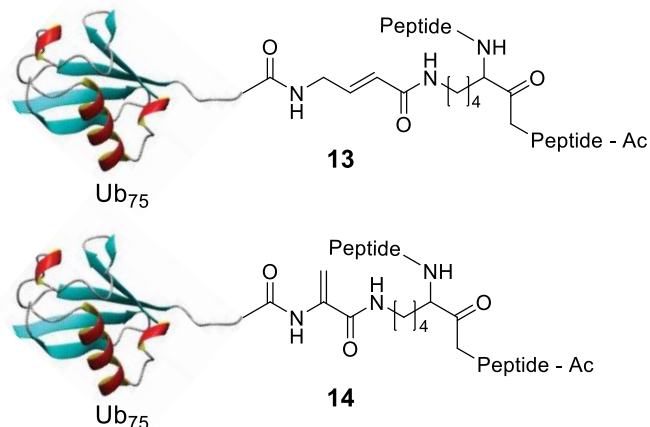


Figure 1.6: Structures of reported Ub-peptide probes.

1.5.2 Diubiquitin ABPs

In addition to the ubiquitin-peptide conjugates, probes consisting of a diubiquitin recognition element have also been developed. Several full length diubiquitin probes were synthesised by McGouran *et al.* (**Figure 1.7A**).¹⁰⁵ All eight linkage types were successfully mimicked, allowing for quantification of DUB selectivity. Another approach to diubiquitin probe synthesis centred around a linker containing an acetal-protected Michael acceptor (**Figure 1.7B**).¹⁰⁶ Acetal deprotection in the final step of the synthesis unmasked a Michael acceptor which functioned as the electrophilic warhead in the probe **16**.

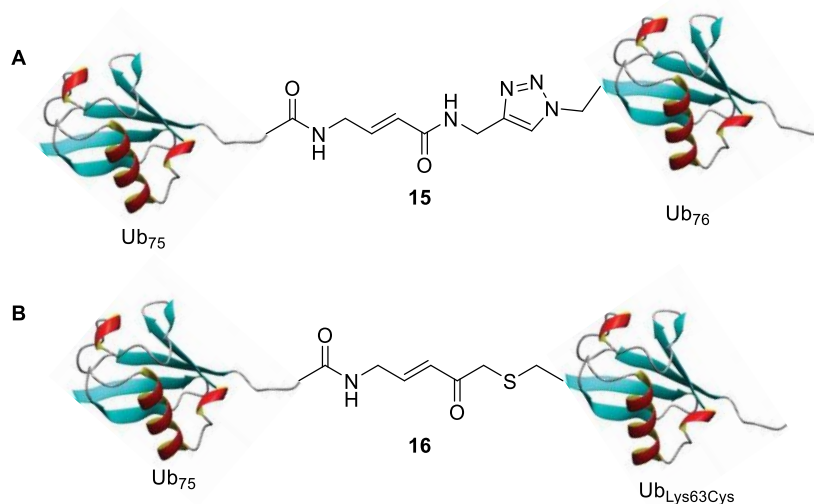


Figure 1.7: Structures of selected ABPs with diubiquitin recognition elements.

Since then, several other ABPs consisting of diubiquitin recognition elements have been synthesised (**Figure 1.8**). They mostly follow the same design with a warhead

positioned between the two ubiquitin monomers. The traps employed are also very similar to the Michael acceptors used in monoubiquitin probes and the first diubiquitin probes, with some using the unnatural amino acid Dha for this purpose (**Figure 1.8A**) and others a vinyl amide (**Figure 1.8B**).¹⁰⁷⁻¹⁰⁹ All diubiquitin probes demonstrated increased DUB selectivity, but only probe **19** synthesised by Weber *et al.* was completely selective for a single class of DUB (**Figure 1.8C**).¹⁰⁹ The probe synthesis followed a similar route to probe **17**, once more using unnatural amino acid DHA as a reactive warhead. This probe structure was selectively bound by OTULIN in cell lysate.¹⁰⁹ Diubiquitin ABPs following this design have significantly enhanced the understanding of DUB linkage selectivity¹¹⁰ and aided in the identification and characterisation on new DUB families.¹¹¹

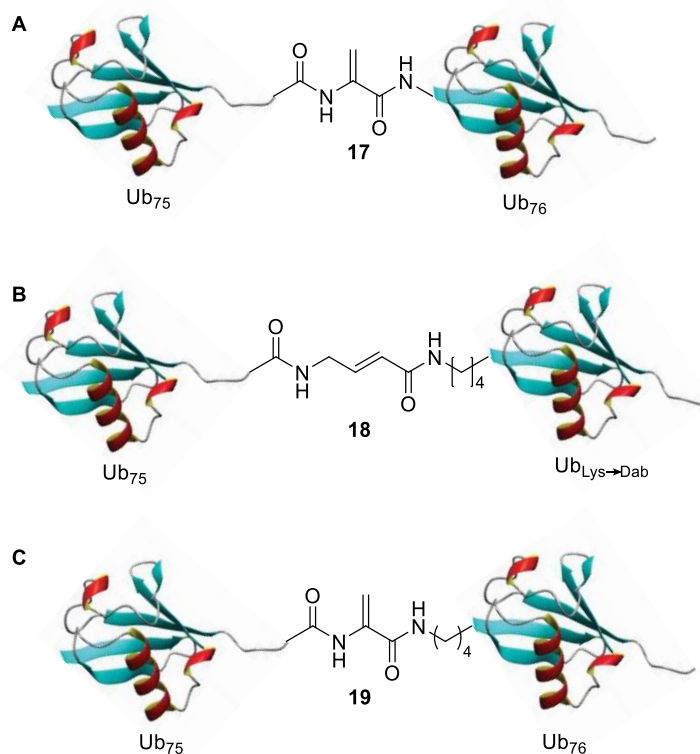


Figure 1.8: Structures of selected ABPs with diubiquitin recognition elements.

All diubiquitin probes discussed thus far probe the S1'-S1 pockets of DUBs, with the warhead positioned between the two ubiquitin components. Flierman *et al.* designed the probe **20** which positioned the warhead proximal to the second ubiquitin monomer, to probe the S1-S2 pocket of DUBs (**Figure 1.9**).¹¹²

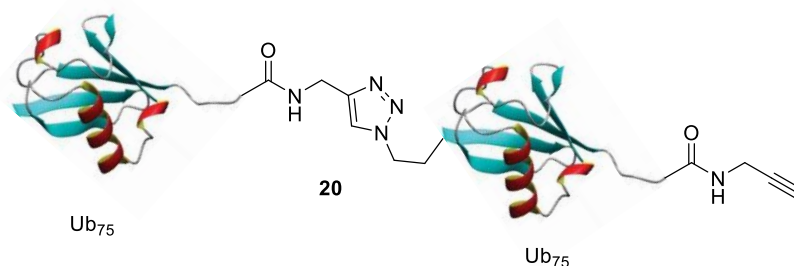


Figure 1.9: Structure of the ABP S1-S2 pocket of DUBs with a diubiquitin recognition element reported by Flierman *et al.*¹¹²

Additionally, Paudel *et al.* synthesised a probe with a triubiquitin recognition element (**Figure 1.10**). The probe **21** consisted of a native isopeptide bond between the proximal and central ubiquitin and the warhead positioned between the central and distal monomers.¹¹⁰

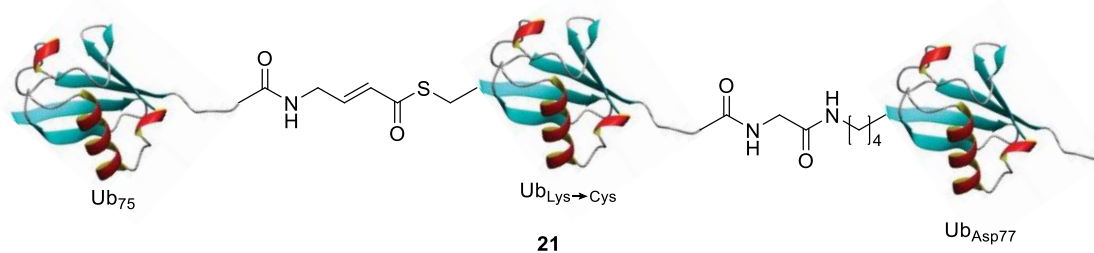


Figure 1.10: Structure of the ABP with a triubiquitin recognition element reported by Paudel *et al.*¹¹⁰

1.5.3 Ubiquitin-protein conjugate probes

To further examine DUB specificity, similar methodologies were employed for probes with ubiquitin conjugated to other protein substrates (**Figure 1.11**). As an extension to their Dha based methodology, Meledin *et al.* designed a probe, **22**, based on ubiquitin conjugated to α -globin (**Figure 1.11A**).¹¹³ The final probe **22** mimicked a ubiquitin- α -globin conjugate with a Dha electrophilic trap between the two proteins. Another probe, **23**, followed a similar principle using Dha as an electrophilic trap and the Zhuang lab reported a probe, **24**, using a Michael acceptor between ubiquitin-PCNA. (**Figure 1.11B and C**).^{114,115} The value of these probes was best demonstrated in studies that demonstrated differing DUB specificity for the ubiquitin-PCNA probe **24** relative to diubiquitin ABPs.¹¹⁵

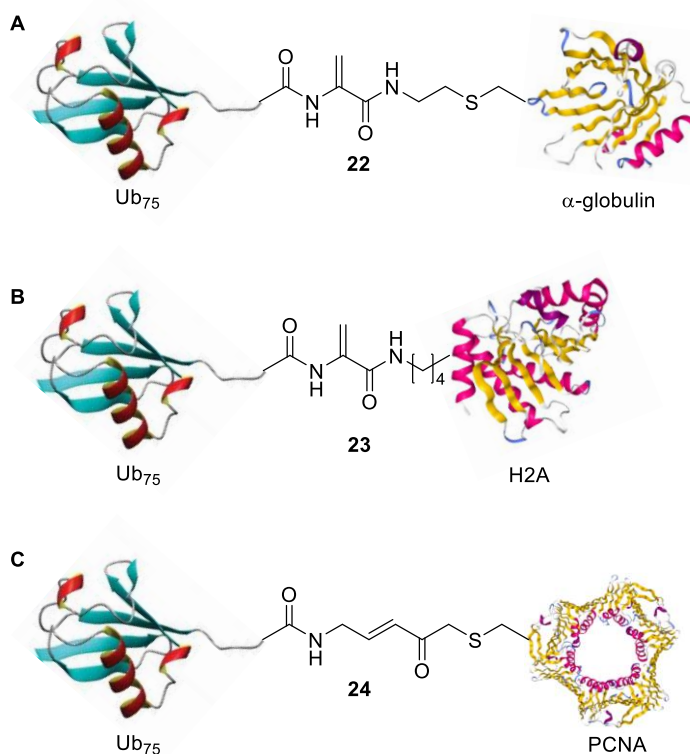


Figure 1.11: Structures of selected ABPs with a ubiquitinated protein as the recognition element.

1.6 Probes for Ubiquitin Conjugation Machinery

Monoubiquitin probes have been demonstrated to label members of the ubiquitin conjugation machinery but they lack specificity.^{71,72,116-119} To broaden the understanding of the complete ubiquitination process, probes targeting members of the ubiquitin conjugation machinery analogous to those targeting DUBs have been developed. The design of these probes followed the same concept of adding groups to the C-terminus to a ubiquitin monomer to make a recognition element targeting specific members of the ubiquitin cascade.

1.6.1 Ubiquitin-adenine probes

The ubiquitin cascade begins with the formation of a high energy ubiquitin-adenylate intermediate within the active site of an E1 enzyme.¹²⁰ Lu *et al.* hypothesised that mimicking this adenylyate intermediate would provide a probe specific for E1 enzymes.¹²¹ A Ub₇₁-thioester was coupled to a modified C-terminus containing an electrophilic trap in place of Gly 74 and a 5'-sulfonyl-adenosine-based modification using NCL to afford the probe **25** (Figure 1.12A). A second E1 specific probe **26** was synthesised by An *et al.* once more using NCL (Figure 1.12B).¹²² A Dha residue

functioned as the electrophilic trap and although the design lacks a phosphate mimic, potentially reducing binding affinity, covalent labelling was observed with UBA1 in recombinant enzyme experiments.

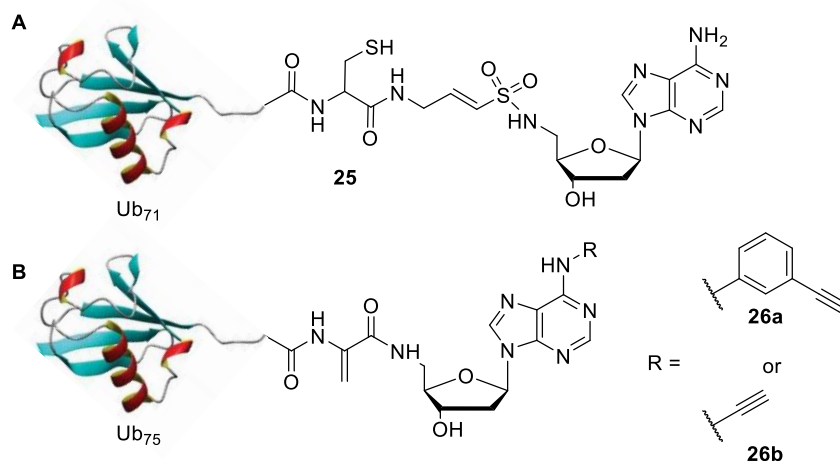


Figure 1.12: ABPs resembling the ubiquitin-adenylate intermediate of the ubiquitin cascade to target E1 enzymes.

Using the knowledge that transthioesterification occurs between E1 and E2 enzymes within the ubiquitin cascade, an alternative probe design using an E2 enzyme as the recognition element was proposed. Stanly *et al.* used tosyl-substituted doubly activated ene (TDAE) compounds to enable sequential functionalisation of two thiols at a single carbon centre and profile E1 activity by studying this transthioesterification step (**Figure 1.13A**).¹²³ In this example, the single Cys residue of the E2 UBE2N was reacted with a TDAE for probe **27** (**Figure 1.13B**). Labelling of E1 UBA1 was observed using the modified E2 probe and this was enhanced by co-incubation with WT ubiquitin and ATP. Endogenous UBA1 was selectively labelled in HEK293T lysate.

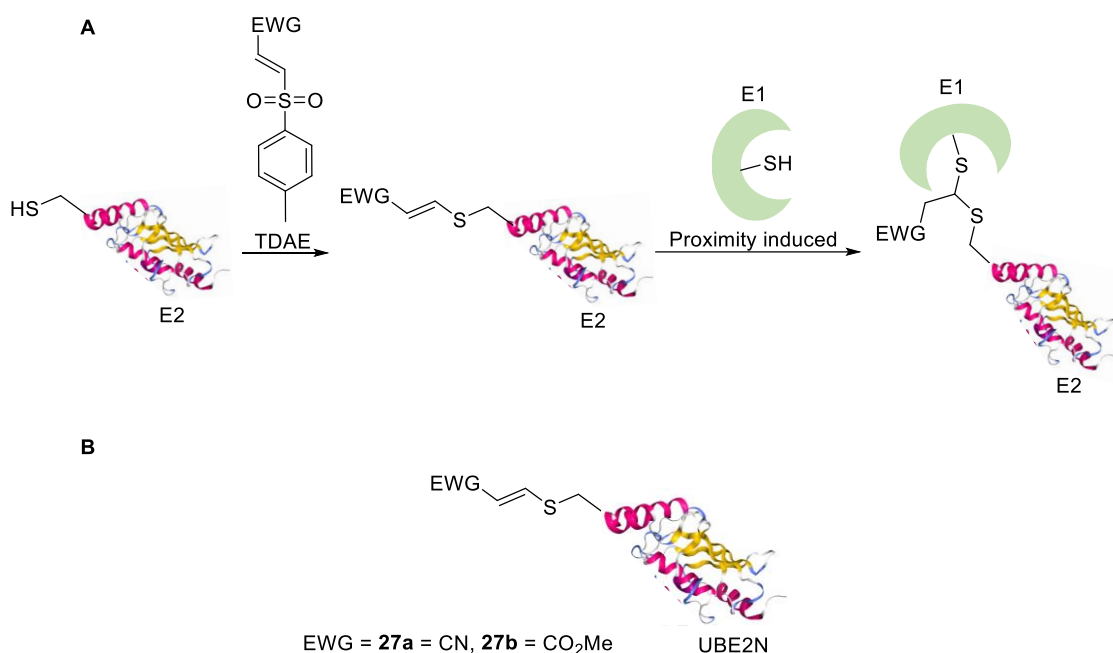


Figure 1.13: Using TDAEs to generate E1 targeting enzymes. (A) Strategy for the formation of ABPs using TDAEs and subsequent binding dependent labelling reaction. (B) Structure of the ABP **27** with an E2 recognition element and warhead formed in reaction with a TDAE reported by Stanly *et al.*¹²³

1.6.2 Ubiquitin-protein Probes for E3 ligases

The concept of the TDAE probes was elaborated upon to create a probe specific for the E3 ligase Parkin (**Figure 1.14A**).¹²³ Two alkyne functionalised acrylate and acrylamide TDAEs were prepared and coupled to ubiquitin monomers. A single Cys mutant of His-UBE2L3 was reacted with the TDAE functionalised monomers to form the final probes **28a–b**. The active-site Cys of Parkin covalently reacted with both probes which were both unreactive with recombinant DUBs. A similar probe **29** consisting of a ubiquitin conjugated E2 enzyme was developed by Xu *et al.* with a Dha residue incorporated as the electrophilic trap (**Figure 1.14B**).¹²⁴ The probes enriched for several E3 enzymes following a reaction in HeLa cells.

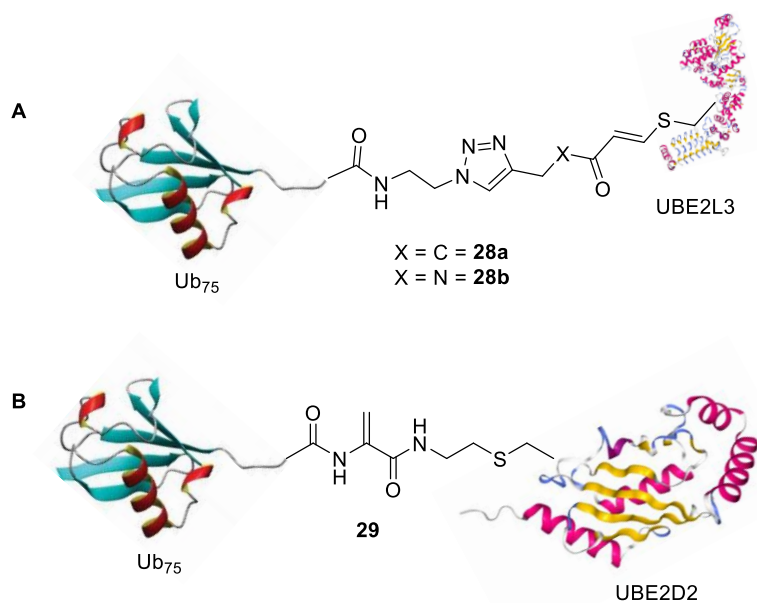


Figure 1.14: Structures of selected ABPs with a ubiquitin-E2 recognition element.

1.7 Radical chemistry in biological systems

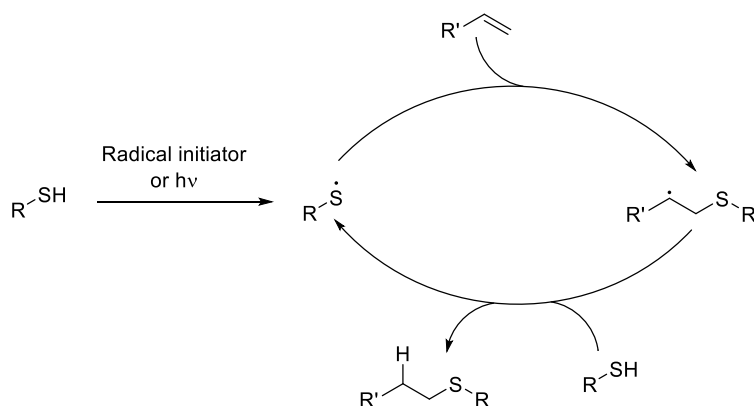
Free radicals are involved in several essential processes in cells including combating pathogens and in cell signalling pathways.¹²⁵ In biological systems, they are generated primarily by electron transfer reactions, but they can also be generated by the direct cleavage of bonds. Such radicals can be generated within the highly controlled environment of an enzyme's active site, by normal oxidative metabolism or alternatively as a result of exogeneous agents such as γ -radiation and ultraviolet (UV) light.¹²⁶⁻¹²⁸ In most cases these processes result in the formation of short-lived radical anions or cations that react rapidly to form new radical species. As a result, there are several different mechanisms by which a variety of radical species and oxidants are formed. The best studied of these are reactive oxygen species (ROS), most notably, peroxide radicals, superoxide radicals and hydroxyl radicals.¹²⁵ In addition to their importance in the previously mentioned processes, the uncontrolled release of these oxygen species is often damaging to proteins, DNA or other biomolecules.¹²⁹

Despite their damaging effects in certain circumstances, free-radical reactions are an attractive prospective tool in chemical biology research for several reasons. They are compatible with aqueous environments and tend to be highly efficient. Free-radical reactions also allow for significantly more temporal control when

compared to other biorthogonal reactions. This allows for the controlled release of a reactive species, enabling the bioconjugation reaction to occur on demand.

1.7.1 Cysteine selective radical-mediated bioconjugations

The thiol-ene reaction is a coupling reaction that involves the addition of a thiyl radical to an alkene.^{130,131} This coupling reaction was the first radical reaction used for the photo conjugation of whole proteins.¹³² The reaction proceeds by a radical mechanism following photochemical or thermal induction and usually requires the inclusion of a radical initiator. The resulting product is an anti-Markovnikov-type thioether (**Scheme 1.7**).¹³³

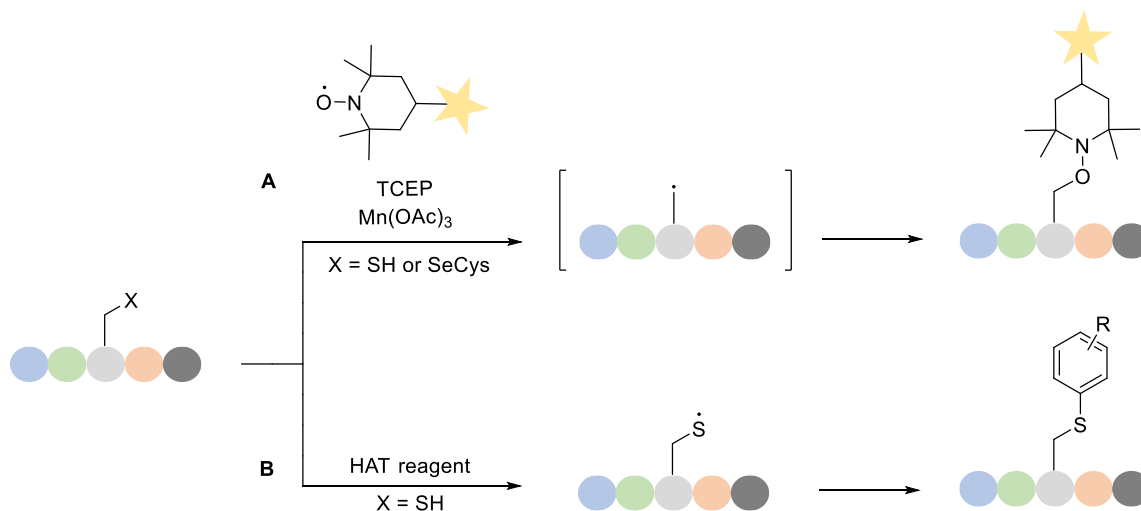



Scheme 1.7: The thiol-ene radical reaction.

Wittrock *et al.* used this reaction to conjugate tumour associated glycopeptides antigens to bovine serum albumin (BSA) due to its compatibility with a wide range of functional groups, and its previously demonstrated efficiency under aqueous conditions.^{132,134} Additionally, the resulting thioether linkage is stable to strong acidic and basic conditions. The coupling reaction was found to proceed efficiently with no observed side-reactions in this case. The resulting thioether linkage was found to not alter the processing of the protein, adding further to the biocompatibility of this reaction.

Subsequently, the thiol-ene reaction has been extensively used in protein chemistry. ‘Biohybrids’ combining synthetic polymers with proteins or amino acids are often synthesised using this technique.¹³⁵ It also remains widely used for selective glycosylation reactions of proteins.¹³⁶ Significantly, the thiol-ene reaction has been used by Valkevich *et al.* to forge an isopeptide bond mimic between two ubiquitin molecules.¹³⁷ The related thiol-yne reaction, in which the alkene functional group is replaced with an alkyne, has also been reported for protein conjugation.^{138,139}

Griffiths *et al.* recently used radical chemistry to target Cys and SeCys residues in a novel way (**Scheme 1.8A**).¹⁴⁰ Using the knowledge that phosphine-mediated desulfurisation and deselenisation pathways used in NCL proceed *via* free-radical processes, a persistent radical species based on 2,2,6,6-tetramethyl-1-piperidine-1-oxyl (TEMPO) was employed as a trapping reagent. This permitted the chemoselective functionalisation of peptides and proteins containing these residues.



 = Handle for further functionaliation

HAT = Hydrogen atom transfer

Scheme 1.8: Radical bioconjugations targeting Cys residues on proteins. (A) and (B) Existing methods targeting Cys residues of whole proteins using radical chemistry.

1.7.1.1 Photocatalysts for visible light-mediated thiyl radical generation

More recently, Cys residues of peptides have also been selectively arylated *via* visible light promoted hydrogen atom transfer (HAT) reactions, using Ni/photoredox complexes,¹⁴¹ palladium reagents¹⁴² or the organic dye Eosin Y (**30**) (**Figure 1.15**).¹⁴³ Of these, only palladium reagents have also been used to perform this conjugation on proteins. The selective generation of radicals upon exposure to visible light is highly desirable for chemical biology applications. Although UV light is widely used for photochemical biotransformations, long exposure times can damage proteins and cause increased ROS production. Compounds that can generate thiyl radicals upon exposure to longer wavelength visible light therefore represent a significant advance.

Eosin Y (**30**) is particularly promising from this point of view. The first reported examples of visible light-mediated generation of thiyl radicals required metal-based catalysts which limits the translation of the methodology to more complex biological systems.^{144,145} Organic photocatalysts are considered more suitable for bioconjugations and the cytocompatibility of Eosin Y (**30**) has already been demonstrated.¹⁴⁶ Shih *et al.*¹⁴³ and Hao *et al.*¹⁴⁴ employed this photocatalyst as the only additive to catalyse thiol-ene reactions in biological systems. Another organic photocatalyst, 9-mesityl-10-methylacridinium tetrafluoroborate (**31**) and the inorganic Bi₂O₃ have also been reported to catalyse visible light-mediated thiol-ene reactions of biomolecules but neither have been applied to proteins thus far (**Figure 1.15**).¹⁴⁷⁻¹⁴⁹

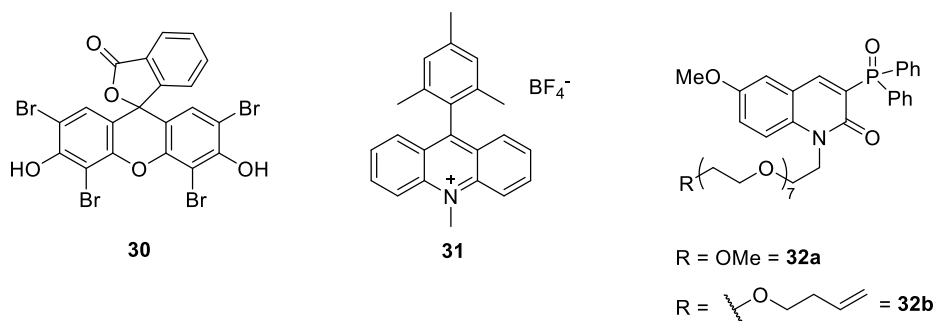


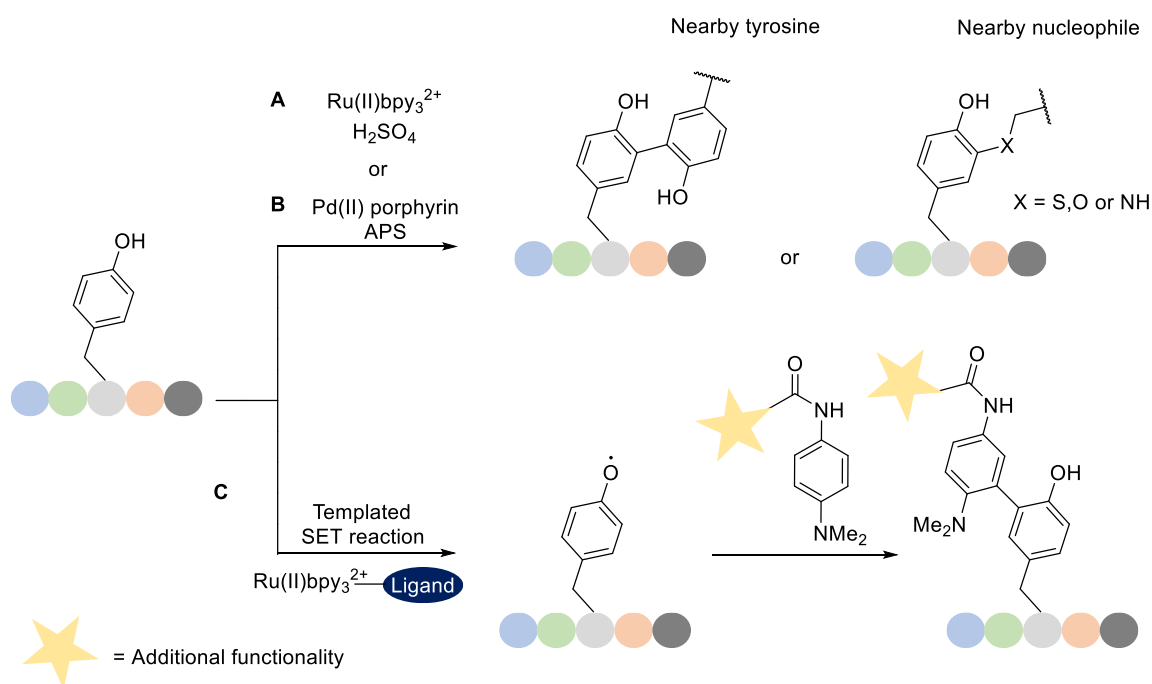
Figure 1.15: Organic photocatalysts used for visible light-mediated thiol-ene reactions.

Choi *et al.* developed an organic photocatalyst **32a** that was demonstrated to catalyse a visible light-mediated thiol-ene reaction (**Figure 1.14**).¹⁵⁰ The catalyst was based on a quinolinone chromophore scaffold. Better yields of the desired conjugate were obtained relative to Eosin Y (**30**) and the methodology was demonstrated to be selective and tolerant of other amino acid side chains. The photocatalyst also exhibited high quantum yields of blue fluorescence in aqueous media. By incorporating a terminal alkene linker into the photocatalyst **32a** to obtain the derivative **32b** (**Figure 1.15**), it catalysed its own conjugation to afford fluorophore labelled biomolecules. However, the catalyst had low solubility in H₂O, so reactions required a high percentage of DMSO or DMF, limiting its applicability to most proteins and in whole cells.

1.7.2 Tyrosine selective radical-mediated bioconjugations

In addition to Cys, the reactivity of other natural amino acids has been exploited for protein crosslinking reactions. Agents capable of oxidising tyrosine (Tyr) residues,

such as ruthenium complexes, have been used to probe protein-protein interactions (**Scheme 1.9A**).^{151,152} By generating tyrosyl radicals at the interface of a protein-protein complex a bond forming reaction can occur and provide valuable information about these interactions. Notably, palladium porphyrin complexes have been demonstrated to catalyse this crosslinking using only visible light (**Scheme 1.9B**).¹⁵² Similar strategies have been employed using ruthenium complexes as single electron transfer (SET) photocatalysts to generate tyrosyl radicals to probe protein-ligand binding interactions (**Scheme 1.9C**).¹⁵³ The ruthenium complexes were conjugated to the ligand of interest and a local SET reaction generated tyrosyl radicals on the binding protein. Tyrosyl radical trapping reagents consisting of an *N*-acyl-*N,N*-dimethyl-1,4-phenylenediamine moiety conjugated to a tag for downstream proteomic analysis were added to the mixture to identify binding proteins.

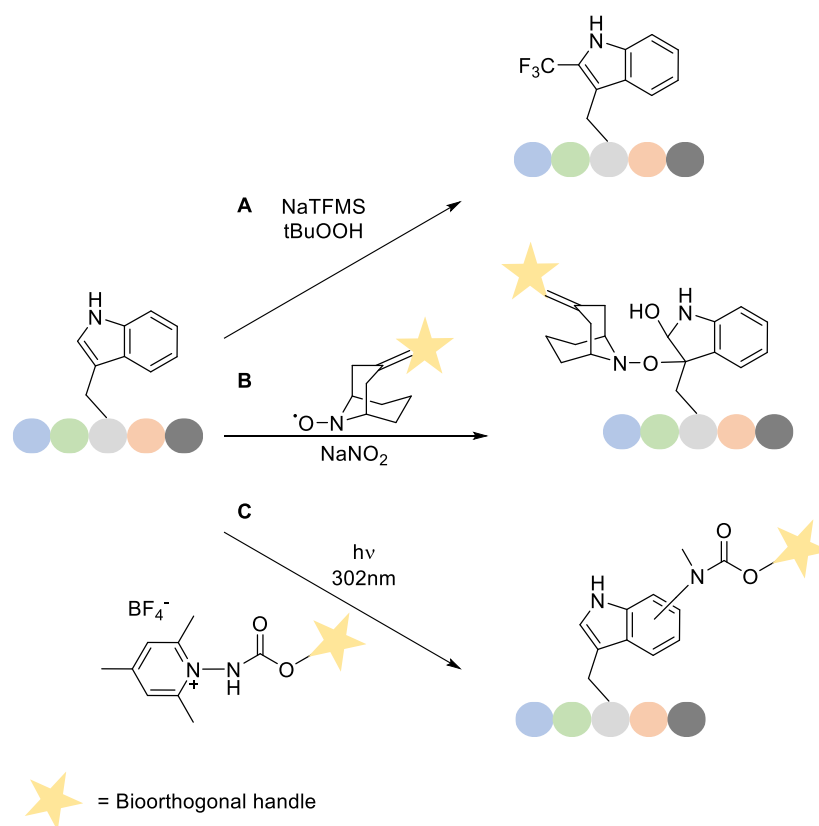


Scheme 1.9: Tyrosine selective radical bioconjugations.

1.7.3 Tryptophan selective radical-mediated bioconjugations

Tryptophan (Trp) has a relatively low natural abundance and a distinct reactivity when compared to other amino acids. It has therefore been the target of numerous residue selective conjugation techniques, including some involving the use of radical chemistry. A radical trifluoromethylation reaction used to conjugate CF_3 to proteins was demonstrated by Sato *et al.* to primarily fluorinate Trp residues, although

reactivity was also observed with Cys and other aromatic residues (**Scheme 1.10A**).¹⁵³ The addition of such groups is useful to add functionality to proteins and monitor them using ¹⁹F NMR. In a separate study, conjugates of the organoradical 9-azabicyclo[3.3.1]nonane-3-one-*N*-oxyl were also shown to be highly selective for Trp conjugation in both peptides and proteins (**Scheme 1.10B**).¹⁵⁴ Seki *et al.* carried out this reaction in aqueous media and required minimal additives.¹⁵⁴ The reaction was elegantly applied to form antibody-fluorophore conjugates which were used in downstream SDS-PAGE analysis with no reduction in antibody binding efficiency.



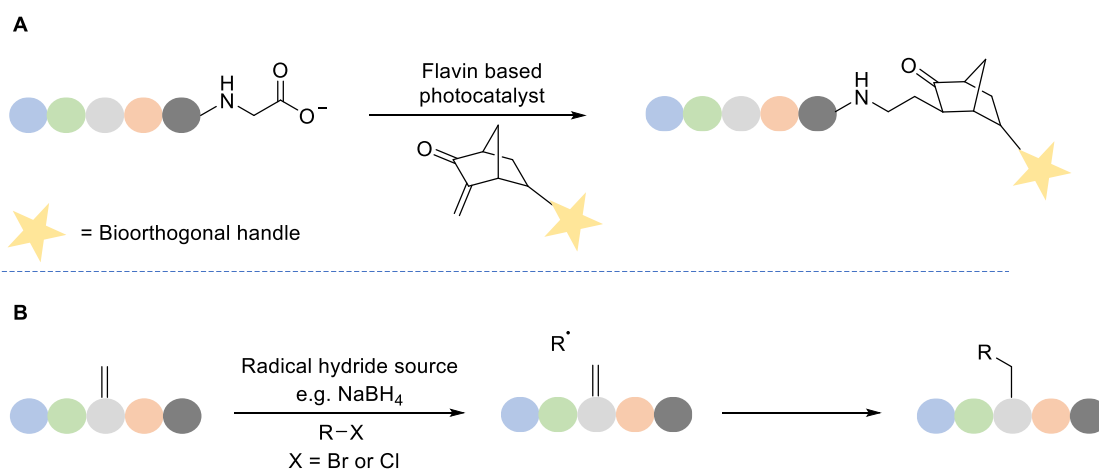
Scheme 1.10: Tryptophan selective radical bioconjugations.

Trp has a known propensity to participate in photoinduced electron transport (PET) reactions.¹⁵⁵ This knowledge was used by Tower *et al.* in the design of *N*-carbamoylpyridinium salts used in a Trp selective conjugation (**Scheme 1.10C**).¹⁵⁶ Various *N*-substituents, including purification tags and linker groups, were linked to the pyridinium salt and ultimately conjugated to the tryptophan residue. It was hypothesised that upon exposure to UV-B light, a PET reaction occurs between the Trp side chain and the pyridinium salt. The N-N bond of the salt undergoes homolytic cleavage following this PET reaction and the

aromaticity of the Katrinsky-type salt is restored. The newly formed nitrogen-centred radical species then participates in a bond forming reaction with Trp. The indole C2 position was the primary site of modification with no detectable off-target labelling in studies using whole proteins.

1.7.4 C-terminal and Dha selective radical bioconjugations

Along with amino acid side chains, the C-terminus of proteins has been targeted for site and chemoselective bioconjugation. Bloom *et al.* used photoredox-catalysed decarboxylation to generate carbon centred radicals that underwent coupling with several electrophilic partners (**Scheme 1.11A**).¹⁵⁷ The C-terminus is more readily oxidised relative to the carboxylates of Asp and Glu side chains and this permits a high degree of selectivity. Flavin based photocatalysts were found to provide the highest alkylation yields and norbornanones bearing bioorthogonal tags gave promising results as radical acceptors. A similar approach that used organic dyes as photocatalysts for the conjugation of alkyne moieties to C-termini has shown promise in the context of peptides but has not yet been applied to proteins.¹⁵⁸



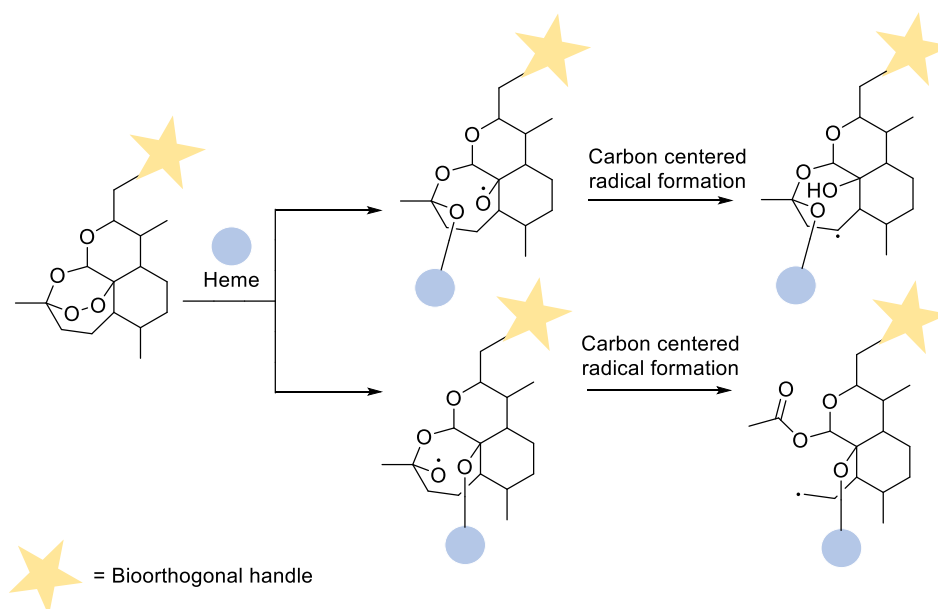
Scheme 1.11: Radical bioconjugation selective for (A) protein C-terminus¹⁵⁷ or (B) Dha amino acids.¹⁵⁹

More recently, radical chemistry was utilised for a biocompatible C-C bond forming reaction by Wright *et al.* (**Scheme 1.11B**).¹⁵⁹ Dha functioned as a protein bound radical acceptor. This provided a highly accessible methodology as Dha is readily installed using a variety of techniques.¹⁶⁰⁻¹⁶³ A range of alkyl halides were employed as radical precursors using various initiators. Remarkably, NaBH₄ was found to be highly effective as a source of hydride radicals. The alkyl radical formed is proposed to participate in a site-selective bond-forming reaction with Dha, forming a carbon

centred radical at the α -carbon of this residue. This is not dissimilar to stabilised radicals that are suggested to form during enzymatic processes.¹²⁹ Several natural and unnatural modifications could be introduced in this way on a variety of proteins scaffolds. These included the addition of polar and non-polar side chains such as cyclo-leucine and citrulline (Cit) to scaffolds including the histones H3 and H4.

1.8 Radicals and other activatable chemistry in ABPP

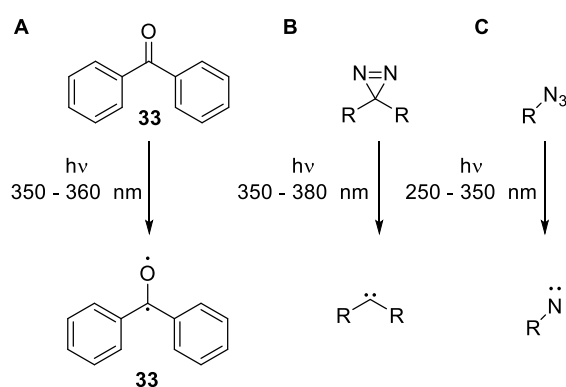
An ABP centred around an artemisinin scaffold was designed by Zhou *et al.* and it worked by a radical labelling mechanism.¹⁶⁴ It was previously established that coordination of haem with the peroxide bridge of artemisinin induces the formation of either a primary or secondary carbon-centred radical that non-specifically crosslinks the artemisinin to proximal residues (**Scheme 1.12**).¹⁶⁵ Using this knowledge, the artemisinin-based probe was incubated in cell lysate and covalent binding was induced by the addition of an oxidised form of haem, hemin (**Scheme 1.12**). Using this strategy numerous protein binders of artemisinin were identified. Recently organohydrazine ABPs developed by Lin *et al.* have been proposed to react *via* a radical mechanism.¹⁶⁶



Scheme 1.12: Radical chemistry in ABPP. Carbon-centred radical forming on artemisinin scaffold following coordination of heme promoting the non-specific crosslinking of the artemisinin-based probe to binding enzyme following addition of hemin.¹⁶⁴

1.8.1 Photoactivatable groups for ABPP

Photoactivated crosslinkers are a very common strategy used to probe enzyme-substrate interactions.¹⁶⁷ Upon irradiation photoactivated crosslinkers can form highly reactive radical species (**Scheme 1.13**) that covalently crosslink to proximal residues within the active site of the target enzyme. This crosslinking is not residue specific or mechanism-based, so probes incorporating these groups are considered to be a measure of enzyme affinity rather than activity. As no active-site residue is required for binding, this strategy is extremely valuable in the probing of metalloenzymes.¹⁶⁸ Benzophenone (**33**) is the most commonly used of these photo crosslinkers. Upon irradiation by long wavelengths of 350 nm to 365 nm it forms a diradical species which reacts by a sequential abstraction-recombination mechanism with relatively high affinity towards methionine (Met) (**Scheme 1.13A**).¹⁶⁹ Along with diazirines (**Scheme 1.13B**), benzophenone was the first crosslinker reported to probe metalloproteases helping to broaden the understanding of this previously difficult to study group of enzymes.^{168,170} A major breakthrough in the use of this crosslinker was the development of the unnatural amino acid *p*-benzoyl-L-phenylalanine which allowed incorporation of benzophenone into proteins to study protein-protein interactions *in vivo*.¹⁷¹



Scheme 1.13: Photocrosslinking groups for affinity-based protein profiling. Formation of reactive species for (A) benzophenone (**33**), (B) diazirines or (C) aryl azides upon exposure to UV light.

Diazirines and aryl azides are also extensively used in ABPP and have been incorporated into unnatural amino acids to facilitate the study of protein-protein interactions.^{167,171,172} However, they rely on a different mode of action, forming carbenes or nitrenes respectively upon irradiation (**Scheme 1.13B and 1.13C**). Diazirines were among the first groups employed for metalloprotease profiling and

their small size and high reactivity upon irradiation make them particularly attractive for probing these interactions.¹⁷³ In most comparative studies, diazirine based probes perform better than other crosslinking groups.¹⁶⁷

The shorter activation wavelength of aryl azides means they are less widely used than diazirines or benzophenones for ABP. Nonetheless, this group was installed between two ubiquitin monomers to form a photoactivated diubiquitin probe **34** (**Figure 1.16**).¹⁷⁴ In this study Tan *et al.* demonstrated reactivity with linkage specific DUBs. A slightly broader reactivity profile was seen in comparison to the corresponding Dha probe in HEK 293F lysate. As this photo-crosslinking does not require an active site Cys, this probe **34** can also profile metalloprotease DUBs. In a separate study, the aryl azide group was once again incorporated into ubiquitin scaffolds to afford photoaffinity-based probes.¹⁷⁵ Comparative analysis of the aryl azide and diazirine groups was carried out with the diazirine group proving more efficient and selective. Linkage specificity was achieved using the diubiquitin based probes but their use as ABPs was limited by the inclusion of the native isopeptide bond.

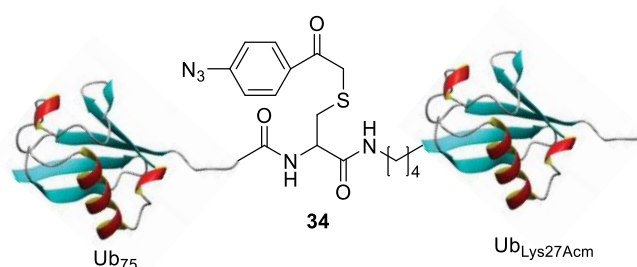
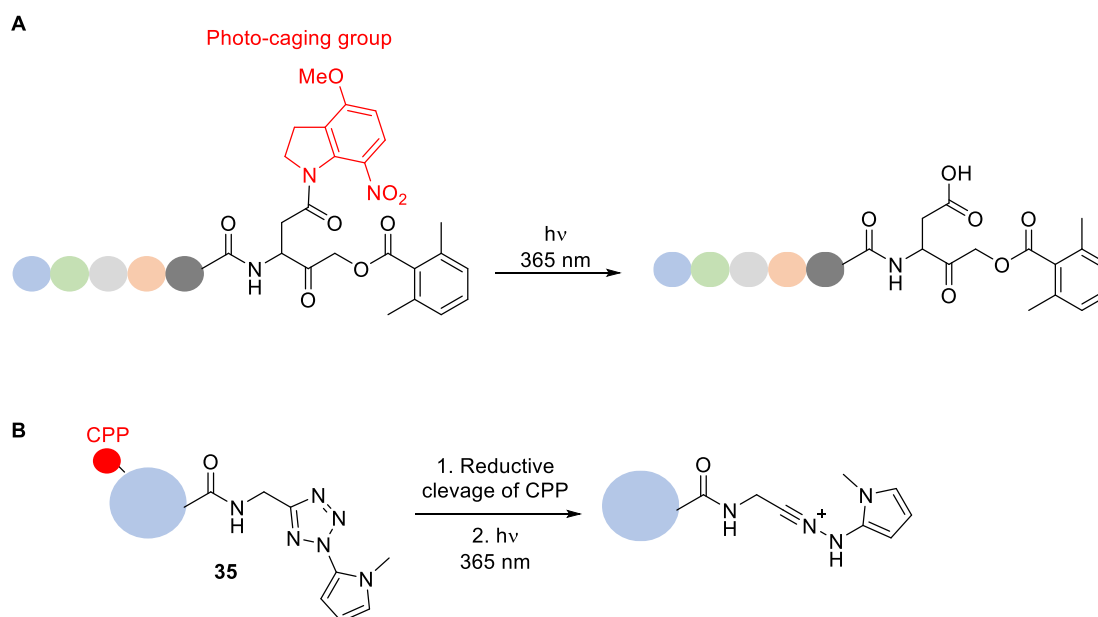


Figure 1.16: Structure of the photocrosslinker ABP with a diubiquitin recognition element reported by Tan *et al.*¹⁷⁴

Another approach towards inducible ABPs is photo-uncaging. This method relies on UV activation and instead of producing a reactive species in the form of a radical, carbene or nitrene species, photo-uncaging typically liberates an electrophile that can then react with an active-site residue. Initial studies in this area focus on profiling specific residues within the proteome such as Cys and those with carboxylic acid sidechains.^{176,177} Chakrabarty *et al.* developed covalent inhibitors targeting caspases in which the electrophilic warhead was sterically hindered by a nitroindoline photocage (**Scheme 1.14A**).¹⁷⁸

The Zhuang group recently expanded on their CPP strategy to design a cell permeable DUB ABP **35** that can be activated using photo-uncaging chemistry (**Scheme 1.14B**).¹⁷⁹ A CPP was conjugated *via* a disulfide bond as in the original probe design (**Figure 1.3**) and a warhead incorporating a tetrazole group was employed. Upon UV irradiation the tetrazole is converted to an electrophilic nitrilimine which reacts with the active-site Cys of the enzyme. The advantages of having improved temporal control over the reaction were elegantly demonstrated by profiling DUBs in whole cells at different points during the cell cycle.



Scheme 1.14: Photo-uncaging groups in ABPs. (A) Uncaging of nitroindoline using UV light to reveal reactive group.¹⁷⁸ (B) Activation of DUB ABP in whole cells using UV light to form a reactive nitrilimine.¹⁷⁹

1.9 Objectives

The importance of DUBs and the ubiquitin conjugation machinery to cell function is overwhelmingly clear.²⁷ Many ABPs targeting these enzymes have been developed and have greatly aided in gaining a better understanding of enzyme activity, structure and function.¹⁸⁰ The objective of this work was to design and test probes that used new chemistry to add to and improve upon this existing panel of DUB ABPs. To achieve this, existing monoubiquitin probes HA-Ub₇₅-CH₂CH₂Br **5** and HA-Ub₇₅-PA **6** were made to optimise the probe synthesis and methodologies required to test the probes (**Figure 1.17A**). Alongside these known probes, two novel derivatives with fluoride warheads, HA-Ub₇₅-CH₂CH₂F **36** and HA-Ub₇₅-CH₂CHF₂ **37**, were designed (**Figure 1.17B**). A fluoride leaving group was

used in place of the other existing halide probes to offer a more stable warhead that could show selectivity for specific subsets of DUBs. Derivatives were designed in which multiple fluorides were attached to a single carbon atom to increase its electrophilicity and promote the attack of the active site Cys. These novel probes were tested for reactivity alongside the reported probes that also react *via* electrophilic mechanisms. This work is presented in Chapter 2.

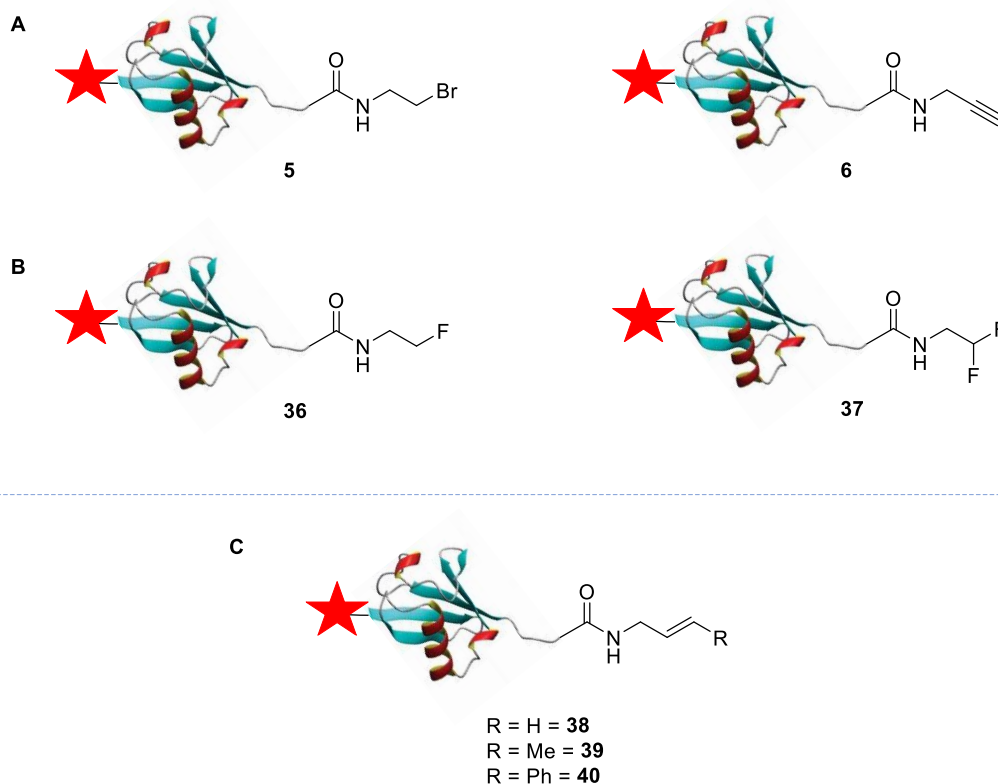


Figure 1.17: Structures of target probes. (A) Previously reported electrophilic probes. (B) Structures of novel fluoride probes designed to work by electrophilic mechanisms. (C) Structures of alkene-based probes designed to label by a thiol-ene reaction.

One common feature of existing Cys reactive DUB ABPs is that once bound, the reactive warhead is positioned next to the active site Cys and a nucleophilic attack occurs. Therefore, there is no external control over the timing of the reaction. The objective of the work described in Chapter 3 was to design and test a probe that can react *via* a radical mechanism. It was hypothesised that this would provide increased control over the timing of the covalent capture of DUBs and allow for more refined studies of these enzymes. Three novel ABPs consisting of a monoubiquitin recognition element and an alkene moiety as the reactive warhead were designed (**Figure 1.17C**). Upon UV irradiation it was hypothesised that radical initiators would catalyse the formation of a thiyl radical on the active-site Cys. This can undergo a

thiol-ene reaction with the alkene warhead which will be held proximal due to the binding interaction of the DUB and monoubiquitin recognition element. Terminal and substituted alkene alternatives were designed to investigate the steric and radical stability requirements of the reaction. The reactivity of the probes was assessed using recombinant enzyme and cell lysate experiments. The specificity and potential applications of these probes were examined using DUB inhibitors, where they were compared to existing electrophilic probes, and proteomic studies.

Finally, to help facilitate the transfer of the thiol-ene labelling methodology to whole cells, the use of a milder source of UV light was investigated in Chapter 4. Additionally, alternative radical initiators were selected to be assessed for use in a visible light-mediated thiol-ene reaction. Avoiding the use of UV light would significantly improve the cytocompatibility of the reaction and enable studies in more physiologically relevant systems. Eosin Y (**30**) was chosen to be tested due to recent studies demonstrating its effectiveness at catalysing thiol-ene conjugations on biomolecules and its cytocompatibility at micromolar concentrations. Bi_2O_3 was also selected due to recent reports showing its efficiency at catalysing visible light mediate thiol-ene reactions. This visible light thiol-ene reaction was investigated for ABPP using recombinant DUBs and those expressed endogenously in cell lysate.

Visible light-mediated thiol-ene and thiol-yne reactions were assessed for non-templated protein-protein conjugations to potentially improve upon existing UV light-dependent conjugations. The thiol-yne reaction using the reported alkyne functionalised probe offers a route towards a diubiquitin probe furnished with an alkene between the monomers. These investigations are described in Chapter 4.

This work provides an alternative methodology by which enzyme activity can be probed and presents how this methodology can be used to study DUB activity and inhibitors in a novel way.

2 Electrophilic probes for DUBs

The existing array of ABPs targeting DUBs means that novel probes targeting these enzymes must represent a significant advance by addressing some of their limitations. In this chapter, existing probes were first synthesised to serve as positive controls when testing novel probes. Additionally, this provided an opportunity to optimise the synthesis of monoubiquitin ABPs and techniques to test their reactivity. A panel of probes examining the suitability of fluoride leaving groups for DUB ABPs were also synthesised and their reactivity was assessed in relative to reported ABPs.

The first literature examples of ABPs targeting DUBs employed Ub₇₅ as a recognition element.^{67,70} This protein is one amino acid shorter than WT ubiquitin but retains a strong binding affinity with DUBs. When acting upon ubiquitinated substrates, DUBs cleave the amide bond of the C-terminal Gly, the 76th residue of WT ubiquitin (**Figure 2.1A**).²⁷ In the original Ub₇₅ based probes, this Gly 76 residue is replaced with an electrophilic warhead in which a leaving group or Michael acceptor is positioned such that the site of attack is analogous to the position of the carbonyl carbon of Gly 76 (**Figure 2.1B**).^{67,70} Once bound by a DUB, a covalent bond is formed between the probe and the enzyme *via* nucleophilic attack by the active site Cys. A tag is incorporated into the probe design to allow for visualisation of this reaction within complex biological samples and subsequent purification of probe-enzyme adducts from these systems.

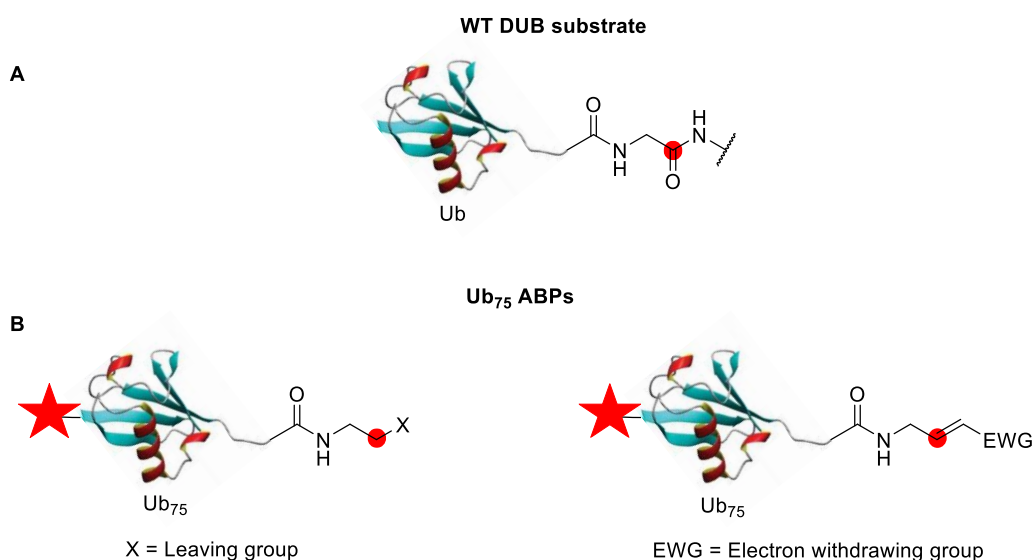


Figure 2.1: Structural basis of DUB ABP design. (A) Structure of WT DUB substrates with site of attack indicated in red on the isopeptide bond between the ubiquitin monomer and substrate Lys. (B) General structure of DUB ABPs with site of attack indicated in red.

Two reported electrophilic probes HA-Ub₇₅-CH₂CH₂Br **5** and HA-Ub₇₅-PA **6** were synthesised (**Figure 2.2A**).^{67,72} All probes synthesised in this work proceeded *via* a common HA-Ub₇₅-thioester **2** intermediate. The HA-Ub₇₅-CH₂CH₂Br **5** and HA-Ub₇₅-PA **6** probes therefore allowed for the optimisation of the formation of this intermediate as well as key methodologies such as recombinant enzyme labellings and an immunoprecipitation. Finally, these known probes were synthesised to serve as positive controls when testing the reactivity of novel probes with recombinant enzyme or cell lysate.

Novel electrophilic probes based on a fluoride leaving group were also synthesised (**Figure 2.2B**). It was anticipated that if these probes demonstrated reactivity against DUBS that they would serve as a more stable alternative to the existing halide probes. Their reactivity was tested with the recombinant DUB OTUB1 and in cell lysate, with existing probes serving as positive controls for these tests. OTUB1 was selected as it is known to have promiscuous reactivity.

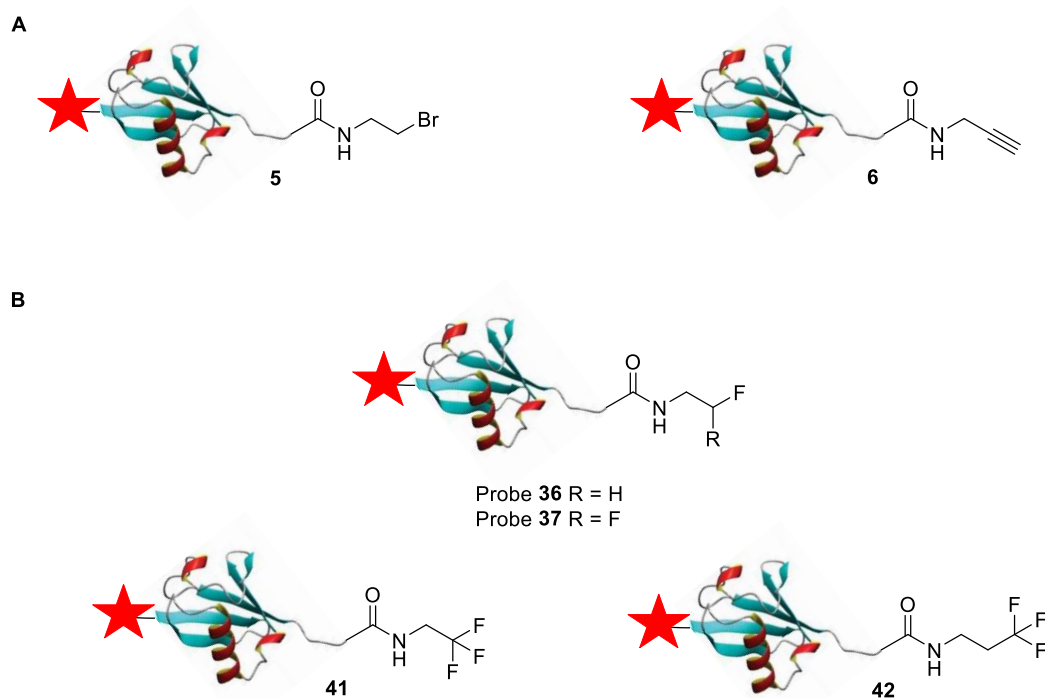


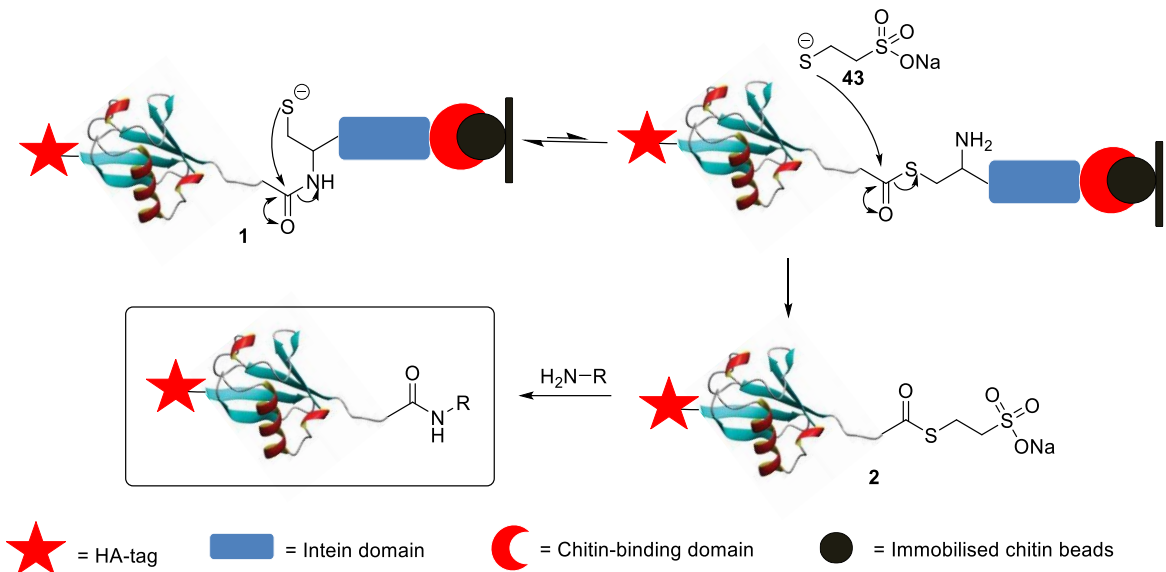
Figure 2.2: Structures of target DUB ABPs. (A) Reported electrophilic probes HA-Ub₇₅-CH₂CH₂Br **5** and HA-Ub₇₅-PA **6**. (B) Novel probes based on fluoride as a leaving group.

2.1 Synthesis and testing of reported electrophilic probes

2.1.1 Expression and purification of HA-Ub₇₅-thioester

The expression and purification of HA-Ub₇₅-thioester **2** was carried out according to literature procedures.¹⁸¹ The first step in the synthesis of this HA-Ub₇₅-thioester **2** was the expression of a HA-Ub₇₅-intein-chitin binding domain (CBD) protein **1** construct in *E. coli* cells. Lysis of these cells allowed for the purification of this construct using over a chitin column (**Scheme 2.1**). The CBD facilitated this purification by immobilizing the construct on the chitin column, with all other proteins removed in a series of washing steps. An Asp to Ala mutation within the intein domain results in a trapped equilibrium forming between an amide and thioester bond at the N-terminus of the intein (**Scheme 2.1**).⁸⁵ The construct could therefore be excised using an excess of MESNa **43** to induce thiolysis. HA-Ub₇₅-thioester **2** was then eluted off the chitin column and the amine precursors of the desired warheads was coupled to this reactive thioester affording the final probes (**Scheme 2.1**). These probes contained an N-terminal HA-tag which facilitated

detection and isolation of this protein construct and the resulting probes (**Scheme 2.1**).



Scheme 2.1: Formation of a reactive HA-Ub₇₅-thioester 2 on an immobilised chitin and amide coupling to the desired warhead.

The protein construct's expression and purification as the HA-Ub₇₅-thioester 2 was followed by SDS-PAGE. Samples were taken at defined stages throughout the process. Following separation by gel electrophoresis they were visualised using an anti-HA western blot, to selectively image proteins containing a HA-tag, or silver staining, to visualise all proteins in the sample (**Figure 2.3**).

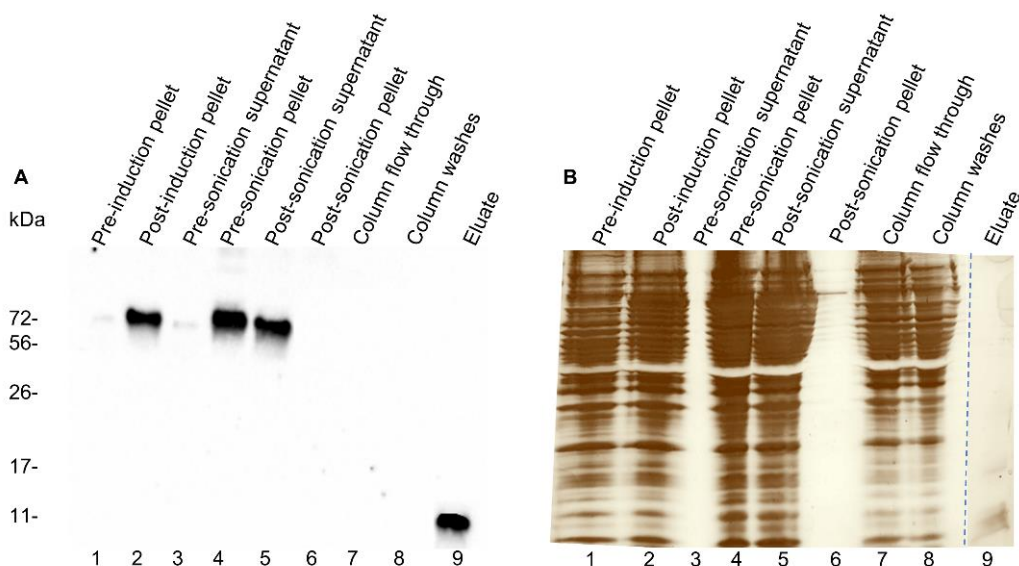


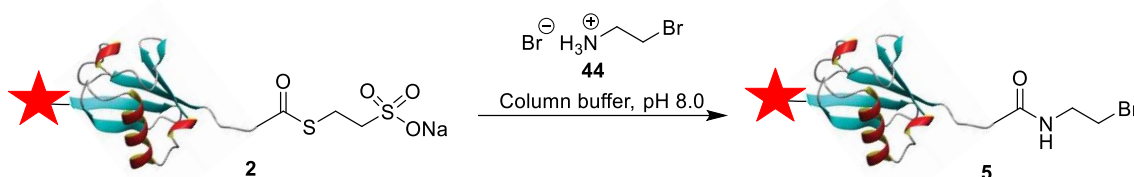
Figure 2.3: Expression and purification of HA-Ub₇₅-Intein-CBD 1. Visualised by (A) Anti HA-tag western blot and (B) Silver stain. The protein construct 1 was expressed in BL21 *E. coli* cells using the pTYB2 plasmid. Expression was induced by the addition of IPTG (0.4 mM). Samples were taken at various points throughout the purification process.

Comparison between pre-induction and post-induction samples indicates the expression of the HA-Ub₇₅-intein-CBD construct 1 was successfully induced (**Figure 2.3A and B, lanes 1 and 2**). A band was observed following induction at around the expected mass of the protein construct, 72 kDa, and it was visible by anti-HA western blot confirming the presence of a HA-tag (**Figure 2.3A, lane 2**). The same band was evident where expected in subsequent steps of the purification confirming the stability of the construct throughout the process (**Figure 2.3A and B, lanes 4 and 5**). The construct 1 was retained on the column during the washing steps as evidenced by the absence of any band in samples taken during the wash steps (**Figure 2.3A and B, lane 8**). In the sample taken following an incubation with MESNa (**43**), a band appeared just below 11 kDa in the elute, the expected mass of HA-Ub₇₅-thioester 2 (**Figure 2.3A and B, lane 9**). Once again, the visualisation of this band by anti-HA western blot confirmed the presence of a HA-tag and the absence of any other bands by silver staining indicated a high level of purity (**Figure 2.3B, lane 9**). The synthesis of the monoubiquitin probes can be realised using this HA-Ub₇₅-thioester 2.

2.1.2 Synthesis and reactivity of the HA-Ub₇₅-CH₂CH₂Br probe

The HA-Ub₇₅-CH₂CH₂Br probe 5 was synthesised according to a modified literature procedure in which 2-bromoethylamine·HBr (**44**) is coupled to HA-Ub₇₅-thioester 2

(**Scheme 2.2**).⁶⁷ Its synthesis from the HA-Ub₇₅-thioester **2** is well established, as is its reactivity towards DUBs.



Scheme 2.2: Synthesis of HA-Ub₇₅-CH₂CH₂Br **5 from HA-Ub₇₅-thioester **2**.**

The activity of the newly synthesised HA-Ub₇₅-CH₂CH₂Br probe **5** was first tested against a purified, recombinant DUB, OTUB1 (**Figure 2.4A and B**). OTUB1 is known to react with HA-Ub₇₅-CH₂CH₂Br **5**. However, in these initial experiments no new band representing a covalent adduct between the probe and the enzyme was observed by anti-HA western blot or silver staining when they were incubated together. (**Figure 2.4A and B, lane 3**).

A second attempt was made to synthesise the HA-Ub₇₅-CH₂CH₂Br probe **5** and this was tested for reactivity alongside the first replicate in HEK 293T cell lysate (**Figure 2.4C**). HEK 293T cell lysate was selected as it is the standard cell line used for the testing and development of DUB ABPs due to its high expression levels of several DUB classes. In this experiment it was used to confirm the lack of observed reactivity between the HA-Ub₇₅-CH₂CH₂Br probe **5** and OTUB1 was due to problems in the probe synthesis and not the condition of the OTUB1. When a covalent bond forms between the HA-tagged probe and a DUB present in the HEK 293T lysate it is visualised as a new band at a molecular weight higher than the probe alone by anti-HA western blot. When both HA-Ub₇₅-CH₂CH₂Br probes **5** were tested for reactivity in cell lysate, very limited labelling was observed (**Figure 2.4C, lanes 4 and 5**). The lack of significant reactivity in both cases confirmed issues in the installation of the reactive warhead of the HA-Ub₇₅-CH₂CH₂Br probe **5**.

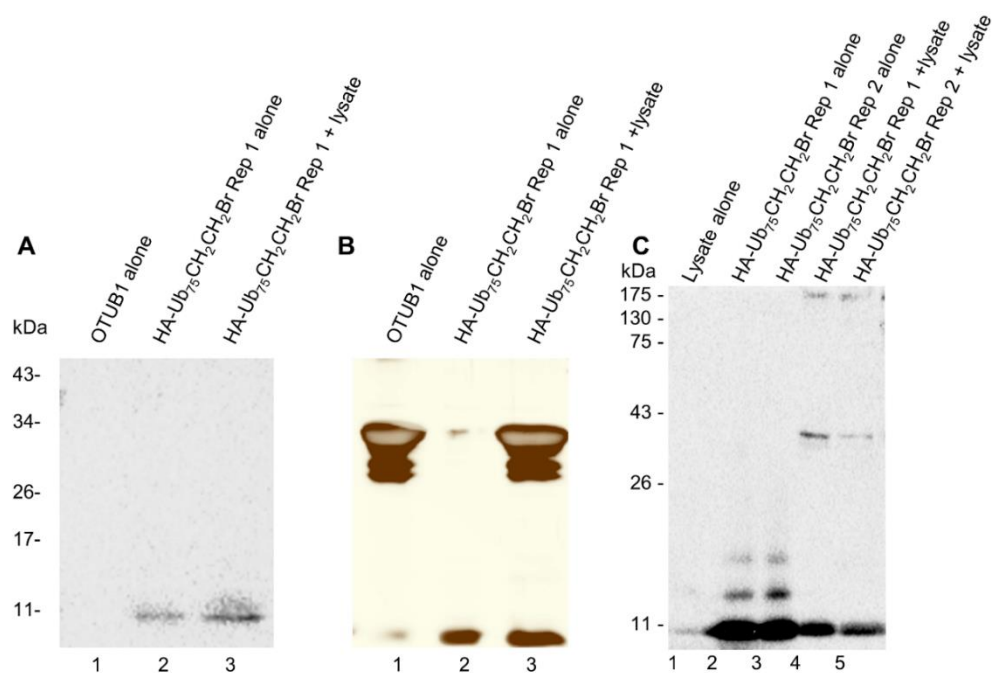


Figure 2.4: Reactivity of the HA-Ub₇₅-CH₂CH₂Br probe 5 against OTUB1 and HEK 293T cell lysate. Visualised by (A) and (C) Anti-HA western blot or (B) silver staining. (A) and (B) HA-Ub₇₅-CH₂CH₂Br 5 (2 µg) was incubated with OTUB1 (1.5 µg) at 37 °C for 60 min in phosphate buffer (50 mM Na₂HPO₄, 50 mM NaH₂PO₄ pH 8.0). (C) HA-Ub₇₅-CH₂CH₂Br 5 (1 µg) was incubated with HEK 293T cell lysate (50 µg) in homogenate buffer at 37 °C for 60 min.

To address the problems with the coupling step of the probe synthesis, changes were made at points of the protocol that were identified as detrimental to probe stability. Prior to the coupling reaction of HA-Ub₇₅-thioester **2** and 2-bromoethylamine·HBr (**44**), the thioester required extended periods of centrifugation to concentrate the protein sample and remove excess MESNa. Similarly, following the coupling reaction, the HA-Ub₇₅-CH₂CH₂Br **5** required a long centrifugation step to concentrate and to remove excess 2-bromoethylamine·HBr (**44**). It was hypothesised that during one or both steps, the elevated temperature inside the centrifuge over time was promoting the hydrolysis of the thioester or the bromide warhead in the aqueous buffer. To overcome this, the centrifugal desalting steps at both stages were replaced by a NAP-5 size exclusion column. Using this new protocol, another attempt was made to synthesise the HA-Ub₇₅-CH₂CH₂Br probe **5** and its reactivity was assessed using recombinant OTUB1 and HEK 293T cell lysate (Figure 2.5A and B).

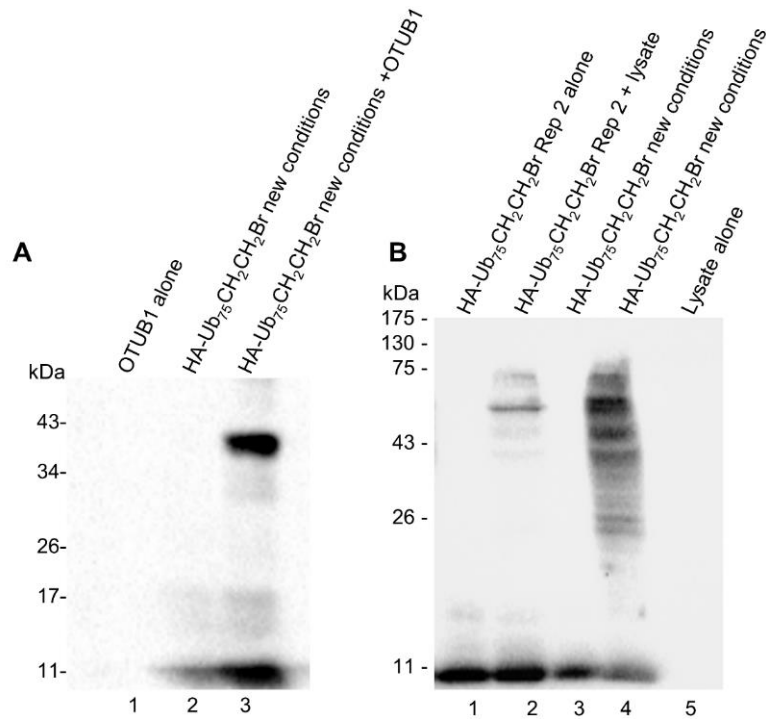


Figure 2.5: Reactivity of the HA-Ub₇₅-CH₂CH₂Br probe 5 against OTUB1 and HEK 293 cell lysate following protocol optimisation. Visualised by anti-HA western blot. (A) HA-Ub₇₅-CH₂CH₂Br 5 (2 µg) was incubated with OTUB1 (1.5 µg) at 37 °C for 60 min in phosphate buffer for 60 min. (B) HA-Ub₇₅-CH₂CH₂Br 5 (1 µg) was incubated with HEK 293T cell lysate (50 µg) in homogenate buffer at 37 °C for 60 min.

Following a 60 min incubation of the new HA-Ub₇₅-CH₂CH₂Br probe 5 with OTUB1, a new band was observed by anti-HA western blot around the 43 kDa molecular weight marker (**Figure 2.5A, lane 3**). This is consistent with the expected molecular weight of around 41 kDa for the probe-enzyme covalent adduct. A second experiment was conducted in which the probe was incubated with HEK 293T cell lysate (**Figure 2.5B**). The probe synthesised using the new protocol was tested in parallel with a HA-Ub₇₅-CH₂CH₂Br probe 5 synthesised following the original protocol. When incubated with cell lysate for 60 min, the HA-Ub₇₅-CH₂CH₂Br probe 5 synthesised following the new protocol showed a marked improvement in reactivity (**Figure 2.5B, lanes 2 and 4**). This is visualised as multiple new bands visible at higher molecular weights, representing covalent adducts between probe and enzymes expressed within the cell lysate. The introduction of a size exclusion column in place of a centrifugation step to desalt the HA-Ub₇₅-thioester 2 and HA-Ub₇₅-CH₂CH₂Br probe 5 limited hydrolysis at key stages and an active probe was generated. This altered protocol was used in all future probe syntheses.

2.1.3 Optimisation of the immunoprecipitation protocol using the HA-Ub₇₅-CH₂CH₂Br probe

The active HA-Ub₇₅-CH₂CH₂Br probe **5** was taken forward and used to optimise the immunoprecipitation protocol. This technique uses agarose beads coupled to antibodies to enrich for proteins that the antibodies target. By using anti-HA antibodies, the HA-Ub₇₅-CH₂CH₂Br probe **5** is bound and enriched for along with any protein that it has covalently bound. Analysis of this enriched material provides valuable information about a probe's specificity and reactivity. The immunoprecipitation was first carried out using amounts 3-fold higher than in previous labelling reactions, 3 µg of HA-Ub₇₅-CH₂CH₂Br **5** and 150 µg of HEK 293T cell lysate. An otherwise standard labelling reaction was carried out and a series of washing steps were carried out using the homogenate buffer used for previous lysate labelling reactions. An equivalent fraction of the sample was taken at multiple stages throughout the protocol to allow for the process to be followed by SDS-PAGE and failed steps to be identified. These samples were visualised by anti-HA western blot (**Figure 2.6A**).

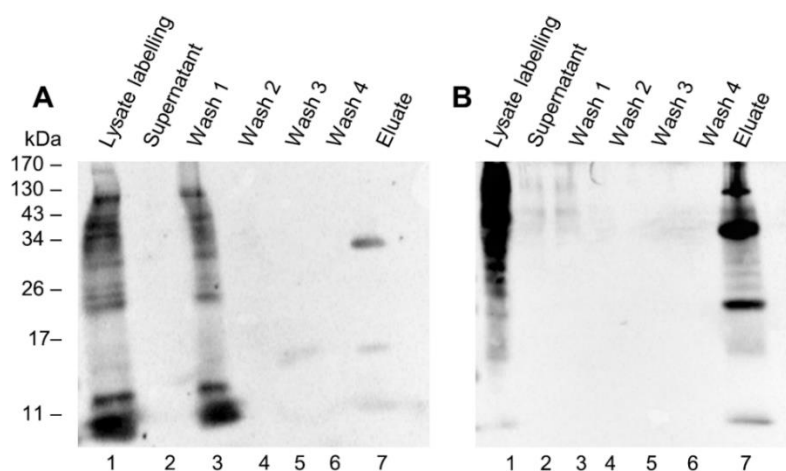


Figure 2.6: Optimisation of immunoprecipitation conditions. Visualised by anti-HA western blot. A lysate labelling was carried out using HEK 293T cell lysate (150 µg) with HA-Ub₇₅-CH₂CH₂Br **5** (3 µg) in (A) homogenate buffer or (B) NET buffer (50 mM Tris pH 7.5, 5 mM EDTA, 150 mM NaCl, 0.5% NP-40). The pulldown was performed with anti-HA coupled agarose beads (60 µL of 50% slurry) for 90 min at 4 °C. After a series of washing steps using (A) homogenate buffer or (B) NET buffer, equivalent fractions of the input, supernatant, washes and eluate samples were taken.

As in the previous cell lysate labelling, the probe was observed to covalently react with several higher molecular weight proteins (**Figure 2.6A, lane 1**). Although the

initial labelling reaction was successful, all captured material was lost in the first washing step (**Figure 2.6A, lane 3**). Therefore, none of this material was carried through the following wash steps (**Figure 2.6A, lanes 4-6**). The elution lane which should represent a sample enriched for the HA-Ub₇₅-CH₂CH₂Br probe **5** and its adducts contains only a negligible amount of unbound probe just below the 11 kDa molecular weight marker and the light and heavy chains of the antibody at 26 kDa and 43 kDa respectively (**Figure 2.6A, lane 7**). To resolve this issue, the experiment was repeated using an alternative buffer, NET buffer (50 mM Tris pH 7.5, 5 mM EDTA, 150 mM NaCl, 0.5% NP-40), that had been used in previous immunoprecipitation studies using monoubiquitin probes (**Figure 2.6B**).⁶⁷

The initial labelling reaction was largely unaffected when carried out in this alternative buffer (**Figure 2.6B, lane 1**). Only very minor protein loss was observed throughout the subsequent washing steps (**Figure 2.6B, lanes 2–6**). A significant increase in material captured by the probe was seen in the elution lane indicating a successful pulldown (**Figure 2.6B, lane 7**). The labelling pattern appeared different to that seen in the input lane of the immunoprecipitation (**Figure 2.6B, lanes 1 vs 7**). This was attributed to the presence of the light and heavy chains of the antibody being present in the eluate sample and the minor loss of material in the various washing steps (**Figure 2.6B, lane 7**). These were promising initial results that indicated that the pulldown was successful. Optimal storage and experimental conditions are unique to each antibody. It was hypothesised that the high sucrose concentration was detrimental to antibody stability when using homogenate buffer. Additionally, the inclusion of the non-ionic detergent, NP-40, in the NET buffer limits non-specific binding interactions, prioritising antibody-antigen binding throughout the immunoprecipitation.

To further optimise the protocol and ensure the number of washing steps was appropriate, another immunoprecipitation was performed and followed by a silver stain in addition to an anti-HA western blot. Once more, samples were taken at defined stages of the protocol to be analysed by these techniques (**Figure 2.7A and B**).

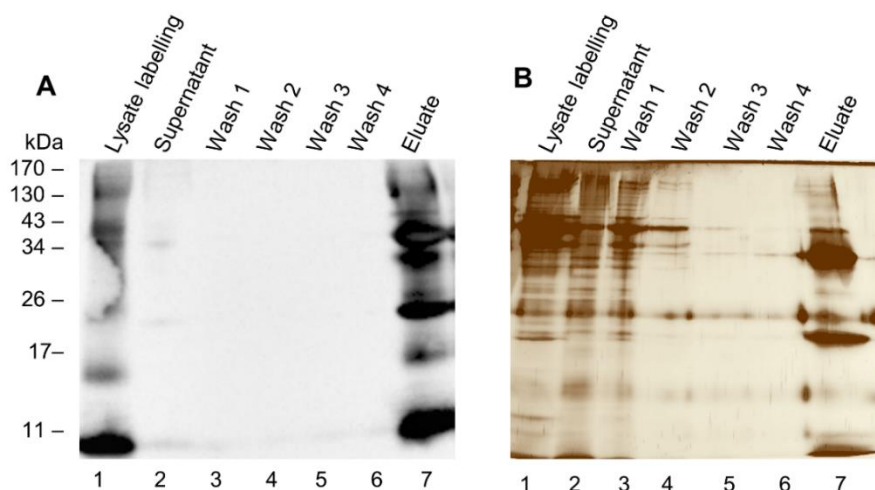


Figure 2.7: Optimisation of immunoprecipitation conditions. Visualised by (A) anti-HA western blot or (B) silver staining. A labelling was carried out using HEK 293T cell lysate (150 μ g) with HA-Ub₇₅-CH₂CH₂Br **5** (3 μ g) in NET buffer. The pulldown was performed with anti-HA coupled agarose beads (60 μ L of 50% slurry) for 90 min at 4 °C. After a series of washing steps using NET buffer equivalent fractions of the input, supernatant, washes and eluate samples were taken.

By western blot, the labelling pattern seen in the eluate sample was more consistent with that seen in the input sample when compared the previous experiment (**Figure 2.6A, lanes 1 vs 7** and **Figure 2.7B, lanes 1 vs 7**). There was also less detectable loss of HA-tagged proteins in any of the washing steps (**Figure 2.7A, lanes 2–6**). The purpose of the washing steps was to remove proteins that were not specifically interacting with the anti-HA antibodies. Tracking the removal of these untagged proteins was possible using the non-specific silver staining technique (**Figure 2.7B**). The removal of unbound proteins was primarily observed in the early washing steps up until the third wash step at which point very few proteins are detected (**Figure 2.7B, lanes 2–5**). The absence of detectable proteins in the final washing step (**Figure 2.7B, lane 6**) strongly suggested that the proteins seen in the eluate lane represented probe-enzyme adducts that were enriched for by the immunoprecipitation (**Figure 2.7B, lane 6**). It was concluded that four washing steps were therefore appropriate for future experiments.

To identify the proteins present in this enriched sample, the remainder of the eluate sample from the previous experiment was digested using trypsin, desalted and the analysed by LC-MS/MS. Several DUBs were identified in this sample along with some DUB associated proteins and proteins with no known connection to DUBs (**Table 2.1**). Additionally, the number of DUBs relative to unrelated proteins in this

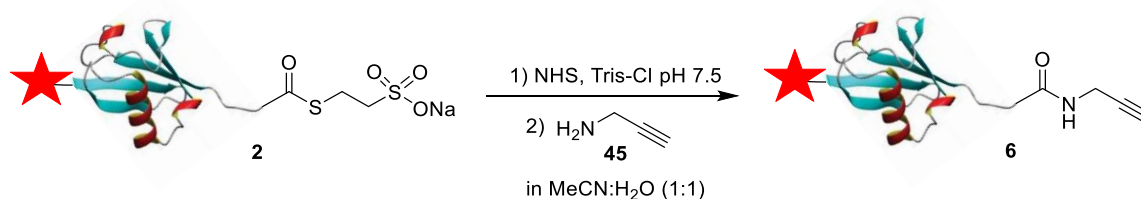
sample represents a significant enrichment relative to expected endogenous levels of DUBs in HEK 293T cell lysate (**Table 2.1**). No quantification was carried out at this point. From these results it was concluded that immunoprecipitation was sufficiently optimised to be carried out using novel probes.

Protein ID	Protein full name	Role
UBP14	Ubiquitin carboxyl-terminal hydrolase 14	DUB
UBP5	Ubiquitin carboxyl-terminal hydrolase 5	DUB
UCHL1	Ubiquitin carboxyl-terminal hydrolase isozyme L1	DUB
UCHL1	Ubiquitin carboxyl-terminal hydrolase isozyme L1	DUB
UCHL3	Ubiquitin carboxyl-terminal hydrolase isozyme L3	DUB
UCHL5	Ubiquitin carboxyl-terminal hydrolase isozyme L5	DUB
OTUB1	Ubiquitin thioesterase OTUB1	DUB
EIF3K	Eukaryotic translation initiation factor 3 subunit K	Forms complex with DUBs
UBB	Polyubiquitin-B	Probe
PSB1	Proteasome subunit beta type-1	Forms complex with DUBs
UB2D3	Ubiquitin-conjugating enzyme E2 D3	Ub conjugation machinery
HS71A	Heat shock 70 kDa protein 1A	Induced by ubiquitination
HS105	Heat shock protein 105 kDa	Induced by ubiquitination
RS6	40S ribosomal protein S6	No known connection to DUBs
YBOX1	Nuclease-sensitive element-binding protein 1	No known connection to DUBs
NDKB	Nucleoside diphosphate kinase B	No known connection to DUBs
RB15B	Putative RNA-binding protein 15B	No known connection to DUBs
SYWC	Tryptophan-tRNA ligase, cytoplasmic	No known connection to DUBs

Table 2.1: Proteins identified by LC-MS/MS following immunoprecipitation of HA-Ub₇₅-CH₂CH₂Br probe 5 after a HEK 293T lysate labelling.

2.1.4 Synthesis and reactivity of HA-Ub₇₅-propargylamine probe

The HA-Ub₇₅CH₂CH₂Br probe **5** suffers stability issues in aqueous buffer. The HA-Ub₇₅-PA probe **6** was therefore synthesised to serve as an alternative positive control. The terminal alkyne group of the HA-Ub₇₅-PA **6** is considerably more stable in aqueous conditions relative to the bromide group of the HA-Ub₇₅CH₂CH₂Br probe **5**. The probe **6** was synthesised following a different literature procedure, originally developed in the synthesis of the Ub₇₅-VME probe (**Scheme 2.3**).⁶⁷



Scheme 2.3: Synthesis of HA-Ub₇₅-PA 6 from HA-UB₇₅-thioester.

To test the activity of the newly synthesised HA-Ub₇₅-PA probe **6**, a recombinant enzyme labelling was carried out using OTUB1 (**Figure 2.8A**). For comparison, an identical experiment was carried out using the HA-Ub₇₅-CH₂CH₂Br probe **5** (**Figure 2.8A**). In both cases a new band was visible around the 43 kDa molecular weight marker in the sample where the probe was incubated with OTUB1 (**Figure 2.8A, lanes 3 and 4**). These bands corresponded to the molecular weight of the probe-OTUB1 covalent adduct and more labelling was observed using the HA-Ub₇₅-PA probe **6** relative to the HA-Ub₇₅-CH₂CH₂Br probe **5** (**Figure 2.8A, lanes 3 vs 4**). Similarly, when both probes were incubated with HEK 293T cell lysate, increased labelling was observed for the HA-Ub₇₅-PA probe **6** (**Figure 2.8B, lanes 6 vs 8**). It was suggested that due to its increased stability, the synthesis of the HA-Ub₇₅-PA probe **6** afforded more active probe than the HA-Ub₇₅-CH₂CH₂Br probe **5** synthesis. Consequently, in several later experiments the HA-Ub₇₅-PA probe **6** served as a positive control in place of the HA-Ub₇₅-CH₂CH₂Br probe **5**.

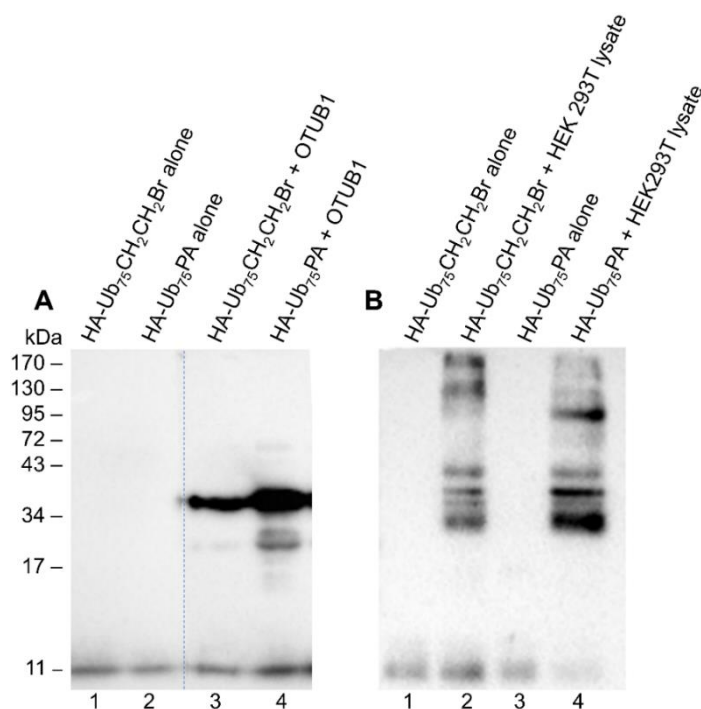


Figure 2.8: Reactivity of the HA-Ub₇₅-CH₂CH₂Br probe 5 and HA-Ub₇₅-PA 6 against (A) OTUB1 and (B) HEK 293T cell lysate visualised by anti-HA western blot. HA-Ub₇₅-CH₂CH₂Br **5** (3 µg) or HA-Ub₇₅-PA **6** (3 µg) was incubated with (A) OTUB1 (2 µg) or (B) HEK 293T cell lysate (50 µg) at 37 °C for 60 min in homogenate buffer.

2.2 Synthesis and reactivity of fluoride probes

In addition to the HA-Ub₇₅-CH₂CH₂Br probe **5**, a monoubiquitin probe using a chloride warhead has also been reported.⁶⁷ Other halide warheads have not yet

been explored in the literature. In line with leaving group ability, it was assumed that an iodide warhead would face even greater stability issues and therefore was not pursued. Conversely, a fluoride-based warhead would be significantly more stable in aqueous buffer and much like the HA-Ub₇₅-PA probe **6** avoid hydrolysis issues in the later stages of the probe synthesis. It was noted that an S_N2 reaction between a thiol and alkyl fluoride group would typically be unanticipated in solution^{182,183} but given the demonstrated reactivity of a terminal alkyne in the context of an active site, it was hypothesised that a reaction may be possible due to stabilising interactions with the oxyanion hole that usually stabilises the oxygen anions formed during peptide bond cleavage (**Scheme 2.9**). Additionally, arylsulfonates have been successfully employed in ABPP, with the stabilisation of the fluoride leaving group through H-bond donation of proximal cationic amino acids residues found to be essential for the labelling reaction (**Scheme 2.9**).¹⁸⁴ It was hypothesised that similar stabilising interactions within the active site of DUBs could achieve similar results.

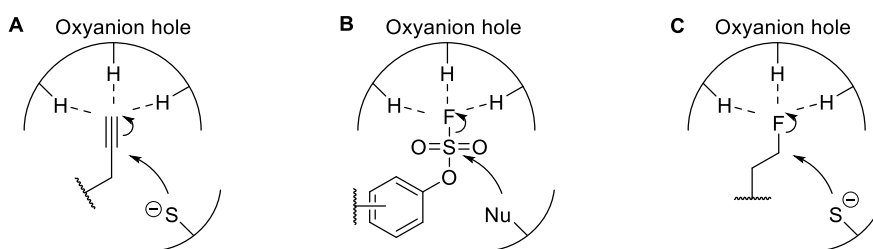
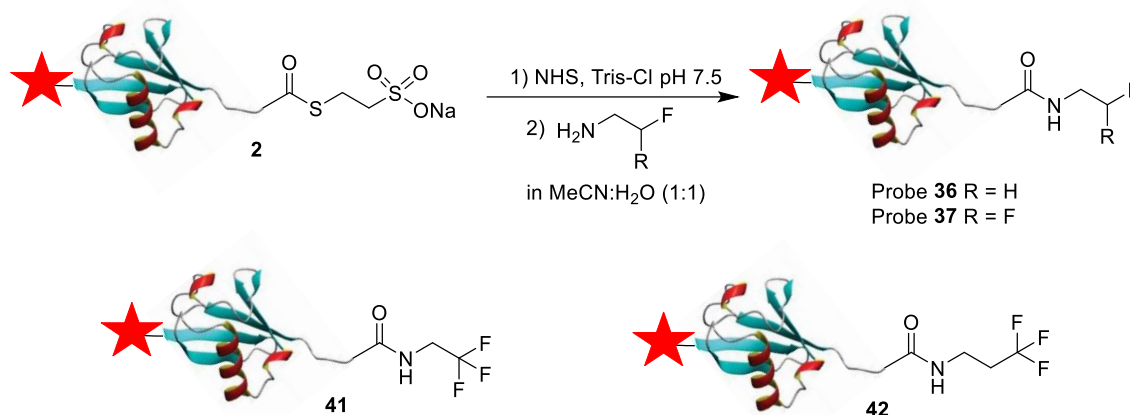


Figure 2.9: Stabilisation within the active site of enzymes promoting the reactivity of (A) HA-Ub₇₅-PA **6 and (B) arylsulfonate based probes. (C) The proposed reactivity of fluoride based ABPs.**

To investigate this, the HA-Ub₇₅-CH₂CH₂F **36** and HA-Ub₇₅-CH₂CHF₂ **37** probes were synthesised (**Scheme 2.4**). The HA-Ub₇₅-CH₂CHF₂ probe **37** was synthesised to investigate if increasing the electrophilicity of the carbon atom by adding multiple fluoride groups would increase reactivity in this context. By the same reasoning, the corresponding HA-Ub₇₅-CH₂CF₃ **41** was synthesised by Dr. Fergus Poynton in the McGouran lab along with a HA-Ub₇₅CH₂CH₂CF₃ probe **42** to examine CF₃ as an alternative leaving group.



Scheme 2.4: Synthesis and structures of the HA-Ub₇₅-CH₂CH₂F 36, HA-Ub₇₅-CH₂CHF₂ 37, HA-Ub₇₅-CH₂CF₃ 41 and HA-Ub₇₅CH₂CH₂CF₃ 42.

The synthesis of the HA-Ub₇₅-CH₂CH₂F **36** and HA-Ub₇₅-CH₂CHF₂ **37** probes was realised using the same procedure as the HA-Ub₇₅-PA probe **6**.⁶⁷ The probes were first tested in HEK 293T cell lysate at concentrations consistent with those used in the previous cell lysate experiments (**Figure 2.9A**). It was expected that the probes would demonstrate reduced reactivity compared to the HA-Ub₇₅-CH₂CH₂Br probe **5**. However, it was hypothesised that the reduced reactivity would provide some specificity, selecting for DUBs with increased active site nucleophilicity or appropriately positioned cationic residues. However, in this experiment no covalent adducts were observed in either case when the probe was incubated with the HEK 293T cell lysate (**Figure 2.9A, lanes 3 and 5**). To definitively confirm the absence of any reactivity, a second experiment was carried out in which the concentration of the probe was increased 3-fold and the incubation time was increased from 60 min to 180 min (**Figure 2.9B**). A labelling with HA-Ub₇₅-CH₂CH₂Br **5** was also carried out as part of this experiment as a positive control (**Figure 2.9B, lane 1**).

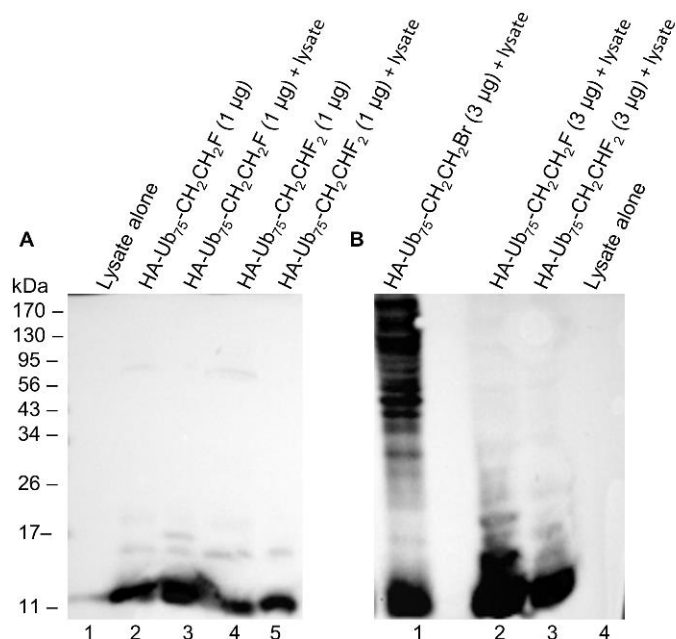


Figure 2.10: Lysate labelling with the HA-Ub₇₅-CH₂CH₂F **36 and HA-Ub₇₅-CH₂CHF₂ **37** probes.** Visualised by anti-HA western blot. (A) and (B) HA-Ub₇₅-CH₂CH₂F **36**, HA-Ub₇₅-CH₂CHF₂ **37** or HA-Ub₇₅-PA **6** was incubated with HEK 293T cell lysate (50 µg) at 37 °C for 60 min at the indicated concentration.

Very faint labelling bands were observed for the HA-Ub₇₅-CH₂CH₂F **36** and HA-Ub₇₅-CH₂CHF₂ **37** probes but when compared to the HA-Ub₇₅-CH₂CH₂Br **5** positive control there is negligible reactivity (**Figure 2.9B, lanes 1–3**). A similar lack of reactivity was observed for the HA-Ub₇₅-CH₂CF₃ **41** and HA-Ub₇₅CH₂CH₂CF₃ **42** when tested by Dr. Fergus Poynton. It was concluded that due to this lack of reactivity the fluoride-based probes were not worth pursuing and no further testing was carried out.

2.3 Conclusions

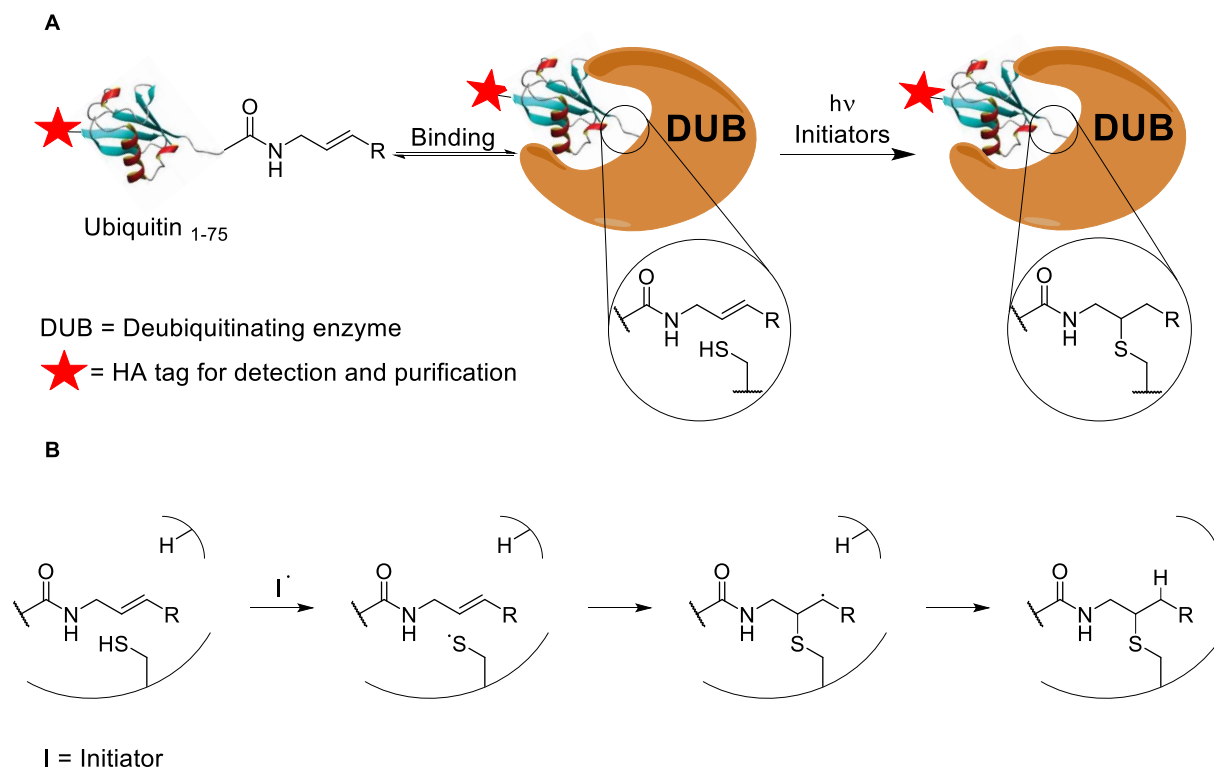
In conclusion, the previously reported HA-Ub₇₅CH₂CH₂Br **5** and HA-Ub₇₅-PA **6** probes were synthesised, and their reactivity was confirmed against the recombinant DUB, OTUB1 and against endogenous DUBs within cell lysate. The synthesis of these probes allowed for the identification of key stages of the protocol during which hydrolysis of key reactive groups was an issue and the subsequent optimisation of these stages. Additionally, the HA-Ub₇₅CH₂CH₂Br **5** probe was used to find appropriate conditions for the immunoprecipitation protocol, an essential method used to characterise the reactivity and selectivity of any new ABP. Two novel probes, HA-Ub₇₅-CH₂CH₂F **36** and HA-Ub₇₅-CH₂CHF₂ **37**, were synthesised to interrogate the applicability of fluoride warheads in monoubiquitin ABPs. These

new probes demonstrated very restricted reactivity in cell lysate and therefore were not taken forward for any further testing.

3 The thiol-ene reaction for ABPP of DUBs

3.1 Introduction and probe design

A novel monoubiquitin probe with a C-terminal alkene warhead was designed to capture active DUBs using the thiol-ene reaction. The labelling assay differs from a typical labelling as the HA-Ub₇₅-propene probe **38** requires a pre-incubation time prior to radical initiation under UV light to initiate covalent bond formation between the probe and the enzyme. This strategy means a binding equilibrium is established between the probe and target enzymes, followed by a short activation period. Therefore, the thiol-ene labelling provides precise temporal control which is not achievable using existing Cys reactive probes (**Scheme 3.1A**).



Scheme 3.1: (A) Proposed covalent bond formation of probes to DUBs via a thiol-ene reaction following the establishment of a binding equilibrium. (B) Stepwise visualisation of bond formation.

Another advantage of this warhead is its increased stability relative to most other monoubiquitin probes, with the exception of the HA-Ub₇₅-PA probe **6**.⁷² The alkene moiety is unreactive under ambient conditions, only forming an adduct with the target enzyme upon exposure to UV light. The probe works *via* a radical mechanism within the enzyme active site with initiators acting as the primary radical source. The radical initiators abstract a hydrogen from the active site Cys and the

resulting thiyl radical reacts with the aligned alkene moiety of the probe affording a carbon-centred radical (**Scheme 3.1B**). This radical is expected to abstract a hydrogen from within the active site. The result is a covalent bond between the C-terminus of the probe and the active site Cys residue. Initiators are expected to have access to the active site even after reversible ubiquitin binding as DUBs typically act upon ubiquitinated substrates, leaving significant space within this pocket.²⁷ Additionally, a water molecule participates in mechanism of action of Cys protease enzymes so this pocket must be solvent accessible. Selected crystal structures of the DUBs OTUB1, OTUB2 and UCHL3 bound to monoubiquitin probes were analysed to visualise solvent accessibility around the C-terminus of ubiquitin (**Figure 3.1**). All structures analysed showed a solvent accessible cavity at the C-terminus of the bound ubiquitin, demonstrating that radical initiators can access the active site Cys.

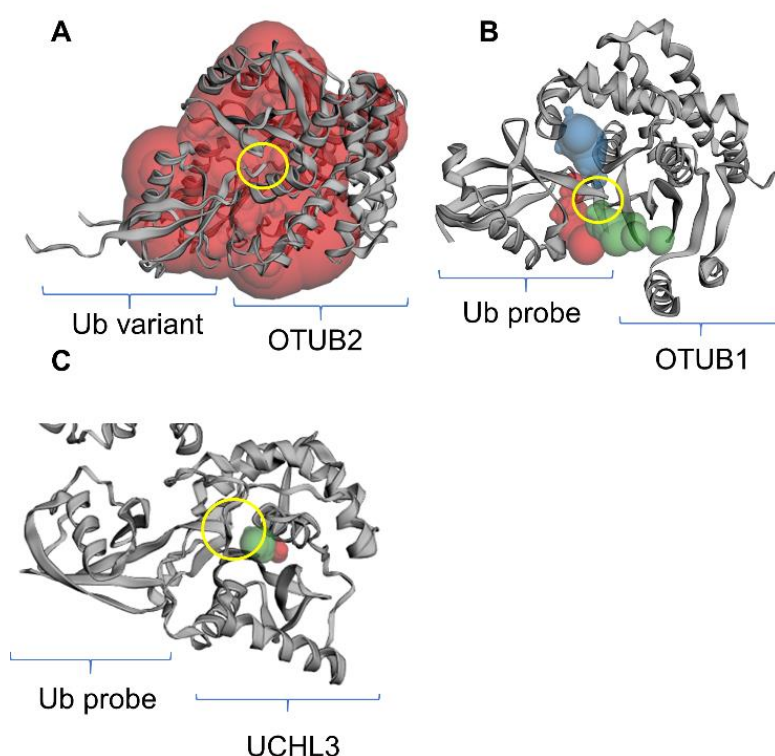
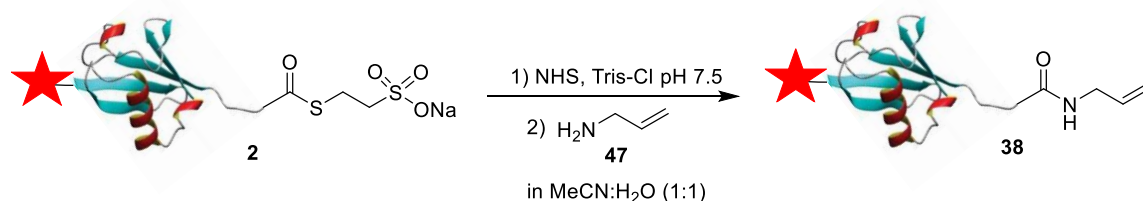


Figure 3.1: Solvent accessibility of the active site Cys of DUBs binding ubiquitin variants. (A) Crystal structure of OTUB2 covalently bound to monoubiquitin probe displaying one solvent accessible pocket (red).¹⁸⁵ (B) Crystal structure of OTUB1 bound to a ubiquitin variant with three solvent accessible pockets highlighted (red, blue, green).⁷⁴ (C) Crystal structure of UCHL3 covalently bound to monoubiquitin suicide probe displaying two solvent accessible pockets (red, green).⁶⁸ In each case the position of the ubiquitin C-terminus is highlighted by a yellow circle. Images obtained using CASTp 3.0 software.¹⁸⁶

DUBs operate in several complex enzymatic networks and are known to be post-translationally modified.²⁷ Therefore, the ability to induce the formation of a probe-enzyme complex *in vitro* at specific times or after different external inputs could offer a greater understanding of how these enzymes act within cells. This coupling reaction represents a promising and novel strategy to target the active form of these enzymes. It differs from existing photocrosslinking strategies as it has high residue selectivity.¹⁸⁷ Although it has been widely used in protein chemistry, including in the formation of ubiquitin dimers and trimers,¹³⁷ the thiol-ene reaction has not previously been used in ABPP. Results presented in this chapter were published in *Chemical Science* in 2020.¹⁸⁸

3.2 Synthesis, characterisation and testing of HA-Ub₇₅-propene

HA-Ub₇₅-propene **38** was the first in a series of alkene-based probes that were synthesised (**Scheme 3.2**). This probe consisted of a functionalised HA-Ub₇₅ in which the C-terminal Gly residue is replaced with an unsubstituted alkene moiety. This was selected as terminal alkenes typically demonstrate increased reactivity in thiol-ene reactions relative to substituted alkenes.¹⁸⁹ As for the HA-Ub₇₅-PA probe **6** the synthesis was adapted from literature procedures used for the synthesis of the Ub₇₅-VME probe.⁶⁷ In a two-step protocol, *N*-hydroxysuccinimide (NHS) (**46**) was incubated with the HA-Ub₇₅-thioester **2**, acting as a nucleophilic catalyst for the coupling. Allylamine (**47**) was added to the mixture in a 1:1 MeCN:H₂O mixture to improve solubility.



Scheme 3.2: Synthesis of HA-Ub₇₅-propene 38.

The synthesis of the probe was confirmed by both MS and gel electrophoresis (**Figure 3.2**). The intact probe was characterised using MALDI mass spectrometry which identified species at 10061 Da and 5034 Da which represented the predicted weights for the singly and doubly charged species respectively (**Figure 3.2A**). LC-MS/MS analysis of the peptides resulting from an elastase digest of this protein resulting in 100% sequence coverage of HA-Ub₇₅ and located a shift in molecular

weight at the C-terminus of the protein, consistent with the incorporation of the allylamide functionality (**Figure 3.2B**). A single band was observed at the expected molecular weight after separation by SDS-PAGE and subsequent silver staining (**Figure 3.2C**). These results indicated the successful synthesis of the HA-Ub₇₅-propene probe **38** with a high level of purity.

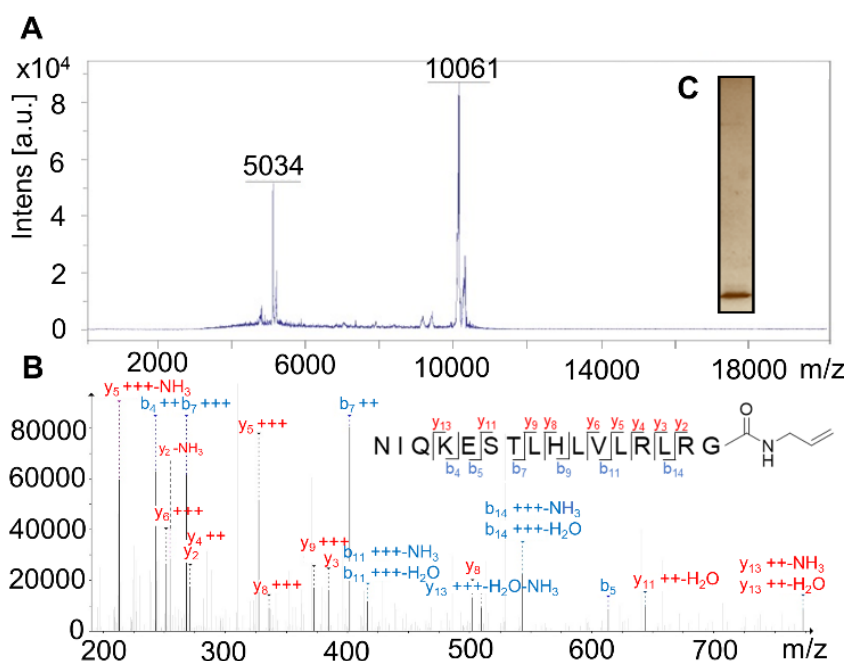


Figure 3.2: Identification of HA-Ub₇₅-propene by MALDI-TOF. (A) MALDI-TOF analysis of HA-Ub₇₅-propene (25 μ g). (B) LC-MS/MS identification of modified C-terminal ubiquitin peptide. (C) Silver stain analysis of 2 μ g of HA-Ub₇₅-propene probe **38**.

3.2.1 Recombinant enzyme experiments using HA-Ub₇₅-propene **38**.

With the HA-Ub₇₅-propene probe **38** in hand, its reactivity was first validated in an assay performed with the His-tagged, recombinant DUB OTUB1 (**Figure 3.3**). The initial reaction conditions were adapted from selected literature examples of thiol-ene reactions involving biomolecules and proteins.^{137,190-192} Following a 60 min preincubation at 37 °C, the radical initiator 2,2-Dimethoxy-2-phenylacetophenone (DPAP) (**48**) was added along with 4'-Methoxyacetophenone (MAP) (**49**). Samples were then degassed with N₂ for 2 min to prevent the formation of reactive oxygen species (ROS). It has been shown that ROS can reversibly inhibit DUBs and DPAP (**48**) mediated thiol-ene couplings required degassing.¹⁹² The samples were exposed to UV light (365 nm) for 10 min. The reaction was analysed by gel electrophoresis and visualised by silver staining and an anti-His western blot to selectively visualise the His-tagged OTUB1 (**Figure 3.3A and B**).

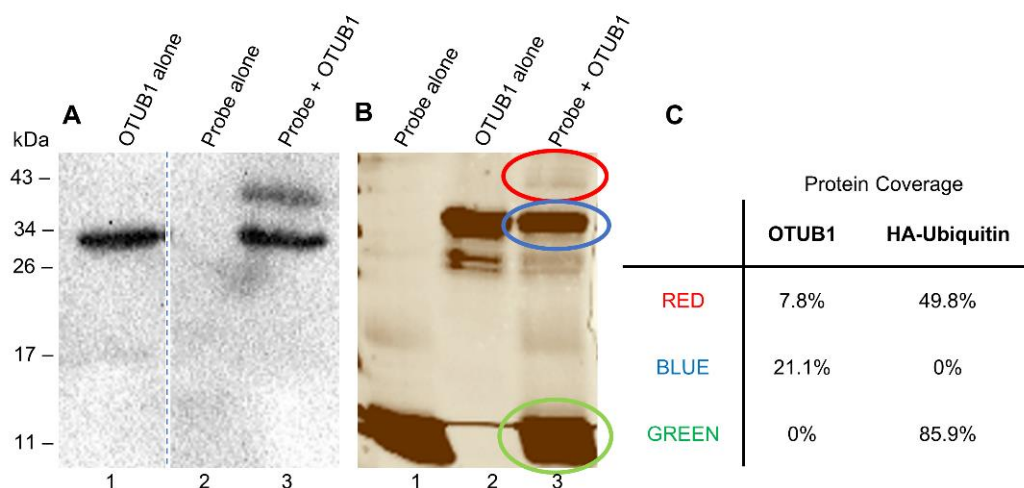


Figure 3.3: Labelling of recombinant OTUB1 with HA-Ub₇₅-propene 38. Visualised using (A) Anti-His western blot and (B) silver stain. HA-Ub₇₅-propene 38 (4 µg) was incubated with OTUB1 (2.5 µg) at 37 °C for 60 min in phosphate buffer (50 mM Na₂HPO₄, 50 mM NaH₂PO₄ pH 8.0) for 60 min. DPAP (48) (0.5 mM) and MAP (49) (0.5 mM) were added, the samples were degassed for 2 min with N₂ and then exposed to UV light (365 nm) for 10 min. Upon completion, 2X reducing sample buffer (30 µL) was added and the proteins were heated to 95 °C for 5 min. (C) LC-MS/MS analysis of proteins found in indicated bands.

A new band corresponding to the expected molecular weight of the probe-enzyme adduct, approximately 43 kDa, was observed in all samples containing the HA-Ub₇₅-propene 38 and the enzyme. This new band strongly suggested that OTUB1 had reacted covalently with a protein of approximately 10 kDa, consistent with the molecular weight of the probe. To confirm the identity of this new band, it was excised from the silver stain gel and subjected to an in-gel digest using trypsin. As controls, the bands corresponding to the expected molecular weight of OTUB1 and the HA-Ub₇₅-propene probe 38 alone, around 34 kDa and 11 kDa respectively, were also excised and digested in parallel (Figure 3.3B, lane 6). LC-MS/MS analysis was used to identify the peptides present in each sample (Figure 3.3C). The results are expressed as the % protein coverage of HA-Ub₇₅ and OTUB1 in the corresponding bands. Both proteins were observed in the newly formed band around the 43 kDa MW marker, while only OTUB1 or HA-Ub₇₅ alone were observed in the other bands analysed. These results add to the evidence that this new band represents a covalent adduct between the probe and the enzyme.

It could not be ruled out that the labelling observed in the previous experiment was due to a non-templated thiol-ene reaction occurring with one of the non-catalytic Cys

residues of OTUB1. A further experiment was devised to confirm that this new band was the result of a reaction with the active-site Cys of OTUB1 following a specific binding interaction (**Figure 3.4**). It was proposed that when OTUB1 was denatured, no specific binding interaction would occur between OTUB1 and the probe and no covalent bond would form, as at these concentrations the reaction will only occur when templated. OTUB1 was denatured by heating it in-solution at 95 °C for 5 min or by sonicating and vortexing the enzyme in a solution containing 0.5% SDS prior to the probe labelling being carried out (**Figure 3.4A and B**). These reactions were run in parallel with an OTUB1 labelling under non-denaturing conditions (**Figure 3.4A and B, lane 5**).

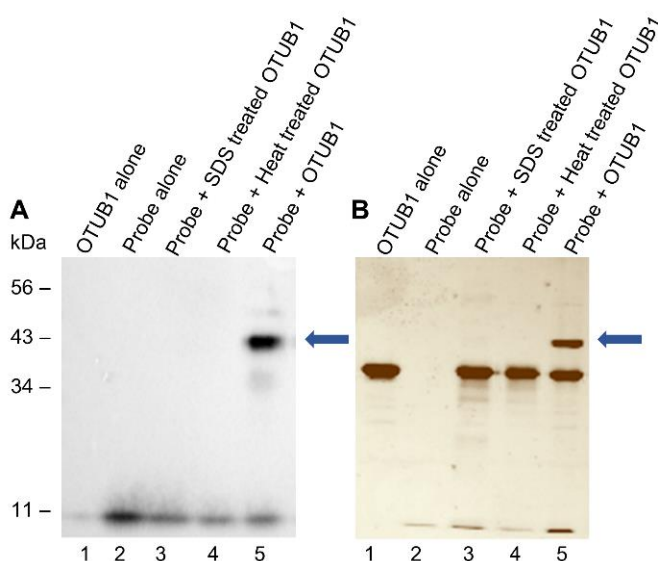


Figure 3.4: Investigating the binding requirement for recombinant enzyme labelling using probe 38. Labelling of recombinant OTUB1 (2 µg) with HA-Ub₇₅-propene probe **38** (4 µg). Visualised using (A) Anti-HA western blot and (B) Silver stain. Recombinant OTUB1 (2µg) was denatured using heat or SDS prior to incubation with the HA-Ub₇₅-propene probe **38** in lanes 3 and 4. HA-Ub₇₅-propene **38** (4 µg) was incubated with OTUB1 (2.5 µg) at 37 °C with gentle shaking in phosphate buffer (50 mM Na₂HPO₄, 50 mM NaH₂PO₄ pH 8.0) for 60 min. DPAP (**48**) (0.5 mM) and MAP (**49**) (0.5 mM) were added, the samples were degassed for 2 min with N₂ and then exposed to UV light (365 nm) for 10 min.

Consistent with this hypothesis, no new band was observed by either silver staining or anti-HA western blot in these samples (**Figure 3.4A and B, lanes 3 and 4**). Conversely, a new band was seen under the standard conditions around the 43 kDa MW marker as seen in the previous experiment (**Figure 3.4A and B, lane 5**). This finding validated the need for a specific binding interaction between the probe and the active form of an enzyme for the reaction to occur. The absence

of a reaction under denaturing conditions also confirmed the probe did not react with off-target Cys residues at these concentrations.

Further to this, it was also demonstrated how the K_d of the probe can be determined using OTUB1 as a model system. Given the unique temporal resolution of this probe and the binding equilibrium that is formed prior to covalent bond formation, it was reasoned that a simple assay could provide information about this equilibrium. The concentration of the probe was increased across several experiments, while the concentration of OTUB1 remained constant. The samples were otherwise treated identically and separated by SDS-PAGE before visualisation by Coomassie blue staining (**Figure 3.5A**). The intensity of the new 43 kDa band was measured using Image Quant software and the band with the highest intensity was taken to be complete saturation of OTUB1. The other values were expressed as a fraction of this and plotted against the concentration of the probe (**Figure 3.5B**). From this graph, the concentration that results in a fractional saturation of 0.5 is taken to be the K_d . A K_d value of 7.8 μM was derived. If applied in combination with reversible inhibitors, this system could be an additional technique to evaluate their potency.

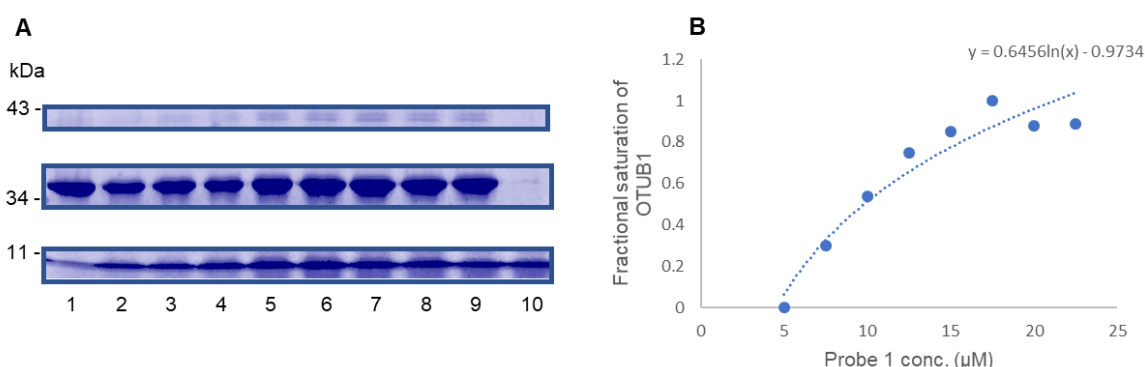


Figure 3.5: Probing the K_d of probe enzyme binding. (A) Visualised by Coomassie blue stain. Recombinant DUB OTUB1 (5 μg) was incubated with increasing concentrations of the HA-Ub₇₅-propene probe **38** in phosphate buffer. DPAP (**48**) (0.5 mM) and MAP (**49**) (0.5 mM) were added, the samples were degassed for 2 min with N_2 and then exposed to UV light (365 nm) for 10 min. Upon completion, 2X reducing sample buffer (30 μL) was added and the proteins were heated to 95 $^\circ\text{C}$ for 5 min. (B) Intensity of the labelled band was analysed on Image Quant and plotted against the concentration of probe.

3.2.2 Cell lysate experiments and optimisation of thiol-ene reaction conditions

Having confirmed its reactivity in a simple two-component system, the HA-Ub₇₅-propene **38** was next tested in HEK 293T cell lysate. The first variables

tested were the time under UV required for maximum labelling to occur and the effect of the preincubation time on the labelling (**Figure 3.6 and 3.7**). Time points under UV ranging from 0 min to 360 min were investigated. In addition to this, several control experiments were also performed. A labelling with HA-Ub₇₅-CH₂CH₂Br **5** was subjected to the same radical conditions as the thiol-ene labelling, a labelling was performed without radical initiators and finally, a labelling experiment was carried out after the cell lysate was preincubated with the thiol alkylator *N*-ethylmaleimide (NEM) (**50**) (**Figure 3.6, lanes 1 and 8–10**).

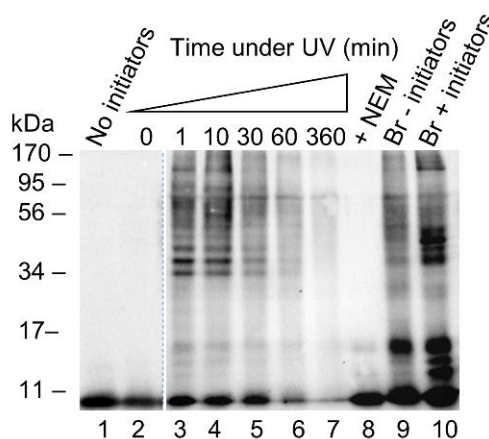


Figure 3.6: Thiol-ene labelling with varying UV exposure. Visualised by anti-HA western blot. Lanes 1–8 all contain HA-Ub₇₅-propene **38** (1 μ g) and HEK 293T cell lysate (50 μ g). Lanes 9 and 10 show a labelling with HA-Ub₇₅-CH₂CH₂Br **5** (2 μ g) and HEK 293T cell lysate (50 μ g) in the presence of DPAP (**48**) and MAP (**49**). Lanes 1–6 exposed to UV light (365 nm) for increasing time periods. *N*-ethylmaleimide (NEM) (13 mM) was added to lane 8 and incubated for 15 min before the addition of the HA-Ub₇₅-propene **38**.

The absence of either UV light or radical initiators resulted in no visible labelling (**Figure 3.6, lanes 1 and 2**). Lane 1 can be directly compared to lane 5 as these samples were exposed to UV light for an equivalent amount of time. Similarly, lane 2 can be compared to lanes 3 to 7 as they were treated with identical amounts of initiators (**Figure 3.6A, lanes 2–7**). The absence of detectable labelling in lanes 1 and 2 validated the requirement of radical initiation for a covalent labelling interaction (**Figure 3.6**). There was no discernible difference between the 1 min and 10 min timepoints (**Figure 3.6, lane 3 vs 4**). 1 min of UV light exposure therefore appeared sufficient for maximum labelling under these conditions. This rapid labelling was reasoned to be due to the templating of the reaction. Prior to UV exposure the samples were incubated at 37 °C for 60 min. Therefore, once the radical reaction was initiated, a binding equilibrium was already established between

the probe and the enzyme and the alkene warhead of HA-Ub₇₅-propene **38** was positioned adjacent to the active site Cys. Continued exposure to UV light started to degrade the proteins at timepoints longer than 10 min resulting in loss of signal in these lanes (**Figure 3.6, lane 5–7**). As a result of these findings, 10 min was taken to as the standard exposure time to ensure complete labelling in future experiments. Additionally, by this time point sample degradation was not observed.

Preincubation of the lysate with the thiol alkylator NEM inhibited labelling by the HA-Ub₇₅-propene probe **38** (**Figure 3.6, lane 8**). The conditions in this lane were otherwise identical to the 10 min time point (**Figure 3.6, lane 4**). This abrogation of labelling strongly indicated the covalent bond formation occurs between the alkene warhead and a Cys residue. A lysate labelling was also performed in which the HA-Ub₇₅-CH₂CH₂Br **5** probe was subject to the same conditions as the HA-Ub₇₅-propene probe **38** to test if these conditions were altering enzymatic activity (**Figure 3.6, lanes 9 and 10**). Interestingly, not only was there no apparent reduction in enzyme activity under these conditions, the intensity of the labelling pattern has increased under these conditions. These results indicated that enzymatic activity was not reduced under these conditions and that the HA-Ub₇₅-CH₂CH₂Br **5** warhead can also react with the active-site cysteine in a radical-mediated reaction.

To test the hypothesis that a binding equilibrium was forming between the HA-Ub₇₅-propene probe **38** and DUBs, an experiment was designed in which the time given to form this equilibrium was varied. Preincubation times from 0 min to 180 min were examined (**Figure 3.7A**). In this experiment the importance of the degassing step was also evaluated along with a test for non-specific reactions with proteins using an inactive probe **51** (**Figure 3.7A**).

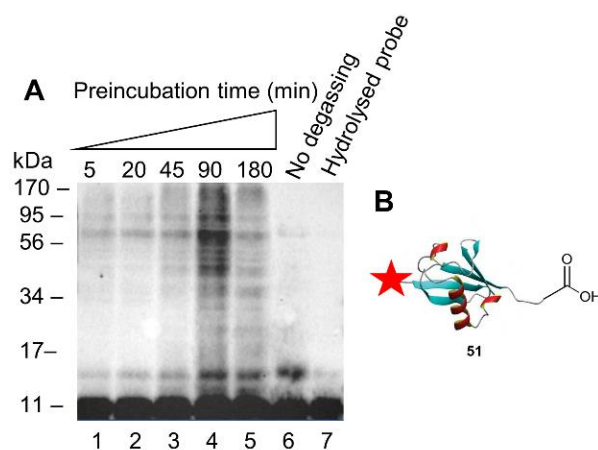


Figure 3.7: Thiol-ene labelling with varying preincubation times. (A) Lanes 1–6 show labellings with HA-Ub₇₅-propene **38** (1 μ g) and HEK 293T lysate (50 μ g). Lane 7 shows a labelling with an inactive HA-Ub₇₅ probe **51** (2 μ g). Pre-incubation time at 37 °C was varied for lanes 1–5. Lanes 6 and 7 were both pre-incubated for 60 min. All lanes contained DPAP (**48**) (0.5 mM) and MAP (**49**) (0.5 mM), were degassed for 2 min and were exposed to UV light for 5 min. (B) Structure of hydrolysed HA-Ub₇₅ **51**.

Following a preincubation time of 5 min, partial labelling was observed in HEK 293T cell lysate (**Figure 3.7A, lane 1**). An increase in the incubation time from 20 min to 90 min correlated to an increase in the intensity of the labelling pattern and therefore an increase in the covalent capture of proteins (**Figure 3.7A, lanes 2–4**). This intensity peaked after 90 min, indicating that the hypothesised binding equilibrium was fully established by this time (**Figure 3.7A, lanes 4 and 5**). The drop in enzyme capture by 180 min was attributed to protease mediated degradation of the sample due to the extended incubation at 37 °C. These results provided evidence for the influence of a preincubation time on the reaction between probe **38** and enzyme. Based on these results, the following experiments were carried out with a 90 min preincubation period to maximise labelling intensity.

The importance of a degassing period before radical initiation was also investigated. Excluding this degassing period lead to marked variation in both labelling pattern and intensity (**Figure 3.7A, lane 6**). It was evident that a thorough degassing step was required to limit the interference of ROS on the reaction (**Figure 3.7A, lane 6**). To validate that an alkene moiety was needed for the reaction to proceed, a control experiment was performed in which a hydrolysed HA-Ub₇₅ **51** was used (**Figure 3.7A, lane 7**). The absence of any labelling when the hydrolysed probe **51** was used confirmed that the alkene warhead was necessary for any covalent bond formation. This result, in combination with previous findings that show that the

reaction does not proceed when Cys residues are alkylated, provides strong evidence that the thiol-ene reaction is responsible for the observed labelling (**Figure 3.7A, lane 7 and figure 3.6, lane 8**).

A panel of radical initiators were tested for their suitability in this system and as alternatives to DPAP (**48**) and MAP (**49**) (**Figure 3.8**). Additionally, alterations in the concentration of DPAP (**48**) and MAP (**49**) were also investigated (**Figure 3.9**). 2,2'-Azobis(2-amidinopropane) dihydrochloride (AAPH) (**52**), 4,4'-Azobis(4-cyanopentanoic acid) (ACPA) (**53**) and *t*-butyl peroxide (**54**) were tested as alternative initiators (**Figure 3.8, lanes 2–4**). *t*-Butyl peroxide proved the most promising of these (**Figure 3.8, lane 2**), with very little protein capture observed when AAPH and ACPA are used as the radical initiators at these concentrations (**Figure 3.8, lanes 4–6**). However, none of these initiators demonstrated the same level of capture as the previously optimised DPAP (**48**) and MAP (**49**) concentration of 0.5 mM (**Figure 3.8, lane 7**). DPAP (**48**) and MAP (**49**) were therefore retained as the radical initiator and stabiliser in future experiments.

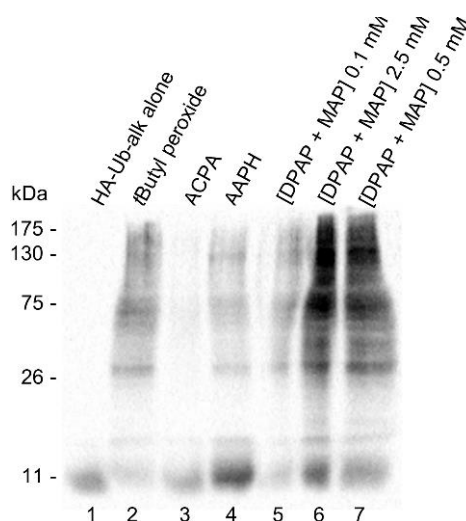


Figure 3.8: Alternative initiator screening. Visualised by anti-HA western blot. HA-Ub₇₅-propene **38** (1 µg) was incubated with HEK 293T lysate (50 µg) for 90 min before the indicated radical initiator was added. All initiators were added at the same concentration (0.5 mM) apart from lanes 5 and 6 which contained 0.1 mM DPAP (**48**) and MAP (**49**) and 2.5 mM DPAP (**48**) and MAP (**49**) respectively. Samples were degassed for 2 min with N₂ and exposed to UV light (365 nm) for 2 min.

In addition to this, DPAP (**48**) and MAP (**49**) were tested at a five-fold increase and five-fold decrease relative to the optimised 0.5 mM (**Figure 3.8, lanes 5 and 6**). The amount of captured protein varied in these samples, increasing or decreasing

corresponding to the change in initiator concentration (**Figure 3.8, lanes 5 and 6**). A second experiment was conducted to investigate if the increase in protein capture observed in the sample containing 2.5 mM of DPAP (**48**) and MAP (**49**) was the result of an increase in the capture of DUBs or an increase of side reactions (**Figure 3.9**). A ten-fold increase in DPAP (**48**) and MAP (**49**) concentrations was investigated in parallel with this five-fold increase.

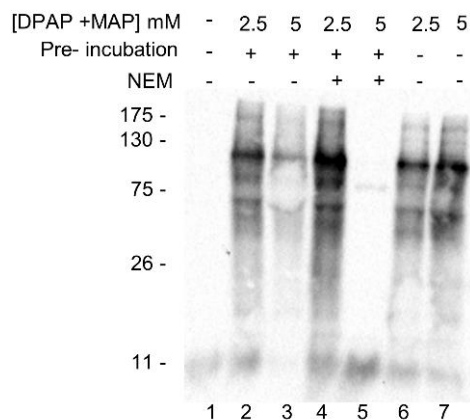


Figure 3.9 Investigating increased concentrations of radical initiators. Visualised by anti-HA western blot. HA-Ub₇₅-propene **38** (1 µg) was incubated with HEK 293T lysate (50 µg) for 90 min before DPAP (**48**) and MAP (**49**) were added at the indicated concentration. Samples were degassed for 2 min with N₂ and exposed to UV light (365 nm) for 2 min.

To validate that these conditions were not promoting off target reactions with other residues, the Cys alkylator NEM was used. At a five-fold increase in concentration significant protein capture is observed, indicating several off-target reactions are occurring (**Figure 3.9, lane 4**). Unexpectedly, less capture is observed in the sample with a ten-fold increase in concentration but in both cases, significant labelling is still visible when the pre-incubation step is omitted (**Figure 3.9, lane 5, 6 and 7**). Consequently, it was concluded that many of the proteins being captured at these concentrations were not specifically interacting with the probe, and off-target reactions were occurring at these higher concentrations. Using higher concentrations of radical initiators was therefore ruled out at this point

A more refined optimisation of the initiator concentration and the time under UV were carried out to investigate if milder conditions could be used to initiate the reaction (**Figure 3.10A and 3.10B**).

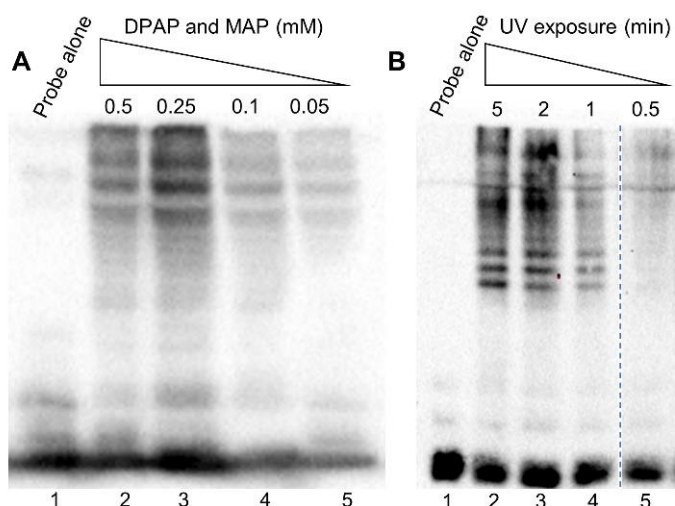


Figure 3.10: Optimisation of reaction conditions. Visualised by anti-HA western blot. (A) HA-Ub₇₅-propene **38** (1 μ g) was incubated with HEK 293T lysate (50 μ g) for 90 min before DPAP (**48**) and MAP (**49**) were added at a range of concentrations. Samples were degassed for 2 min and exposed to UV light (365 nm) for 2 min. (B) Time under UV was investigated using DPAP (**48**) and MAP (**49**) (0.25 mM). The initiators were added to the samples after a 90 min incubation of HA-Ub₇₅-propene **38** (1 μ g) with HEK 293T lysate (50 μ g) and samples were exposed to UV light (365 nm) for the time indicated.

Decreasing concentrations ranging from the optimised 0.5 mM to 0.05 mM were examined (**Figure 3.10A**, lanes 2–5). No decrease in labelling intensity was observed after a reduction in concentration from 0.5 mM to 0.25 mM, but at lower concentrations there was a clear reduction in the number of proteins captured (**Figure 3.10A**, lanes 2–5). Future experiments were therefore carried out at 0.25 mM DPAP (**48**) and MAP (**49**). Similarly, the relative amount of captured proteins appears to decrease as the time under UV is reduced (**Figure 3.10B**, lanes 2–5). In this more refined study, it appears that the reaction is complete after 5 min with no evident difference between this and the 5 min timepoint (**Figure 3.10B**, lanes 2 and 3). Based on these results, DPAP (**48**) and MAP (**49**) were used at a final concentration of 0.25 mM in future experiments. To ensure the reactions had gone to completion, samples were exposed to UV light for 5 min.

3.3 Investigating the specificity of the thiol-ene labelling using PR-619

The specificity of the HA-Ub₇₅-propene probe **38** towards DUBs was investigated by observing the changes in labelling pattern following a preincubation of the known pan DUB inhibitor, PR-619 with cell lysate (**Figure 3.11**).¹⁹³

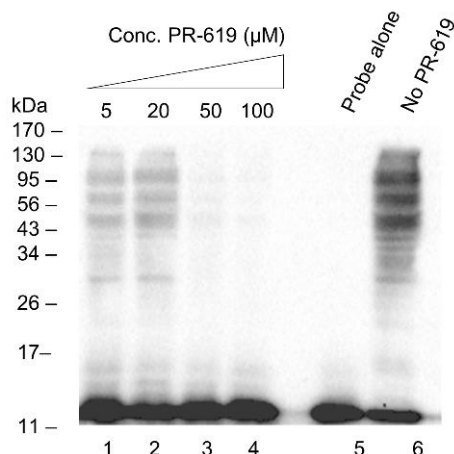


Figure 3.11: Testing specificity with DUB inhibitor PR-619 (55). Visualised by anti-HA western blot. (A) HEK 293T cell lysate (50 μg) was preincubated for 90 min with increasing concentrations of PR-619 before the addition of HA-Ub₇₅-propene **38** (1 μg). Samples were incubated for a further 90 min at 37 °C before DPAP (**48**) (0.25 mM) and MAP (0.25 mM) were added. Samples were degassed for 2 min with N₂ and exposed to UV light (365 nm) for 2 min.

PR-619 was incubated with cell lysate for 30 min prior to the addition of HA-Ub₇₅-propene **38** and the optimised conditions of 0.25 mM initiator and 2 min under UV were used to carry out the labelling. A clear concentration-dependent reduction in labelling intensity was observed in samples where PR-619 was preincubated with the lysate (**Figure 3.11A, lanes 1–4**). This provided compelling evidence that the labelling bands observed in previous experiments represent covalent adducts of the probe bound to DUBs and indicated specificity of the probe towards these enzymes.

To demonstrate how this methodology can be used advantageously in inhibitor studies, an additional experiment was performed whereby the HA-Ub₇₅-propene **38** was preincubated with the lysate to form a binding equilibrium with any DUBs present. PR-619 was added to the samples at concentrations analogous to the previous experiment and incubated for a further 30 min before initiators were added and the samples were exposed to UV light (**Figure 3.12B**). This experiment analysed the displacement of the reversibly bound probe by the inhibitor.

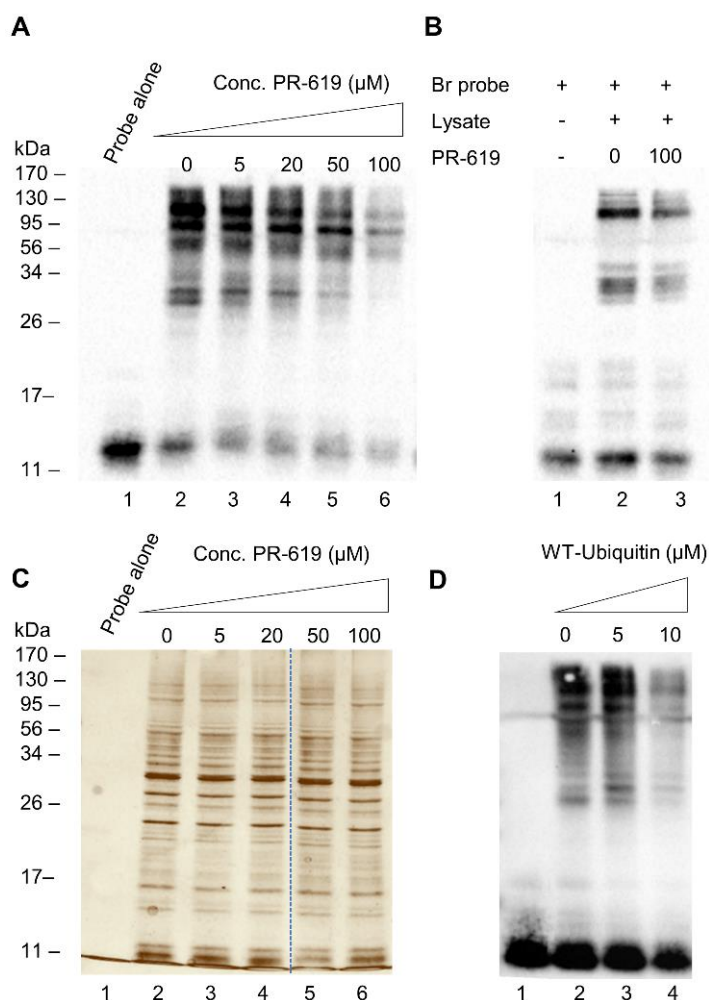


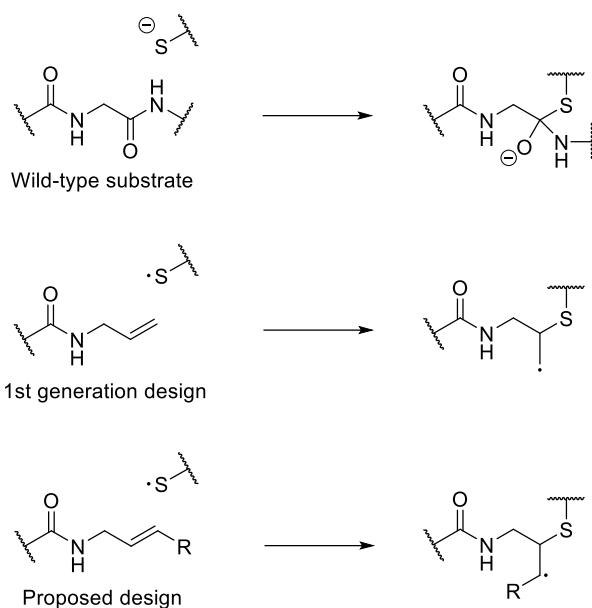
Figure 3.12: Displacement of the probe with inhibitors. Visualised by (A), (B) and (D) anti-HA western blot and (C) Silver stain. (A) and (C) HEK 293T cell lysate (50 μg) was preincubated with HA-Ub₇₅-propene **38** (1 μg) for 90 min before PR-619 was added at increasing concentrations. Samples were incubated for a further 90 min at 37 °C before DPAP (**48**) (0.25 mM) and MAP (0.25 mM) were added. Samples were degassed for 2 min with N₂ and exposed to UV light (365 nm) for 2 min. (B) HEK 293T cell lysate (50 μg) was incubated with HA-Ub₇₅-CH₂CH₂Br **5** and PR-619 (100 μM) was added to one sample. Samples were incubated for a further 90 min at 37 °C before DPAP (**48**) (0.25 mM) and MAP (**49**) (0.25 mM) were added. Samples were degassed for 2 min with N₂ and exposed to UV light (365 nm) for 2 min. (D) HEK 293T cell lysate (50 μg) was preincubated with HA-Ub₇₅-propene **38** (1 μg) for 90 min before WT-ubiquitin was added at increasing concentrations. Samples were incubated for a further 90 min at 37 °C before DPAP (**48**) (0.25 mM) and MAP (**49**) (0.25 mM) were added. Samples were degassed for 2 min with N₂ and exposed to UV light (365 nm) for 2 min.

The inhibition of labelling appears less pronounced than in the previous experiment as access to DUB active sites is limited by the presence of the HA-Ub₇₅-propene probe **38** (Figure 3.12A, lanes 2–6). However, the effect of the inhibitor is clearly

visible, reducing enzyme capture in a concentration dependent manner (**Figure 3.12A, lanes 2–6**). This experiment demonstrated how PR-619 can disrupt the binding of the probe and providing a novel way to study inhibitors. A parallel experiment was performed using the HA-Ub₇₅CH₂CH₂Br probe **5** for contrast (**Figure 3.12B**). When it is subject to identical conditions as lanes 2 and 6, 0 μ M and 100 μ M PR-619 respectively, only a minor reduction in protein capture is observed (**Figure 3.12C, lanes 2 and 3**). These results demonstrated that as the HA-Ub₇₅-CH₂CH₂Br probe **5** reacts once bound by a DUB and does not form the same reversible binding equilibrium as HA-Ub₇₅-propene probe **38**. Therefore, it cannot be used to study inhibitors in the same way. A silver stain was performed for all samples on this gel to confirm the stability of the probe in this experiment (**Figure 3.12C**). Similar results were obtained using an excess of WT ubiquitin in place of PR-619 (**Figure 3.12D**). At higher concentrations the WT ubiquitin disrupted the binding equilibrium of the HA-Ub₇₅-propene probe and reduced overall DUB capture (**Figure 3.12D, lane 4**). These results illustrated how this methodology can be utilised to study reversible protein binding events as well as covalent and irreversible inhibitor interactions. This methodology therefore allows for the study of inhibitors and protein binding events with much greater temporal control, with the potential to provide valuable information about binding affinities.

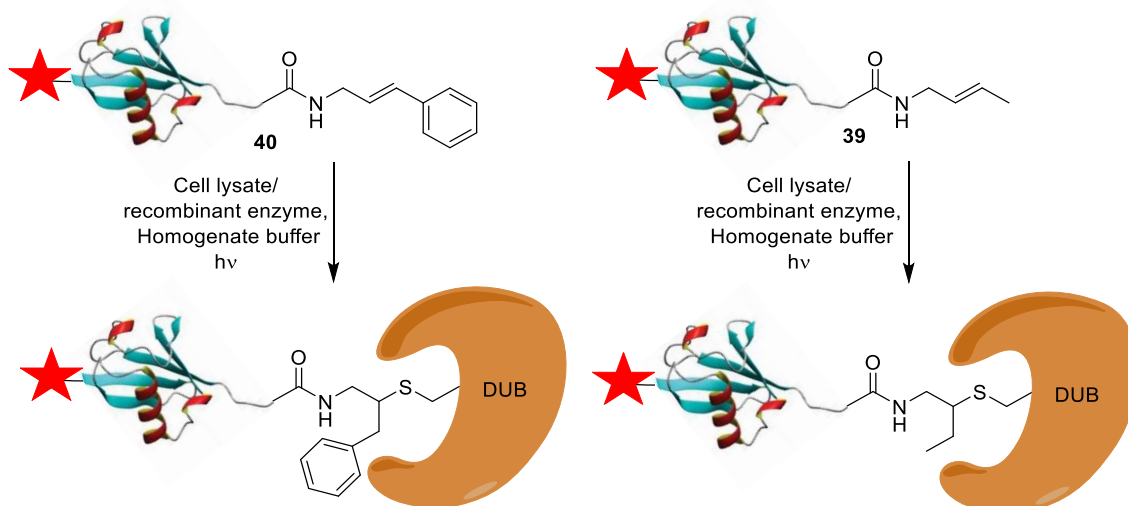
3.4 Design, synthesis and testing of substituted alkene probes.

Two further alkene-based probes were designed and synthesised to study the effects of alkene substitution on labelling efficiency. Assuming the labelling reaction using HA-Ub₇₅-propene **38** forms a covalent bond at the expected site of attack by analogy with the WT substrate, an unstable primary alkyl radical will form (**Scheme 3.3**). If the bond forms at the terminal carbon of the alkene, forming a more stable secondary radical, attack must occur at a non-optimal position. It was hypothesised that if a substituted alkene was used instead of the terminal alkene, attack at the optimal site would form a more stable radical, increasing the efficiency of the reaction (**Scheme 3.3**).



Scheme 3.3: Effect of alkene substitution on potential radical stability. Site of attack on WT DUB substrate and radicals resulting from covalent bond formation at the equivalent position using the thiol-ene labelling.

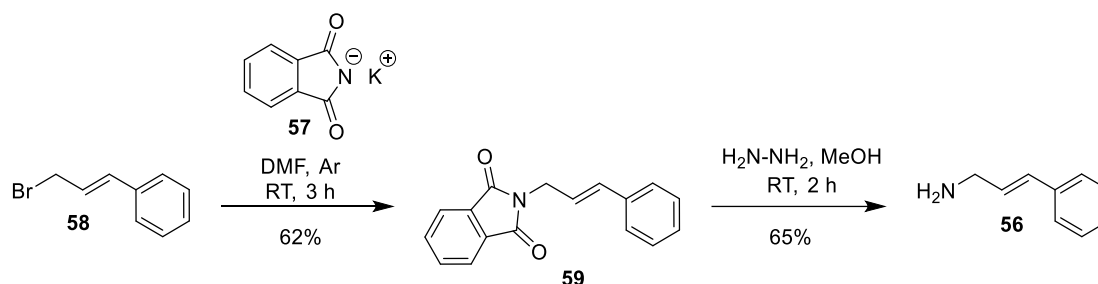
Two new warheads were designed for this purpose (**Scheme 3.4**). The first of these two consisted of a methyl substituted alkene, while the other was a phenyl substituted alkene, affording the HA-Ub₇₅-butene **39** and HA-Ub₇₅-phenylpropene **40** probes respectively.



Scheme 3.4: Structure and reactivity of new alkene probes.

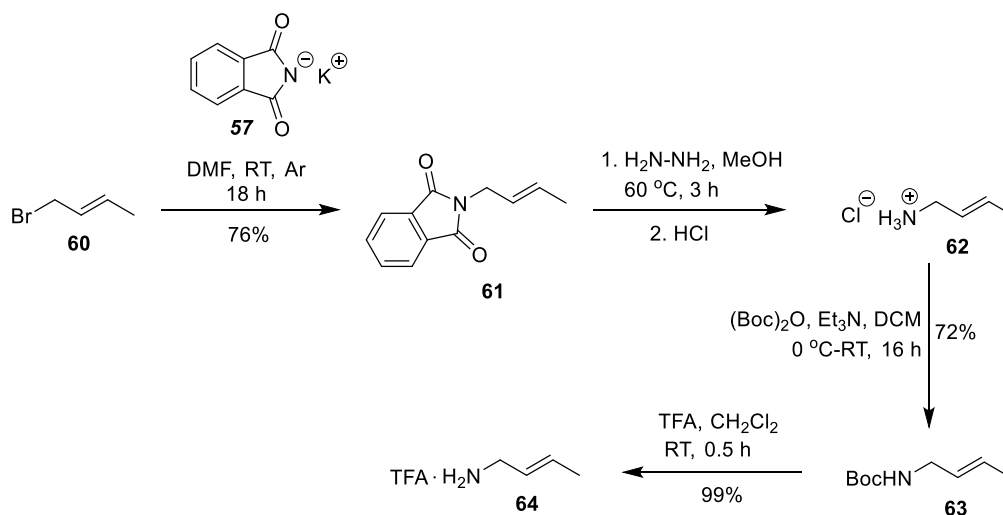
The synthesis of the (*E*)-3-phenylprop-2-en-1-amine warhead (**56**) was carried out using modified literature procedures^{194,195} in a 40% yield over two steps (**Scheme 3.5**). The reaction was carried out using standard Gabriel amine synthesis conditions with potassium phthalimide (**57**) used to introduce amino functionality.

The amine group was freed using hydrazine and the new warhead was available for coupling to the HA-Ub₇₅-thioester **3** as in the synthesis of the HA-Ub₇₅-propene **38**.



Scheme 3.5: Synthesis of (*E*)-3-phenylprop-2-en-1-amine **56.**

The second warhead was synthesised over four steps in 54% yield (**Scheme 3.6**). It was initially synthesised as the (*E*)-but-2-ene-amine hydrochloride salt (**62**) following literature procedures (**Scheme 3.6**).^{196,197} As in the previous synthesis, potassium phthalimide (**57**) was used to introduce amino functionality and hydrazine was employed to deprotect the phthalimide. However, purification of the hydrochloride salt **62** by column chromatography proved difficult due to retention of the salt on silica. To overcome this, the amine was Boc-protected using modified literature procedures¹⁹⁸ and purified by flash column chromatography to afford **63**. The amine was deprotected using standard deprotection conditions¹⁹⁹ and the warhead was available for coupling to the HA-Ub₇₅-thioester **2** as the TFA salt **64**.



Scheme 3.6: Synthesis of (*E*)-but-2-ene-amine trifluoroacetate **64.**

Two new warheads **56** and **64** were successfully synthesised, coupled to the HA-Ub₇₅-thioester **2** and tested in cell lysate (**Figure 3.13**). The new probes, HA-Ub₇₅-butene **39** and HA-Ub₇₅-phenylpropene **40**, both showed restricted

labelling patterns compared to the HA-Ub₇₅-propene **38** (**Figure 3.13**, lanes **1 vs 3** and **5**).

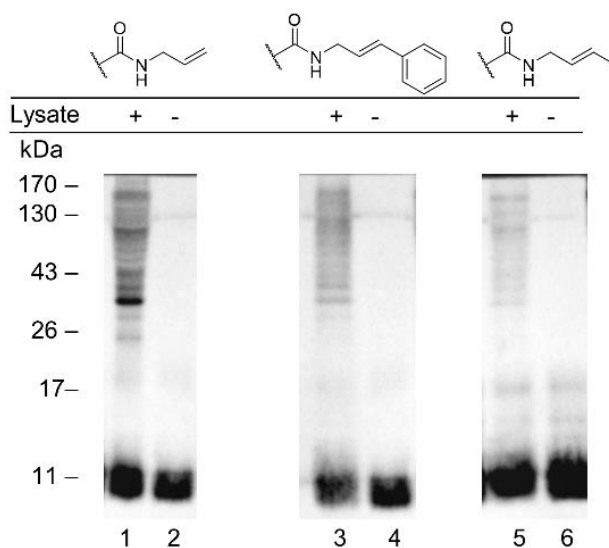


Figure 3.13: Testing of new alkene warheads. Visualised by anti-HA western blot. HA-Ub₇₅-propene **38** (1 μ g), HA-Ub₇₅-phenylpropene **40** (1 μ g) or HA-Ub₇₅-butene **39** (1 μ g) was incubated with HEK 293T lysate (50 μ g) for 90 min before DPAP (**48**) (0.25 mM) and MAP (**49**) (0.25 mM) were added. Samples were degassed for 2 min with N₂ and exposed to UV light (365 nm) for 2 min.

These results suggest that the least sterically hindered warhead reacts most efficiently, despite the potential formation of a less stable radical. Conversely, when comparing HA-Ub₇₅-butene **39** and HA-Ub₇₅-phenylpropene **40** there is an apparent reduction in labelling intensity (**Figure 3.13**, lane **3 vs 5**). It is important to note that the efficiency of the coupling reaction for the different warheads during probe synthesis was not quantified so the differences in labelling efficiency observed could be explained by different levels of coupling. Furthermore, the coupling reaction for the HA-Ub₇₅-butene probe **39** required modification as the warhead was synthesised as the TFA salt. The reduction in labelling intensity may be due to a less efficient coupling as the reaction was not optimised in this case. A more definitive comparison can therefore be drawn between the HA-Ub₇₅-phenylpropene **40** and HA-Ub₇₅-propene **39** probes. Additionally, these probes represented the biggest contrast in terms of steric bulk and potential radical stability so were both taken forward for further analysis at this point.

3.5 Immunoprecipitation analysis of thiol-ene labelling

An immunoprecipitation was carried out on material captured by a thiol-ene labelling to unambiguously identify the enzymes captured by the probe and compare the reactivity of the HA-Ub₇₅-propene probe **38** to the HA-Ub₇₅ phenylpropene probe **40**. As discussed, the protocol for the immunoprecipitation was optimised using the HA-Ub₇₅-CH₂CH₂Br probe **5** (**Section 2.3.1, figure 2.7**). To confirm compatibility of the thiol-ene labelling strategy with these conditions, it was first carried out on a small scale (**Figure 3.14A and B**). Additionally, one extra elution step was introduced at this point in addition to the Gly elution. Following this elution, the anti-HA coupled agarose beads were incubated at 95 °C for 5 min in reducing sample buffer as in the previous immunoprecipitation. This step was introduced to help visualise the efficiency of the Gly elution and allow for any proteins still bound after this elution to be included in subsequent analysis.

Western blotting revealed both eluates afforded pulled down material with labelling patterns consistent to the initial lysate labelling, or input (**Figure 3.14A and B, lanes 1, 7 and 8**). Once again, the heavy and light chains of the antibodies are visible in these samples around 26 kDa and 43 kDa (**Figure 3.14A and B, lanes 7 and 8**). Silver staining of the same samples revealed that although some material remained bound following incubation in the Gly buffer, most of the sample was eluted in this step. The difference between the two elution steps was more apparent using this technique (**Figure 3.14B, lane 7 vs 8**). Furthermore, silver staining also confirmed that the four washing steps effective in removing all detectable unbound material (**Figure 3.14B, lane 6**). These results suggested that the conditions optimised using the HA-Ub₇₅-CH₂CH₂Br probe translated well to the thiol-ene methodology on this smaller scale.

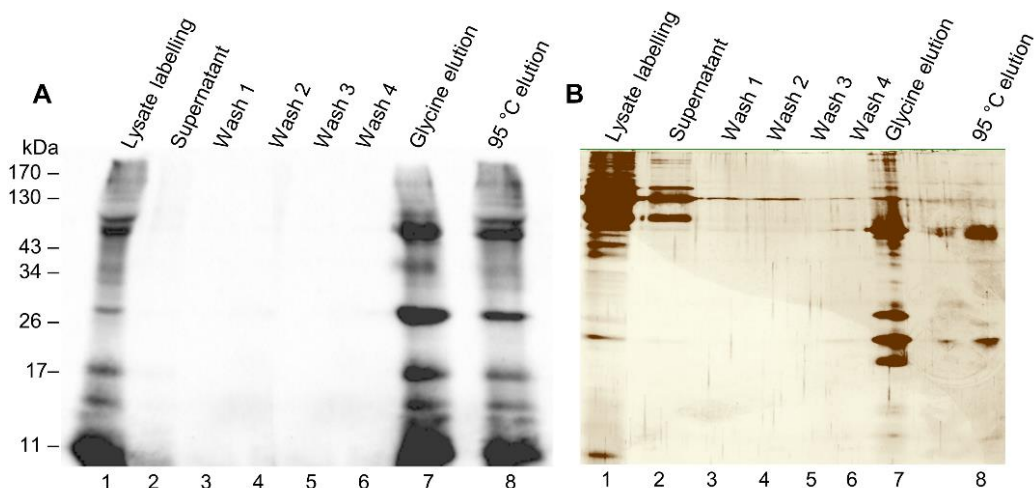


Figure 3.14: Optimisation of immunoprecipitation conditions. Visualised by (A) anti-HA western blotting or (B) silver staining. A standard labelling was carried out under optimised conditions using HEK 293T cell lysate (150 μ g) with HA-Ub₇₅-propene **38** (3 μ g) in NET buffer. The pull-down was performed with anti-HA coupled agarose beads (60 μ L of 50% slurry) for 90 min at 4 °C. After a series of washing steps, equivalent fractions of the input, supernatant and washes were taken.

The remainder of the eluate samples were subjected to a tryptic digest and submitted for analysis by LC-MS/MS. Although the immunoprecipitation appeared to work well when analysed by gel electrophoresis methods, a very limited number of proteins were confidently identified in a search against a Uniprot database of human proteins. It was expected that proteins visible by silver staining would also be identified by LC-MS/MS due to the high sensitivity of this technique. It was therefore hypothesised that either the exposure to UV light or subsequent off-target radical reactions were resulting in the formation of undesired protein adducts which were affecting the identification of the peptides. To investigate this hypothesis, a series of lysate samples were exposed to a variety of conditions in which the time under UV and the presence of initiators were varied (**Table 3.1**). To replicate the conditions of the immunoprecipitation as accurately as possible the samples were incubated at 4 °C for 2 h following this treatment and then analysed by LC-MS/MS.

Entry	UV (min)	Initiators	Protein IDs	≥ 80% confidence
1	0	No	2775	612
2	5	Yes	2578	30
3	1	Yes	2225	540
4	2	Yes	2835	471
5	5	No	1938	10

Table 3.1: Protein IDs by LC-MS/MS following UV light and radical exposure. All samples contained HEK 293T cell lysate (50 µg). Samples treated with radical initiators contained DPAP (**48**) (0.25 mM) and MAP (**49**) (0.25 mM) and the UV light wavelength was 365 nm. After treatment samples were subject to tryptic digest then desalted and concentrated by zip-tipping prior to analysis by LC-MS/MS.

A control sample was left untreated and incubated for 2 hrs at 4 °C (**Table 3.1, entry 1**). A total of 2775 proteins were identified in this sample, with 612 of these having over 80% confidence (**Table 3.1, entry 1**). Conversely, in the sample that was exposed to standard labelling conditions, a similar number of proteins were identified but a much smaller fraction of these had confidence level over 80% (**Table 3.1, entry 2**). To examine if this reduction in confidence was primarily due to the UV light or off-target radical reactions, samples were prepared in which the effect of one of these variables was limited or removed (**Table 3.1, entries 3–5**). When UV exposure was reduced to 1 min or 2 min and the radical initiator concentration was kept consistent, a significant improvement in confidently identified proteins (**Table 3.1, entry 3 and 4**). In contrast to this, when the time under UV remained at 5 min and radical initiators were omitted, protein confidence was comparable to standard labelling conditions (**Table 3.1, entry 5**). Based on these results, it was concluded that the exposure time to UV was significantly degrading the protein sample by 5 min and this was affecting peptide identification by LC-MS/MS. To overcome this, the exposure time for a standard labelling reaction was reduced to 2 min. Although a drop in confidently identified proteins is observed between the 1 min and 2 min time points, previous experiments demonstrated that there was a substantial difference between these time points in terms of protein capture (**Section 3.2.2, Figure 3.10, lanes 3 vs 4**). In the same experiment, no difference was seen between 2 min and 5 min timepoints.

Using these newly optimised conditions of 2 min exposure to UV light, another immunoprecipitation was carried out (**Figure 3.15**). In addition to these new conditions, two minor changes were made to the protocol. Firstly, the initial labelling was carried out on a larger scale than previously, with 5 μg of probe compared to 3 μg . Concentrations of the other components of the reaction were increased accordingly with the aim of increasing the final amount of enriched material. Additionally, the elution step in Gly buffer was increased in time from 30 sec to 2 min with the microcentrifuge tube being inverted twice during this time ensuring the beads were fully resuspended each time. This was done to ensure complete elution of bound material during this step.

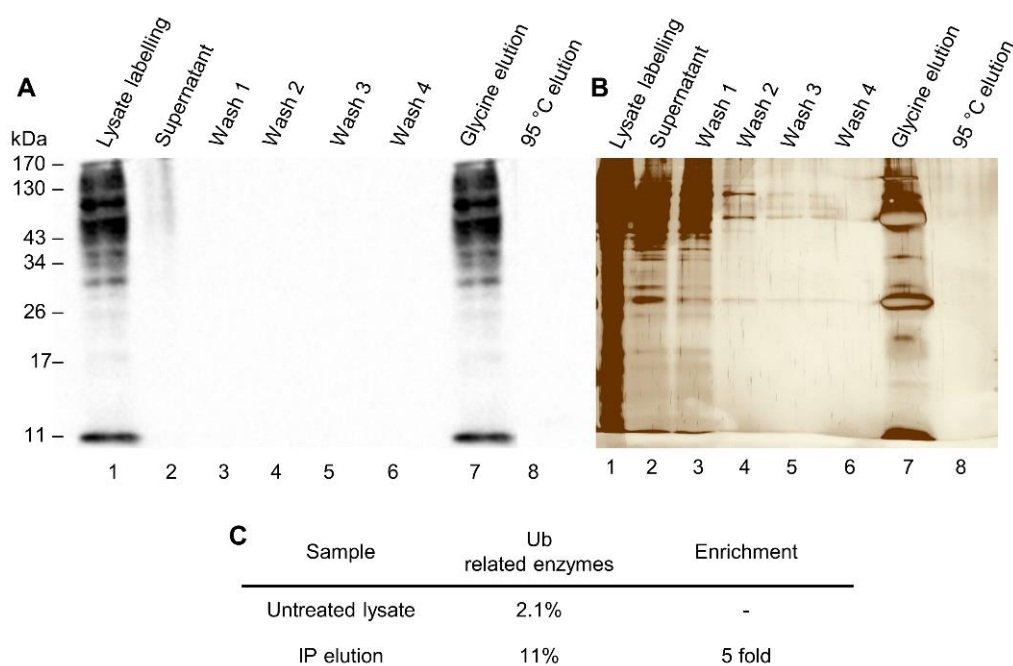


Figure 3.15: Optimisation of immunoprecipitation conditions. Visualised by (A) anti-HA western blotting or (B) silver stain. A standard labelling was carried out under optimised conditions using HEK 293T cell lysate (250 μg) with HA-Ub₇₅-propene **38** (5 μg) in NET buffer. The pull-down was performed with anti-HA coupled agarose beads (100 μL of 50% slurry) for 90 min at 4 °C. After a series of washing steps, equivalent fractions of the input, supernatant, washes and eluate samples were taken. (C) The remainder of the input and eluate samples were digested using trypsin and then desalted and concentrated by zip-tipping prior to analysis by LC-MS/MS.

Analysis by silver staining and western blotting confirmed that the immunoprecipitation successfully enriched for captured material (**Figure 3.15A and B**). The changes to the protocol resulted in an increased amount of protein visible in the Gly elution relative to previous gels, and all proteins appeared to be

eluted in this step (**Figure 3.15A and B, lanes 7 and 8**). As with previous immunoprecipitations the labelling pattern observed in the elution lane is consistent with that of the input lane (**Figure 3.15A, lane 1 vs 7**). The remainder of the eluate sample was digested and analysed by LC-MS/MS. An equivalent fraction of the input sample was also digested in parallel (**Figure 3.15A**). In contrast to previous results several proteins were confidently identified in both samples with a five-fold enrichment of DUBs and ubiquitin conjugation machinery in the eluate sample relative to the input (**Figure 3.15C**). These were promising initial results that suggested specificity of the HA-Ub₇₅-propene probe **38** towards these enzymes. As no negative control was run in parallel, no more quantification was carried out at this stage.

One further experiment was carried out following this immunoprecipitation. Sections of the Gly elution lane were excised and were subjected to an in-gel digest (**Table 3.2**). A selection of DUBs and members of the conjugation machinery were identified in these samples. These were largely found in the section of the gel corresponding to their MW (**Table 3.2**). These result once more pointed towards specificity of the HA-Ub₇₅-propene probe **38** towards DUBs. However, to confirm this, an immunoprecipitation was carried out in with an appropriate negative control to allow for definitive quantification of enrichment.

kDa	Section	Protein ID	MW	Type
170 –	A	UBP32	182 kDa	DUB
130 –		UBP8	127 kDa	DUB
95 –		UBP21	113 kDa	DUB
72 –	B	UBP37	110 kDa	DUB
43 –		UBP13	97 kDa	DUB
34 –		UI7L3	81 kDa	DUB
		UBP14	75 kDa	DUB
		UBP27	60 kDa	DUB
26 –		DCST9	56 kDa	E3
	TRIM18	50kDa	E3	
	C	MYCB2	51 kDa	E3
17 –		RNF26	47 kDa	E3
		UBE2A	17 kDa	E2
	D	-		
11 –	E	Ub		Probe

Table 3.2: In-gel digestion and LC-MS/MS analysis of immunoprecipitation eluate. Indicated sections were excised from the gel and subjected to an in-gel digestion using trypsin. Resulting samples were desalted and concentrated by zip-tipping prior to analysis by LC-MS/MS.

An immunoprecipitation was carried out in triplicate using the HA-Ub₇₅-propene **38** and HA-Ub₇₅-phenylpropene **40** probes. The results were analysed by both western blot analysis and LC-MS/MS (**Figures 3.16 and 3.17**).

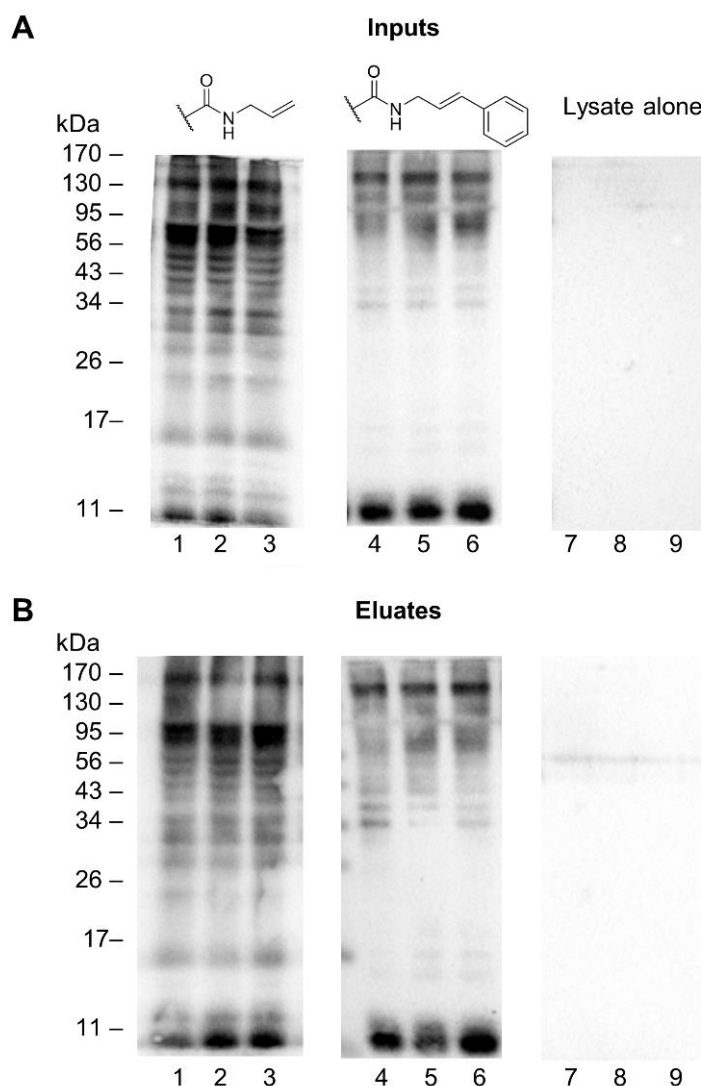


Figure 3.16: Analysis of immunoprecipitation. Visualised by anti-HA western blot. A standard labelling was carried out in triplicate under optimised conditions using HEK 293T cell lysate (250 μ g) with HA-Ub₇₅-propene **38** (5 μ g), HA-Ub₇₅-phenylpropene **40** (5 μ g) or no probe in NET buffer. (A) A fraction of this labelling was taken for analysis. The pulldown was performed with anti-HA coupled agarose beads (100 μ L of 50% slurry) for 90 min at 4 °C. (B) After a series of washing steps, equivalent fractions of the eluate samples were taken for analysis.

A labelling was performed under optimised conditions with each probe and a small fraction of the sample was removed for analysis by anti-HA western blot (**Figure 3.16A, lanes 1–6**). The only variable in the negative control sample was the exclusion of any probe, the sample was otherwise treated identically (**Figure 3.16A,**

lanes 7–9). The proteins were then enriched using agarose beads coupled to anti-HA antibodies and an equivalent fraction of the resulting sample was again analysed by anti-HA western blot (**Figure 3.16B**).

For both probes, comparison of the inputs against the eluate samples confirms the labelling and the subsequent immunoprecipitation were successful (**Figure 3.16A and B**). The remainder of the eluate sample was subjected to tryptic digest and submitted for analysis by LC-MS/MS. The samples were analysed using label-free quantification (LFQ). This is a method whereby the abundance of each protein detected in sample is quantified relative to a negative or positive control run in parallel. The results of this analysis are expressed as a relative intensity and visualised as a heat map (**Figure 3.17**). The replicate that had the highest intensity for an individual protein was taken as 100% and if that protein was detected in another sample, its intensity was expressed as a percentage of this.

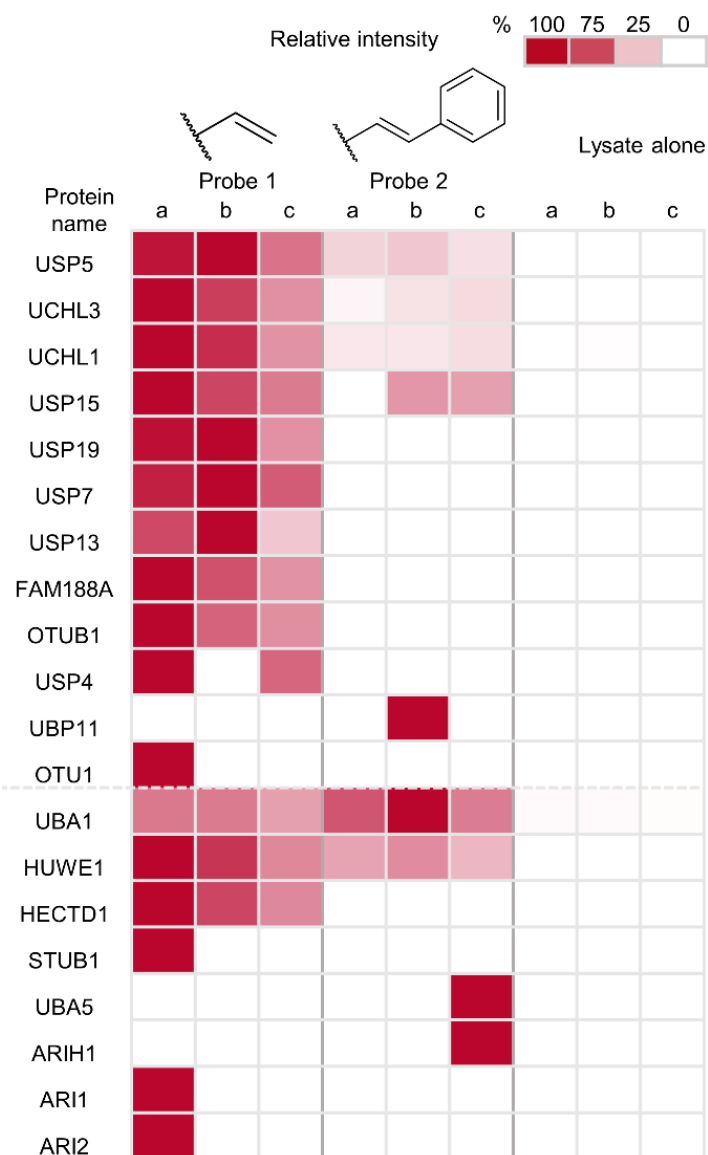


Figure 3.17: LC-MS/MS analysis of immunoprecipitation in triplicate. Heatmap showing the enrichment of DUBs and ubiquitin conjugation machinery after immunoprecipitation with anti-HA coupled agarose beads using HA-Ub₇₅-propene **38**, HA-Ub₇₅-phenylpropene **40** and lysate alone. Intensities calculated using label-free quantification following LC-MS/MS analysis. The replicate that had the highest intensity for each individual enzyme was taken as 100% and the values of other replicates for the enzyme are expressed as a percentage of this value.

Twelve DUBs were identified following the IP as well as eight components of the ubiquitin conjugation machinery. Enrichment of eleven DUBs was observed in samples treated with the HA-Ub₇₅-propene probe **38** (Figure 3.17). Some enrichment was also seen for HA-Ub₇₅-phenylpropene **40**, although this was less pronounced (Figure 3.17). The HA-Ub₇₅-propene probe **38** therefore yields more efficient capture in this case. This finding further indicates that less steric bulk is

favoured over the formation of a more stable radical species, consistent with the earlier western blot results (**Section 3.4, Figure 3.13**).

Additionally, enrichment of ubiquitin conjugation machinery was also observed in both cases. Our probe design is therefore also applicable to labelling the less nucleophilic active site Cys of these enzymes. Interestingly, the HA-Ub₇₅-phenylpropene **40** warhead appeared to be more efficient at capturing these conjugation machinery enzymes, even enriching for enzymes not observed in any of the replicates for the alkene probe. This result may be an indication that these enzymes have a greater tolerance for the extra steric bulk of this probe

3.6 Conclusion

In conclusion, a novel activity-based monoubiquitin probe that is completely inactive under ambient conditions and can be selectively activated to label DUBs and enzymes of the ubiquitin conjugation machinery was synthesised. This occurs via a thiol-ene reaction between the active site Cys of the enzyme and an alkene warhead on the probe. This is the first successful application of thiol-ene chemistry in ABPP. The probe's reactivity was demonstrated against recombinant, purified DUB OTUB1 and HEK 293T lysate and the methodology was made compatible for downstream analysis by LC-MS/MS. Experiments using heat and SDS treated recombinant enzyme showed the probe is selective for the active form of the DUB, requiring a specific binding interaction. This new HA-Ub₇₅-propene probe **38** was also used to study the effects of inhibitors displacing bound probe, providing novel information about these binding interactions. Finally, DUB selectivity was shown using a combination of inhibitor assays and immunoprecipitations and this selectivity could be influenced by the addition groups proximal to the alkene.

The short activation period of the probe following specific binding provides a snapshot of the DUBs bound at that time. The consequence of capturing the equilibrium in such a way results in a small proportion of DUBs captured relative to similar existing probes. However, it does provide an opportunity to study binding affinity and inhibitor potency in new ways for both reversible and irreversible binding interactions. Unlike existing photocrosslinking probes this technique offers a residue specific method to provide a time-resolved readout of enzyme activity rather than protein binding. This radical labelling approach is broadly applicable and provides

further opportunities in chemical proteomics beyond the study of reactivity and selectivity in the ubiquitin system as any enzyme bearing an active site Cys could be targeted in this way. The alkene moiety is chemically inert and sterically undemanding to introduce to other biological entities, such as carbohydrates, DNA or inhibitor scaffolds to access a wide variety of enzyme classes.

4 Towards the application of the thiol-ene reaction for ABPP in cells

The thiol-ene methodology developed in Chapter 3 was optimised to effectively profile DUB activity in HEK 293T cell lysate. Certain aspects of this methodology make it unsuitable for whole cell analysis. The UV photoreactor consisted of ten 8 W UV bulbs. These levels of UV light exposure afforded a rapid and extremely time-resolved reaction, but extended exposure times resulted in degradation of proteins, which was observed by SDS-PAGE and LC-MS/MS analysis (**Section 3.2.2, Figure 3.6**). It was anticipated that even short exposures would be cytotoxic if applied to whole cells. Additionally, such photoreactors are not in widespread use in biological contexts, limiting the accessibility of the technique. Finally, the oxygen sensitivity of the reaction would be limiting in more complex systems.

In this chapter, two routes towards a milder photoinitiation of the thiol-ene coupling were explored. Firstly, a weaker source of UV irradiation was investigated using the previously optimised conditions with DPAP (**48**) and MAP (**49**) (**Figure 4.1A**). Low wattage UV lamps are widely available and offer a more affordable and milder alternative to the previously used photoreactor.

Secondly, the radical initiators Eosin Y (**30**) and Bi_2O_3 were examined as alternatives to DPAP (**48**) and MAP (**49**) (**Scheme 4.1B**). Both Eosin Y (**30**) and Bi_2O_3 have been demonstrated to catalyse thiol-ene coupling reactions of biomolecules using only visible light.^{147,200} Additionally, Eosin Y (**30**) has been used to generate thiyl radicals for Cys arylation reactions on peptides and is known to be cytocompatible at micromolar concentrations.^{146,201} Eosin Y (**30**) is often used in combination with a coinitiator such as triethanolamine, but recent studies have demonstrated that it can be used as the sole photoinitiator to generate thiyl radicals.²⁰⁰ Furthermore, these couplings did not require degassing, and are tolerant of oxygen.²⁰⁰ Therefore, it was hypothesised that Eosin Y (**30**) would provide a milder photoinitiation by avoiding the need for UV light, while also eliminating the requirement for a degassing step. Conversely, couplings reported using Bi_2O_3 required degassing and the inclusion of an organohalide, BrCCl_3 , as a chain carrier.¹⁴⁷ Bi_2O_3 has also been used as part of a nanocomposite to catalyse a thiol-ene coupling.¹⁴⁹ The cytocompatibility of Bi_2O_3 and BrCCl_3 are not well characterised. However due the relative simplicity of the

system and previously demonstrated tolerance in biomolecule functionalisation they were examined for use in ABPP.

A combination of recombinant enzyme and cell lysate studies were used to evaluate Eosin Y (**30**) and Bi_2O_3 as initiators for this templated thiol-ene reaction. Both ambient light and a 10 W white light source were employed, and the concentration and time dependencies of the reaction were examined. Additionally, the distance from the light source was varied.

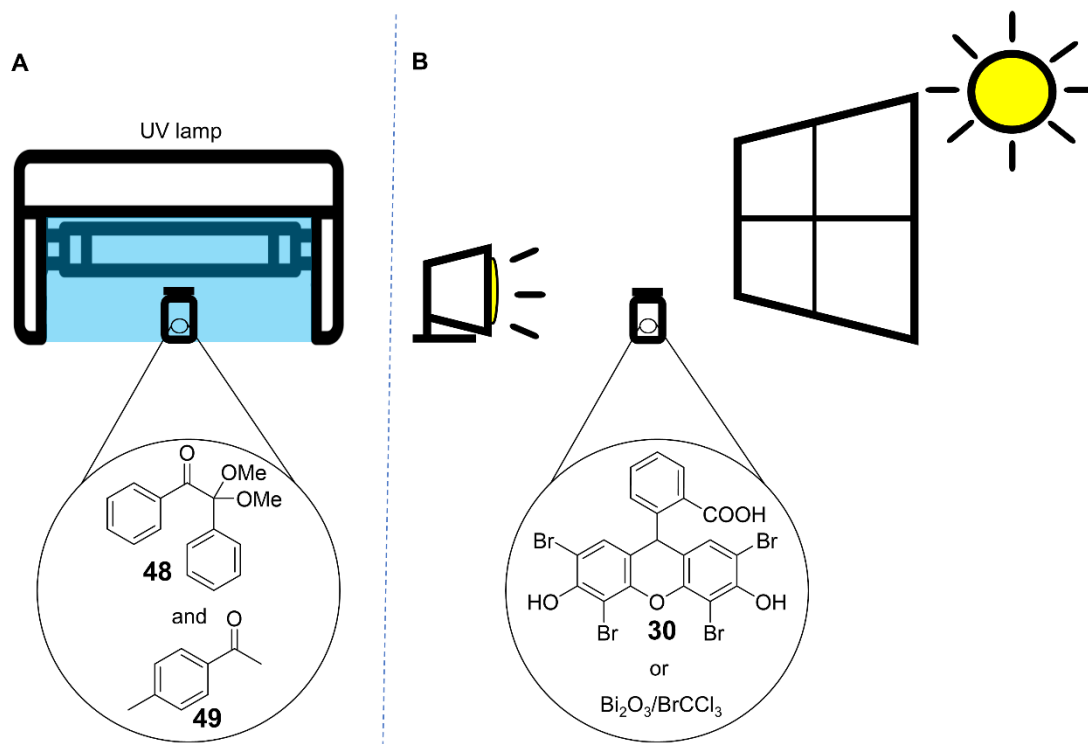
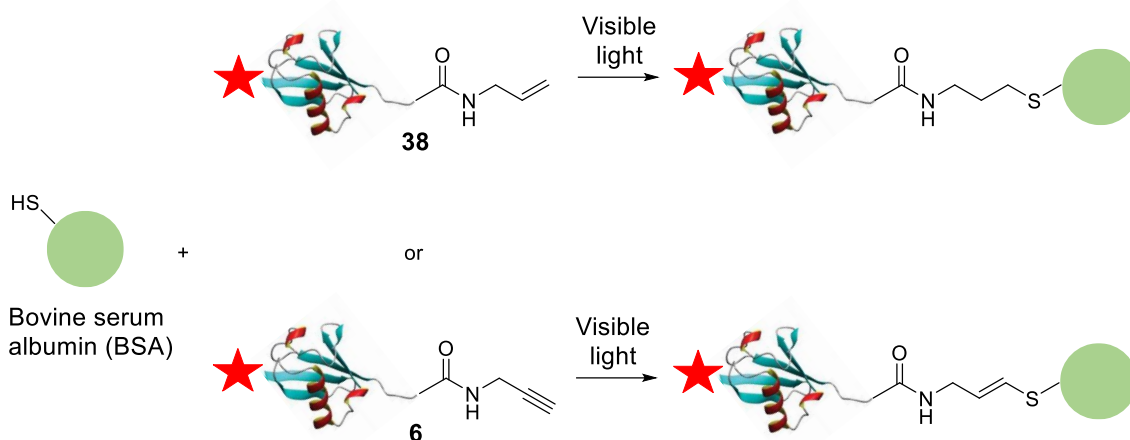


Figure 4.1. Further development of the thiol-ene reaction in biological systems. (A) A milder source of UV was investigated using conditions optimised in Chapter 3. (B) Visible light induced thiol-ene reaction was examined using the initiators Eosin Y (**30**) and Bi_2O_3 .

Further studies were carried out with Eosin Y (**30**) to assess its ability to catalyse a non-templated thiol-ene reaction between the HA-Ub₇₅-propene probe **38** and BSA. Although the thiol-ene reaction has been used previously to conjugate proteins in this non-templated manner, this required UV light irradiation.¹³⁷ Achieving comparable coupling efficiency with visible light would significantly improve the biocompatibility of the reaction, providing a mild and facile route towards protein conjugation. Further to this, carrying out the analogous thiol-yne coupling with HA-Ub₇₅-PA **6** and BSA could potentially be used to afford a dimer with an alkene positioned between the monomers. The resulting conjugate could therefore be designed to mimic specific ubiquitin dimer linkages or known ubiquitination targets

and used for ABPP using the thiol-ene methodology. Once more, ambient light and a 10 W source of white light were employed to initiate the thiol-ene and thiol-yne reactions using BSA as a model system (**Scheme 4.1**).



Scheme 4.1: Visible light-mediated thiol-ene and thiol-yne coupling of HA-Ub₇₅ probes and BSA.

4.1 Examining a milder UV source for the thiol-ene methodology

In order to evaluate the use of a commercially available UV lamp to initiate labelling, a time-course was performed using the conditions optimised in Chapter 3 (**Section 3.2.2**), with a low wattage UV lamp in place of the UV photoreactor (**Figure 4.2**). This lamp consisted of four 9 W UV bulbs, compared to ten 8 W bulbs in the photoreactor, resulting in a significantly lower cumulative UV exposure. The HA-Ub₇₅-propene probe **38** was used in this experiment and all others in this chapter unless stated otherwise.

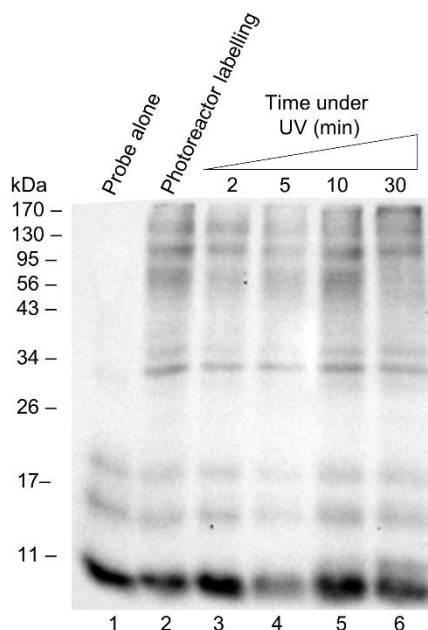


Figure 4.2: Time dependence of low wattage UV lamp light exposure time. Visualised by anti-HA western blot. HA-Ub₇₅-propene **38** (1 µg) was incubated with HEK 293T cell lysate (50 µg) at 37 °C with gentle shaking in homogenate buffer for 60 min. DPAP (**48**) (0.25 mM) and MAP (**49**) (0.25 mM) were added, the samples were degassed for 2 min with N₂ and then exposed to UV light (365 nm) for 2 min in a UV photoreactor or the indicated time (2–30 min) in a low wattage UV lamp.

As a positive control, a standard labelling reaction was carried out in the UV photoreactor (**Figure 4.2, lane 2**). A series of exposure times, ranging from the optimised photoreactor time of 2 min to 30 min were examined using the low wattage UV lamp (**Figure 4.2, lanes 3–6**). Comparison of the 2 min timepoint for both conditions showed reduced labelling intensity for the milder source of UV (**Figure 4.2, lane 2 vs 3**). By the 10 min timepoint, labelling intensity is comparable to that seen for the optimised methodology (**Figure 4.2, lane 2 vs 5**). Interestingly, no degradation of the sample is observed at the 30 min timepoint (**Figure 4.2, lane 6**). Using the original conditions, sample degradation was typically observed at this timepoint using western blot analysis (**Section 3.2.2, Figure 3.6, lanes 5–7**). From these observations it was concluded that using this milder source of UV sacrifices some of the time resolution but still maintains a rapid coupling with greater preservation of protein integrity. It is expected that this change would greatly enhance the cytocompatibility of the methodology while also improving its accessibility due to the significantly lower cost of equipment.

4.2 Ambient light-mediated thiol-ene labelling experiments

4.2.1 Recombinant enzyme ambient light labelling

To investigate whether ambient light could initiate the thiol-ene coupling reaction, a recombinant enzyme experiment was performed using Eosin Y (**30**) as the only initiator in place of DPAP (**48**) and MAP (**49**) (**Figure 4.3A and B**). The concentration of Eosin Y (**30**) was consistent with that of DPAP (**48**) and MAP (**49**), 0.25 mM, which were also used as a positive control. Both samples underwent a 90 min pre-incubation and were degassed for 2 min prior to the addition of initiators, as previously optimised. The sample containing DPAP (**48**) and MAP (**49**) was exposed to UV light for 10 min in the low wattage UV lamp using the newly optimised conditions. As it was assumed radical initiation would be slower under ambient light, this reaction was incubated for 30 min following the addition of Eosin Y (**30**) at a concentration of 0.25 mM. The resulting samples were analysed by anti-HA western blot and silver staining (**Figure 4.3A and B**).

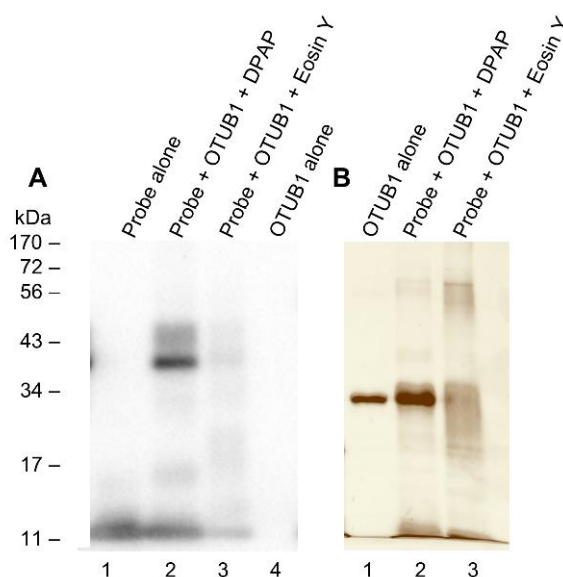


Figure 4.3: Comparative labelling of recombinant OTUB1 using DPAP (48**) and MAP (**49**) or Eosin Y (**30**).** Visualised using (A) Anti-His western blot; (B) silver stain. HA-Ub₇₅-propene **38** (3 µg) was incubated with OTUB1 (2 µg) at 37 °C with gentle shaking in homogenate buffer for 90 min. DPAP (**48**) (0.25 mM) and MAP (**49**) (0.25 mM) or Eosin Y (**30**) (0.25 mM) were added, the samples were degassed for 2 min with N₂ and then exposed to UV light (365 nm) for 10 min or ambient light for 30 min.

As expected, a new band was visible by anti-HA western blot and silver staining around the 43 kDa marker using the original conditions (**Figure 4.3A and B, lane 2**).

By western blot, no corresponding band was seen in the sample incubated with Eosin Y (**30**) (**Figure 4.3A, lane 3**). However, a faint streak was visible around the expected molecular weight, with similar streaking observed for the unbound probe in the same sample (**Figure 4.3A, lane 3**). It was hypothesised that significant protein degradation was causing a loss of signal. To investigate this, a silver stain was performed with all samples containing OTUB1 (**Figure 4.3B**). By comparison of the OTUB1 alone lane and the sample treated with Eosin Y (**30**) (**Figure 4.3B, lane 1 vs 3**), it is apparent the protein sample was degraded. The faint labelling observed by western blot indicated that some labelling may have been achieved but substantial optimisation of the reaction was required.

The first variable examined to avoid this degradation was the Eosin Y (**30**) concentration (**Figure 4.4**). As degradation was observed at the optimised DPAP (**48**) and MAP (**49**) concentration (250 μ M), lower concentrations were examined. The incubation time with Eosin Y (**30**) was also reduced to 10 min to avoid this degradation, and the degassing step was omitted to examine the air sensitivity of the reaction.

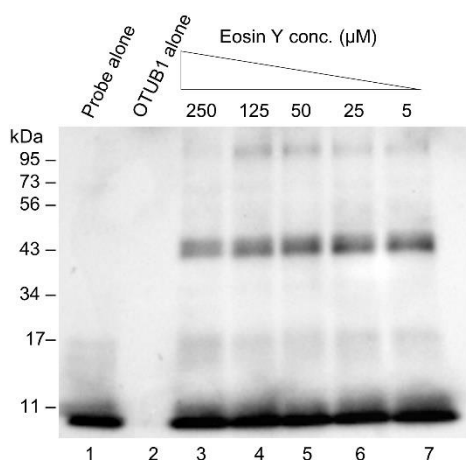


Figure 4.4: Concentration dependence of recombinant OTUB1 labelling using Eosin Y (30). Visualised by anti-HA western blot. HA-Ub₇₅-propene **38** (3 μ g) was incubated with OTUB1 (2 μ g) at 37 °C with gentle shaking in homogenate buffer for 90 min. Eosin Y (**30**) was added at the indicated concentration and the samples were exposed to ambient light for 10 min.

The reduced incubation time and/or the lack of degassing had a positive effect on the labelling reaction (**Figure 4.4, lane 3**). A clear band was visible by anti-HA western blot at the 43 kDa marker for all concentrations tested in this assay (**Figure 4.4, lanes 3–7**). Surprisingly, only minor concentration dependence was

observed for the reaction (**Figure 4.4, lanes 3–7**). At the highest concentrations tested less labelling was observed (**Figure 4.4, lanes 3 and 4**). OTUB1 capture appeared to peak at the 50 μM concentration point with no major drop in capture by the final concentration which is ten-fold lower in Eosin Y (**30**) concentration (**Figure 4.4, lanes 5–7**). Encouragingly, the conjugation of the HA-Ub₇₅-propene probe **38** to OTUB1 can be carried out using only ambient light at significantly lower concentrations than DPAP (**48**) and MAP (**49**). Furthermore, this conjugation did not require a degassing step.

The incubation time of the sample after the addition of Eosin Y (**30**) was examined further (**Figure 4.5**). The HA-Ub₇₅-propene probe **38** was preincubated with OTUB1 for 90 min followed by the addition of Eosin Y (**30**) and incubation for a range of times. Samples were analysed by anti-HA western blot (**Figure 4.5**).

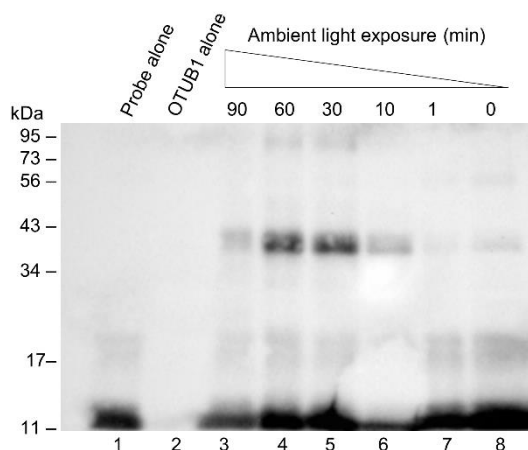


Figure 4.5: Time dependence of recombinant OTUB1 labelling using Eosin Y (30). Visualised by anti-HA western blot. HA-Ub₇₅-propene **38** (3 μg) was incubated with OTUB1 (2 μg) at 37 °C with gentle shaking in homogenate buffer for 90 min. Eosin Y (**30**) (5 μM) was added and the samples were exposed to ambient light for the indicated time.

A time dependent increase in OTUB1 capture was observed until the 30 min timepoint (**Figure 4.5, lanes 5–8**). Beyond this timepoint, no increase in labelling was observed, with similar capture seen after 60 min (**Figure 4.5, lane 4**). By the longest timepoint, 90 min, sample degradation had occurred (**Figure 4.5, lane 3**). Based on these results it was concluded that a 30 min incubation following Eosin Y (**30**) addition was optimal for a labelling using ambient light at this concentration.

4.2.2 HEK 293T lysate experiments using ambient light

The ambient light labelling methodology was next examined in cell lysate. An initial experiment was performed comparing the concentration used for DPAP (**48**) and MAP lysate labellings, 0.25 mM, to the concentration reported by Shih *et al.* for an Eosin Y (**30**) catalysed thiol-ene reaction using visible light (**Figure 4.6**).²⁰⁰ Additionally, an analogous experiment was performed using Bi₂O₃ and BrCCl₃, also comparing the optimised DPAP (**48**) and MAP (**49**) concentration to that reported by Fadeyi *et al.* (**Figure 4.6**).¹⁴⁷

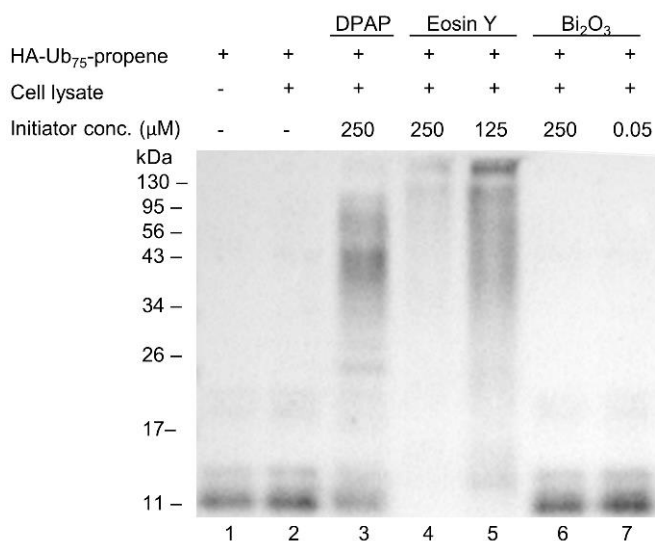


Figure 4.6: Ambient light catalysed labelling of HEK 293T lysate. Visualised by anti-HA western blot. HA-Ub₇₅-propene **38** (1 μg) was incubated with HEK 293T cell lysate (50 μg) at 37 °C with gentle shaking in homogenate buffer for 90 min. Eosin Y (**30**), DPAP (**48**) and MAP (**49**) or Bi₂O₃ and BrCCl₃ were added at the indicated concentrations and the samples were degassed for 2 min with N₂. Samples containing DPAP (**48**) and MAP (**49**) were exposed to UV light (365 nm) in the low wattage UV lamp for 10 min and all other samples were exposed to ambient light for 30 min.

As a positive control, a labelling was carried out using the optimised DPAP (**48**) and MAP (**49**) conditions (**Figure 4.6, lane 3**). As with the recombinant enzyme labelling, substantial protein degradation was seen at Eosin Y (**30**) concentrations equivalent to those optimised for DPAP (**48**) and MAP (**49**) (**Figure 4.6, lane 4**). At the lower Eosin Y (**30**) concentration, less damage was observed, and a streaking was apparent at higher molecular weight (**Figure 4.6, lane 5**). Neither concentration of Bi₂O₃ and BrCCl₃ resulted in any detectable labelling (**Figure 4.6, lanes 6 and 7**). No loss of signal was observed for the unbound probe band of these samples when

compared to the equivalent band in the probe alone lane (**Figure 4.6, lanes 1 vs 6 and 7**). This implied the absence of labelling was due to the lack of radical initiation rather than protein damage. Ambient light catalysed labelling with Bi₂O₃ was therefore not pursued any further. As with the recombinant enzyme studies, initial experiments using Eosin Y (**30**) in lysate showed that protein degradation occurred, and further optimisation was required.

A concentration dependence experiment was performed using the same concentrations as the OTUB1 labelling (**Figure 4.7**). As before, following a preincubation of 90 min, Eosin Y (**30**) was added to the reaction which was incubated for a further 10 min.

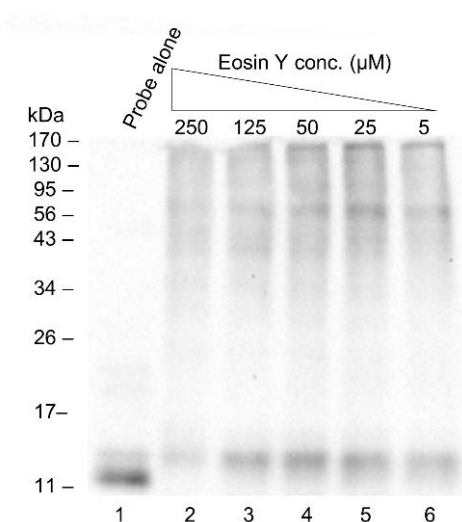


Figure 4.7: Concentration dependence of HEK 293T cell lysate labelling using Eosin Y (30). Visualised using anti-HA western blot. HA-Ub₇₅-propene **38** (1 µg) was incubated with HEK 293T cell lysate (50 µg) at 37 °C with gentle shaking in homogenate buffer for 90 min. Eosin Y (**30**) was added at the indicated concentration and the reaction was exposed to ambient light for 30 min.

As in the OTUB1 labelling and the initial cell lysate experiment, streaking and loss of signal are observed at the highest concentration, indicating the integrity of the protein sample was compromised (**Figure 4.7, lane 2**). Protein capture peaks at the 50 µM and 25 µM concentrations (**Figure 4.7, lanes 4 and 5**) before a drop in intensity at the lowest concentration, 5 µM (**Figure 4.7, lane 6**). A time dependence analysis was therefore carried out using the 25 µM concentration (**Figure 4.8**).

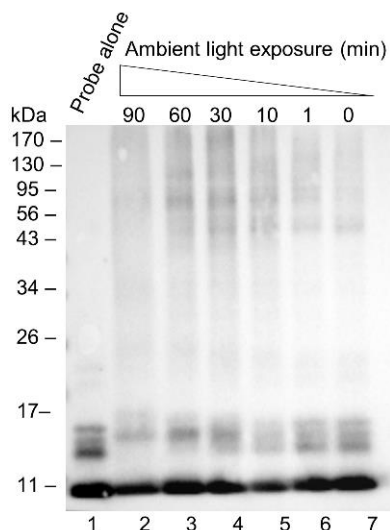


Figure 4.8: Time dependence of HEK 293T cell lysate labelling using Eosin Y (30). Visualised by anti-HA western blot. HA-Ub₇₅-propene **38** (1 µg) was incubated with HEK 293T cell lysate (50 µg) at 37 °C with gentle shaking in homogenate buffer for 90 min. Eosin Y (**30**) (25 µM) was added and the reaction was exposed to ambient light for the indicated time.

As expected, streaking and loss of signal was observed at the longest timepoint of 90 min (**Figure 4.8, lane 2**). As with the recombinant enzyme labelling, signal intensity peaks after a 30 min incubation (**Figure 4.8, lane 4**), indicating maximum protein capture has occurred by this time. There is a time-dependent decrease in labelling intensity at shorter intervals (**Figure 4.8, lanes 5–7**). It was noted that protein labelling appeared less efficient under these conditions in cell lysate relative to the optimised DPAP (**48**) and MAP (**49**) labelling conditions. Additionally, problems with reproducibility were encountered as there was limited control over the levels of ambient light.

4.3 Controlled visible light source thiol-ene labelling experiments

4.3.1 Recombinant enzyme 10 W lamp thiol-ene labelling

To overcome the reproducibility problems and provide a stronger, more controlled light source, a 10 W white lamp was introduced. To analyse the dependence of the reaction on the light source, three OTUB1 labellings were carried out in parallel and analysed by anti-HA western blot and silver staining (**Figure 4.9A and B**). The conditions optimised for the ambient light labelling of OTUB1 were used in each case.

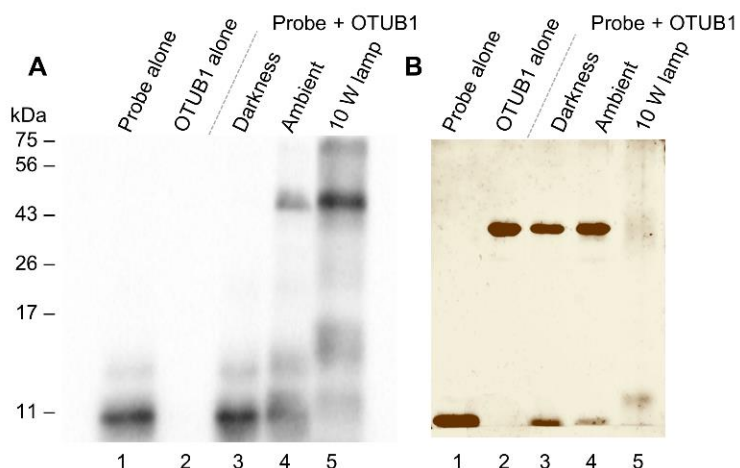


Figure 4.9: Comparative labelling of recombinant OTUB1 in darkness, ambient light or using a 10 W light source. Visualised using (A) Anti-His western blot, (B) silver stain. HA-Ub₇₅-propene **38** (3 µg) was incubated with OTUB1 (2 µg) at 37 °C with gentle shaking in homogenate buffer for 90 min. Eosin Y (**30**) (5 µM) was added, the samples were incubated for 30 min either in the dark, exposed to ambient light for or exposed to white light (10 W) from 10 cm.

A covalent adduct was formed at the expected molecular weight when HA-Ub₇₅-propene **38** was incubated with OTUB1 and Eosin Y (**30**) while exposed to ambient light (**Figure 4.9A, lane 4**). To confirm the requirement of light to initiate the labelling, a control experiment was carried out in which the sample was incubated in darkness (**Figure 4.9A and B, lane 3**). No band corresponding to the probe-OTUB1 adduct is visible in this sample, signifying that without light no radical reaction is initiated and no covalent bonds are formed (**Figure 4.9A and B, lane 3**). The adduct band is clearly visible by anti-HA western blot in the sample irradiated with the 10 W lamp (**Figure 4.9A, lane 5**). The band formed is more intense than that seen for the sample exposed to ambient light (**Figure 4.9A, lanes 4 and 5**). However, the increased capture was offset by the increased sample damage which is particularly evident by silver staining (**Figure 4.9A and B, lane 5**).

It was anticipated that increasing the distance between the sample and the light source would maintain a strong labelling reaction while avoiding sample degradation. According to Lambert's law, when the distance from the light source is doubled, the light intensity reaching the sample is a quarter of the original intensity. This was investigated in an OTUB1 labelling experiment and analysed by western blotting and silver staining (**Figure 4.10A and B**).

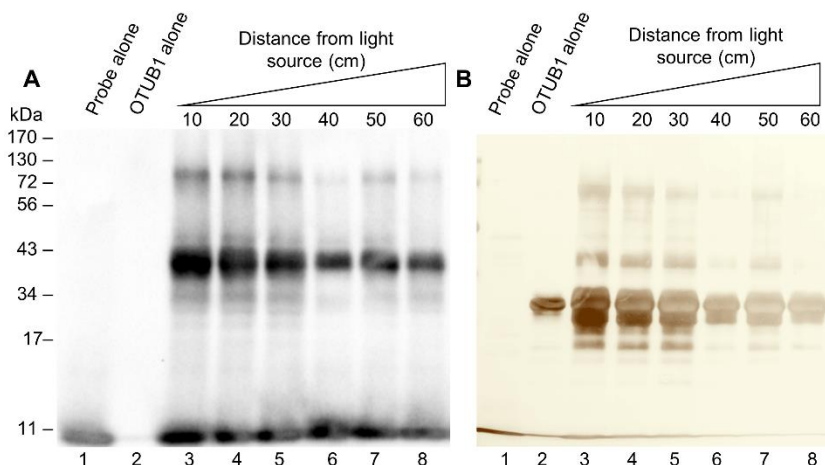


Figure 4.10: Lamp distance variation for OTUB1 labelling. Visualised using (A) Anti-His western blot, (B) silver stain. HA-Ub₇₅-propene **38** (3 µg) was incubated with OTUB1 (2 µg) at 37 °C with gentle shaking in homogenate buffer for 90 min. Eosin Y (**30**) (5 µM) was added, the samples were either incubated in the dark for 10 min, exposed to ambient light for 10 min or exposed to white light (10 W) from the indicated distance for 10 min.

Based on the previous experiment, a 30 min exposure from 10 cm was too long, so the irradiation time was reduced to 10 min (**Figure 4.10A and 4.10B**). Covalent adduct formation was observed by anti-HA western blot and silver stain at all distances tested (**Figure 4.10A and 4.10B, lanes 3–8**). A decrease in adduct formation was seen as the distance was increased in 10 cm increments (**Figure 4.10A and 4.10B, lanes 3–8**). The formation of lower molecular weight bands representing broken down protein also reduced as this distance was increased (**Figure 4.10A and 4.10B, lanes 3–8**). To maintain sufficient adduct formation for detection by silver staining while also limiting protein damage, a distance of 50 cm was considered optimal based on these results. However, it is expected that the optimal distance will change if the initiator concentration or light exposure time is changed.

The formation of an unanticipated band at the 72 kDa marker was also observed in all samples containing the probe and OTUB1 (**Figure 4.10A and B**). It is possible that this band represented off-target crosslinking. The molecular weight of this band is consistent with an adduct between the HA-Ub₇₅-propene probe **38** and two OTUB1 enzymes. Its formation was more pronounced at closer lamp distances, suggesting it is dependent on radical initiation suggesting Eosin Y (**30**) is causing off-target crosslinking.

4.3.2 HEK 293T lysate experiments using a 10 W lamp

Initial experiments aiming to initiate a thiol-ene coupling in cell lysate using ambient light using Bi_2O_3 and BrCCl_3 were unsuccessful (**Section 4.2.2, Figure 4.6, lanes 6 and 7**). A similar experiment was conducted to investigate if higher light intensity and longer incubation times would facilitate a coupling in lysate (**Figure 4.11**). A standard HEK 293T lysate labelling using optimised DPAP (**48**) and MAP (**49**) conditions was included as a positive control (**Figure 4.11, lane 2**).

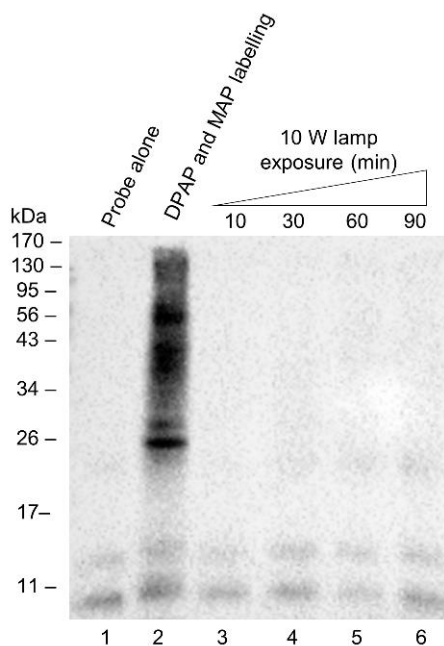


Figure 4.11: Time dependence of HEK 293T cell lysate labelling using Bi_2O_3 and BrCCl_3 . Visualised by anti-HA western blot. HA-Ub₇₅-propene **38** (1 μg) was incubated with HEK 293T cell lysate (50 μg) at 37 °C with gentle shaking in homogenate buffer for 90 min. Bi_2O_3 (250 μM) and BrCCl_3 (600 μM) were added and the samples were degassed for 2 min with N_2 . Samples were exposed to white light (10 W) from 5 cm for the indicated time.

Samples were exposed to white light from 5 cm, and the initiator concentration was the same as the optimised DPAP (**48**) and MAP (**49**) concentrations. At the shortest timepoint tested, no labelling is apparent (**Figure 4.11, lane 3**). Labelling increased slightly as the exposure time increased up to 90 min (**Figure 4.11, lanes 4–6**). Despite indications that some labelling was occurring, it was deemed not worth pursuing any further due to the relative success of Eosin Y (**30**) (**Section 4.2.2**).

For Eosin Y (**30**), when ambient light was used to initiate the reaction, samples in lysate required higher initiator concentrations compared to recombinant enzyme labelling under ambient light (**Section 4.2, Figure 4.4 vs Section 4.2.2, Figure 4.7**).

To explore if lower concentrations could be used when higher intensity light was applied, a concentration dependence study was carried out (**Figure 4.12**). Irradiation time and lamp distance were kept consistent with optimised conditions for OTUB1 labelling.

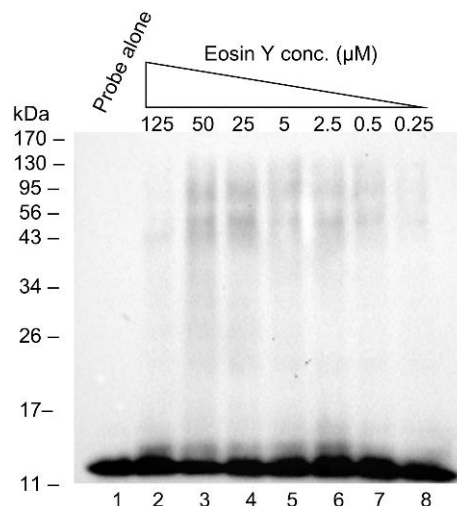


Figure 4.12: Concentration dependence of HEK 293T cell lysate labelling using Eosin Y (30). Visualised by anti-HA western blot. HA-Ub₇₅-propene **38** (1 μg) was incubated with HEK 293T cell lysate (50 μg) at 37 °C with gentle shaking in homogenate buffer for 90 min. Eosin Y (**30**) was added at the indicated concentration and exposed to white light (10 W) for 10 min from 50 cm.

Interestingly, even with the additional light intensity, similar initiator concentrations to the ambient light experiment were required to achieve maximal labelling (**Figure 4.7 vs Figure 4.12**). Increased sample degradation was observed at the 125 μM concentration (**Figure 4.12, lane 2**) but protein capture peaks around the 50 μM and 25 μM concentrations as before (**Figure 4.12, lanes 3 and 4**). Additionally, the increase in labelling intensity moving from ambient light exposure to white light exposure from the lamp was not comparable to that seen for OTUB1. To examine if altering either the distance from the light source or the irradiation time would improve this labelling, both these parameters were varied (**Figure 4.13A and B**).

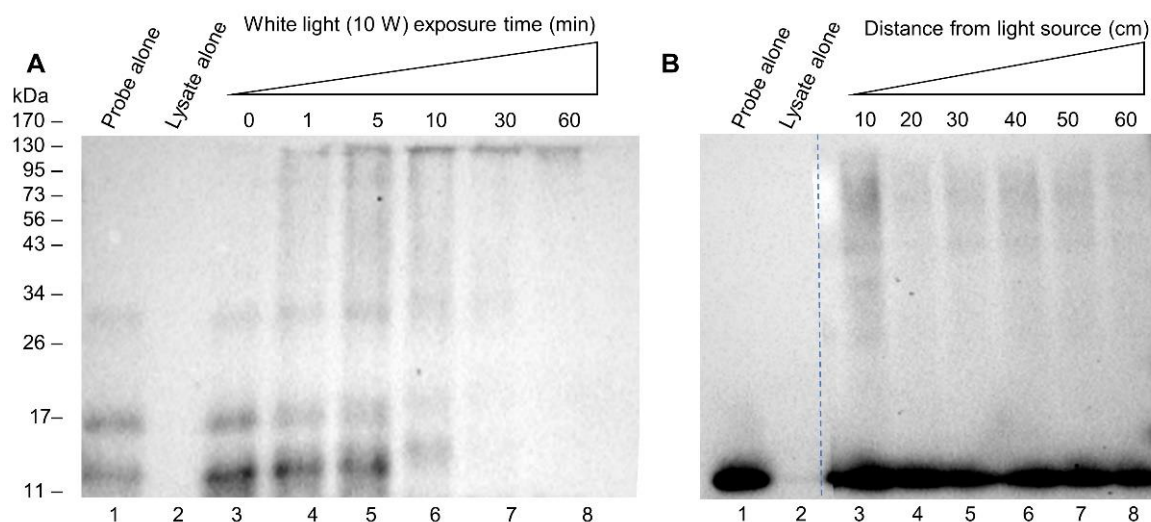


Figure 4.13: Time dependence of HEK 293T cell lysate labelling using Eosin Y (30). Visualised by anti-HA western blot. HA-Ub₇₅-propene **38** (1 μ g) was incubated with HEK 293T cell lysate (50 μ g) at 37 °C with gentle shaking in homogenate buffer for 90 min. Eosin Y (**30**) (50 μ M) was added and reactions were exposed to white light (10 W) for (A) a range of times from 50 cm or (B) 10 min from a range of distances.

As anticipated, longer exposure times led to a loss of signal due to protein damage (**Figure 4.13A, lanes 6–8**). The optimal exposure time appeared to be 5 min but only a very faint signal was detected (**Figure 4.13A, lane 5**). Similarly, only weak labelling was obtained when the distance from the light source was varied (**Figure 4.13B**). A closer distance of 10 cm proved optimal for a cell lysate labelling at this concentration and exposure time (**Figure 4.13B, lane 3**). The addition of the high intensity light source did not have the desired effect on the labelling reaction in cell lysate. It was apparent that ABPP using Eosin Y (**30**) was significantly more successful in recombinant enzyme studies than in more complex cell lysate.

4.4 Investigating the influence of degassing on the Eosin Y catalysed labelling

The omission of a degassing step was one of the primary advantages of this methodology. However, in a bid to improve reactivity in cell lysate the importance of this step was analysed. Firstly, recombinant OTUB1 labellings were carried out at increasing concentrations of Eosin Y (**30**) with evaluation of the degassing step at each concentration (**Figure 4.14A and B**).

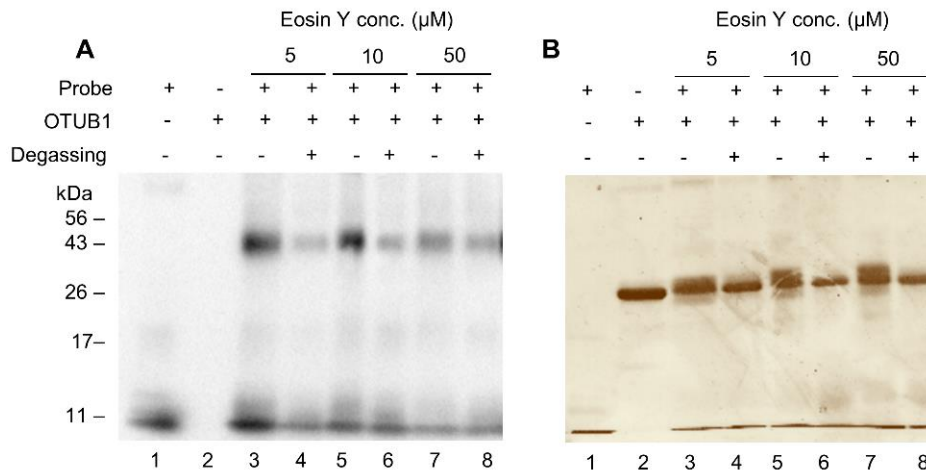


Figure 4.14: Effect of degassing of recombinant enzyme sample on labelling using Eosin Y (30). Visualised using (A) Anti-His western blot; (B) silver stain. HA-Ub₇₅-propene 38 (3 μg) was incubated with OTUB1 (2 μg) at 37 °C with gentle shaking in homogenate buffer for 90 min. Eosin Y (30) was added at the indicated concentration and indicated samples were degassed for 2 min using N₂. Samples were exposed to white light (10 W) for 5 min from 50 cm.

Unexpectedly, despite avoiding some protein degradation, degassing reduced the extent of labelling at all concentrations examined (**Figure 4.14A and B, lanes 3–8**). This was attributed to the mechanical stress of the degassing step, which involved bubbling gas through the sample, reducing enzyme activity. An equivalent experiment was carried out using cell lysate to see if the same phenomenon was observed (**Figure 4.15**).

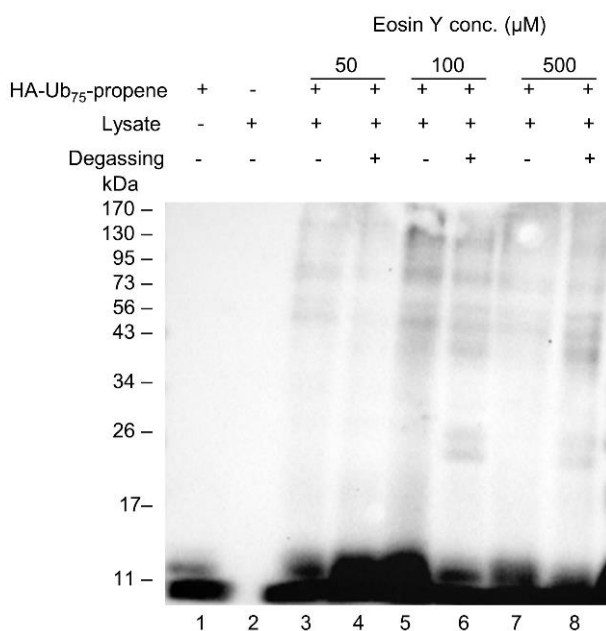


Figure 4.15: Effect of degassing of HEK 293T cell lysate sample on labelling using Eosin Y (30). Visualised by anti-HA western blot. HA-Ub₇₅-propene **38** (1 μg) was incubated with HEK 293T cell lysate (50 μg) at 37 °C with gentle shaking in homogenate buffer for 90 min. Eosin Y (**30**) was added at the indicated concentration and indicated samples were degassed for 2 min using N₂. Samples were exposed to white light (10 W) for 10 min from 10 cm.

A similar reduction in labelling intensity as a result of degassing was not observed in cell lysate (**Figure 4.15**). However, there was no improvement in protein capture at any of the concentrations examined (**Figure 4.15, lanes 3–8**). Following these experiments, it was concluded that a degassing step was not required in future experiments and its omission was not causing the lack of reactivity observed in cell lysate. Instead it was hypothesised that unanticipated off-target reactivity of Eosin Y (**30**) may be affecting the reaction in this more complex system.

4.5 Investigating the off-target reactivity of Eosin Y

4.5.1 Fluorescent gel studies

Eosin Y (**30**) is known to associate with positively-charged amino acids *via* electrostatic interactions and its binding to proteins has previously been well characterised.^{202,203} It is plausible that in cell lysate experiments, Eosin Y (**30**) was being sequestered by off-target proteins due to these interactions. It was noted that the unbound probe band was often shifted slightly higher in molecular weight in previous western blots (**Section 4.3.1, Figure 4.9**). This was particularly apparent

for conditions that resulted in high protein degradation. This was consistent with the hypothesis that Eosin Y (**30**) as binding to off-target proteins and being sequestered.

To investigate the potential off-target reactivity of Eosin Y (**30**), two fluorescent gels were performed along with an anti-HA western blot (**Figure 4.16A, B and C**).

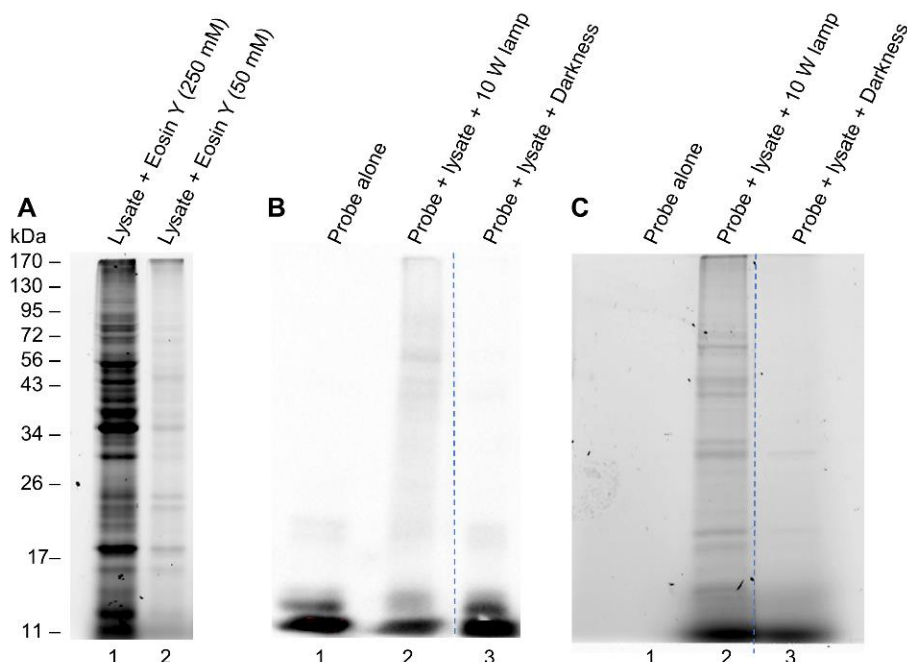


Figure 4.16: Formation of Eosin Y (30**) adducts following visible light excitation.** Samples were visualised by (A) and (C) fluorescent imaging or (B) anti-HA western blot. HA-Ub₇₅-propene **38** (1 μ g) was incubated with HEK 293T cell lysate (50 μ g) at 37 °C with gentle shaking in homogenate buffer for 90 min. Eosin Y (**30**) (50 μ M or as indicated) was added and reactions were exposed to white light (10 W) from 10 cm for 10 min or kept in darkness for 10 min.

Two reactions were carried out in parallel, comparing a higher Eosin Y (**30**) concentration of 0.25 mM, at which protein degradation was previously observed, to the newly optimised 50 μ M for cell lysate reaction (**Figure 4.16A**). Using fluorescent gel imaging, Eosin Y (**30**) adducts were visible at both concentrations and, as expected, less adducts formed at the lower concentration (**Figure 4.16A, lane 1 vs 2**). To elucidate if these adducts were the result of off-target radical reactions, a negative control reaction was carried out in darkness (**Figure 4.16B and C**). No labelling was observed by western blot without light exposure, indicating no radical reaction was initiated (**Figure 4.16B, lane 2**). Similarly, when the same sample was visualised by fluorescent imaging, negligible protein-Eosin Y adducts were observed despite their formation in the analogous light-exposed sample

(**Figure 4.16C, lane 2 vs 3**). These results strongly suggested that Eosin Y (**30**) was reacting with off-target amino acid residues in a radical-dependent manner.

To elucidate if the low abundance of specific amino acids within the OTUB1 sequence resulted in it being highly compatible with Eosin Y (**30**), further experiments were carried out with a second recombinant DUB UCHL1. Labelling reactions were carried out for the recombinant enzymes OTUB1 and UCHL1 using optimised conditions for DPAP (**48**) and MAP (**49**) and Eosin Y (**30**) (**Figure 4.17A and B**). Lysate labellings using the optimised conditions for both initiators were also carried out to observe if a greater reduction in labelling intensity was seen in this case relative to the recombinant enzymes (**Figure 4.17A**).

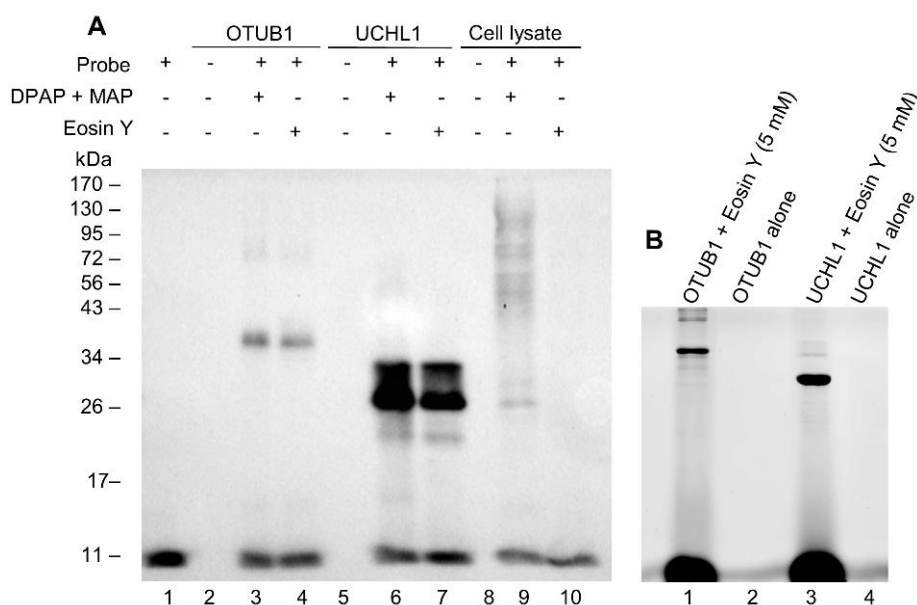


Figure 4.17: Comparing DPAP (48**) and MAP (**49**) labelling to Eosin Y (**30**) labelling for recombinant enzyme and cell lysate.** Visualised using (A) anti-HA western blot or (B) fluorescent imaging. HA-Ub₇₅-propene **38** (3 μ g) was incubated with OTUB1 (2 μ g), UCHL1 (2 μ g) or cell lysate (150 μ g) at 37 °C with gentle shaking in homogenate buffer for 90 min. Eosin Y (**30**) (5 μ M for recombinant enzyme or 50 μ M for cell lysate) was added and reactions were exposed to white light (10 W) from 50 cm for recombinant enzyme or 10 cm for lysate for 10 min. Upon completion, 2X reducing sample buffer (30 μ L) was added and the proteins were heated to 95 °C for 5 min.

For the recombinant enzyme experiments, comparable probe-enzyme binding was achieved using both initiators (**Figure 4.17A, lanes 3 vs 4, 6 vs 7**). Conversely, a clear reduction in enzyme capture was observed between the optimised DPAP (**48**) and MAP (**49**) conditions relative to Eosin Y (**30**) in cell lysate (**Figure 4.17A, lane 9 vs 10**). Interestingly, adduct formation between enzyme and Eosin Y (**30**)

was observed for both OTUB1 and UCHL1 using fluorescence imaging (**Figure 4.17B, lanes 1 and 3**). Despite differing abundances of key amino acids, no significant differences were seen in probe-enzyme labelling or adduct formation for the recombinant enzymes (**Figure 4.17A and B**). For example, OTUB1 does not contain any Trp residues. Therefore, Trp alone is not responsible for either the loss in reactivity moving into lysate or the off-target adduct formation. Both OTUB1 and UCHL1 consist of relative high amounts of positively charged amino acids. It was therefore unlikely that sequestering of Eosin Y (**30**) by these amino acids was the major cause of the problems observed moving into cell lysate. Notably, the HA-Ub₇₅ recognition element does not contain any Cys residues and adduct formation was also seen for this protein (**Figure 4.17B, lanes 1 and 3**).

4.5.2 Analysing the effects of certain amino acids on the Eosin Y labelling

To better characterise the influence of different amino acid side chains, a series of OTUB1 labelling experiments were conducted in which an excess of several amino acids were included in the reaction (**Figure 4.18**). Additionally, the tripeptide glutathione (GSH) was also used in a similar experiment at a physiologically relevant concentration. GSH is an important cellular component responsible for reducing oxidative stress within the cell and is typically present at a concentration of 0.5 mM to 10 mM.²⁰⁴ Another experiment was carried out in which BSA was added in 24-fold excess (**Figure 4.18**). The abundance of the positively charged amino acids Lys, arginine (Arg) and His in BSA is 10%, 4.3% and 2.8% respectively. The average abundance of these residues in proteins is 7.2%, 4.2% and 2.9%, respectively. This makes BSA an appropriate model for Eosin Y (**30**) sequestering in an environment with an excess of off-target proteins, such as cell lysate.

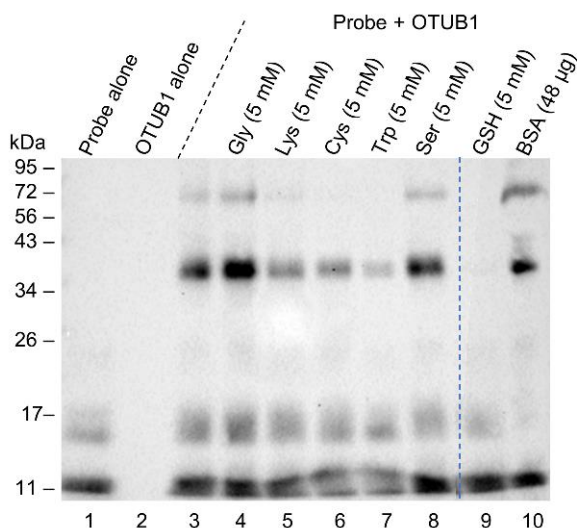


Figure 4.18: Recombinant OTUB1 labelling with amino acid spike. Visualised by anti-HA western blot. The indicated amino acid (5 mM) was incubated with OTUB1 (2 µg) at 37 °C in homogenate buffer for 5 min. HA-Ub₇₅-propene **38** (3 µg) was added and the solution was incubated at 37 °C for 90 min. Eosin Y (**30**) (5 µM) was added and reactions were exposed to white light (10 W) from 50 cm for 5 min.

As positive controls, a standard labelling using Eosin Y (**30**) was carried out along with one containing an excess of Gly (**Figure 4.18, lanes 3 and 4**). No reduction in probe-enzyme bond formation was observed when Gly was added in excess (**Figure 4.18, lane 4**). As a representative for positively charged amino acids, the effect of excess Lys was analysed (**Figure 4.18, lane 5**). There was a small reduction in the intensity of the band representing the probe-enzyme adduct (**Figure 4.18, lane 5**). A similar effect was observed for an excess of Cys (**Figure 4.18, lane 6**). An even greater inhibition was observed for Trp which was included as a representative aromatic amino acid (**Figure 4.18, lane 7**). Excess Ser had little effect on the OTUB1 labelling (**Figure 4.18, lane 8**). This amino acid was selected to examine the influence of hydroxyl groups due to the abundance of amino acids with this functional group. The addition of BSA to bring the total protein amount present to 50 µg, as in the cell lysate experiments, had little effect on the reaction (**Figure 4.18, lane 10**). In the context of cell lysate, Lys, Cys, Trp and residues with similar reactivity may have a cumulative effect of reducing labelling efficiency. However, the presence of off-target proteins such as BSA appears to have negligible effects on the reaction indicating that reactivity with off-target amino acids is not the primary cause of the observed problems.

Fascinatingly, the addition of GSH completely inhibited the labelling reaction (**Figure 4.18, lane 9**). This was even more noteworthy given GSH had such a marked effect relative to Cys alone at the same concentration (**Figure 4.18, lane 6 vs 9**). The negative influence on labelling resulting from the degassing step was initially attributed to mechanical stress on the enzyme. However, these results, in combination with the knowledge that GSH inhibits the reaction, imply that ROS may play a critical role in this reaction. Previous studies have found that the production of ROS from O₂ facilitates the regeneration of Eosin Y (**30**) from intermediate radical species.²⁰⁵ It is also possible that ROS are acting as radical carriers for the reaction. GSH can convert these ROS to H₂O *via* the formation of disulfide bonds, ultimately reducing the concentration of O₂ in solution and preventing catalytic turnover of Eosin Y (**30**).²⁰⁴ Trp metabolites and derivatives have also been reported as ROS scavengers,²⁰⁶ and this amino acid had the greatest effect of all single amino acids in this experiment. However, it would be expected that the addition of excess Cys would have a similar effect to GSH. To further investigate this and analyse the influence of individual amino acids on the Eosin Y (**30**) catalysed labelling, a silver stain and fluorescent gel of this amino acid spike experiment were conducted (**Figure 4.19A and B**).

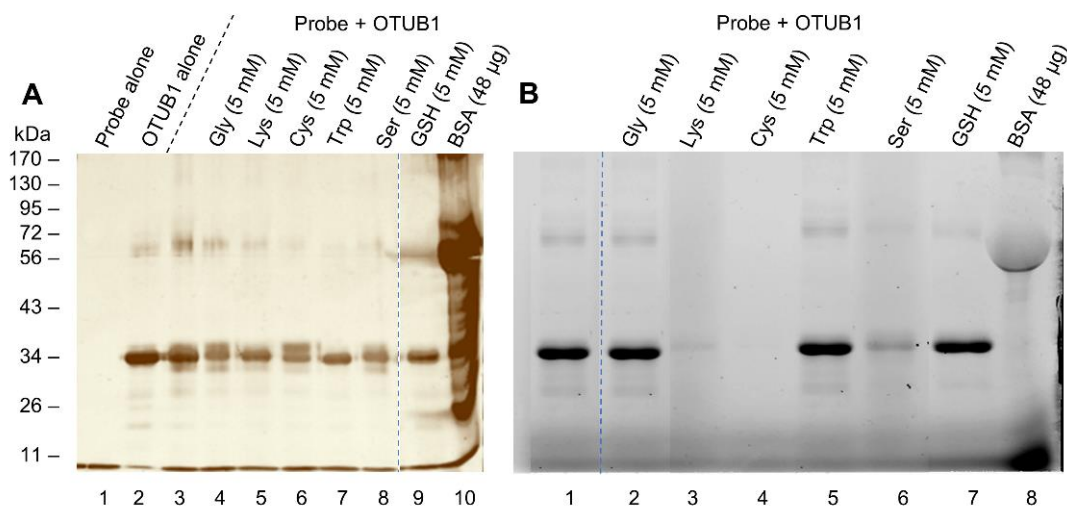


Figure 4.19: Recombinant OTUB1 labelling with amino acid spike. Visualised by (A) silver staining and (B) fluorescent gel imaging. The indicated amino acid (5 mM) was incubated with OTUB1 (2 µg) at 37 °C in homogenate buffer for 5 min. HA-Ub₇₅-propene **38** (3 µg) was added and the solution was incubated at 37 °C for 90 min. Eosin Y (**30**) (5 µM) was added and reactions were exposed to white light (10 W) from 50 cm for 5 min.

By silver staining, varying effects were observed on OTUB1 in samples containing different additives (**Figure 4.19A, lanes 2–10**). Interestingly, a new band was observed just above the band representing OTUB1 alone at around 34 kDa when Cys was added in excess (**Figure 4.19A, lane 6**). The same band was not observed for OTUB1 alone (**Figure 4.19A, lane 2**). This indicates that multiple Cys residues crosslinked with OTUB1 following the formation of thiyl radicals, causing a small but discernible increase in molecular weight for OTUB1. The same band was not observed for GSH (**Figure 4.19A, lane 9**). Lower molecular weight bands, indicative of OTUB1 degradation, were apparent in all samples apart from those spiked with GSH and Trp (**Figure 4.19A, lanes 3–6, 8**). This was hypothesised to be due to the ROS scavenging of these additives.

As in the western blot and silver stain, Cys and GSH had differing effects when analysed by fluorescent gel (**Figure 4.19, lanes 4 and 7**). The formation of Eosin Y-OTUB1 adducts is apparent in the sample containing an optimised labelling reaction without additives (**Figure 4.19B, lane 1**). Added Gly does not impact the formation of these adducts (**Figure 4.19B, lane 2**). An excess of Cys eliminated the formation of Eosin Y-OTUB1 adducts and appeared to have quenched Eosin Y (**30**) (**Figure 4.19, lane 4**). In contrast to this, despite containing a Cys residue in its structure, GSH had no effect on the formation of these adducts (**Figure 4.19, lane 7**).

Based on these results, it can be proposed that Cys reacted directly with Eosin Y (**30**). Similar results were obtained for Lys and Ser in this experiment, which can feasibly react by nucleophilic addition with Eosin Y (**30**) (**Figure 4.19, lanes 3 and 6**). The increased steric bulk and overall negative charge of GSH at pH 7.4 are possible reasons for the lack of similar reactivity with Eosin Y (**30**), which is also negatively charged at this pH. This allows GSH to modulate ROS formation and prevent regeneration of Eosin Y (**30**), while the zwitterionic Cys reacted more directly with Eosin Y (**30**). It is important to note that GSH and Trp, which had the greatest negative effect on the labelling reaction (**Figure 4.18, lanes 7 and 9**), demonstrated no impact on the formation of Eosin Y adducts on OTUB1 (**Figure 4.19, lanes 5 and 7**). Therefore, this adduct formation is not the primary mechanism by which the methodology failed in cell lysate, but it is still important to consider for these applications.

4.6 Using Eosin Y for non-templated thiol-ene conjugation of proteins

In addition to its application in ABPP, Eosin Y (**30**) was also investigated as a catalyst for the thiol-ene conjugation of proteins using visible light. BSA was selected as a model protein for these initial experiments as despite containing multiple Cys residues, all but one of these are involved in disulfide bonds. Therefore, using the HA-Ub₇₅-propene probe **38**, a site-selective thiol-ene reaction with a Cys residue could be achieved. Initial experiments were carried out using ambient light and varying amounts of protein (**Figure 4.20**).

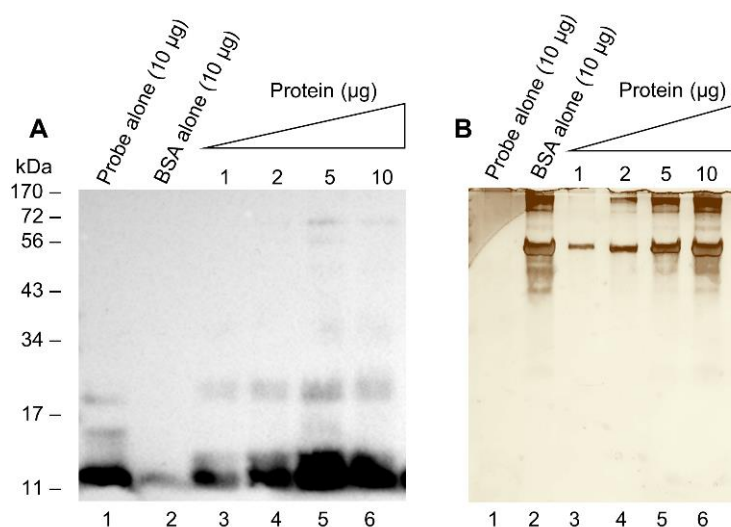


Figure 4.20: HA-Ub₇₅-propene **38** and BSA conjugation concentration curve. Visualised using (A) anti-His western blot; (B) silver stain. HA-Ub₇₅-propene **38** (1–10 µg) was incubated with BSA (1–10 µg) at 37 °C with gentle shaking in NaOAc buffer (250 mM, pH 6.8). Eosin Y (**30**) (50 µM) was added and the samples were incubated in ambient light for 30 min.

At the highest concentrations, a faint band was seen above the 72 kDa marker by anti-HA western blot consistent with the molecular weight of a covalent adduct between the HA-Ub₇₅-propene **38** and BSA (**Figure 4.20A, lanes 5 and 6**). The same adduct was seen by silver staining at the highest concentration examined (**Figure 4.20A, lane 6**). Significantly less covalent bond formation was observed relative to experiments with DUBs, demonstrating the importance of templating the reaction. While these were promising initial results, optimisation was required. The first step of optimisation was increasing the time samples were exposed to light for (**Figure 4.21A and B**).

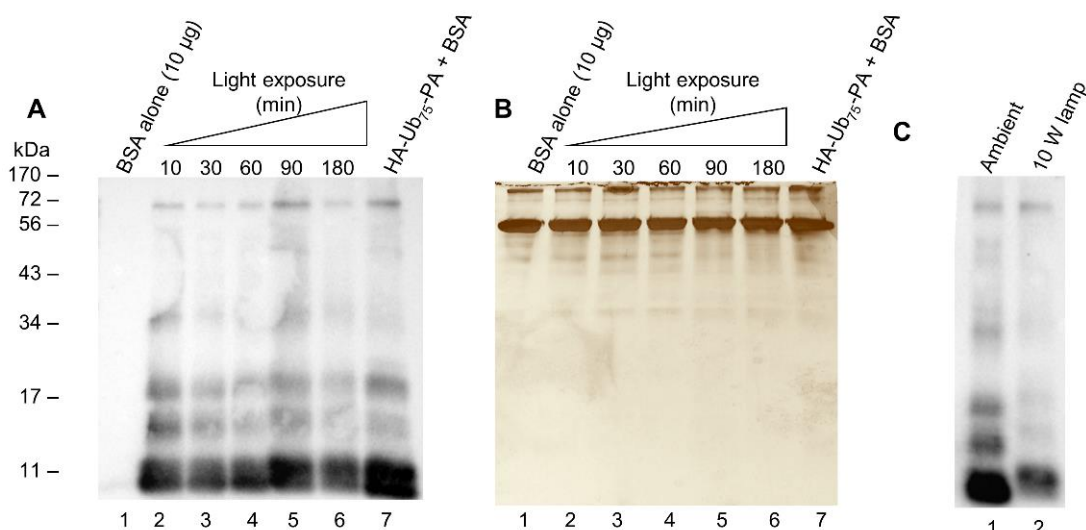


Figure 4.21 HA-Ub₇₅-propene 38 and BSA conjugation time dependence experiment.

Visualised using (A) and (C) anti-HA western blot; (B) silver stain. HA-Ub₇₅-propene **38** (10 µg, 5 µM) or HA-Ub₇₅-PA **6** was incubated with BSA (10 µg, 30 µM) at 37 °C with gentle shaking in NaOAc buffer (250 mM, pH 6.8). Eosin Y (**30**) (50 µM) was added and the samples were either incubated in ambient light for (A) and (B) the indicated time or (C) 30 min or white light (10 W) from 10 cm for 30 min.

Times ranging from 10 min to 180 min were examined with no significant time dependence on the amount of adduct formed (**Figure 4.21A and B, lanes 2–6**). The HA-Ub₇₅-PA probe **6** was used in equivalent conditions to carry out the similar thiol-ene reaction (**Figure 4.21A, lane 7**). Similar coupling efficiency to the HA-Ub₇₅-propene **38** was observed (**Figure 4.21A, lane 5 vs 7**). The resulting adduct contains an alkene bond between the HA-Ub₇₅ recognition element and BSA. As expected, double addition of the BSA was not observed. It is expected that following the thiol-ene reaction, steric clashes surrounding the newly formed alkene will prevent the second addition *via* a thiol-ene reaction. It is proposed that this can be overcome by templating the second addition in an enzyme-substrate binding interaction which would position an active-site Cys proximal to this alkene. Although the Ub-BSA adduct does not represent a substrate of any target enzyme, it allows for the optimisation of the methodology to then be applied for more desirable couplings such as diubiquitin.¹⁰²

Introducing a stronger source of white light did not provide any improve the amount of adduct formed for a coupling with the HA-Ub₇₅-propene probe **38** (**Figure 4.21C, lane 1 vs 2**). In a final attempt to optimise the reaction, the concentration of both the

BSA and HA-Ub₇₅-propene **38** were increased further, and a time dependence analysis was performed at this higher concentration (**Figure 4.22**).

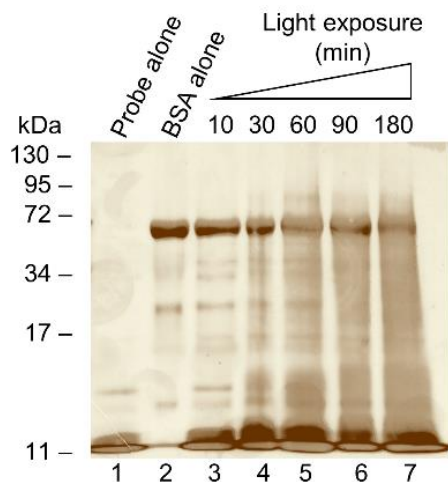


Figure 4.22: High concentration HA-Ub₇₅-propene **38 and BSA conjugation time dependence.** Visualised by silver staining. HA-Ub₇₅-propene **38** (10 µg, 15 µM) was incubated with BSA (10 µg, 90 µM) at 37 °C with gentle shaking in NaOAc buffer (250 mM, pH 6.8). Eosin Y (**30**) (50 µM) was added and the samples were incubated while exposed to white light (10 W) for the indicated time from 5 cm.

The time dependency of the coupling was investigated using times ranging from 10 min to 180 min (**Figure 4.22, lanes 2–7**). No improvement in coupling efficiency was seen at the 10 min timepoint (**Figure 4.22, lane 3**). Additionally, significant degradation of the sample was apparent at longer times (**Figure 4.22, lanes 4–7**). Shorter exposure times were therefore preferable, but the coupling achieved by this time is minimal and does not represent a significant improvement of literature procedures.

Overall, promising initial results were obtained for both the HA-Ub₇₅-propene probe **38** and the HA-Ub₇₅-PA probe **6** but the coupling appears to have significant limitations. While the methodology for HA-Ub₇₅-propene **38** does not provide an improvement on current methods in this form, it could allow for the facile synthesis of a range of ABPs when alkyne HA-Ub₇₅-PA **6** is used. Using this methodology, a wide range of alkene probes mimicking ubiquitinated proteins can potentially be synthesised in a facile manner but degradation observed when using higher concentrations of Eosin Y (**30**) will be limiting for the approach.

4.7 Conclusions

In conclusion, milder conditions for the thiol-ene labelling of DUBs were explored. A less intense UV light source was found to sacrifice some time resolution when used to catalyse the thiol-ene reaction for ABPP. Nonetheless, comparable labelling was attained within a slightly longer timeframe and the integrity of the protein sample was retained for longer. This represented a small change to the methodology but is expected to have significant impact on the cytocompatibility and availability of the approach.

Bi_2O_3 and Eosin Y (**30**) were assessed as radical initiators for a visible light catalysed thiol-ene reaction to be used for ABPP of DUBs. Bi_2O_3 was tested in cell lysate in combination with the radical propagator BrCCl_3 using ambient light and a source of white light to initiate the reaction. In this context, only negligible levels of capture were observed between the HA-Ub₇₅-propene probe **38** and endogenous DUBs. The requirement of degassing for Bi_2O_3 was another limiting factor for the purpose of translating the methodology into whole cells. Due to the observed lack of reactivity, this radical initiator and propagator combination was not pursued any further.

Eosin Y (**30**) was successfully employed in recombinant enzyme labelling experiments using both ambient light and a source of white light to initiate the reaction. This represents the first time a visible light thiol-ene reaction has been used to conjugate two proteins. Significantly, the methodology avoided using UV light, did not require a degassing step and lower concentrations of radical initiators were required than for DPAP (**48**) and MAP (**49**). Significant limitations of Eosin Y (**30**) were identified when moving into cell lysate. Reactivity was observed using both ambient light and a white light source to catalyse the reaction, but it was not comparable to what was seen in recombinant enzyme studies.

Off-target reactivity of Eosin Y (**30**) was identified with certain amino acid side chains. This was found to be dependent on visible light exposure and was observed following incubation of Eosin Y (**30**) with cell lysate and subsequent fluorescent imaging analysis. The negative influence on labelling of specific amino acid residues was identified in experiments using OTUB1 and the tripeptide GSH was found to completely prevent the labelling reaction. The known ROS scavenging function of GSH in the cell coupled with results demonstrating that degassing had a negative

effect on the reaction indicate the potential requirement for O₂ in the reaction. Other initiators may prove more successful for this application.

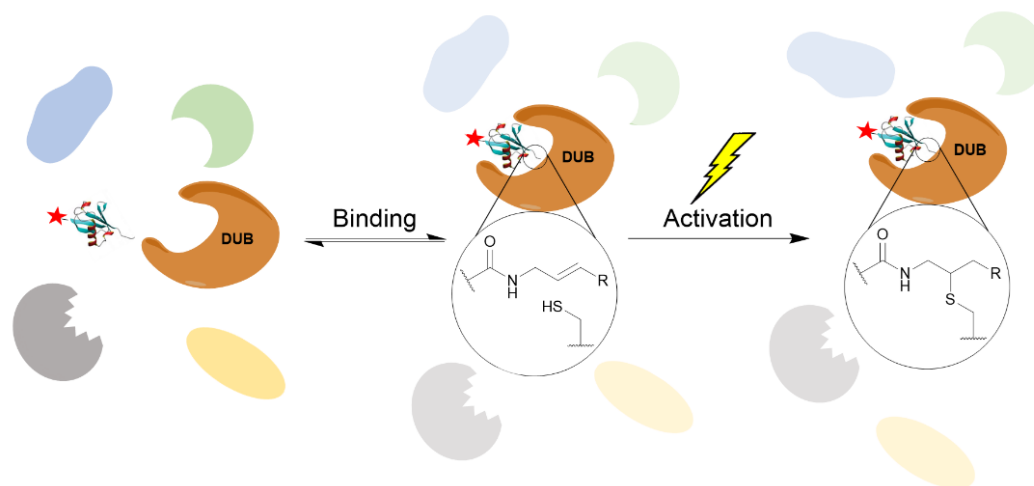
Finally, Eosin Y (**30**) was also investigated as an initiator for non-templated visible light induced thiol-ene coupling. Modest coupling was achieved using the HA-Ub₇₅-propene probe **38** and BSA using both ambient and white light. The observed coupling does not represent an improvement relative to literature methods that rely on UV light to induce this coupling. The off-target reactivity of Eosin Y (**30**) resulting in unwanted adducts may also limit the protocol going forward. Further investigations of the technique at lower initiator concentrations and longer incubation times may prove more successful.

The HA-Ub₇₅-PA probe **6** and BSA coupled with comparable efficiency to the HA-Ub₇₅-propene probe **38**. This is the first example of the thiol-yne reaction being used for a protein-protein conjugation and potentially represents a facile route towards ABPs. Their application in this context was not yet explored, but double addition of the BSA to the HA-Ub₇₅-PA probe **6** was not observed under these conditions. This finding indicates that a second thiol addition would require enzyme binding to template it. As before, the formation of Eosin Y adducts may be limiting as they would disrupt protein structure and enzyme binding. Investigation of alternative initiators would therefore be desirable.

5 Conclusions and outlook

This work describes investigations into novel ABPs that target the cysteine protease classes of DUBs, exploring fluoride and alkene warheads. Novel probes using fluoride warheads were designed and evaluated. As part of this work, the reported probes HA-Ub₇₅CH₂CH₂Br **5** and HA-Ub₇₅-PA **6** were synthesised, and their reactivity was confirmed against recombinant DUBs and those within cell lysate. Problems were encountered during the generation of the HA-Ub₇₅-thioester **2** and the synthesis of this intermediate was optimised. Additionally, key protocols required for the evaluation of novel probes were optimised using the probe HA-Ub₇₅CH₂CH₂Br **5**. Two novel probes, HA-Ub₇₅-CH₂CH₂F **36** and HA-Ub₇₅-CH₂CHF₂ **37**, were generated to investigate fluoride warheads in monoubiquitin ABPs, but no significant labelling was observed in either case. These results show that the anticipated stabilisation of the fluoride leaving group either did not occur or was insufficient to drive the reaction, making these warheads unsuitable for probing cysteine-containing DUBs.

To develop a time-resolved labelling strategy, a novel ABP, HA-Ub₇₅-propene **38**, was designed and synthesised. This probe is inert under ambient conditions and is activated using UV light and radical initiators to label the active-site Cys of DUBs *via* a thiol-ene reaction (**Scheme 7.1**). This was the first successful application of thiol-ene chemistry in ABPP. The probe's reactivity was demonstrated against the recombinant, purified DUB OTUB1 and HEK293T lysate and the methodology was made compatible for downstream analysis by LC-MS/MS. This new HA-Ub₇₅-propene probe **38** was confirmed to be specific for only the active form of DUBs and novel methods to evaluate inhibitors were demonstrated. Immunoprecipitation and proteomic analysis allowed for characterisation of the probe reactivity and exhibited the potential to confer specificity by adding substituents to the alkene moiety. While the methodology captured fewer DUBs relative to reported monoubiquitin probes, it provides opportunities to examine both reversible and irreversible inhibitors in a new way, thus generating information that cannot be obtained using existing probes. The potential of this methodology can be fully realised by examining DUB activity in more physiologically relevant settings such as whole cells and designing derivatives that are specific for particular DUBs.



Scheme 5.1: ABPP of DUBs within cell lysate using a UV light-initiated thiol-ene reaction.

As an extension to this work, a less intense UV light source was successfully applied to initiate this reaction. Although some time resolution was sacrificed, this enhances the biocompatibility of the reaction and provide opportunities for future investigations in whole cells. Bi_2O_3 and Eosin Y were assessed as radical initiators for a visible light catalysed thiol-ene reaction to be used for ABPP of DUBs. Although only negligible capture was observed in the case of Bi_2O_3 , Eosin Y was found to work well in recombinant enzyme labelling experiments using both ambient light and a source of white light to initiate the reaction. Off-target reactivity of Eosin Y was identified with certain amino acid side chains and the tripeptide GSH. This was hypothesised to be primarily due to the ROS scavenging ability of GSH and Trp metabolites and limits the applicability of this radical initiator in HEK 293T cell lysate. Other initiators may prove more suitable for a more biocompatible visible light-mediated thiol-ene reaction.

Finally, Eosin Y was also investigated as an initiator for non-templated visible light induced thiol-ene and thiol-yne couplings between proteins. Modest coupling was achieved using the HA-Ub₇₅-propene probe **38** and HA-Ub₇₅-PA probe **6** with BSA using both ambient and white light. The off-target reactivity of Eosin Y observed in cell lysate experiments is assumed to also be limiting in this case and optimisation of this methodology will require the implementation of alternative initiators.

Overall, a novel radical labelling approach was successfully developed for the ABPP of DUBs in complex biological systems. This works adds to the repertoire of existing ABPs for these enzymes and provides opportunities for more finely resolved

examinations of DUB activity and inhibitors. Furthermore, as the alkene warhead is chemically inert and sterically undemanding, it is expected that this approach will be broadly applicable to study other enzymatic processes. Although promising initial results were obtained in improving the cytocompatibility of the approach, more optimisation is required for the method to be applied in whole cells. However, the methodology already has high biocompatibility in complex cell lysate systems.

6 Experimental

6.1 General biological methods

6.1.1 Buffers

2X Reducing sample buffer: 0.2 M Tris-Cl pH 6.8, 30% glycerol, 0.4% β -mercaptoethanol, 9% SDS, 0.1 % bromophenol blue.

PBS: 8 mM Na_2HPO_4 , 150 mM NaCl, 2 mM KH_2PO_4 , 3 mM KCl.

PBST: 8 mM Na_2HPO_4 , 150 mM NaCl, 2 mM KH_2PO_4 , 3 mM KCl, 0.1% Tween 20.

Column buffer: 50 mM HEPES pH 6.8, 100 mM NaOAc

Homogenate buffer: 50 mM Tris-Cl pH 7.4, 5 mM MgCl_2 , 250 mM sucrose, 1 mM dithiothreitol (DTT) or 1 mM tris (2-carboxyethyl) phosphine) (TCEP)

NET buffer: 50 mM Tris-Cl pH 7.5, 5 mM EDTA, 150 mM NaCl, 0.5% NP-40

NaOAc buffer: 250 mM, pH 6.8 with TCEP 1 mM

MS buffer A: 98% dH_2O , 2% MeCN, 0.1 % formic acid

MS buffer B: for peptides; 80% MeCN, 20% H_2O , 0.1% TFA; for full proteins; 65% MeCN, 35% H_2O , 0.1% TFA

6.1.2 SDS-PAGE

Proteins were separated on a 12% acrylamide gel (resolving gel: 1.3 mL 1.5 M Tris-Cl pH 6.8, 1.5 mL 40% acrylamide/bis-acrylamide (29:1), 2 mL dH_2O , 50 μL 10% SDS, 50 μL 10% ammonium persulfate (APS), 5 μL Tetramethylethylenediamine (TEMED); stacking gel: 630 μL 0.5 M Tris-Cl pH 6.8, 300 μL acrylamide/bis-acrylamide (29:1), 1.3 mL dH_2O , 25 μL 10% SDS, 25 μL 10% APS, 2.5 μL TEMED). Samples were prepared for separation by adding 2X reducing sample buffer followed by heating at 95 °C for 5 min. The proteins were loaded along with Fisher's EZ-Run™ Pre-Stained Rec Protein Ladder. Separation was achieved at 150 V for 1–2 h in running buffer (25 mM Tris, 190 mM Gly, 1% SDS) and visualised either by western blotting or silver staining. All gels were imaged using

Chemidoc XRS+ (Biorad, California USA) and Typhoon FLA9500 (GE Healthcare, Illinois USA).

6.1.3 Silver staining

Gels were treated with fixative (40% EtOH, 10% AcOH) at RT for 1 h or at 4 °C for 16 h. Gels were washed in 20% EtOH (2 x 10 min), then in dH₂O (2 x 10 min). Gels were sensitised in aq. Na₂S₂O₃ (0.02%) for 45 s and then immediately washed with dH₂O (2 x 1 min). Gels were incubated in a solution of AgNO₃ (12 mM) with formaldehyde (0.02%) at 4 °C for a minimum of 20 min and up to 2 h. Following this, gels were washed in dH₂O (2 x 30 s) and transferred to developer solution (3% K₂CO₃, 0.05% formaldehyde). Development was stopped using 5% AcOH.

6.1.4 Coomassie blue staining

Gels were treated with fixative (50% MeOH, 10% AcOH) at RT for 30 min or at 4 °C for 16 h. Gels were incubated in 0.25% Coomassie blue R-250 for 2–4 h until the gel was a uniform blue colour. After this time, the gels were incubated at RT in destaining solution (5% MeOH, 7% AcOH) for up to 18 h. At this point the saturated solution was removed, replaced with fresh destaining solution and incubated at RT until the background was clear.

6.1.5 Western Blotting

A nitrocellulose membrane (GE Healthcare, Illinois USA) was soaked in blotting transfer buffer (25 mM Tris, 190 mM Gly, 20% MeOH) along with the filter papers and sponges that will form the transfer sandwich. The sandwich was assembled, and proteins were transferred onto nitrocellulose membranes in blotting transfer buffer overnight at 15 V and 4 °C. The membrane was incubated in blocking buffer (5% skimmed milk powder in PBST) for 1 h at RT or 16 h at 4 °C prior to immunoblotting. The primary mouse monoclonal anti-HA antibody (Biolegend, California USA) was diluted 1:2,000 in blocking buffer and incubated with the membrane for 1 h at RT with gentle shaking. The membrane was washed with PBST (2 x 5 min) and PBS (2 x 5 min). The secondary antibody, Peroxidase conjugated AffiniPure Goat Anti-Mouse IgG (H+L) (Jackson ImmunoResearch, Cambridgeshire UK), was diluted in blocking buffer 1:4,000, added to the membrane and incubated for 1 h at RT with gentle shaking. The membrane was washed with PBST (3 x 5 min),

PBS (2 x 5 min) and dH₂O (1 x 5 min). Pierce ECL western blotting substrate (ThermoFisher, Massachusetts USA) was used to visualise the chemiluminescence.

6.1.6 Expression and purification of WT ubiquitin

BL21 (DE3) *E. coli* cells containing a pET-15b expression plasmid were transferred from a glycerol stock into LB broth (10 mL) containing ampicillin (100 µg/mL) and grown for 16 hrs at 37°C with vigorous shaking. This culture was transferred into fresh LB broth (300 mL) containing ampicillin (100 µg/mL) and grown until an OD₆₀₀ of 0.6–0.9 was reached. Isopropyl β-D-1-thiogalactopyranoside (IPTG, 0.4 mM) was added and the bacteria were incubated at 37°C for a further 4 hrs. The cells were centrifuged at 8,000 rpm for 15 min. The resulting pellet was re-suspended in column buffer and lysed using a sonication tip. Sonication was carried out for 5 min on ice with the tip set to pulse for 3 sec on and 3 sec off. The lysate was centrifuged at 14,000 rpm for 45 min. The clarified supernatant was stirred vigorously on ice while perchloric acid (200 µL) was added dropwise. The resulting white precipitate was pelleted. The supernatant was transferred into MEMBRA-CEL dialysis tubing (Serva, Heidelberg Germany) and left for 16 h in dialysis buffer (2 L; NH₄OAc 50 mM, 1 mM EDTA, 1 mM DTT; pH 4.5). The protein concentration was checked on the nanodrop (1.33 mg/mL in 15 mL).

6.1.7 Expression and purification of OTUB1

The expression and purification of His tagged OTUB1 Cys91Ser mutant was carried out according to literature procedures.^{67,207} BL21 (DE3) cells transfected with a pET28a-LIC vector containing an N-terminal His6 tagged OTUB1 was transferred from a glycerol stock into LB medium (8 mL) containing kanamycin (100 µg/mL) and grown for 18 h at 37 °C at 180 rpm. The cells were transferred into fresh LB medium (300 mL) containing kanamycin (100 µg/mL) and grown at 37 °C at 180 rpm until an OD₆₀₀ of 0.6 to 0.9 was reached. IPTG was added at a final concentration of 0.4 mM and the bacteria were incubated at 18 °C for 16 h with vigorous shaking. The cells were centrifuged at 6,000 rpm for 15 min. The resulting pellet was re-suspended in homogenate buffer (25 mL) containing PMSF (20 µM) and lysed *via* sonication. The lysate was centrifuged at 13,000 rpm for 45 min. Ni NTA agarose resin (Sigma-Aldrich, Missouri, USA) (1.5 mL, 1:1 suspension in 20 % EtOH) was centrifuged at 2,200 rpm for 5 min and the supernatant was discarded. dH₂O (2 x 0.7 mL) was added to the beads which were gently inverted until the resin was fully resuspended.

The resulting solution was centrifuged at 2,200 rpm and the supernatant was discarded. Ni wash buffer (1.4 mL, 50 mM sodium phosphate pH 8.0, 300 mM NaCl, 10 mM imidazole) was added to the resin which was transferred to the clarified supernatant and incubated overnight at 4 °C with rolling. The resin was centrifuged at 2,200 rpm and the supernatant was discarded. Ni wash buffer (1 mL) was added to the resin which was fully resuspended by gentle inversion and centrifuged at 2,200 rpm for 5 min. This wash step was repeated four times. The supernatant was discarded after each washing step. Ni elution buffer A (4 x 0.7 mL; 50 mM sodium phosphate pH 8.0, 300 mM NaCl, 150 mM imidazole) was added to the resin that was resuspended by gentle inversion. The solution was centrifuged at 2,200 rpm for 5 min and the supernatants from these washes were pooled in clean microcentrifuge tubes. A final wash step was carried out with Ni elution buffer B (1 mL; 50 mM sodium phosphate pH 8.0, 300 mM NaCl, 300 mM imidazole) at 2,200 rpm for 5 min. The supernatant was discarded, and the beads were stored in 20% EtOH. The pooled supernatants were concentrated in a 10 kDa MW cut-off Vivaspin 500 centrifugal concentrators in a centrifuge at 9,000 rpm to a final concentration of 50 μ L. Ni wash buffer (450 μ L) was added to the tubes and concentrated to 50 μ L in a centrifuge at 9,000 rpm. This wash step was repeated, and the solution was resuspended in storage buffer (150 μ L, 20 mM Tris-Cl pH 8.0, 1mM DTT, 10% glycerol, 50 mM NaCl). The concentration was measured by nanodrop (13.78 μ g/ μ L in 150 μ L).

6.2 Mass spectrometry

6.2.1 CHCl₃/MeOH extraction

MeOH (600 μ L) and CHCl₃ (150 μ L) were added to a sample of protein (200 μ L) and the solution was vortexed for 20 s. dH₂O (450 μ L) was added and the sample was vortexed for a further 20 s. The sample was centrifuged at 14,000 rpm for 2 min. The upper layer was aspirated off and discarded. The sample was diluted with MeOH (450 μ L), vortexed for 20 s and centrifuged at 14,000 rpm for 1 min. The supernatant was aspirated and discarded. The pellet was prepared for an in-solution digestion.

6.2.2 In-solution digest following CHCl₃/MeOH extraction

A protein pellet obtained using a CHCl₃/MeOH extraction was diluted in urea buffer (50 µL; 6 M urea, 33 mM Tris-Cl pH 7.8) and dissolved by vortexing for 20 s and sonicating for 2 min. The sample was diluted with dH₂O (250 µL), vortexed for 20 s and sonicated for a further 2 min. Elastase was added in a 1:15 dilution relative to the protein concentration. The digest was carried out at 37 °C with gentle shaking for 16 h. Samples were prepared for MS analysis by zip-tipping and analysed by captive spray ionisation mass spectrometry

6.2.3 In-gel digest

Samples were separated by SDS-PAGE and visualised by silver staining. Bands of interest were excised, cut into small pieces and incubated for 18 h in wash solution (200 µL; 50% MeOH, 45% dH₂O, 5% formic acid). The wash solution was aspirated, and fresh wash solution was added. The samples were incubated for a further 2 h at RT. The wash solution was removed, and the gel pieces were dehydrated for 5 min in MeCN (200 µL). This dehydration step was repeated, DTT buffer (30 µL; 100 mM NH₄HCO₃, 10 mM DTT) was added to the gel pieces and they were incubated for 30 min at RT. The DTT buffer was aspirated and iodoacetamide solution (30 µL, 50 mM in dH₂O) was added. The samples were incubated for a further 30 min. After the removal of the iodoacetamide solution the gel pieces were dehydrated for 5 min in MeCN (200 µL). Rehydration was performed in NH₃HCO₃ solution (200 µL, 100 mM). Dehydration and rehydration steps were repeated. Trypsin, modified sequencing grade (Sigma-Aldrich, Missouri, USA) stock was diluted in NH₃HCO₃ solution and this 1X stock (30 µL, 20 µg/mL) was added to the dehydrated gel pieces. The solution was incubated on ice for 10 min with gentle mixing. Following this incubation step, NH₃HCO₃ solution (5 µL, 50 mM) was added to the mixture and it was incubated for 18 h at 37 °C with gentle shaking. After this incubation, NH₃HCO₃ solution (50 µL, 50 mM) was added. The gel pieces were incubated in this mixture for 10 min with occasional vortexing. The supernatant was transferred to a fresh microcentrifuge tube. Extraction buffer 1 (50 µL; 50% MeCN, 45% dH₂O, 5% formic acid) was added to the gel pieces. The pieces were incubated for 10 min in this buffer with occasional vortexing. The supernatant was then added to the collection tube and the gel pieces were incubated for a further 10 min in extraction buffer 2 (85% MeCN, 10% dH₂O, 5% formic acid) with periodic vortexing.

The supernatant was again added to the collection tube. For more abundant protein bands an additional extraction with extraction buffer 2 was performed. The combined supernatants were dried in a vacuum centrifuge, resuspended in MS buffer A (20 μ L) and analysed by captive spray ionisation mass spectrometry.

6.2.4 Filter Aided Sample Preparation (FASP)

FASP²⁰⁸ was carried out using a 10 kDa MW cut-off Vivaspin 500 centrifugal concentrators (10 kDa MW cut-off). The concentrator was conditioned with 50 μ L dH₂O. It was spun at 11,800 rpm for 2 min. The protein solution to be digested was transferred to the filter and centrifuged at 13000 rpm until concentrated to a maximum of 25 μ L. UA buffer (200 μ L, 8 M urea in 0.1 M Tris-Cl pH 8.5) was added to the filter and centrifuged at 11,800 rpm for 15 min. This step was repeated twice. DTT solution (100 μ L, 10 mM in UA buffer) was added to the concentrator and vortexed for 5 s. The concentrator was centrifuged at 11,800 rpm for 15 min. IAA solution (100 μ L, 50 mM) was added and the solution was vortexed for 5 s and then centrifuged again at 11,800 rpm for 15 min. Washes were performed using UA buffer (3 x 100 μ L) followed by NH₄HCO₃ solution (3 x 100 μ L, 50 mM). After the final wash, trypsin solution (200 μ L, 50 mM NH₄HCO₃ solution, 1:50 enzyme:protein) was added and the concentrator was incubated overnight at 37 °C. The concentrator was centrifuged at 11,800 rpm for 15 min. NaCl solution (50 μ L, 0.5 M) was added and it was centrifuged at 11,800 rpm until all the of the solution had passed the filter. Samples were de-salted by zip-tipping and analysed by LC-MS/MS.

6.2.5 Zip-tip purification

A 10 μ L zip-tip with 0.6 μ L C₁₈ resin (Merk Millipore, Massachusetts USA) was equilibrated by aspirating and MS buffer B four times and further four times with MS buffer A. 10 μ L of the protein sample was aspirated across the tip ten times. Buffer A (10 μ L) was used to wash the sample by aspirating and dispensing four times. The protein or peptides were then eluted in buffer B (2 x 10 μ L) and dried using a vacuum centrifuge. The sample was analysed by MALDI or LC-MS/MS.

6.2.6 MALDI-TOF mass spectrometry

MALDI-TOF analysis was carried out by Dr Edel Durack on a Bruker Ultraflex extreme MALDI-TOF/TOF mass spectrometer. The matrix used was a saturated solution of HCCA (α -Cyano-4-hydroxycinnamic acid) in TA 85% (85% ACN with 0.1% TFA),

and the calibrant was prepared in the same matrix. The matrix (1 μ L) was mixed with the sample (1 μ L) and 1 μ L of this mixture was deposited onto a ground steel MALDI target plate and allowed to dry in air. Mass spectra were recorded in positive reflection mode.

6.2.7 Orbitrap mass spectrometry

Orbitrap mass spectrometry was carried out by Dr. Holger Kramer. Protein digests were redissolved in 0.1% TFA (30 μ L per sample) by agitation (1,200 rpm, 15 min) and sonication in an ultrasonic water bath (10 min). This was followed by centrifugation (14,000 rpm, 5 °C, 10 min) and transfer to MS sample vials. LC-MS/MS analysis was carried out in technical duplicates (4.0 μ L per injection) and separation was performed using an Ultimate 3,000 RSLC nano liquid chromatography system (Thermo Scientific) coupled to an Orbitrap Velos mass spectrometer (Thermo Scientific) *via* an Easy-Spray nano-electrospray source (Thermo Scientific). Samples were injected and loaded onto a trap column (Acclaim PepMap 100 C18, 100 μ m \times 2 cm) for desalting and concentration at 8 μ L/min in 2% MeCN, 0.1% TFA. Peptides were then eluted on-line to an analytical column (Acclaim Pepmap RSLC C18, 75 μ m \times 50 cm) at a flow rate of 250 nL/min. Peptides were separated using a 120 min gradient, 4–25% of buffer A for 90 min followed by 25–45% buffer B for another 30 min (buffer A: 5% DMSO, 0.1% FA; buffer B: 75% MeCN, 5% DMSO, 0.1% FA) and subsequent column conditioning and equilibration. Eluted peptides were analysed by the mass spectrometer operating in positive polarity using a data-dependent acquisition mode. Ions for fragmentation were determined from an initial MS1 survey scan at 30,000 resolution, followed by CID (Collision-Induced Dissociation) of the top 10 most abundant ions. MS1 and MS2 scan AGC targets were set to 1^6 and 3^4 for maximum injection times of 500 ms and 100 ms respectively. A survey scan m/z range of 350–1500 was used, normalised collision energy set to 35%, charge state screening enabled with +1 charge state rejected and minimal fragmentation trigger signal threshold of 500 counts. Data was processed using the MaxQuant²⁰⁹ software platform (v1.6.7.0), with database searches carried out by the in-built Andromeda search engine against the Swissprot *H.sapiens* database (version 20180104, number of entries: 20,244). A reverse decoy database approach was used at a 1% false discovery rate (FDR) for peptide spectrum matches. Search parameters included: maximum missed cleavages set

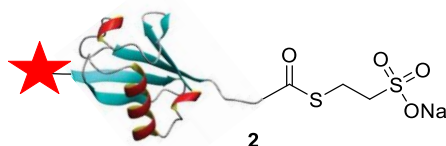
to 3, fixed modification of Cys carbamidomethylation and variable modifications of methionine oxidation, Asp deamidation and protein N-terminal acetylation. Label-free quantification was enabled with an LFQ minimum ratio count of 1.

6.2.8 Captive spray ionisation mass spectrometry

Captive spray ionisation was carried out by Dr. Gary Hessman. It was performed using a Thermo Scientific UltiMate 3000RSLCnano LC (Waltham, MA USA) equipped with an Acclaim PepMap C18 (2 μm , 0.075 mm x 150 mm) column. For each injection, 5 μL of a (1 $\mu\text{g}/\mu\text{L}$) digested peptide was loaded onto a Nano Trap Column (100 μm I.D. x 2 cm, packed with Acclaim PepMap100 C18) at 10 $\mu\text{L}/\text{min}$ in 95% water, 5% MeCN, 0.1% formic acid for 3 min. Trapped peptides were eluted onto the analytical column using a multi-step gradient with a flow rate of 0.3 $\mu\text{L}/\text{min}$. The gradient utilised two mobile phases (buffer A, H₂O, 0.1% formic acid; buffer B MeCN : 0 min, A (98%), B (2%); 3 min, A (98%), B (2%); 63 min A (65%), B (35%); 64 min A (5%), B (95%); 66 min A (5%), B (95%); 67 min A (98%), B (2%); 75 min A (98%), B (2%). Peptide digest were analysed on a Bruker compact Qq-TOF mass spectrometer via CaptiveSpray nanoBooster (Bremen Germany). Precursor ions were scanned from 150 m/z to 2200 m/z at 2 Hz with a cycle time of 3.0 seconds, with fixed windows excluded (20–350, 1,221–1,225, 2,200–40,000). Smart Exclusion was used to ensure only chromatographic peaks were selected as precursors. Active Exclusion enabled the analysis of less-abundant ions to be analysed and not excluded from precursor selection. Data acquired on the Bruker compact was converted to mzXML format and searched against a custom database containing the probe sequence inserted into a uniprot database with taxonomy restricted to human on PeptideShaker. ²¹⁰

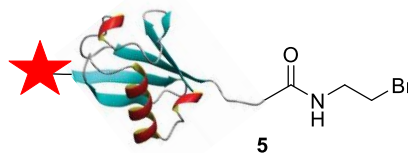
6.3 Synthesis of HA-tagged activity-based monoubiquitin probes

6.3.1 Expression and purification of HA-Ub₇₅-thioester **2**



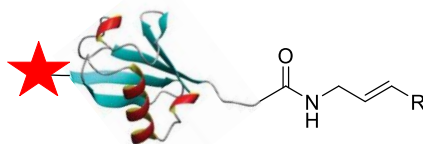
The expression and purification of HA-Ub₇₅-thioester **2** was carried out according to literature procedures.^{67,207} BL21 (DE3) cells transfected with a pTYB2 plasmid encoding for a HA-tagged ubiquitin₇₅ fusion protein containing an intein domain and chitin-binding domain (HA-Ub₇₅-intein-CBD) **1** were transferred from a glycerol stock into LB medium (8 mL) containing ampicillin (100 µg/mL) and grown for 18 h at 37 °C at 180 rpm. The cells were transferred into fresh LB medium (300 mL) containing ampicillin (100 µg/mL) and grown at 37 °C at 180 rpm until an OD₆₀₀ of 0.6 to 0.9 was reached. IPTG was added at a final concentration of 0.4 mM and the bacteria were incubated at 18 °C for 16 h with vigorous shaking. The cells were centrifuged at 8,000 rpm for 15 min. The resulting pellet was re-suspended in column buffer and lysed using a sonication tip. Sonication was carried out for 5 min with the tip set to pulse for 3 sec on and 3 sec off. The lysate was centrifuged at 14,000 rpm for 45 min. A column containing chitin resin (2.5 mL) (New England Biolabs) was equilibrated with column buffer (25 mL). The clarified supernatant was run over this column. The column was washed with column buffer (25 mL). After this wash, column buffer containing MESNa **43** (7.5 mL; 50 mM) was run through the column before incubation in this buffer for 18 h at 37 °C with gentle shaking. HA-Ub₇₅-thioester **2** was eluted in column buffer (5 mL) before concentration by spinning at 14,000 rpm in 5 kDa MW cut-off Vivaspin 500 centrifugal concentrators (Sartorius, Göttingen Germany). HA-Ub₇₅-thioester **2** was desalted using a NAP-5 column (GE Healthcare, Illinois USA) and eluted in column buffer according to manufacturer's instructions. The sample was concentrated again at 14,000 rpm using 5 kDa MW cut-off Vivaspin centrifugal concentrators and the protein concentration was measured on a nanodrop (4.8 mg/mL, 100 µL).

6.3.2 Synthesis of HA-Ub₇₅-CH₂CH₂Br **5**



HA-Ub₇₅-CH₂CH₂Br **5** was synthesised using literature procedures.⁶⁷ 2-bromoethylamine·HBr **44** (31 mg, 0.15 mmol) was dissolved in column buffer (200 μ L) and the pH of the solution was adjusted to pH 8.0 by the addition of aq. NaOH (1 M). HA-Ub₇₅-thioester **2** in column buffer (2.2 mg/mL, 100 μ L) was added to this solution and it was shaken gently for 90 min at RT. The reaction mixture was desalted using a NAP-5 column according to manufacturer's instructions, eluted in column buffer and concentrated by centrifuging at 14,000 rpm in a 5 kDa MW cut-off Vivaspin centrifugal concentrator. The protein concentration was measured on a nanodrop (1.5 mg/mL, 100 μ L).

6.3.3 Synthesis of HA-Ub₇₅-alkene probes **38–40**

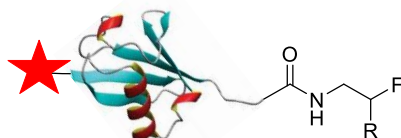


Probe **38**: R = H
 Probe **39**: R = Me
 Probe **40**: R = Ph

N-Hydroxysuccinimide **46** solution (0.2 M, 45 μ L) and Tris-Cl (100 mM, 10 μ L, pH 7.5) were added to HA-Ub₇₅-thioester **2** in column buffer (1.2 mg/mL, 500 μ L) and incubated for 10 min at RT. Allylamine **47** (23 μ L, 0.3 mmol), *E*-but-2-en-1-amine.TFA **57** or cinnamylamine **56** (40 mg, 0.3 mmol) was added to a solution of MeCN-H₂O (1:1, 56 μ L). This solution was added to the reaction mixture and the pH was adjusted to 9.0. The reaction was incubated for 18 h at 37 °C with gentle shaking. After this time, the reaction mixture was desalted using a NAP-5 column according to manufacturer's instructions and concentrated in a 5 kDa MW cut-off Vivaspin centrifugal concentrator at 14,000 rpm. The protein concentration was measured on a nanodrop, probe **38** = (3.4 mg/mL, 100 μ L); probe **39** = (2.3 mg/mL, 100 μ L) probe **40** = (5.6 mg/mL, 100 μ L). Samples of the probe were

concentrated and desalted using a combination of $\text{CHCl}_3/\text{MeOH}$ and zip tipping prior to a tryptic digest or submission for MALDI analysis.

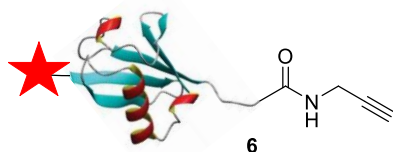
6.3.4 Synthesis of HA-Ub₇₅-alkyl fluoride probes 36–37



Probe **36** R = H
Probe **37** R = F

N-Hydroxysuccinimide **46** (0.2 M, 45 μL) and Tris-Cl (100 mM, 10 μL , pH 7.5) were added to HA-Ub₇₅-thioester **2** in column buffer (1.2 mg/mL, 500 μL) and incubated for 10 min at RT. 2-Fluoroethanamine hydrochloride (30 mg, 0.3 mmol) or 2,2-Difluoroethylamine (21 μL , 0.3 mmol) was added to a solution of MeCN-H₂O (1:1, 56 μL). This solution was added to the reaction mixture and the pH was adjusted to 9.0 with 1M NaOH or 1M HCl as appropriate. The reaction was incubated for 18 h at 37 °C with gentle shaking. After this time, the reaction mixture was desalted using a NAP-5 column according to manufacturer's instructions and concentrated in a 5 kDa MW cut off Vivaspin centrifugal concentrator at 14,000 rpm. The protein concentration was measured on a nanodrop, probe **36** = (3.9 mg/mL, 150 μL); probe **37** = (4.2 mg/mL, 100 μL).

6.3.5 Synthesis of HA-Ub₇₅-PA 6



N-Hydroxysuccinimide **46** (0.2 M, 45 μL) and Tris-Cl (100 mM, 10 μL , pH 7.5) were added to HA-Ub₇₅-thioester **2** in column buffer (1.2 mg/mL, 500 μL) and incubated for 10 min at RT. Propargyl amine **45** (19 μL , 0.3 mmol) was added to a solution of MeCN-H₂O (1:1, 56 μL). This solution was added to the reaction mixture and the pH was adjusted to 9.0. The reaction was incubated for 18 h at 37 °C with gentle shaking. After this time, the reaction mixture was desalted using a NAP-5 column according to manufacturer's instructions and concentrated in a Vivaspin centrifugal

concentrator at 14,000 rpm. The protein concentration was measured on a nanodrop, HA-Ub₇₅-PA **6** = (8.7 mg/mL, 200 μ L).

6.4 *In vitro* DUB labelling

6.4.1 HEK 293T cell lysate preparation

A HEK 293T cell pellet was lysed using glass beads. To a 100 μ L cell pellet, 100 μ L of glass beads (0.5 mm, Sigma-Aldrich, Missouri, USA) were added. Homogenate buffer (200 μ L) was added. The mixture was vortexed for 20 s before being placed on ice for 90 s. This sequence was repeated 20 times. Cell debris and glass beads were pelleted by centrifuging at 14,000 rpm for 5 min. The resulting supernatant was aspirated off. The protein concentration of the clarified extract was measured by nanodrop (19.9 mg/mL, 200 μ L)

6.4.2 *In vitro* HA-Ub₇₅CH₂CH₂Br **5** labelling

HA-Ub₇₅-CH₂CH₂Br **5** (0.75 μ L, 1.5 mg/mL in column buffer) was incubated with HEK 293T cell lysate (2.5 μ L, 19.9 mg/mL in homogenate buffer). The final volume of the labelling was adjusted to 30 μ L with homogenate buffer. Incubation was carried out for 90 min at 37 °C with gentle shaking. Upon completion, 2X reducing sample buffer (15 μ L) was added and the proteins were heated to 95 °C for 5 min. Proteins were visualised using silver staining and anti-HA western blotting after being separated on a 12% SDS-PAGE.

6.4.3 Optimised *in vitro* thiol-ene labelling with alkene probes

All thiol-ene reactions were carried out in 2 mL transparent glass vials with a PTFE/silicone septum (Sigma-Aldrich, Missouri, USA). UV light (365 nm) was applied in a Luzchem LZC photoreactor oven containing 10 x 8 W UV lamps or Mylee UV Gel Nail Curing Lamp 4 x 9 W UV bulbs. The relevant probe (1–4 μ g) was incubated with HEK 293T cell lysate (2.5 μ L, 19.9 mg/mL in homogenate buffer) or OTUB1 (2 μ g). The final volume of the labelling was adjusted to 30 μ L with homogenate buffer containing TCEP (1 mM) for the lysate labelling, or phosphate buffer (pH 8.0) containing TCEP (1 mM) for the OTUB1 labelling. The probes were pre-incubated with the DUBs for 90 min at 37 °C with gentle shaking before the addition of radical initiator DPAP (**48**) (0.25 mM) and MAP (**49**) (0.25 mM). The reaction mixture was degassed for 2 min with N₂ and exposed to UV light (365 nm)

for 2 min in the Luzchem LZC photoreactor or 10 min in Mylee UV Gel Nail Curing Lamp. Upon completion, 2X reducing sample buffer (30 μ L) was added and the proteins were heated to 95 °C for 5 min. Proteins were visualised using silver staining and anti-HA western blotting following separation on a 12% SDS-PAGE.

6.4.4 Lysate labelling with *N*-ethylmaleimide (NEM)

HEK 293T cell lysate (2.5 μ L, 19.9 mg/mL) was incubated at 37 °C for 15 min with *N*-ethylmaleimide (NEM) (13 mM final concentration) in homogenate buffer containing TCEP (1 mM). The relevant probe (1 μ g) was added to the solution so final volume of the labelling was adjusted to 30 μ L. The probes were incubated with the lysate for 90 min at 37 °C with gentle shaking before the addition of radical initiator DPAP (**48**) (0.25 mM) and MAP (**49**) (0.25 mM). The reaction mixture was degassed for 2 min with N₂ and exposed to UV light (365 nm, Luzchem photoreactor, 10 x 8 W UV bulbs) for 2 min. Upon completion, 2X reducing sample buffer (30 μ L) was added and the proteins were heated to 95 °C for 5 min. Proteins were visualised using silver staining and anti-HA western blotting following separation on a 12% SDS-PAGE.

6.4.5 Screening of alternative initiators

HA-Ub₇₅-propene **38** (0.3 μ L, 3.4 mg/mL in column buffer) and was incubated with HEK 293T cell lysate (2.5 μ L, 19.9 mg/mL) in homogenate buffer at a final volume at 30 μ L. (2,2'-Azobis(2-amidinopropane) dihydrochloride (AAPH) (0.25 mM), 4,4'-azobis(4-cyanopentanoic acid) (ACPA) (0.25 mM) or t-butyl peroxide (0.25 mM) was added to the sample. The solutions were degassed for 2 min using N₂ and exposed to UV light (365 nm, Luzchem photoreactor, 10 x 8 W UV bulbs) for times ranging from 0 min to 5 min. Upon completion, 2X reducing sample buffer (30 μ L) was added and the proteins were heated to 95 °C for 5 min. Proteins were visualised using silver staining and anti-HA western blotting following separation on a 12% SDS-PAGE.

6.4.6 Investigating increasing DPAP and MAP concentrations

HA-Ub₇₅-propene **38** (0.3 μ L, 3.4 mg/mL in column buffer) was incubated with HEK 293T cell lysate (2.5 μ L, 19.9 mg/mL) in homogenate buffer at a final volume of 30 μ L. Across two different experiments DPAP (**48**) and MAP (**49**) were added at

four different concentrations (0.05 mM, 0.25 mM, 1.25 mM and 2.5 mM). The solutions were degassed for 2 min using N₂ and exposed to UV light (365 nm, Luzchem photoreactor, 10 x 8 W UV bulbs) for times ranging from 0 min to 5 min. Upon completion, 2X reducing sample buffer (30 µL) was added and the proteins were heated to 95 °C for 5 min. Proteins were visualised using silver staining and anti-HA western blotting following separation on a 12% SDS-PAGE

6.4.7 Optimisation of labelling conditions for LC-MS/MS

HEK 293T cell lysate (2.5 µL, 19.9 mg/mL) was added to homogenate buffer (30 µL) and all samples which were incubated at 37 °C for 90 min. At this point DPAP (**48**) (0.25 mM) and MAP (**49**) (0.25 mM) were added where appropriate. The solutions were degassed for 2 min using N₂ and exposed to UV light (365 nm, Luzchem photoreactor, 10 x 8 W UV bulbs) for times ranging from 0 min to 5 min. They were incubated at 4 °C for 90 min with rolling to mimic the immunoprecipitation protocol. The samples were subject to tryptic digest using the FASP protocol, desalted by zip tipping and analysed by LC-MS/MS using captive spray ionisation mass spectrometry.

6.4.8 *In vitro* thiol-ene labelling with alkene probes and denatured OTUB1

OTUB1 (0.25 µL, 8.0 mg/mL) was denatured either by heating at 95 °C for 10 min or by the addition of SDS (0.5% final concentration). The final volume of the labelling was adjusted to 30 µL with phosphate buffer (pH 8.0) containing TCEP (1 mM). In this step SDS concentration was reduced fifteen-fold. The HA-Ub₇₅-propene **38** was pre-incubated with the DUBs for 90 min at 37 °C with gentle shaking before the addition of radical initiator DPAP (**48**) (0.25 mM) and MAP (**49**) (0.25 mM). The reaction mixture was degassed for 2 min with N₂ and exposed to UV light (365 nm, Luzchem photoreactor, 10 x 8 W UV bulbs) for 2 min. Upon completion, 2X reducing sample buffer (30 µL) was added and the proteins were heated to 95 °C for 5 min. Proteins were visualised using silver staining and anti-HA western blotting following separation on a 12% SDS-PAGE

6.4.9 PR-619 (55**) pre-incubation assay**

Inhibitor PR-619 (**55**) was pre-incubated with HEK 293T cell lysate (2.5 µL, 19.9 mg/mL) on ice for 30 min at a range of concentrations (0 µM–100 µM).

HA-Ub₇₅-propene **38** (0.3 µL, 3.4 mg/mL in column buffer) was added giving the labelling a final volume of 30 µL. The reaction mixture was incubated for a further 90 min before addition of DPAP (**48**) (0.25 mM) and MAP (**49**) (0.25 mM) and degassing for 2 min with N₂. The mixture was exposed to UV light (365 nm, Luzchem photoreactor, 10 x 8 W UV bulbs) for 2 min. Upon completion, 2X reducing sample buffer (30 µL) was added and the proteins were heated to 95 °C for 5 min. Proteins were visualised using silver staining and anti-HA western blotting following separation on a 12% SDS-PAGE

6.4.10 Probe displacement assay

HA-Ub₇₅-propene **38** (0.3 µL, 3.4 mg/mL in column buffer) or HA-Ub₇₅-CH₂CH₂Br **5** (0.75 µL, 1.5 mg/mL in column buffer) was incubated with HEK 293T cell lysate (2.5 µL, 19.9 mg/mL) at 37 °C for 60 min. PR-619 (**55**) was added at a range of concentrations (0 µM–100 µM) and the mixture was incubated for a further 30 min at 37 °C. DPAP (**48**) (0.25 mM) and MAP (**49**) (0.25 mM) were added and the mixture was degassed for 2 min with N₂. The mixture was exposed to UV light (365 nm, Luzchem photoreactor, 10 x 8 W UV bulbs) for 2 min. Upon completion, 2X reducing sample buffer (30 µL) was added and the proteins were heated to 95 °C for 5 min. Proteins were visualised using silver staining and anti-HA western blotting following separation on a 12% SDS-PAGE

6.4.11 Determining the K_d of the probe-OTUB1 complex

Recombinant OTUB1 (5 µg) was incubated at 37 °C for 90 min with increasing concentrations of HA-Ub₇₅-propene **38** (5 µM–22.5 µM in Homogenate buffer). DPAP (**48**) (0.25 mM) and MAP (**49**) (0.25 mM) were added and the reaction mixture was degassed for 2 min with N₂ and exposed to UV light (365 nm, Luzchem photoreactor, 10 x 8 W UV bulbs) for 2 min. 2X reducing sample buffer (30 µL) was added and the samples were heated at 95 °C for 5 min. The reaction was visualised by Coomassie blue staining following separation on a 12% SDS-PAGE. The intensity of the labelled band was quantified on Image Quant and plotted against the concentration of probe.

6.5 Immunoprecipitation (IP)

The relevant alkene probe (5 µg) was pre-incubated with HEK 293T cell lysate (12.5 µL, 19.9 mg/mL in homogenate buffer) in NET buffer (136 µL; 50 mM Tris-Cl pH 7.5, 5 mM EDTA, 150 mM NaCl, 0.5% NP-40) containing TCEP (1 mM) for 90 min at 37 °C. DPAP (**48**) (0.25 mM) and MAP (**49**) (0.25 mM) were added and the solution was degassed with N₂ for 2 min. The solution was exposed to UV light (365 nm, Luzchem photoreactor, 10 x 8 W UV bulbs) for 2 min. SDS solution (10% in dH₂O, 7.5 µL) was added to the reaction before vortexing for 30 s and sonication for 2 min. The mixture was diluted with homogenate buffer (1.5 mL). EZview™ Red Anti-HA Affinity Gel (Sigma-Aldrich, Missouri, USA) (100 µL of 50% slurry) was equilibrated by adding NET buffer (750 µL), gently inverting and centrifuging at 9,000 rpm. The supernatant was aspirated, and the equilibration step was repeated. The lysate was added to the equilibrated beads and incubated at 4 °C for 90 min with rolling. The mixture was centrifuged at 9,000 rpm for 30 s and the supernatant was aspirated. NET buffer (750 µL) was added to the beads which were inverted until the beads were fully resuspended before being centrifuged at 9,000 rpm for 30 s. This washing step was repeated four times. After the final wash Gly buffer (250 µL, 150 mM, pH 2.5) was added to the beads. The solution was inverted until the beads were resuspended and then left on ice for 2 min. The solution was centrifuged at 9,000 rpm for 30 s. The resulting supernatant was transferred to a clean microcentrifuge tube, and this elution step was repeated. 1X reducing sample buffer (250 µL) was added to the beads which were heated at 95 °C for 5 min. A small % of the samples were separated by 12 % SDS-PAGE and visualised by western blotting. The remainder of the samples was transferred to a clean microcentrifuge tube and subject to tryptic digest using the FASP protocol along with the Gly elution. Samples were desalted by zip tipping and analysed by LC-MS/MS using an Orbitrap.

6.6 Optimised Eosin Y lysate labelling

The HA-Ub₇₅-propene probe **38** (1 µg) was incubated with HEK 293T cell lysate (2.5 µL, 19.9 mg/mL in homogenate buffer). The final volume of the labelling was adjusted to 30 µL with homogenate buffer containing TCEP (1 mM). A stock solution of Eosin Y (**30**) (2.9 mM in DMSO–homogenate buffer, 4:1) was prepared fresh before use and protected from light. The reaction was preincubated for 90 min at

37 °C with gentle shaking before the addition of Eosin Y (0.5 µL of stock, final conc. = 50 µM). Samples were exposed to white light (10 W) from 10 cm for 5 min at 37 °C or ambient light for 30 min at 37 °C. Upon completion, 2X reducing sample buffer (30 µL) was added and the proteins were heated to 95 °C for 5 min. Proteins were visualised using silver staining and anti-HA western blotting after being separated on a 12% SDS-PAGE.

6.6.1 Optimised Eosin Y recombinant enzyme labelling

The HA-Ub₇₅-propene probe **38** (2 µg) was incubated with OTUB1 (0.2 µL, 13.78 µg/µL in storage buffer) or UCHL1 (3.3 µL, 0.9 µg/µL in storage buffer). The final volume of the labelling was adjusted to 30 µL with homogenate buffer containing TCEP (1 mM). A stock solution of Eosin Y (**30**) (0.29 mM in DMSO–homogenate buffer, 4:1) was prepared fresh before use and protected from light. The reaction was preincubated for 90 min at 37 °C with gentle shaking before the addition of Eosin Y (0.5 µL of stock for recombinant enzyme labelling, final conc. = 5 µM). Samples were exposed to white light (10 W) from 50 cm for 5 min or ambient light for 30 min at 37 °C. Upon completion, 2X reducing sample buffer (30 µL) was added and the proteins were heated to 95 °C for 5 min. Proteins were visualised using silver staining and anti-HA western blotting after being separated on a 12% SDS-PAGE.

6.6.2 Amino acid spike OTUB1 labelling using Eosin Y

A stock solution (0.15 M in H₂O) of the amino acids Gly, Lys, Cys, Trp and Ser and the tripeptide GSH were prepared and adjusted to pH 7.5. Each amino acid or tripeptide (1 µL, for 5 mM final conc.) was added to OTUB1 (0.2 µL, 13.78 µg/µL in storage buffer) and incubated for 5 min at 37 °C. The HA-Ub₇₅-propene probe **38** (1.2 µL, 3.4 mg/mL in column buffer) was added to the reaction and the final volume of the labelling was adjusted to 30 µL with homogenate buffer containing TCEP (1 mM). The solution was preincubated for 90 min at 37 °C with gentle shaking before the addition of Eosin Y (**30**) (0.5 µL of 0.29 mM stock, final conc. = 5 µM). Samples were exposed to white light (10 W) from 50 cm for 5 min. Upon completion, 2X reducing sample buffer (30 µL) was added and the proteins were heated to 95 °C for 5 min. Proteins were visualised using silver staining and anti-HA western blotting after being separated on a 12% SDS-PAGE.

6.6.3 Eosin Y for the conjugation of ubiquitin monomers and BSA

BSA (1–10 μg) was incubated with HA-Ub₇₅-propene **38** (1–10 μg) or HA-Ub₇₅-PA **6** (10 μg) in NaOAc buffer (250 mM, pH 6.8) at a final volume of 30 μL . A stock solution of Eosin Y (2.9 mM in DMSO: homogenate buffer, 4:1) was prepared fresh before each use and protected from light. Eosin Y (**30**) (0.5 μL of 2.9 mM stock, final conc. = 50 μM) was added and samples were incubated at 37 °C for the specified time (10–180 min) while exposed to ambient light or white light (10 W) from 10 cm. Upon completion, 2X reducing sample buffer (30 μL) was added and the proteins were heated to 95 °C for 5 min. Proteins were visualised using silver staining and anti-HA western blotting after being separated on a 12% SDS-PAGE.

6.6.4 Bi₂O₃ labelling

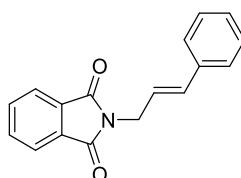
The HA-Ub₇₅-propene probe **38** (1–4 μg) was incubated with HEK 293T cell lysate (2.5 μL , 19.9 mg/mL in homogenate buffer). The final volume of the labelling was adjusted to 30 μL with homogenate buffer containing TCEP (1 mM). The HA-Ub₇₅-propene probe **38** was pre-incubated for 90 min at 37 °C with gentle shaking before the addition of Bi₂O₃ (250 μM or 0.2 μM) and BrCCl₃ (600 μM or 0.48 μM). The solution was degassed with N₂ for 2 min and exposed to white light from 5 cm for the specified time (2–90 min) or ambient light for 60 min at 37 °C. Upon completion, 2X reducing sample buffer (30 μL) was added and the proteins were heated to 95 °C for 5 min. Proteins were visualised using silver staining and anti-HA western blotting after being separated on a 12% SDS-PAGE.

6.7 General chemical methods

¹H and ¹³C NMR spectra were recorded on Bruker 400 MHz or 600 MHz system spectrometers. Spectra were recorded in DMSO-d₆ or CDCl₃ relative to residual DMSO (δ = 2.50 ppm) or CHCl₃ (δ = 7.26 ppm). Chemical shifts are reported in parts per million (ppm), coupling constants are reported in Hertz (Hz) and are accurate to 0.2 Hz. NMR spectra were assigned using HSQC and HMBC experiments. Mass spectrometry measurements were carried out on a Bruker ESI or APCI HRMS. Melting points were measured using a Griffin melting points apparatus and are uncorrected. Infrared (IR) spectra were obtained on a Perkin Elmer spectrophotometer. Flash column chromatography was carried out using silica gel, particle size 0.04-0.063 mm. TLC analysis was performed on precoated 60F₂₅₄

slides and visualised by UV irradiation, potassium permanganate stain (3 g KMnO_4 , 20 g K_2CO_3 , 300 mL dH_2O) and ninhydrin stain (1.5 g ninhydrin, 5 mL, AcOH, 500 mL EtOH 95%). All solvents were obtained from commercial sources and used as received. Petroleum ether refers to the fraction of petroleum ether that boils at 40–60 °C.

6.7.1 Synthesis of (*E*)-1-phenyl-3-phthalimido-2-propene **59**



59

Cinnamyl bromide **58** (500 mg, 2.54 mmol) and potassium phthalimide **57** (729 mg, 3.94 mmol) were dissolved in dry DMF (10 mL) under argon. The reaction mixture was stirred at RT for 3 h. TLC analysis (petroleum ether) showed complete consumption of cinnamyl bromide ($R_f = 0.6$) and formation of the product ($R_f = 0.1$) after this time. The solution was diluted with Et_2O (40 mL) and brine (30 mL) and the white precipitate formed was collected by vacuum filtration. The aqueous layer was extracted with Et_2O (2 x 30 mL). The combined organic layers were dried over MgSO_4 , filtered and concentrated to afford the crude product as a yellow solid. This was combined with the precipitated product and recrystallised from toluene to afford the product **59** as colourless crystals (411 mg, 62%); mp 152–154 °C (toluene). Lit.¹⁹⁴ 154–155 °C.

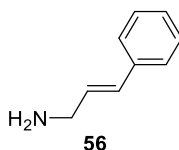
$\nu_{\text{max}}/\text{cm}^{-1}$ (neat) 3461 (C-H_{ar}), 3102 (C-H_{ar}), 3083 (C-H_{ar}), 3026 (C-H), 2915 (C-H), 1769 (C=O), 1701 (C=O), 1426 (C=C), 1394, 1321, 1106, 969, 952, 724.

^1H NMR (400 MHz, CDCl_3) δ = 7.86 (dd, $J = 2.9$ Hz, $J = 5.5$ Hz, 2H, CH_{Phth}), 7.72 (dd, $J = 2.9$ Hz, $J = 5.5$ Hz, 2H, CH_{Phth}), 7.37–7.32 (m, 2H, CH_{Ph}), 7.31–7.27 (m, 2H, CH_{Ph}), 7.24–7.20 (m, 1H, CH_{Ph}), 6.66 (d, $J = 16.1$ Hz, 1H, $\text{CH}=\underline{\text{C}}\text{H}-\text{Ph}$), 6.28 (dt, $J = 6.7$ Hz, $J = 16.0$ Hz, 1H, $\underline{\text{C}}\text{H}=\text{CH}-\text{Ph}$), 4.45 (d, $J = 6.7$ Hz, 2H, CH_2) ppm.

^{13}C NMR (100 MHz, CDCl_3) δ = 168.2 (C=O), 136.2 (q C_{Ph}), 134.0 (q C_{Phth}), 133.7 (CH_{Phth}), 132.2 ($\underline{\text{C}}\text{H}=\text{CH}-\text{Ph}$), 128.5 (CH_{Ph}), 127.9 (CH_{Ph}), 126.5 (CH_{Ph}), 123.3 (CH_{Phth}), 122.8 ($\text{CH}=\underline{\text{C}}\text{H}-\text{Ph}$), 39.7 (CH_2) ppm.

HRMS (APCI⁺): m/z calc. 264.1025 [$\text{M}+\text{H}$]⁺, found 264.1014

The spectroscopic data are in agreement with those reported in the literature.²¹¹

6.7.2 Synthesis of (*E*)-3-phenyl-prop-2-en-1-amine 56

(*E*)-1-phenyl-3-phthalimido-2-propene **59** (700 mg, 2.66 mmol) was dissolved in MeOH (12 mL). Hydrazine hydrate solution (80%, 150 μ L, 2.95 mmol) was added dropwise and the reaction was stirred at RT for 2 h. TLC analysis after this time showed the complete consumption of the starting material (petroleum ether-EtOAc, 3:1; R_f = 0.8) and formation of the product **56** (H₂O-IPA-EtOAc, 1:2:2; R_f = 0.2). The reaction was cooled to 4 °C resulting in the formation of a white precipitate. The white precipitate was collected by vacuum filtration and washed with MeOH (3 x 10 mL). The filtrate was concentrated under reduced pressure and the residue was dissolved in DCM (20 mL) and washed with aq. KOH (20 mL, 0.5 M). The aqueous layer was extracted with DCM (3 x 20 mL) and the combined organic layers were concentrated to afford the product **56** as a yellow oil (228 mg, 65%).

$\nu_{\max}/\text{cm}^{-1}$ (neat) 3676 (NH₂), 3261 (C-H_{ar}), 2988 (C-H), 2902 (C-H), 1570 (C=C), 1447, 1403, 1315, 1274, 1067, 1057, 964, 739, 689.

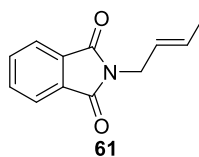
¹H NMR (400 MHz, CDCl₃) δ = 7.37 (d, J = 7.4 Hz, 2H, CH_{Ph}), 7.33–7.27 (m, 2H, CH_{Ph}), 7.25–7.15 (m, 1H, CH_{Ph}), 6.50 (d, J = 15.9 Hz, 1H, CH=C $\underline{\text{H}}$ -Ph), 6.32 (dt, J = 5.9 Hz, J = 15.9 Hz, 1H, C $\underline{\text{H}}$ =CH-Ph), 3.48 (d, J = 5.9 Hz, 2H, CH₂) ppm.

¹³C NMR (100 MHz, CDCl₃) δ = 137.2 (qC), 131.1 (CH_{Ph}), 129.6 (CH_{Ph}), 128.5 (CH_{Ph}), 127.3 (CH=C $\underline{\text{H}}$ -Ph), 125.8 (C $\underline{\text{H}}$ =CH-Ph), 44.3 (CH₂) ppm.

HRMS (ESI⁺): m/z calc. 136.1121 [M+H]⁺, found: 136.1126

The spectroscopic data are in agreement with those reported in the literature.²¹²

6.7.3 Synthesis of (E)-1-phthalimido-2-butene **61**



Potassium phthalimide **61** (4.12 g, 22.2 mmol) was dissolved in dry DMF (10 mL) under argon. Crotyl bromide **60** (2.00 g, 10.8 mmol) was added dropwise and the reaction mixture was stirred for 18 h at RT. TLC analysis (petroleum ether-EtOAc, 3:1) showed the complete consumption of crotyl bromide **60** ($R_f = 0.9$) and formation of the product **61** ($R_f = 0.6$) in this time. The reaction mixture was poured into H₂O-ice (1:1, 480 mL) and stirred vigorously until the ice had melted. A white precipitate formed and was collected by vacuum filtration. The precipitate was washed with H₂O (3 x 10 mL) and dissolved in DCM (20 mL). The aqueous filtrate was extracted with DCM (2 x 100 mL). The combined organic layers were dried over MgSO₄, filtered and concentrated. Recrystallisation from DCM-petroleum ether (4:1) afforded the product **61** as colourless crystals. (2.26 g, 76% yield); mp 72–75 °C (DCM-petroleum ether, 4:1). Lit.¹⁹⁶ 62–65 °C

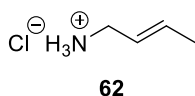
$\nu_{\max}/\text{cm}^{-1}$ (neat) 3461 (C-H_{ar}), 2919 (C-H), 1765 (C=O), 1611 (C=C), 1465, 1426, 1394, 1355, 981, 954, 716.

¹H NMR (400 MHz, CDCl₃) δ = 7.84 (dd, $J = 2.9$ Hz, $J = 5.5$ Hz, 2H, CH_{Phth}), 7.70 (dd, $J = 2.9$ Hz, $J = 5.5$ Hz, 2H, H-1), 5.81–5.69 (m, 1H, CH=CH-CH₃), 5.58–5.48 (m, 1H, CH=CH-CH₃), 4.22 (dd, $J = 1.2$ Hz, $J = 6.3$ Hz, 2H, CH₂), 1.67 (dd, $J = 1.2$ Hz, $J = 6.5$ Hz, 3H, CH₃)

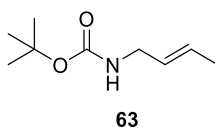
¹³C NMR (100 MHz, CDCl₃) δ = 168.2 (C=O), 133.8 (CH_{Phth}), 132.8 (qC_{Phth}), 130.1 (CH=CH-CH₃), 124.8 (CH=CH-CH₃), 123.5 (CH_{Phth}), 39.5 (CH₂), 17.6 (CH₃).

HRMS (ESI⁺): m/z calc. 202.0862 [M+H]⁺, found: 202.0855

The spectroscopic data are in agreement with those reported in the literature.¹⁹⁶

6.7.4 (E)-but-2-ene-amine hydrochloride **62**

(E)-1-phthalimido-2-butene **61** (1.20 g, 5.9 mmol) was dissolved in EtOH (30 mL). Hydrazine monohydrate (311 μ L, 6.4 mmol) was added dropwise and the reaction was heated to 60 °C for 3 h. After this time, TLC analysis showed the consumption of the starting material (petroleum ether-EtOAc, 7:3; R_f = 0.8) and formation of the product (H₂O-IPA-EtOAc, 2:2:1; R_f = 0.1). The reaction mixture was cooled to 4 °C and the resulting white precipitate was removed by vacuum filtration. The filtrate was acidified to pH 3.0 using HCl (2 M). Following concentration under reduced pressure the crude intermediate **62** was obtained as a yellow solid and carried forward without further purification.

6.7.5 (E)-tert-butyl but-2-en-1-ylcarbamate **63**

(E)-but-2-ene-amine hydrochloride **62** (150 mg, 1.4 mmol) was added to DCM (5 mL) and the suspension was cooled to 0 °C. Et₃N (440 μ L, 3.2 mmol) was added dropwise. (Boc)₂O (500 mg, 2.3 mmol) was added and the reaction mixture was stirred and warmed slowly to RT. After 16 h TLC analysis showed the complete consumption of the intermediate amine **62** (H₂O-IPA-EtOAc, 2:2:1; R_f = 0.1) and the formation of the product **63** (petroleum ether-EtOAc, 47:3; R_f = 0.3). The reaction mixture was diluted with aq. NH₄Cl (10 mL) and the aqueous layer was extracted with DCM (3 x 20 mL). The combined organic layers were dried with MgSO₄, filtered and concentrated. Purification by flash column chromatography (petroleum ether-EtOAc, 47:3) afforded the product **63** as a colourless oil (633 mg, 72%).

$\nu_{\text{max}}/\text{cm}^{-1}$ (CHCl₃) 3350 (N-H), 2978 (C-H), 2934 (C-H), 1680 (C=O), 1505 (C=C), 1366 (C-H), 1249 (C-O), 1169 (C-O), 910, 732

¹H NMR (400 MHz, CDCl₃) δ = 5.65–5.53 (m, 1H, CH=CH-CH₃), 5.24 (dtq, J = 1.4 Hz, J = 5.8 Hz, J = 15.2 Hz, 1H, CH=CH-CH₃), 4.51 (bs, 1H, NH), 3.65 (d, J =

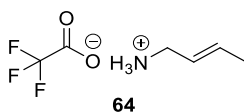
5.8 Hz, 2H, CH₂), 1.66 (dd, $J = 1.4$ Hz, $J = 6.3$ Hz, 3H, CH=CH-CH₃), 1.43 (s, 9H, CH₃BOC) ppm.

¹³C NMR (100 MHz, CDCl₃) $\delta = 168.0$ (C=O), 127.9 (CH=CH-CH₃), 127.3 (CH=CH-CH₃), 80.2 (C_{BOC}), 42.3 (CH₂), 128.1 (CH₃BOC), 17.3 (CH=CH-CH₃) ppm.

HRMS (ESI⁺): m/z calc. 194.1151 [M+Na]⁺, found: 194.1159

The spectroscopic data are in agreement with those reported in the literature.²¹³

6.7.6 (E)-but-2-ene-amine trifluoroacetate **64**



(*E*)-tert-butyl but-2-en-1-ylcarbamate **63** (118 mg, 0.7 mmol) was dissolved in DCM (12 mL). TFA (3 mL) was added dropwise and the reaction was stirred for 30 min. TLC analysis showed the complete conversion of the starting material (petroleum ether–EtOAc, 3:1; $R_f = 0.5$) to the product **64** (H₂O-IPA-EtOAc, 2:2:1; $R_f = 0.1$). The reaction mixture was diluted with toluene (12 mL) and concentrated under reduced pressure. The product was obtained as a white solid and used without further purification (128 mg, 99%).

$\nu_{\max}/\text{cm}^{-1}$ (neat) 3037 (N-H), 2960 (C-H), 2937 (C-H), 1775 (C=O), 1665 (C=C), 1199 (C-O), 1145 (C-O), 967, 704

¹H NMR (400 MHz, CDCl₃) $\delta = 7.82$ (bs, 3H, NH₃⁺), 5.84–5.71 (m, 1H, CH=CH-CH₃), 5.52–5.42 (m, CH=CH-CH₃), 3.40–3.30 (m, 2H, CH₂) 1.67 (dd, $J = 1.2$ Hz, $J = 6.6$ Hz 3H, CH₃) ppm.

¹³C NMR (100 MHz, CDCl₃) $\delta = 159.0$ (q, $J = 34.1$ Hz, C=O), 132.0 (CH=CH-CH₃), 124.0 (CH=CH-CH₃), 118.2 (qC), 40.9 (CH₂), 17.9 (CH₃) ppm.

The spectroscopic data are in agreement with those reported in the literature.¹⁹⁹

7 References

1. Goldstein, G.; Scheid, M.; Hammerling, U.; Schlesinger, D. H.; Niall, H. D.; Boyse, E. A., Isolation of a polypeptide that has lymphocyte-differentiating properties and is probably represented universally in living cells. *Proc. Natl. Acad. Sci. U.S.A* **1975**, *72* (1), 11-5.
2. Ciechanover, A.; Elias, S.; Heller, H.; Hershko, A., "Covalent affinity" purification of ubiquitin-activating enzyme. *J. Biol. Chem.* **1982**, *257* (5), 2537-42.
3. Hershko, A.; Heller, H.; Elias, S.; Ciechanover, A., Components of ubiquitin-protein ligase system. Resolution, affinity purification, and role in protein breakdown. *J. Biol. Chem.* **1983**, *258* (13), 8206-14.
4. Ciechanover, A.; Hod, Y.; Hershko, A., A heat-stable polypeptide component of an ATP-dependent proteolytic system from reticulocytes. *Biochem. Biophys. Res. Commun.* **1978**, *81* (4), 1100-5.
5. Jentsch, S.; McGrath, J. P.; Varshavsky, A., The yeast DNA repair gene RAD6 encodes a ubiquitin-conjugating enzyme. *Nature* **1987**, *329* (6135), 131-4.
6. Hochstrasser, M.; Varshavsky, A., In vivo degradation of a transcriptional regulator: the yeast alpha 2 repressor. *Cell* **1990**, *61* (4), 697-708.
7. Ciechanover, A.; Finley, D.; Varshavsky, A., Ubiquitin dependence of selective protein degradation demonstrated in the mammalian cell cycle mutant ts85. *Cell* **1984**, *37* (1), 57-66.
8. Finley, D.; Ciechanover, A.; Varshavsky, A., Thermolability of ubiquitin-activating enzyme from the mammalian cell cycle mutant ts85. *Cell* **1984**, *37* (1), 43-55.
9. Komander, D., The emerging complexity of protein ubiquitination. *Biochem. Soc. Trans.* **2009**, *37* (5), 937-953.
10. Carlson, N.; Rogers, S.; Rechsteiner, M., Microinjection of ubiquitin: changes in protein degradation in HeLa cells subjected to heat-shock. *J. Cell. Biol.* **1987**, *104* (3), 547-55.
11. Carlson, N.; Rechsteiner, M., Microinjection of ubiquitin: intracellular distribution and metabolism in HeLa cells maintained under normal physiological conditions. *J. Cell. Biol.* **1987**, *104* (3), 537-46.
12. Hunt, L. T.; Dayhoff, M. O., Amino-terminal sequence identity of ubiquitin and the nonhistone component of nuclear protein A24. *Biochem. Biophys. Res. Commun.* **1977**, *74* (2), 650-5.

13. Hoegel, C.; Pfander, B.; Moldovan, G. L.; Pyrowolakis, G.; Jentsch, S., RAD6-dependent DNA repair is linked to modification of PCNA by ubiquitin and SUMO. *Nature* **2002**, *419* (6903), 135-41.
14. Carter, S.; Bischof, O.; Dejean, A.; Vousden, K. H., C-terminal modifications regulate MDM2 dissociation and nuclear export of p53. *Nat. Cell. Biol.* **2007**, *9* (4), 428-35.
15. Haglund, K.; Sigismund, S.; Polo, S.; Szymkiewicz, I.; Di Fiore, P. P.; Dikic, I., Multiple monoubiquitination of RTKs is sufficient for their endocytosis and degradation. *Nat. Cell Biol.* **2003**, *5* (5), 461-6.
16. Hershko, A.; Heller, H., Occurrence of a polyubiquitin structure in ubiquitin-protein conjugates. *Biochem. Biophys. Res. Commun.* **1985**, *128* (3), 1079-86.
17. Chau, V.; Tobias, J. W.; Bachmair, A.; Marriott, D.; Ecker, D. J.; Gonda, D. K.; Varshavsky, A., A multiubiquitin chain is confined to specific lysine in a targeted short-lived protein. *Science* **1989**, *243* (4898), 1576-83.
18. Peng, J.; Schwartz, D.; Elias, J. E.; Thoreen, C. C.; Cheng, D.; Marsischky, G.; Roelofs, J.; Finley, D.; Gygi, S. P., A proteomics approach to understanding protein ubiquitination. *Nat. Biotechnol.* **2003**, *21* (8), 921-6.
19. Xu, P.; Duong, D. M.; Seyfried, N. T.; Cheng, D.; Xie, Y.; Robert, J.; Rush, J.; Hochstrasser, M.; Finley, D.; Peng, J., Quantitative proteomics reveals the function of unconventional ubiquitin chains in proteasomal degradation. *Cell* **2009**, *137* (1), 133-45.
20. Elsasser, S.; Finley, D., Delivery of ubiquitinated substrates to protein-unfolding machines. *Nat. Cell Biol.* **2005**, *7* (8), 742-749.
21. Dong, Y.; Zhang, S.; Wu, Z.; Li, X.; Wang, W. L.; Zhu, Y.; Stoilova-McPhie, S.; Lu, Y.; Finley, D.; Mao, Y., Cryo-EM structures and dynamics of substrate-engaged human 26S proteasome. *Nature* **2019**, *565* (7737), 49-55.
22. Xu, P.; Peng, J., Characterization of Polyubiquitin Chain Structure by Middle-down Mass Spectrometry. *Anal. Chem.* **2008**, *80* (9), 3438-3444.
23. Mani, A.; Gelmann, E. P., The Ubiquitin-Proteasome Pathway and Its Role in Cancer. *J. Clin. Oncol.* **2005**, *23* (21), 4776-4789.
24. Huber, C.; Dias-Santagata, D.; Glaser, A.; O'Sullivan, J.; Brauner, R.; Wu, K.; Xu, X.; Pearce, K.; Wang, R.; Uzielli, M. L. G.; Dagoneau, N.; Chemaitilly, W.; Superti-Furga, A.; Santos, H. D.; Mégarbané, A.; Morin, G.; Gillissen-Kaesbach, G.; Hennekam, R.; Burgt, I. V. d.; Black, G. C. M.; Clayton, P. E.;

- Read, A.; Merrer, M. L.; Scambler, P. J.; Munnich, A.; Pan, Z.-Q.; Winter, R.; Cormier-Daire, V., Identification of mutations in CUL7 in 3-M syndrome. *Nat. Genet.* **2005**, *37* (10), 1119-1124.
25. Popovic, D.; Vucic, D.; Dikic, I., Ubiquitination in disease pathogenesis and treatment. *Nat. Med.* **2014**, *20* (11), 1242-53.
26. Hough, R.; Rechsteiner, M., Ubiquitin-lysozyme conjugates. Purification and susceptibility to proteolysis. *J. Biol. Chem.* **1986**, *261* (5), 2391-9.
27. Hanpude, P.; Bhattacharya, S.; Dey, A. K.; Maiti, T. K., Deubiquitinating enzymes in cellular signaling and disease regulation. *IUBMB Life* **2015**, *67* (7), 544-55.
28. Abdul Rehman, S. A.; Kristariyanto, Y. A.; Choi, S. Y.; Nkosi, P. J.; Weidlich, S.; Labib, K.; Hofmann, K.; Kulathu, Y., MINDY-1 Is a Member of an Evolutionarily Conserved and Structurally Distinct New Family of Deubiquitinating Enzymes. *Mol. Cell.* **2016**, *63* (1), 146-55.
29. Komander, D.; Barford, D., Structure of the A20 OTU domain and mechanistic insights into deubiquitination. *Biochem. J.* **2008**, *409* (1), 77-85.
30. Storer, A. C.; Ménard, R., Catalytic mechanism in papain family of cysteine peptidases. *Methods Enzymol.* **1994**, *244*, 486-500.
31. Shrestha, R. K.; Ronau, J. A.; Davies, C. W.; Guenette, R. G.; Strieter, E. R.; Paul, L. N.; Das, C., Insights into the mechanism of deubiquitination by JAMM deubiquitinases from cocrystal structures of the enzyme with the substrate and product. *Biochemistry* **2014**, *53* (19), 3199-217.
32. Tran, H. J.; Allen, M. D.; Löwe, J.; Bycroft, M., Structure of the Jab1/MPN domain and its implications for proteasome function. *Biochemistry* **2003**, *42* (39), 11460-5.
33. Maytal-Kivity, V.; Reis, N.; Hofmann, K.; Glickman, M. H., MPN+, a putative catalytic motif found in a subset of MPN domain proteins from eukaryotes and prokaryotes, is critical for Rpn11 function. *B.M.C. Biochem.* **2002**, *3*, 28.
34. Hurley, J. H.; Lee, S.; Prag, G., Ubiquitin-binding domains. *Biochem. J.* **2006**, *399* (3), 361-72.
35. Drag, M.; Mikolajczyk, J.; Bekes, M.; Reyes-Turcu, F. E.; Ellman, J. A.; Wilkinson, K. D.; Salvesen, G. S., Positional-scanning fluorogenic substrate libraries reveal unexpected specificity determinants of DUBs (deubiquitinating enzymes). *Biochem. J.* **2008**, *415* (3), 367-75.

36. Wiener, R.; Zhang, X.; Wang, T.; Wolberger, C., The mechanism of OTUB1-mediated inhibition of ubiquitination. *Nature* **2012**, *483* (7391), 618-22.
37. Iphoefer, A.; Kummer, A.; Nimtz, M.; Ritter, A.; Arnold, T.; Frank, R.; van den Heuvel, J.; Kessler, B. M.; Jaensch, L.; Franke, R., Profiling Ubiquitin Linkage Specificities of Deubiquitinating Enzymes with Branched Ubiquitin Isopeptide Probes. *ChemBioChem* **2012**, *13* (10), 1416-1420.
38. Todi, S. V.; Paulson, H. L., Balancing act: deubiquitinating enzymes in the nervous system. *Trends Neurosci.* **2011**, *34* (7), 370-82.
39. Welchman, R. L.; Gordon, C.; Mayer, R. J., Ubiquitin and ubiquitin-like proteins as multifunctional signals. *Nat. Rev. Mol. Cell Biol.* **2005**, *6* (8), 599-609.
40. Chen, Z. J.; Sun, L. J., Nonproteolytic functions of ubiquitin in cell signaling. *Mol. Cell* **2009**, *33* (3), 275-86.
41. Lam, Y. A.; Xu, W.; DeMartino, G. N.; Cohen, R. E., Editing of ubiquitin conjugates by an isopeptidase in the 26S proteasome. *Nature* **1997**, *385* (6618), 737-40.
42. Fischer-Vize, J. A.; Rubin, G. M.; Lehmann, R., The fat facets gene is required for Drosophila eye and embryo development. *Development* **1992**, *116* (4), 985-1000.
43. King, R. C.; Storto, P. D., The role of the otu Gene in Drosophila oogenesis. *BioEssays* **1988**, *8* (1), 18-24.
44. Knobloch, K. P.; Utermöhlen, O.; Kisser, A.; Prinz, M.; Horak, I., Reexamination of the role of ubiquitin-like modifier ISG15 in the phenotype of UBP43-deficient mice. *Mol. Cell. Biol.* **2005**, *25* (24), 11030-4.
45. Wang, L.; Dent, S. Y., Functions of SAGA in development and disease. *Epigenomics* **2014**, *6* (3), 329-39.
46. Yang, W.; Lee, Y. H.; Jones, A. E.; Woolnough, J. L.; Zhou, D.; Dai, Q.; Wu, Q.; Giles, K. E.; Townes, T. M.; Wang, H., The histone H2A deubiquitinase Usp16 regulates embryonic stem cell gene expression and lineage commitment. *Nat. Commun.* **2014**, *5*, 3818.
47. Nandakumar, V.; Chou, Y.; Zang, L.; Huang, X. F.; Chen, S. Y., Epigenetic control of natural killer cell maturation by histone H2A deubiquitinase, MYSM1. *Proc. Natl. Acad. Sci. U. S. A.* **2013**, *110* (41), E3927-36.

48. Kim, J. M.; Parmar, K.; Huang, M.; Weinstock, D. M.; Ruit, C. A.; Kutok, J. L.; D'Andrea, A. D., Inactivation of Murine Usp1 Results in Genomic Instability and a Fanconi Anemia Phenotype. *Dev. Cell* **2009**, *16* (2), 314-320.
49. Knobel, P. A.; Belotserkovskaya, R.; Galanty, Y.; Schmidt, C. K.; Jackson, S. P.; Stracker, T. H., USP28 Is Recruited to Sites of DNA Damage by the Tandem BRCT Domains of 53BP1 but Plays a Minor Role in Double-Strand Break Metabolism. *Mol. Cell. Biol.* **2014**, *34* (11), 2062-2074.
50. Sharma, N.; Zhu, Q.; Wani, G.; He, J.; Wang, Q. E.; Wani, A. A., USP3 counteracts RNF168 via deubiquitinating H2A and γ H2AX at lysine 13 and 15. *Cell Cycle* **2014**, *13* (1), 106-14.
51. Joo, H. Y.; Zhai, L.; Yang, C.; Nie, S.; Erdjument-Bromage, H.; Tempst, P.; Chang, C.; Wang, H., Regulation of cell cycle progression and gene expression by H2A deubiquitination. *Nature* **2007**, *449* (7165), 1068-72.
52. Atanassov, B. S.; Dent, S. Y., USP22 regulates cell proliferation by deubiquitinating the transcriptional regulator FBP1. *EMBO Rep.* **2011**, *12* (9), 924-30.
53. Nicassio, F.; Corrado, N.; Vissers, J. H.; Areces, L. B.; Bergink, S.; Marteijn, J. A.; Geverts, B.; Houtsmuller, A. B.; Vermeulen, W.; Di Fiore, P. P.; Citterio, E., Human USP3 is a chromatin modifier required for S phase progression and genome stability. *Curr. Biol.* **2007**, *17* (22), 1972-7.
54. Sun, X. X.; Dai, M. S., Deubiquitinating enzyme regulation of the p53 pathway: A lesson from Otub1. *World J. Biol. Chem.* **2014**, *5* (2), 75-84.
55. De, A.; Dainichi, T.; Rathinam, C. V.; Ghosh, S., The deubiquitinase activity of A20 is dispensable for NF- κ B signaling. *EMBO Rep.* **2014**, *15* (7), 775-83.
56. Herhaus, L.; Sapkota, G. P., The emerging roles of deubiquitylating enzymes (DUBs) in the TGF β and BMP pathways. *Cell. Signal.* **2014**, *26* (10), 2186-92.
57. Meenhuis, A.; Verwijmeren, C.; Roovers, O.; Touw, I. P., The deubiquitinating enzyme DUB2A enhances CSF3 signalling by attenuating lysosomal routing of the CSF3 receptor. *Biochem. J.* **2011**, *434* (2), 343-51.
58. Zhao, Y.; Thornton, A. M.; Kinney, M. C.; Ma, C. A.; Spinner, J. J.; Fuss, I. J.; Shevach, E. M.; Jain, A., The deubiquitinase CYLD targets Smad7 protein to regulate transforming growth factor β (TGF- β) signaling and the development of regulatory T cells. *J. Biol. Chem.* **2011**, *286* (47), 40520-30.

59. Carneiro, A. P.; Reis, C. F.; Morari, E. C.; Maia, Y. C.; Nascimento, R.; Bonatto, J. M.; de Souza, M. A.; Goulart, L. R.; Ward, L. S., A putative OTU domain-containing protein 1 deubiquitinating enzyme is differentially expressed in thyroid cancer and identifies less-aggressive tumours. *Br. J. Cancer* **2014**, *111* (3), 551-8.
60. Bhattacharyya, B. J.; Wilson, S. M.; Jung, H.; Miller, R. J., Altered neurotransmitter release machinery in mice deficient for the deubiquitinating enzyme Usp14. *Am. J. Physiol. Cell Physiol.* **2012**, *302* (4), C698-708.
61. Imai, S.; Mamiya, T.; Tsukada, A.; Sakai, Y.; Mouri, A.; Nabeshima, T.; Ebihara, S., Ubiquitin-specific peptidase 46 (Usp46) regulates mouse immobile behavior in the tail suspension test through the GABAergic system. *PLoS One* **2012**, *7* (6), e39084.
62. Xilouri, M.; Kyratzi, E.; Pitychoutis, P. M.; Papadopoulou-Daifoti, Z.; Perier, C.; Vila, M.; Maniati, M.; Ulusoy, A.; Kirik, D.; Park, D. S.; Wada, K.; Stefanis, L., Selective neuroprotective effects of the S18Y polymorphic variant of UCH-L1 in the dopaminergic system. *Hum. Mol. Genet.* **2012**, *21* (4), 874-89.
63. Bernassola, F.; Karin, M.; Ciechanover, A.; Melino, G., The HECT family of E3 ubiquitin ligases: multiple players in cancer development. *Cancer Cell* **2008**, *14* (1), 10-21.
64. Altun, M.; Kramer, H. B.; Willems, L. I.; McDermott, J. L.; Leach, C. A.; Goldenberg, S. J.; Kumar, K. G.; Konietzny, R.; Fischer, R.; Kogan, E.; Mackeen, M. M.; McGouran, J.; Khoronenkova, S. V.; Parsons, J. L.; Dianov, G. L.; Nicholson, B.; Kessler, B. M., Activity-based chemical proteomics accelerates inhibitor development for deubiquitylating enzymes. *Chem. Biol.* **2011**, *18* (11), 1401-12.
65. Velculescu, V. E.; Zhang, L.; Vogelstein, B.; Kinzler, K. W., Serial Analysis of Gene Expression. *Science* **1995**, *270* (5235), 484.
66. Sanman, L. E.; Bogoy, M., Activity-based profiling of proteases. *Annu. Rev. Biochem.* **2014**, *83*, 249-73.
67. Borodovsky, A.; Ovaa, H.; Kolli, N.; Gan-Erdene, T.; Wilkinson, K. D.; Ploegh, H. L.; Kessler, B. M., Chemistry-based functional proteomics reveals novel members of the deubiquitinating enzyme family. *Chem. Biol.* **2002**, *9* (10), 1149-59.
68. Misaghi, S.; Galardy, P. J.; Meester, W. J.; Ovaa, H.; Ploegh, H. L.; Gaudet, R., Structure of the ubiquitin hydrolase UCH-L3 complexed with a suicide substrate. *J. Biol. Chem.* **2005**, *280* (2), 1512-20.

69. Kramer, H. B.; Nicholson, B.; Kessler, B. M.; Altun, M., Detection of ubiquitin-proteasome enzymatic activities in cells: application of activity-based probes to inhibitor development. *Biochim. Biophys. Acta.* **2012**, *1823* (11), 2029-37.
70. Borodovsky, A.; Kessler, B. M.; Casagrande, R.; Overkleeft, H. S.; Wilkinson, K. D.; Ploegh, H. L., A novel active site-directed probe specific for deubiquitylating enzymes reveals proteasome association of USP14. *EMBO J.* **2001**, *20* (18), 5187-96.
71. Love, K. R.; Pandya, R. K.; Spooner, E.; Ploegh, H. L., Ubiquitin C-terminal electrophiles are activity-based probes for identification and mechanistic study of ubiquitin conjugating machinery. *ACS Chem. Biol.* **2009**, *4* (4), 275-87.
72. Ekkebus, R.; van Kasteren, S. I.; Kulathu, Y.; Scholten, A.; Berlin, I.; Geurink, P. P.; de Jong, A.; Goerdayal, S.; Neefjes, J.; Heck, A. J.; Komander, D.; Ovaa, H., On terminal alkynes that can react with active-site cysteine nucleophiles in proteases. *J. Am. Chem. Soc.* **2013**, *135* (8), 2867-70.
73. de Jong, A.; Witting, K.; Kooij, R.; Flierman, D.; Ovaa, H., Release of Enzymatically Active Deubiquitinating Enzymes upon Reversible Capture by Disulfide Ubiquitin Reagents. *Angew. Chem., Int. Ed. Engl.* **2017**, *56* (42), 12967-12970.
74. Ernst, A.; Avvakumov, G.; Tong, J.; Fan, Y.; Zhao, Y.; Alberts, P.; Persaud, A.; Walker, J. R.; Neculai, A. M.; Neculai, D.; Vorobyov, A.; Garg, P.; Beatty, L.; Chan, P. K.; Juang, Y. C.; Landry, M. C.; Yeh, C.; Zeqiraj, E.; Karamboulas, K.; Allali-Hassani, A.; Vedadi, M.; Tyers, M.; Moffat, J.; Sicheri, F.; Pelletier, L.; Durocher, D.; Raught, B.; Rotin, D.; Yang, J.; Moran, M. F.; Dhe-Paganon, S.; Sidhu, S. S., A strategy for modulation of enzymes in the ubiquitin system. *Science* **2013**, *339* (6119), 590-5.
75. Zhang, Y.; Zhou, L.; Rouge, L.; Phillips, A. H.; Lam, C.; Liu, P.; Sandoval, W.; Helgason, E.; Murray, J. M.; Wertz, I. E.; Corn, J. E., Conformational stabilization of ubiquitin yields potent and selective inhibitors of USP7. *Nat. Chem. Biol.* **2013**, *9* (1), 51-8.
76. Gabrielsen, M.; Buetow, L.; Nakasone, M. A.; Ahmed, S. F.; Sibbet, G. J.; Smith, B. O.; Zhang, W.; Sidhu, S. S.; Huang, D. T., A General Strategy for Discovery of Inhibitors and Activators of RING and U-box E3 Ligases with Ubiquitin Variants. *Mol. Cell* **2017**, *68* (2), 456-470 e10.

77. Zhang, W.; Wu, K. P.; Sartori, M. A.; Kamadurai, H. B.; Ordureau, A.; Jiang, C.; Mercedi, P. Y.; Murchie, R.; Hu, J.; Persaud, A.; Mukherjee, M.; Li, N.; Doye, A.; Walker, J. R.; Sheng, Y.; Hao, Z.; Li, Y.; Brown, K. R.; Lemichez, E.; Chen, J.; Tong, Y.; Harper, J. W.; Moffat, J.; Rotin, D.; Schulman, B. A.; Sidhu, S. S., System-Wide Modulation of HECT E3 Ligases with Selective Ubiquitin Variant Probes. *Mol. Cell* **2016**, *62* (1), 121-36.
78. Gorelik, M.; Sidhu, S. S., Specific targeting of the deubiquitinase and E3 ligase families with engineered ubiquitin variants. *Bioeng. Transl. Med.* **2017**, *2* (1), 31-42.
79. Gjonaj, L.; Sapmaz, A.; Gonzalez-Prieto, R.; Vertegaal, A. C. O.; Flierman, D.; Ovaa, H., USP7: combining tools towards selectivity. *Chem. Commun. (Camb.)* **2019**, *55* (35), 5075-5078.
80. Mulder, M. P.; Witting, K.; Berlin, I.; Pruneda, J. N.; Wu, K. P.; Chang, J. G.; Merckx, R.; Bialas, J.; Groettrup, M.; Vertegaal, A. C.; Schulman, B. A.; Komander, D.; Neefjes, J.; El Oualid, F.; Ovaa, H., A cascading activity-based probe sequentially targets E1-E2-E3 ubiquitin enzymes. *Nat. Chem. Biol.* **2016**, *12* (7), 523-30.
81. Erlich, L. A.; Kumar, K. S. A.; Haj-Yahya, M.; Dawson, P. E.; Brik, A., N-Methylcysteine-mediated total chemical synthesis of ubiquitin thioester. *Org. Biomol. Chem.* **2010**, *8* (10), 2392-2396.
82. El Oualid, F.; Merckx, R.; Ekkebus, R.; Hameed, D. S.; Smit, J. J.; de Jong, A.; Hilkmann, H.; Sixma, T. K.; Ovaa, H., Chemical Synthesis of Ubiquitin, Ubiquitin-Based Probes, and Diubiquitin. *Angew. Chem., Int. Ed.* **2010**, *49* (52), 10149-10153.
83. Bavikar, S. N.; Spasser, L.; Haj-Yahya, M.; Karthikeyan, S. V.; Moyal, T.; Ajish Kumar, K. S.; Brik, A., Chemical Synthesis of Ubiquitinated Peptides with Varying Lengths and Types of Ubiquitin Chains to Explore the Activity of Deubiquitinases. *Angew. Chem., Int. Ed.* **2012**, *51* (3), 758-763.
84. Colston, M. J.; Davis, E. O., The ins and outs of protein splicing elements. *Mol. Microbiol.* **1994**, *12* (3), 359-63.
85. Mootz, H. D., Split inteins as versatile tools for protein semisynthesis. *ChemBiochem* **2009**, *10* (16), 2579-89.

86. Wilkinson, K. D.; Audhya, T. K., Stimulation of ATP-dependent proteolysis requires ubiquitin with the COOH-terminal sequence Arg-Gly-Gly. *J. Biol. Chem.* **1981**, *256* (17), 9235-41.
87. Dang, L. C.; Melandri, F. D.; Stein, R. L., Kinetic and Mechanistic Studies on the Hydrolysis of Ubiquitin C-Terminal 7-Amido-4-Methylcoumarin by Deubiquitinating Enzymes. *Biochemistry* **1998**, *37* (7), 1868-1879.
88. Wilkinson, K. D.; Cox, M. J.; Mayer, A. N.; Frey, T., Synthesis and characterization of ubiquitin ethyl ester, a new substrate for ubiquitin carboxyl-terminal hydrolase. *Biochemistry* **1986**, *25* (21), 6644-6649.
89. Ovaa, H., Active-site directed probes to report enzymatic action in the ubiquitin proteasome system. *Nat. Rev. Cancer* **2007**, *7* (8), 613-620.
90. Pickart, C. M.; Rose, I. A., Ubiquitin carboxyl-terminal hydrolase acts on ubiquitin carboxyl-terminal amides. *J. Biol. Chem.* **1985**, *260* (13), 7903-10.
91. Hewings, D. S.; Heideker, J.; Ma, T. P.; AhYoung, A. P.; El Oualid, F.; Amore, A.; Costakes, G. T.; Kirchhofer, D.; Brasher, B.; Pillow, T.; Popovych, N.; Maurer, T.; Schwerdtfeger, C.; Forrest, W. F.; Yu, K.; Flygare, J.; Bogoy, M.; Wertz, I. E., Reactive-site-centric chemoproteomics identifies a distinct class of deubiquitinase enzymes. *Nat. Commun.* **2018**, *9* (1), 1162.
92. Pinto-Fernández, A.; Davis, S.; Schofield, A. B.; Scott, H. C.; Zhang, P.; Salah, E.; Mathea, S.; Charles, P. D.; Damianou, A.; Bond, G.; Fischer, R.; Kessler, B. M., Comprehensive Landscape of Active Deubiquitinating Enzymes Profiled by Advanced Chemoproteomics. *Front. Chem.* **2019**, *7*, 592.
93. Claessen, J. H. L.; Witte, M. D.; Yoder, N. C.; Zhu, A. Y.; Spooner, E.; Ploegh, H. L., Catch-and-release probes applied to semi-intact cells reveal ubiquitin-specific protease expression in *Chlamydia trachomatis* infection. *Chembiochem* **2013**, *14* (3), 343-52.
94. Gui, W.; Ott, C. A.; Yang, K.; Chung, J. S.; Shen, S.; Zhuang, Z., Cell-Permeable Activity-Based Ubiquitin Probes Enable Intracellular Profiling of Human Deubiquitinases. *J. Am. Chem. Soc.* **2018**, *140* (39), 12424-12433.
95. Neumann, E.; Schaefer-Ridder, M.; Wang, Y.; Hofschneider, P. H., Gene transfer into mouse lymphoma cells by electroporation in high electric fields. *The EMBO journal* **1982**, *1* (7), 841-845.
96. Bak, R. O.; Dever, D. P.; Porteus, M. H., CRISPR/Cas9 genome editing in human hematopoietic stem cells. *Nat. Protoc.* **2018**, *13* (2), 358-376.

97. Ward, J. A.; McLellan, L.; Stockley, M.; Gibson, K. R.; Whitlock, G. A.; Knights, C.; Harrigan, J. A.; Jacq, X.; Tate, E. W., Quantitative Chemical Proteomic Profiling of Ubiquitin Specific Proteases in Intact Cancer Cells. *ACS Chem. Biol.* **2016**, *11* (12), 3268-3272.
98. Ward, J. A.; Pinto-Fernandez, A.; Cornelissen, L.; Bonham, S.; Díaz-Sáez, L.; Riant, O.; Huber, K. V. M.; Kessler, B. M.; Feron, O.; Tate, E. W., Re-Evaluating the Mechanism of Action of α,β -Unsaturated Carbonyl DUB Inhibitors b-AP15 and VLX1570: A Paradigmatic Example of Unspecific Protein Cross-linking with Michael Acceptor Motif-Containing Drugs. *J. Med. Chem.* **2020**, *63* (7), 3756-3762.
99. Panyain, N.; Godinat, A.; Lanyon-Hogg, T.; Lachiondo-Ortega, S.; Will, E. J.; Soudy, C.; Mondal, M.; Mason, K.; Elkhalifa, S.; Smith, L. M.; Harrigan, J. A.; Tate, E. W., Discovery of a Potent and Selective Covalent Inhibitor and Activity-Based Probe for the Deubiquitylating Enzyme UCHL1, with Antifibrotic Activity. *J. Am. Chem. Soc.* **2020**, *142* (28), 12020-12026.
100. Krabill, A. D.; Chen, H.; Hussain, S.; Feng, C.; Abdullah, A.; Das, C.; Aryal, U. K.; Post, C. B.; Wendt, M. K.; Galardy, P. J.; Flaherty, D. P., Ubiquitin C-Terminal Hydrolase L1: Biochemical and Cellular Characterization of a Covalent Cyanopyrrolidine-Based Inhibitor. *ChemBioChem* **2020**, *21* (5), 712-722.
101. Kooij, R.; Liu, S.; Sapmaz, A.; Xin, B.-T.; Janssen, G. M. C.; van Veelen, P. A.; Ovaa, H.; Dijke, P. t.; Geurink, P. P., Small-Molecule Activity-Based Probe for Monitoring Ubiquitin C-Terminal Hydrolase L1 (UCHL1) Activity in Live Cells and Zebrafish Embryos. *J. Am. Chem. Soc.* **2020**, *142* (39), 16825-16841.
102. Taylor, N. C.; McGouran, J. F., Strategies to Target Specific Components of the Ubiquitin Conjugation/Deconjugation Machinery. *Front. Chem.* **2020**, *7*, 914.
103. Iphofer, A.; Kummer, A.; Nimtz, M.; Ritter, A.; Arnold, T.; Frank, R.; van den Heuvel, J.; Kessler, B. M.; Jansch, L.; Franke, R., Profiling ubiquitin linkage specificities of deubiquitinating enzymes with branched ubiquitin isopeptide probes. *Chembiochem* **2012**, *13* (10), 1416-20.
104. Whedon, S. D.; Markandeya, N.; Rana, A. S.; Weller, C. E.; Senger, N. A.; Turecek, F.; Strieter, E. R.; Chatterjee, C., Selenocysteine as a latent bioorthogonal electrophilic probe for deubiquitylating enzymes. *J. Am. Chem. Soc.* **2016**.
105. McGouran, J. F.; Gaertner, S. R.; Altun, M.; Kramer, H. B.; Kessler, B. M., Deubiquitinating enzyme specificity for ubiquitin chain topology profiled by di-ubiquitin activity probes. *Chem. Biol.* **2013**, *20* (12), 1447-55.

106. Li, G.; Liang, Q.; Gong, P.; Tencer, A. H.; Zhuang, Z., Activity-based diubiquitin probes for elucidating the linkage specificity of deubiquitinating enzymes. *Chem. Commun. (Camb.)* **2014**, *50* (2), 216-8.
107. Haj-Yahya, N.; Hemantha, H. P.; Meledin, R.; Bondalapati, S.; Seenaiyah, M.; Brik, A., Dehydroalanine-based diubiquitin activity probes. *Org. Lett.* **2014**, *16* (2), 540-3.
108. Mulder, M. P.; El Oualid, F.; ter Beek, J.; Ovaa, H., A native chemical ligation handle that enables the synthesis of advanced activity-based probes: diubiquitin as a case study. *Chembiochem* **2014**, *15* (7), 946-9.
109. Weber, A.; Elliott, P. R.; Pinto-Fernandez, A.; Bonham, S.; Kessler, B. M.; Komander, D.; El Oualid, F.; Krappmann, D., A Linear Diubiquitin-Based Probe for Efficient and Selective Detection of the Deubiquitinating Enzyme OTULIN. *Cell Chem. Biol.* **2017**, *24* (10), 1299-1313 e7.
110. Paudel, P.; Zhang, Q.; Leung, C.; Greenberg, H. C.; Guo, Y.; Chern, Y. H.; Dong, A.; Li, Y.; Vedadi, M.; Zhuang, Z.; Tong, Y., Crystal structure and activity-based labeling reveal the mechanisms for linkage-specific substrate recognition by deubiquitinase USP9X. *Proc. Natl. Acad. Sci. U S A* **2019**, *116* (15), 7288-7297.
111. Hermanns, T.; Pichlo, C.; Woiwode, I.; Klopffleisch, K.; Witting, K. F.; Ovaa, H.; Baumann, U.; Hofmann, K., A family of unconventional deubiquitinases with modular chain specificity determinants. *Nat. Commun.* **2018**, *9* (1), 799.
112. Flierman, D.; van der Heden van Noort, G. J.; Ekkebus, R.; Geurink, P. P.; Mevissen, T. E.; Hospenthal, M. K.; Komander, D.; Ovaa, H., Non-hydrolyzable Diubiquitin Probes Reveal Linkage-Specific Reactivity of Deubiquitylating Enzymes Mediated by S2 Pockets. *Cell Chem. Biol.* **2016**, *23* (4), 472-82.
113. Meledin, R.; Mali, S. M.; Kleifeld, O.; Brik, A., Activity-Based Probes Developed by Applying a Sequential Dehydroalanine Formation Strategy to Expressed Proteins Reveal a Potential alpha-Globin-Modulating Deubiquitinase. *Angew. Chem. Int. Ed. Engl.* **2018**, *57* (20), 5645-5649.
114. Jbara, M.; Laps, S.; Morgan, M.; Kamnesky, G.; Mann, G.; Wolberger, C.; Brik, A., Palladium prompted on-demand cysteine chemistry for the synthesis of challenging and uniquely modified proteins. *Nat. Commun.* **2018**, *9* (1), 3154.

115. Gong, P.; Davidson, G. A.; Gui, W.; Yang, K.; Bozza, W. P.; Zhuang, Z., Activity-based ubiquitin-protein probes reveal target protein specificity of deubiquitinating enzymes. *Chem. Sci.* **2018**, *9* (40), 7859-7865.
116. Byrne, R.; Mund, T.; Licchesi, J. D. F., Activity-Based Probes for HECT E3 Ubiquitin Ligases. *Chembiochem* **2017**, *18* (14), 1415-1427.
117. Kim, H. C.; Steffen, A. M.; Oldham, M. L.; Chen, J.; Huibregtse, J. M., Structure and function of a HECT domain ubiquitin-binding site. *EMBO Rep.* **2011**, *12* (4), 334-41.
118. Maspero, E.; Valentini, E.; Mari, S.; Cecatiello, V.; Soffientini, P.; Pasqualato, S.; Polo, S., Structure of a ubiquitin-loaded HECT ligase reveals the molecular basis for catalytic priming. *Nat. Struct. Mol Biol.* **2013**, *20* (6), 696-701.
119. Kamadurai, H. B.; Souphron, J.; Scott, D. C.; Duda, D. M.; Miller, D. J.; Stringer, D.; Piper, R. C.; Schulman, B. A., Insights into ubiquitin transfer cascades from a structure of a Ubch5B approximately ubiquitin-HECT(NEDD4L) complex. *Mol. Cell.* **2009**, *36* (6), 1095-102.
120. Witting, K. F.; Mulder, M. P. C.; Ovaa, H., Advancing our Understanding of Ubiquitination Using the Ub-Toolkit. *J. Mol. Biol.* **2017**, *429* (22), 3388-3394.
121. Lu, X.; Olsen, S. K.; Capili, A. D.; Cisar, J. S.; Lima, C. D.; Tan, D. S., Designed semisynthetic protein inhibitors of Ub/Ubl E1 activating enzymes. *J. Am. Chem. Soc.* **2010**, *132* (6), 1748-9.
122. An, H.; Statsyuk, A. V., Facile synthesis of covalent probes to capture enzymatic intermediates during E1 enzyme catalysis. *Chem. Commun. (Camb.)* **2016**, *52* (12), 2477-80.
123. Stanley, M.; Han, C.; Knebel, A.; Murphy, P.; Shpiro, N.; Virdee, S., Orthogonal thiol functionalization at a single atomic center for profiling transthiolation activity of E1 activating enzymes. *ACS Chem. Biol.* **2015**, *10* (6), 1542-54.
124. Xu, L.; Fan, J.; Wang, Y.; Zhang, Z.; Fu, Y.; Li, Y. M.; Shi, J., An activity-based probe developed by a sequential dehydroalanine formation strategy targets HECT E3 ubiquitin ligases. *Chem. Commun. (Camb.)* **2019**, *55* (49), 7109-7112.
125. Milkovic, L.; Cipak Gasparovic, A.; Cindric, M.; Mouthuy, P.-A.; Zarkovic, N., Short Overview of ROS as Cell Function Regulators and Their Implications in Therapy Concepts. *Cells* **2019**, *8* (8), 793.

126. Gruber, J.; Schaffer, S.; Halliwell, B., The mitochondrial free radical theory of ageing--where do we stand? *Front. Biosci.* **2008**, *13*, 6554-79.
127. van der Vliet, A., NADPH oxidases in lung biology and pathology: host defense enzymes, and more. *Free. Radic. Biol. Med.* **2008**, *44* (6), 938-55.
128. Bedard, K.; Krause, K. H., The NOX family of ROS-generating NADPH oxidases: physiology and pathophysiology. *Physiol. Rev.* **2007**, *87* (1), 245-313.
129. Hawkins, C. L.; Davies, M. J., Generation and propagation of radical reactions on proteins. *Biochim. Biophys. Acta.* **2001**, *1504* (2-3), 196-219.
130. Kolb, H. C.; Finn, M. G.; Sharpless, K. B., Click Chemistry: Diverse Chemical Function from a Few Good Reactions. *Angew. Chem., Int. Ed.* **2001**, *40* (11), 2004-2021.
131. Posner, T., Beiträge zur Kenntniss der ungesättigten Verbindungen. II. Ueber die Addition von Mercaptanen an ungesättigte Kohlenwasserstoffe. *Ber. Dtsch. Chem. Ges.* **1905**, *38* (1), 646--657.
132. Wittrock, S.; Becker, T.; Kunz, H., Synthetic Vaccines of Tumor-Associated Glycopeptide Antigens by Immune-Compatible Thioether Linkage to Bovine Serum Albumin. *Angew. Chem., Int. Ed.* **2007**, *46* (27), 5226-5230.
133. Griesbaum, K., Probleme und Möglichkeiten der radikalischen Addition von Thiolen an ungesättigte Verbindungen. *Angew. Chem.* **1970**, *82* (7), 276-290.
134. Dondoni, A., The Emergence of Thiol–Ene Coupling as a Click Process for Materials and Bioorganic Chemistry. *Angew. Chem., Int. Ed.* **2008**, *47* (47), 8995-8997.
135. Geng, Y.; Discher, D. E.; Justynska, J.; Schlaad, H., Grafting Short Peptides onto Polybutadiene-block-poly(ethylene oxide): A Platform for Self-Assembling Hybrid Amphiphiles. *Angew. Chem.* **2006**, *118* (45), 7740-7743.
136. Floyd, N. a. V. B. a. K. J. R. a. D. B. G., Thiol Glycosylation of Olefinic Proteins: S-Linked Glycoconjugate Synthesis. *Angew. Chem., Int. Ed.* **2009**, *48* (42), 7798--7802.
137. Valkevich, E. M.; Guenette, R. G.; Sanchez, N. A.; Chen, Y. C.; Ge, Y.; Strieter, E. R., Forging isopeptide bonds using thiol-ene chemistry: site-specific coupling of ubiquitin molecules for studying the activity of isopeptidases. *J. Am. Chem. Soc.* **2012**, *134* (16), 6916-9.

138. Conte, M. L.; Staderini, S.; Marra, A.; Sanchez-Navarro, M.; Davis, B. G.; Dondoni, A., Multi-molecule reaction of serum albumin can occur through thiol-yne coupling. *Chem. Commun.* **2011**, 47 (39), 11086-11088.
139. Li, Y.; Pan, M.; Huang, Y.; Guo, Q., Thiol-yne radical reaction mediated site-specific protein labeling via genetic incorporation of an alkynyl-L-lysine analogue. *Org. Biomol. Chem.* **2013**, 11 (16), 2624-9.
140. Griffiths, R. C.; Smith, F. R.; Long, J. E.; Williams, H. E. L.; Layfield, R.; Mitchell, N. J., Site-Selective Modification of Peptides and Proteins via Interception of Free-Radical-Mediated Dechalcogenation. *Angew. Chem., Int. Ed. Engl.* **2020**.
141. Vara, B. A.; Li, X.; Berritt, S.; Walters, C. R.; Petersson, E. J.; Molander, G. A., Scalable thioarylation of unprotected peptides and biomolecules under Ni/photoredox catalysis. *Chem. Sci.* **2018**, 9 (2), 336-344.
142. Vinogradova, E. V.; Zhang, C.; Spokoiny, A. M.; Pentelute, B. L.; Buchwald, S. L., Organometallic palladium reagents for cysteine bioconjugation. *Nature* **2015**, 526 (7575), 687-691.
143. Bottecchia, C.; Rubens, M.; Gunnoo, S. B.; Hessel, V.; Madder, A.; Noël, T., Visible-Light-Mediated Selective Arylation of Cysteine in Batch and Flow. *Angew. Chem., Int. Ed. Engl.* **2017**, 56 (41), 12702-12707.
144. Tyson, E. L.; Ament, M. S.; Yoon, T. P., Transition Metal Photoredox Catalysis of Radical Thiol-Ene Reactions. *J. Org. Chem.* **2013**, 78 (5), 2046-2050.
145. Keylor, M. H.; Park, J. E.; Wallentin, C.-J.; Stephenson, C. R. J., Photocatalytic initiation of thiol-ene reactions: synthesis of thiomorpholin-3-ones. *Tetrahedron* **2014**, 70 (27), 4264-4269.
146. Sawhney, A. S.; Pathak, C. P.; Hubbell, J. A., Interfacial photopolymerization of poly(ethylene glycol)-based hydrogels upon alginate-poly(L-lysine) microcapsules for enhanced biocompatibility. *Biomaterials* **1993**, 14 (13), 1008-1016.
147. Fadeyi, O. O.; Mousseau, J. J.; Feng, Y.; Allais, C.; Nuhant, P.; Chen, M. Z.; Pierce, B.; Robinson, R., Visible-Light-Driven Photocatalytic Initiation of Radical Thiol-Ene Reactions Using Bismuth Oxide. *Org. Lett.* **2015**, 17 (23), 5756-9.
148. Zhao, G.; Kaur, S.; Wang, T., Visible-Light-Mediated Thiol-Ene Reactions through Organic Photoredox Catalysis. *Org. Lett.* **2017**, 19 (12), 3291-3294.
149. Maffei, V.; McCourt, R. O.; Petracca, R.; Laethem, O.; Camisasca, A.; Colavita, P. E.; Giordani, S.; Scanlan, E. M., Photocatalytic Initiation of Radical

Thiol–ene Reactions Using Carbon-Bi₂O₃ Nanocomposites. *ACS Appl. Nano Mater.* **2018**, *1* (8), 4120-4126.

150. Choi, H.; Kim, M.; Jang, J.; Hong, S., Visible-Light-Induced Cysteine-Specific Bioconjugation: Biocompatible Thiol–Ene Click Chemistry. *Angew. Chem., Int. Ed.* **2020**, doi.org/10.1002/anie.202010217.

151. Fancy, D. A.; Kodadek, T., Chemistry for the analysis of protein–protein interactions: Rapid and efficient cross-linking triggered by long wavelength light. *Proc. Natl. Acad. Sci.* **1999**, *96* (11), 6020.

152. Kim, K.; Fancy, D. A.; Carney, D.; Kodadek, T., Photoinduced Protein Cross-Linking Mediated by Palladium Porphyrins. *J. Am. Chem. Soc.* **1999**, *121* (50), 11896-11897.

153. Sato, S.; Nakamura, H., Ligand-Directed Selective Protein Modification Based on Local Single-Electron-Transfer Catalysis. *Angew. Chem., Int. Ed.* **2013**, *52* (33), 8681-8684.

154. Seki, Y.; Ishiyama, T.; Sasaki, D.; Abe, J.; Sohma, Y.; Oisaki, K.; Kanai, M., Transition Metal-Free Tryptophan-Selective Bioconjugation of Proteins. *J. Am. Chem. Soc.* **2016**, *138* (34), 10798-10801.

155. Lee, Y.; Lee, H.; Lee, M., Photoinduced electron transfer between flavin and tryptophan in a poly(vinyl alcohol) film. *Dyes Pigm.* **2015**, *112*, 54-58.

156. Tower, S. J.; Hetcher, W. J.; Myers, T. E.; Kuehl, N. J.; Taylor, M. T., Selective Modification of Tryptophan Residues in Peptides and Proteins Using a Biomimetic Electron Transfer Process. *J. Am. Chem. Soc.* **2020**, *142* (20), 9112-9118.

157. Bloom, S.; Liu, C.; Kölmel, D. K.; Qiao, J. X.; Zhang, Y.; Poss, M. A.; Ewing, W. R.; MacMillan, D. W. C., Decarboxylative alkylation for site-selective bioconjugation of native proteins via oxidation potentials. *Nat. Chem.* **2018**, *10* (2), 205-211.

158. Garreau, M.; Le Vaillant, F.; Waser, J., C-Terminal Bioconjugation of Peptides through Photoredox Catalyzed Decarboxylative Alkynylation. *Angew. Chem., Int. Ed.* **2019**, *58* (24), 8182-8186.

159. Wright, T. H.; Bower, B. J.; Chalker, J. M.; Bernardes, G. J. L.; Wiewiora, R.; Ng, W.-L.; Raj, R.; Faulkner, S.; Vallée, M. R. J.; Phanumartwiwath, A.; Coleman, O. D.; Thézénas, M.-L.; Khan, M.; Galan, S. R. G.; Lercher, L.; Schombs, M. W.; Gerstberger, S.; Palm-Espling, M. E.; Baldwin, A. J.; Kessler,

- B. M.; Claridge, T. D. W.; Mohammed, S.; Davis, B. G., Posttranslational mutagenesis: A chemical strategy for exploring protein side-chain diversity. *Science* **2016**, *354* (6312), aag1465.
160. Wang, J.; Schiller, S. M.; Schultz, P. G., A Biosynthetic Route to Dehydroalanine-Containing Proteins. *Angew. Chem., Int. Ed.* **2007**, *46* (36), 6849-6851.
161. Seebeck, F. P.; Szostak, J. W., Ribosomal Synthesis of Dehydroalanine-Containing Peptides. *J. Am. Chem. Soc.* **2006**, *128* (22), 7150-7151.
162. Bernardes, G. J. L.; Chalker, J. M.; Errey, J. C.; Davis, B. G., Facile Conversion of Cysteine and Alkyl Cysteines to Dehydroalanine on Protein Surfaces: Versatile and Switchable Access to Functionalized Proteins. *J. Am. Chem. Soc.* **2008**, *130* (15), 5052-5053.
163. Chalker, J. M.; Gunnoo, S. B.; Boutureira, O.; Gerstberger, S. C.; Fernández-González, M.; Bernardes, G. J. L.; Griffin, L.; Hailu, H.; Schofield, C. J.; Davis, B. G., Methods for converting cysteine to dehydroalanine on peptides and proteins. *Chem. Sci.* **2011**, *2* (9), 1666-1676.
164. Zhou, Y.; Li, W.; Xiao, Y., Profiling of Multiple Targets of Artemisinin Activated by Hemin in Cancer Cell Proteome. *ACS Chem. Biol.* **2016**, *11* (4), 882-8.
165. Wei, C.; Zhao, C. X.; Liu, S.; Zhao, J. H.; Ye, Z.; Wang, H.; Yu, S. S.; Zhang, C. J., Activity-based protein profiling reveals that secondary-carbon-centered radicals of synthetic 1,2,4-trioxolanes are predominately responsible for modification of protein targets in malaria parasites. *Chem. Commun. (Camb.)* **2019**, *55* (64), 9535-9538.
166. Lin, Z.; Wang, X.; Bustin, K. A.; He, L.; Suciu, R. M.; Schek, N.; Ahmadi, M.; Hu, K.; Olson, E. J.; Parsons, W. H.; Witze, E. S.; Morton, P. D.; Gregus, A. M.; Buczynski, M. W.; Matthews, M. L., Hydrazines as versatile chemical biology probes and drug-discovery tools for cofactor-dependent enzymes. *bioRxiv* **2020**, 2020.06.17.154864.
167. Murale, D. P.; Hong, S. C.; Haque, M. M.; Lee, J. S., Photo-affinity labeling (PAL) in chemical proteomics: a handy tool to investigate protein-protein interactions (PPIs). *Proteome Sci.* **2016**, *15*, 14.
168. Saghatelian, A.; Jessani, N.; Joseph, A.; Humphrey, M.; Cravatt, B. F., Activity-based probes for the proteomic profiling of metalloproteases. *Proc. Natl. Acad. Sci. U. S. A.* **2004**, *101* (27), 10000-5.

169. Galardy, R. E.; Craig, L. C.; Jamieson, J. D.; Printz, M. P., Photoaffinity Labeling of Peptide Hormone Binding Sites. *J. Biol. Chem.* **1974**, *249* (11), 3510-3518.
170. Chan, E. W. S.; Chattopadhyaya, S.; Panicker, R. C.; Huang, X.; Yao, S. Q., Developing Photoactive Affinity Probes for Proteomic Profiling: Hydroxamate-based Probes for Metalloproteases. *J. Am. Chem. Soc.* **2004**, *126* (44), 14435-14446.
171. Chin, J. W.; Martin, A. B.; King, D. S.; Wang, L.; Schultz, P. G., Addition of a photocrosslinking amino acid to the genetic code of Escherichia coli. *Proc. Natl. Acad. Sci. U. S. A.* **2002**, *99* (17), 11020.
172. Yanagisawa, T.; Hino, N.; Iraha, F.; Mukai, T.; Sakamoto, K.; Yokoyama, S., Wide-range protein photo-crosslinking achieved by a genetically encoded N ϵ -(benzyloxycarbonyl)lysine derivative with a diazirinyl moiety. *Mol. Biosyst.* **2012**, *8* (4), 1131-1135.
173. Hill, J. R.; Robertson, A. A. B., Fishing for Drug Targets: A Focus on Diazirine Photoaffinity Probe Synthesis. *J. Med. Chem.* **2018**, *61* (16), 6945-6963.
174. Tan, X.-D.; Pan, M.; Gao, S.; Zheng, Y.; Shi, J.; Li, Y.-M., A diubiquitin-based photoaffinity probe for profiling K27-linkage targeting deubiquitinases. *Chem. Commun. (Camb.)* **2017**, *53* (73), 10208-10211.
175. Liang, J.; Zhang, L.; Tan, X. L.; Qi, Y. K.; Feng, S.; Deng, H.; Yan, Y.; Zheng, J. S.; Liu, L.; Tian, C. L., Chemical Synthesis of Diubiquitin-Based Photoaffinity Probes for Selectively Profiling Ubiquitin-Binding Proteins. *Angew. Chem., Int. Ed. Engl.* **2017**, *56* (10), 2744-2748.
176. Abo, M.; Bak, D. W.; Weerapana, E., Optimization of Caged Electrophiles for Improved Monitoring of Cysteine Reactivity in Living Cells. *Chembiochem* **2017**, *18* (1), 81-84.
177. Bach, K.; Beerkens, B. L. H.; Zanon, P. R. A.; Hacker, S. M., Light-Activatable, 2,5-Disubstituted Tetrazoles for the Proteome-wide Profiling of Aspartates and Glutamates in Living Bacteria. *ACS Cent. Sci.* **2020**, *6* (4), 546-554.
178. Chakrabarty, S.; Verhelst, S. H. L., Controlled Inhibition of Apoptosis by Photoactivatable Caspase Inhibitors. *Cell Chem. Biol.* **2020**.
179. Gui, W.; Shen, S.; Zhuang, Z., Photocaged Cell-Permeable Ubiquitin Probe for Temporal Profiling of Deubiquitinating Enzymes. *J. Am. Chem. Soc.* **2020**.

180. Gui, W.; Paudel, P.; Zhuang, Z., 4.23 - Activity-Based Ubiquitin Probes for Investigation of Deubiquitinases. In *Compr. Nat. Prod. III*, Liu, H.-W.; Begley, T. P., Eds. Elsevier: Oxford, 2020; pp 589-602.
181. Wilkinson, K. D.; Gan-Erdene, T.; Kolli, N., Derivatization of the C-terminus of ubiquitin and ubiquitin-like proteins using intein chemistry: methods and uses. *Methods Enzymol.* **2005**, *399*, 37-51.
182. Blanksby, S. J.; Ellison, G. B., Bond Dissociation Energies of Organic Molecules. *Acc. Chem. Res.* **2003**, *36* (4), 255-263.
183. Amii, H.; Uneyama, K., C–F Bond Activation in Organic Synthesis. *Chem. Rev.* **2009**, *109* (5), 2119-2183.
184. Mortenson, D. E.; Brighty, G. J.; Plate, L.; Bare, G.; Chen, W.; Li, S.; Wang, H.; Cravatt, B. F.; Forli, S.; Powers, E. T.; Sharpless, K. B.; Wilson, I. A.; Kelly, J. W., "Inverse Drug Discovery" Strategy To Identify Proteins That Are Targeted by Latent Electrophiles As Exemplified by Aryl Fluorosulfates. *J. Am. Chem. Soc.* **2018**, *140* (1), 200-210.
185. Altun, M.; Walter, T. S.; Kramer, H. B.; Herr, P.; Iphöfer, A.; Boström, J.; David, Y.; Komsany, A.; Ternette, N.; Navon, A.; Stuart, D. I.; Ren, J.; Kessler, B. M., The human otubain2-ubiquitin structure provides insights into the cleavage specificity of poly-ubiquitin-linkages. *PLoS One* **2015**, *10* (1), e0115344.
186. Tian, W.; Chen, C.; Lei, X.; Zhao, J.; Liang, J., CASTp 3.0: computed atlas of surface topography of proteins. *Nucleic Acids Res.* **2018**, *46* (W1), W363-W367.
187. Braxton, C. N.; Quartner, E.; Pawloski, W.; Fushman, D.; Cropp, T. A., Ubiquitin Chains Bearing Genetically Encoded Photo-Cross-Linkers Enable Efficient Covalent Capture of (Poly)ubiquitin-Binding Domains. *Biochemistry* **2019**, *58* (7), 883-886.
188. Taylor, N. C.; Hessman, G.; Kramer, H. B.; McGouran, J. F., Probing enzymatic activity – a radical approach. *Chem. Sci.* **2020**, *11* (11), 2967-2972.
189. Hoyle, C. E.; Bowman, C. N., Thiol-ene click chemistry. *Angew. Chem., Int. Ed. Engl.* **2010**, *49* (9), 1540-73.
190. Dondoni, A.; Massi, A.; Nanni, P.; Roda, A., A New Ligation Strategy for Peptide and Protein Glycosylation: Photoinduced Thiol–Ene Coupling. *Chem. – Eur. J.* **2009**, *15* (43), 11444-11449.
191. Malone, A.; Scanlan, E. M., Applications of thiy radical cyclizations for the synthesis of thiosugars. *Org. Lett.* **2013**, *15* (3), 504-507.

192. Gopinath, P.; Mahammed, A.; Ohayon, S.; Gross, Z.; Brik, A., Understanding and predicting the potency of ROS-based enzyme inhibitors, exemplified by naphthoquinones and ubiquitin specific protease-2. *Chem. Sci.* **2016**, 7 (12), 7079-7086.
193. Tian, X.; Isamididnova, N. S.; Peroutka, R. J.; Goldenberg, S. J.; Mattern, M. R.; Nicholson, B.; Leach, C., Characterization of selective ubiquitin and ubiquitin-like protease inhibitors using a fluorescence-based multiplex assay format. *Assay Drug Dev. Technol.* **2011**, 9 (2), 165-73.
194. Jensen, T.; Pedersen, H.; Bang-Andersen, B.; Madsen, R.; Jørgensen, M., Palladium-Catalyzed Aryl Amination–Heck Cyclization Cascade: A One-Flask Approach to 3-Substituted Indoles. *Angew. Chem., Int. Ed.* **2008**, 47 (5), 888-890.
195. Rodrigues, N.; Bennis, K.; Vivier, D.; Pereira, V.; C. Chatelain, F.; Chapuy, E.; Deokar, H.; Busserolles, J.; Lesage, F.; Eschalier, A.; Ducki, S., Synthesis and structure–activity relationship study of substituted caffeate esters as antinociceptive agents modulating the TREK-1 channel. *Eur. J. Med. Chem.* **2014**, 75, 391-402.
196. Mowery, B. P.; Lee, S. E.; Kissounko, D. A.; Epand, R. F.; Epand, R. M.; Weisblum, B.; Stahl, S. S.; Gellman, S. H., Mimicry of antimicrobial host-defense peptides by random copolymers. *J. Am. Chem. Soc.* **2007**, 129 (50), 15474-6.
197. Więcek, M.; Kottke, T.; Ligneau, X.; Schunack, W.; Seifert, R.; Stark, H.; Handzlik, J.; Kieć-Kononowicz, K., N-Alkenyl and cycloalkyl carbamates as dual acting histamine H3 and H4 receptor ligands. *Bioorg. Med. Chem.* **2011**, 19 (9), 2850-2858.
198. Taylor, E. C.; Liu, B., A new route to 7-substituted derivatives of n-[4-(2-[2-amino-3,4-dihydro-4-oxo-7H-pyrrolo(2,3-d)pyrimidin-5-yl]ethyl)benzoyl] -L-glutamic acid. *J. Org. Chem.* **2001**, 66 (11), 3726-38.
199. Sergejev, S.; Hesse, M., A New Convenient Method for the Preparation of Enamides from N-Allylamides. *Synlett.* **2002**, 2002 (08), 1313-1317.
200. Shih, H.; Lin, C. C., Visible-light-mediated thiol-ene hydrogelation using eosin-Y as the only photoinitiator. *Macromol. Rapid Commun.* **2013**, 34 (3), 269-73.
201. Bottecchia, C.; Rubens, M.; Gunnoo, S. B.; Hessel, V.; Maddar, A.; Noël, T., Visible-Light-Mediated Selective Arylation of Cysteine in Batch and Flow. *Angew. Chem., Int. Ed. Eng.* **2017**, 56 (41), 12702-12707.

202. Waheed, A. A.; Rao, K. S.; Gupta, P. D., Mechanism of dye binding in the protein assay using eosin dyes. *Anal. Biochem.* **2000**, *287* (1), 73-9.
203. Gao, D.; Tian, Y.; Liang, F.; Jin, D.; Chen, Y.; Zhang, H.; Yu, A., Investigation on the pH-dependent binding of Eosin Y and bovine serum albumin by spectral methods. *J. Lumin.* **2007**, *127* (2), 515-522.
204. Pompella, A.; Visvikis, A.; Paolicchi, A.; Tata, V. D.; Casini, A. F., The changing faces of glutathione, a cellular protagonist. *Biochem. Pharmacol.* **2003**, *66* (8), 1499-1503.
205. Aguirre-Soto, A.; Kaastrup, K.; Kim, S.; Ugo-Beke, K.; Sikes, H. D., Excitation of Metastable Intermediates in Organic Photoredox Catalysis: Z-Scheme Approach Decreases Catalyst Inactivation. *ACS Catal.* **2018**, *8* (7), 6394-6400.
206. Tan, D.-X.; Manchester, L. C.; Terron, M. P.; Flores, L. J.; Reiter, R. J., One molecule, many derivatives: A never-ending interaction of melatonin with reactive oxygen and nitrogen species? *J. Pineal Res.* **2007**, *42* (1), 28-42.
207. Chong, S.; Mersha, F. B.; Comb, D. G.; Scott, M. E.; Landry, D.; Vence, L. M.; Perler, F. B.; Benner, J.; Kucera, R. B.; Hirvonen, C. A.; Pelletier, J. J.; Paulus, H.; Xu, M. Q., Single-column purification of free recombinant proteins using a self-cleavable affinity tag derived from a protein splicing element. *Gene* **1997**, *192* (2), 271-81.
208. Manza, L. L.; Stamer, S. L.; Ham, A. J.; Codreanu, S. G.; Liebler, D. C., Sample preparation and digestion for proteomic analyses using spin filters. *Proteomics* **2005**, *5* (7), 1742-5.
209. Cox, J.; Mann, M., MaxQuant enables high peptide identification rates, individualized p.p.b.-range mass accuracies and proteome-wide protein quantification. *Nat. Biotechnol.* **2008**, *26* (12), 1367-72.
210. Vaudel, M.; Burkhardt, J. M.; Zahedi, R. P.; Oveland, E.; Berven, F. S.; Sickmann, A.; Martens, L.; Barsnes, H., PeptideShaker enables reanalysis of MS-derived proteomics data sets. *Nat Biotechnol* **2015**, *33* (1), 22-4.
211. Lambert, K. M.; Bobbitt, J. M.; Eldirany, S. A.; Kissane, L. E.; Sheridan, R. K.; Stempel, Z. D.; Sternberg, F. H.; Bailey, W. F., Metal-Free Oxidation of Primary Amines to Nitriles through Coupled Catalytic Cycles. *Chem. – Eur. J.* **2016**, *22* (15), 5156-5159.

212. Hari Babu, M.; Ranjith Kumar, G.; Kant, R.; Sridhar Reddy, M., Ni-Catalyzed regio- and stereoselective addition of arylboronic acids to terminal alkynes with a directing group tether. *Chem. Commun.* **2017**, 53 (27), 3894-3897.
213. Walters, M. A.; Hoem, A. B., In situ Preparation and Subsequent Use of Isomerically Pure E- and Z-Crotylamines in a 3-Aza-Claisen Rearrangement. *J. Org. Chem.* **1994**, 59 (9), 2645-2647.